LUND UNIVERSITY

Effective Field Theory for QCD-like Theories and Constraints on the Two Higgs Doublet Model

Lu, Jie

2011

Effective Field Theory for QCD-like Theories and Constraints on the Two Higgs Doublet Model

Jie Lu

Department of Astronomy and Theoretical Physics
Lund University

Thesis for the degree of Doctor of Philosophy

Thesis Advisor: *Johan Bijnens*
Faculty Opponent: *José R. Peláez*

To be presented, with the permission of the Faculty of Science of Lund University, for public criticism in lecture hall F of the Department of Physics on Friday, the 3th of February 2012, at 10.15.

Organization	Document name
LUND UNIVERSITY Department of Astronomy and Theoretical Physics Sölvegatan 14A SE–223 62 LUND Sweden	**DOCTORAL DISSERTATION**
	Date of issue November 2011
	Sponsoring organization
Author(s) Jie Lu	

Title and subtitle
Effective Field Theory for QCD-like Theories and Constraints on the Two Higgs Doublet Model

Abstract

This thesis includes two topics.
The first three papers is the major part of this thesis, which is about higher order calculations in the effective field theories of three QCD-like theories. These three QCD-like theories are distinguished by having quarks in a complex, real or pseudo-real representation of gauge group. We wrote their effective field theories in a very similar way so that the calculations can be done using techniques from chiral perturbation theory. We calculated the vacuum-expectation-value, the mass and the decay constant of pseudo-Goldstone bosons up to next-to-next-to leading order (NNLO) in paper I. The various channels of general meson-meson scattering of the three cases were calculated up to NNLO in paper II. In paper III, we calculated the vector, axial-vector, scalar, pseudo-scalar two-point functions and pseudo-scalar decay constant G_M up to two-loop level. We also calculated the S parameter for those different QCD-like theories at the TeV scale.
The second topic concerns the evolution of Yukawa couplings in general two Higgs doublet models (2HDM). In paper IV, using the updated experimental and theoretical data, we give the latest constraints on the parameters λ_{ij}^F of the Cheng-Sher ansatz for 2HDM. We show the constraints from the Landau poles and large nondiagonal λ_{ij}^F at a high scale with various input at electroweak scale for three different cases: models with Z_2 symmetry, models with Z_2 symmetry breaking but still aligned or diagonal, and models with the Cheng-Sher ansatz.

Key words:
QCD-like, effective field theory, symmetry breaking, renormalization group, two Higgs doublet model

Classification system and/or index terms (if any):

Supplementary bibliographical information:		Language English
ISSN and key title:		ISBN 978-91-7473-222-1
Recipient's notes	Number of pages 214	Price
	Security classification	

Distributor
Jie Lu
Department of Astronomy and Theoretical Physics, Sölvegatan 14A, SE–223 62 Lund, Sweden

Department of Astronomy and Theoretical Physics, Lund University
ISBN 978-91-7473-222-1

Printed in Sweden by Media-Tryck, Lund University
Lund 2011

Sammanfattning

Denna avhandling handlar om teoretisk partikelfysik. Partikelfysik handlar om elementarpartiklar och hur dessa växelverkar med varandra, dvs vilka krafter som verkar mellan dem. Detta är hur materien ser ut på den minsta skala vi har kunnat studera experimentellt. Den teori som beskriver de starka, svaga och elektromagnetiska krafterna och de materiepartiklar som vi känner till, kvarkar och leptoner, kallas för standardmodellen. Standardmodellen består av tre så kallade gauge symmetrier för den elektrosvaga, som är en gemensam beskrivning av den svaga och den elektromagnetiska, och den starka kraften. Den elektrosvaga symmetrin måste vara bruten via en mekanism som kallas för spontant symmetribrott för att elementarpartiklarna ska kunna få massor i överenstämmelse med vad som mäts upp experimentellt.

Standardmodellen som helhet är en stor framgång i vår förståelse av universums all minsta beståndsdelar. Icke desto mindre finns det forfarande en del oklarheter i teorin och framförallt när det gäller hur den elektorsvaga symmetrin bryts. Den del av teorin, den så kallade Higgs sektorn, som står för hur elementarpartiklar får massa är ännu inte experimentellt bekräftad. Det enklaste sättet att göra detta är med ett enda Higgsfält som har ett nollskilt värde i vakuum, dvs i universums grundtillstånd, kallad vakuumförväntansvärde. Denna avhandling bidrar på två olika sätt till att ersätta Higgs sektorn i standardmodellen.

Det första tre artiklarna handlar om så kallade QCD-lika teorier. De liknar teorin för den starka kraften (QCD) på det sättet att de fundamentala partiklarna, ofta kallad technikvarkar i detta sammanhang, inte är direkt synliga utan bara kan finnas i bundna tillstånd. I stället för att som i standardmodellen det är Higgsfältet som får ett förväntansvärde är det en kombination av technikvarkfälten som får det. Denna allmänna typ av alternativa Higgs sektorer kallas för technicolor och går under namnet dynamiskt elektrosvagt symmetribrott. Eftersom dessa teorier också har en stark kraft kan man inte direkt använda vanlig störningsräkning för att studera dem. I stället behöver man använda ickesörningsmässiga metoder. De tre första artiklarna i avhandlingen handlar om studier av QCD-lika teorier med en metod som kallas effektiv fältteori. Ett antal fysikaliska storheter har utvecklats till tredje ordningen. Dessa formler gör det möjligt att extrapolera stora numeriska simuleringar för QCD-lika teorier som man måste göra med massan för technikvarkarna till det masslösa fall man behöver för dynamiskt elektrosvagt symmetribrott.

Det sista artikeln handlar om ett av de enklaste sätten att utvidga standardmodellen. Man antar att det finns två Higgsfält i stället för ett. Teorin blir därigenom mer allmän, men man har redan nu begränsningar på denna typ av modeller från experimentella mätningar. I denna avhandling studerar vi en av dessa begränsningar. Man antar att modellen måste vara komplett

också för mycket högre energiskalor än vi har experimentell tillgång till. De begränsningar som detta antagande ger för kopplingarna av Higgsfälten till kvarkar och leptoner, så kallade Yukawa kopplingar, är mycket starka och studiet av dessa är innehållet för den sista artikeln.

To my family —

This thesis is based on the following publications:

I Johan Bijnens, Jie Lu
Technicolor and other QCD-like theories at next-to-next-to-leading order
Journal of High Energy Physics **0911** (2009) 116 [arXiv:0910.5424].

II Johan Bijnens, Jie Lu
Meson-meson Scattering in QCD-like Theories
Journal of High Energy Physics **1103** (2011) 028 [arXiv:1102.0172].

III Johan Bijnens, Jie Lu
Two-Point Functions and S-Parameter in QCD-like Theories
Submitted to *Journal of High Energy Physics* [arXiv:1111.1886].

IV Johan Bijnens, Jie Lu and Johan Rathsman
Constraining General Two Higgs Doublet Models by the Evolution of Yukawa Couplings
arXiv:1111.5760

Contents

i Introduction **1**

i.1 Introduction to the Thesis 1
i.2 From Classical to Quantum 2
i.3 Symmetry and Symmetry Breaking 5
i.3.1 Principle of Least Action and Noether's Theorem . . . 5
i.3.2 Symmetry: Global vs Local 6
i.3.3 Symmetry Breaking: Explicit vs Spontaneous 7
i.4 Standard Model of Particle Physics 12
i.4.1 Overview 12
i.4.2 Electroweak Theory 13
i.4.3 Quantum Chromodynamics 16
i.5 Chiral Perturbation Theory 18
i.5.1 Effective Field Theory 18
i.5.2 Global Chiral Symmetry 19
i.5.3 Making the Chiral Symmetry Local 22
i.5.4 Power Counting 23
i.5.5 Beyond the Leading Order 24
i.6 Physics Beyond the Standard Model 26
i.6.1 Two Higgs Doublet Model 27
i.6.2 Supersymmetry 29
i.6.3 Strong Dynamical Electroweak Symmetry Breaking . 29
i.7 Introduction to the Papers 32
i.7.1 Paper I 32
i.7.2 Paper II 32
i.7.3 Paper III 33
i.7.4 Paper IV 33
i.7.5 List of Contributions 33
Acknowledgments 35
References 36

I Technicolor and other QCD-like theories at NNLO **39**

I.1 Introduction . . . 40
I.2 Quark level . . . 41
I.2.1 QCD . . . 41
I.2.2 Adjoint . . . 42
I.2.3 $N_c = 2$ . . . 43
I.3 Effective field theory . . . 44
I.3.1 QCD . . . 44
I.3.2 Adjoint . . . 47
I.3.3 Two colours . . . 49
I.4 The divergence structure at NLO . . . 50
I.5 The calculation: mass, decay constant and condensate . . . 51
I.6 Conclusions . . . 58
References . . . 62

II Meson-meson Scattering in QCD-like Theories **65**

II.1 Introduction . . . 66
II.2 Effective Field Theory . . . 67
II.2.1 Generators . . . 67
II.2.2 Lagrangians . . . 69
II.2.3 Renormalization . . . 70
II.3 General results for the amplitudes . . . 71
II.3.1 $\pi\pi$ case . . . 71
II.3.2 General amplitude . . . 72
II.3.3 QCD case: channels and amplitudes . . . 73
II.3.4 Real case: channels and amplitudes . . . 78
II.3.5 Pseudo-real case: channels and amplitudes . . . 80
II.4 Results for the amplitude $M(s,t,u)$ . . . 82
II.4.1 Lowest order . . . 83
II.4.2 Next-to-leading order . . . 83
II.4.3 Next-to-next-to-leading order . . . 84
II.5 Scattering lengths . . . 84
II.5.1 Large n behaviour . . . 88
II.6 Conclusions . . . 91
II.A Next-to-next-to leading order result . . . 92
II.A.1 Complex or QCD . . . 92
II.A.2 Real or adjoint . . . 94
II.A.3 Pseudo-real or two-colour . . . 97
II.B Polynomial parts . . . 101
II.B.1 Complex or QCD . . . 101
II.B.2 Real or adjoint . . . 104
II.B.3 Pseudo-real or two-colour . . . 107

II.C Scattering lengths . . . 111
II.C.1 Complex or QCD case . . . 111
II.C.2 Real or adjoint case . . . 113
II.C.3 Pseudo-real or two-colour case . . . 117
II.D Loop integrals . . . 121
II.D.1 One-loop integrals . . . 121
II.D.2 Sunset integrals . . . 122
II.D.3 Vertex integrals . . . 124
References . . . 133

III Two-Point Functions and S-Parameter in QCD-like Theories 137

III.1 Introduction . . . 138
III.2 Effective Field Theory . . . 139
III.2.1 Complex representation: QCD and CHPT . . . 139
III.2.2 Real and Pseudo-Real representation . . . 140
III.2.3 High Order Lagrangians and Renormalization . . . 142
III.3 Two-Point Functions . . . 143
III.3.1 Definition . . . 143
III.3.2 The Vector Two-Point Function . . . 145
III.3.3 The Axial-Vector Two-Point Function . . . 147
III.3.4 The Scalar Two-Point Functions . . . 152
III.3.5 The Pseudo-Scalar Two-Point Functions . . . 155
III.3.6 Large n . . . 161
III.4 The Oblique Corrections and S-parameter . . . 161
III.5 Conclusion . . . 164
III.A Loop integrals . . . 165
III.A.1 One-loop integrals . . . 165
III.A.2 Sunset integrals . . . 166
References . . . 168

IV Constraining General Two Higgs Doublet Models by the Evolution of Yukawa Couplings 171

IV.1 Introduction . . . 172
IV.2 The general 2HDM . . . 173
IV.2.1 The Scalar Sector . . . 173
IV.2.2 The Yukawa Sector . . . 175
IV.2.3 RGE for Yukawa Couplings in 2HDM . . . 178
IV.3 Constraints and SM input . . . 182
IV.3.1 Low-energy constraints on λ_{ij}^F . . . 182
IV.3.2 General input . . . 184
IV.4 RGE analysis . . . 186
IV.4.1 Z_2-symmetric models . . . 186

IV.4.2 Z_2-breaking models 187
IV.5 Conclusion 196
References 200

i

Introduction

i.1 Introduction to the Thesis

This thesis can be divided into two parts: the introduction and the papers of my Ph.D. research.

In the introduction part, I will give a brief review of particle physics. Section *i*.2 contains a little bit of the history of physics and where we stand today. In section *i*.3, I focus on some basic principles of particle physics, mainly about the symmetries and related subjects. From section *i*.4, I start to introduce some topics of the Standard Model that relate to my work during PhD studies. An overview of the Standard Model is given in section *i*.4.1, and its parts, the electroweak theory in section *i*.4.2 and Quantum Chromodynamics in section *i*.4.3. Afterwards we introduce Effective Field Theory and Chiral Perturbation Theory in section *i*.5.1. This section is strongly related to the methods used in the first three papers of my research work. In section *i*.6, I explain a bit about why we need theories beyond the Standard Model. Three examples of such theories are described very shortly, they are: the general Two Higgs Doublet Model (section *i*.6.1), Supersymmetry (section *i*.6.2) and Strong Dynamical electroweak symmetry breaking (section *i*.6.3). Section *i*.6.1 contains the background of my fourth paper, and section *i*.6.3 contains the motivation for our work about QCD like theories. In the last section of the introduction, a brief summary of the four papers and my own contributions is given. In the second part, the four papers are attached with a few additional references.

i.2 From Classical to Quantum

"Nature and nature's laws lay hid in night;
God said "Let Newton be" and all was light."
– Alexandre Pope

Back to three hundred years ago, the nature of the universe was dark and mysterious for people. At that time, some people already knew that we are living on earth, but nobody knew why we can stand on this "sphere". Such a basic question was not answered until Newton discovered his laws of motion and gravity.

In the following 200 years, scientists developed and refined Newton's theory, which is now called classical mechanics. Apart from classical mechanics, the laws of electricity and magnetism have also been discovered by Maxwell and other pioneers. In the late 19th century, most physicists believed the major part of physics was done, the remainder was just a matter of calculations.

However, as we know, the famous "Two Clouds on the Horizon" [1] brought a storm of revolution, not only in physics, but also in many other science areas. In the early 20th century, the discovery of the theory of relativity and quantum mechanics took us to understand the next level of structure of nature. Furthermore, much of modern science and technology is also based on those two theories.

In the early 20th century, physicists knew we cannot apply classical mechanics to the quantum world, which was probably the first time people realized the limits of the validity of the physical law in the spatial scale.

Today, from the point view of physics, we may divide nature into different "Worlds" according to the spatial scale. There is a famous "snake" drawn by Sheldon Glashow that shows how our worlds looks like from the smallest scale to the whole universe, see fig. *i*.1.

The world we are familiar with is the "Macro World" whose sizes are from about 10^{-10}m to about $\sim 10^{18}$m. Most phenomena in this world can be described by classical mechanics and electromagnetism. In the cosmos scale which is about $10^{18}\text{m} \sim 10^{28}\text{m}$, we could call it ''Cosmos World". This world is dominated by gravity that can be explained by the theory of general relativity and cosmology.

When the scale become as small as the size of an atom which is about 10^{-10}m, quantum effects become important. In this case we reach the "Quantum World" that can be understood by quantum mechanics. Many research areas sit in this world, e.g., atomic physics, nanophysics,condensed matter physics, and chemistry.

If we want to explore the even smaller world, which we can call "Particle World", we often have to use particle colliders as the main experimental tool.

[1] The Michelson-Morley experiment and blackbody radiation.

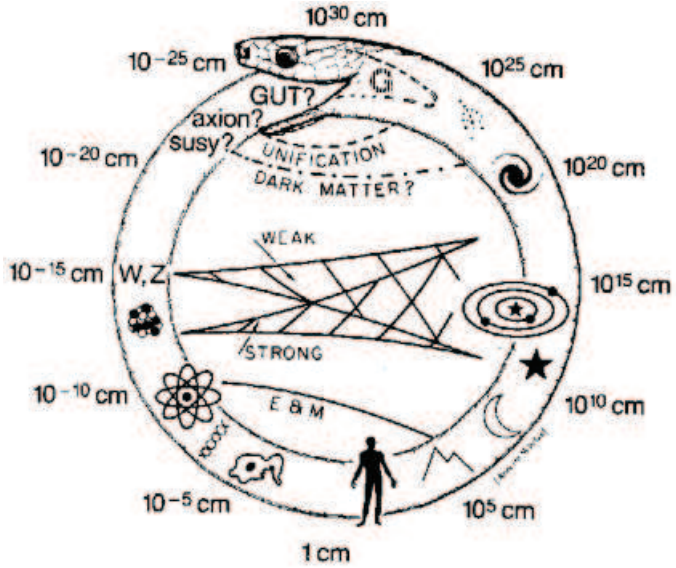

Figure *i*.1: Glashow's snake showing characteristic structure scales of nature [1].

In this world, special relativity and quantum mechanics are still the basic theory but they need to be upgraded to quantum field theory (QFT). Based on quantum field theory, the "Standard Model" of particle physics has been built to describe the small and fast moving particles during the 1960's and 1970's.

One of the key features of QFT is "renormalization", from which we learn that many fundamental parameters in the Standard Model, e.g. the coupling constants, actually change with the energy scale. That implies the Standard Model might fail at a certain high energy above the electroweak scale. But on the other side, renormalization of QFT also predicts that the strength of the interactions of the Standard Model will be comparable to each other and also to gravity at a very high energy scale, which implies that we probably can find a unified theory for gravitation, QCD and electroweak theory. This theory is called grand unification theory (GUT), where the energy scale can be as high as $10^{15} \sim 10^{16}$ GeV.

Nowadays, particle physics has strong interactions with cosmology. According to the big bang theory of cosmology, the energy scale of the early universe can be as high as the GUT scale or even higher, where all the fundamental interactions could be equally important. That's why the snake is eating its own tail in fig. *i*.1, where physics at the smallest scale meets the one at the largest scale.

The grand unification theory may be still faraway from us, but physicists

believe that physics beyond the standard model should be reachable at the Large Hadron Collider (LHC) in Geneva. We will come back to this point in section *i*.6.

In particle physics, people often choose natural units to simplify the mathematical formulas. In these units,

$$\hbar = c = 1$$

where $\hbar$ and c are Plank constant and the speed of light. In this way length and time become the inverse of mass

$$[L] = [T] = [M]^{-1}$$

In this paper, all dimensional quantities are given in units of energy.

i.3 Symmetry and Symmetry Breaking

Tao generate one.
After one come two,
after two come three,
after three come all things.
—Tao Te Ching

Over thousands of years, scientists were dreaming to find a unified theory based on which the whole complicate world can be deduced from some simple principles. Physics are thought to be the correct way to achive this goal by many people.

One of the most fundamental principles in physics is the "principle of least action" which came from classical mechanics. The Euler-Lagrange equations, which basically contain all the information of the physical system, can be derived from this principle. However this is not enough to do something practical. We need to know how the Lagrangian looks like, but there are endless possibilities of how the Lagrangian can be constructed.

Fortunately, today we have a powerful tool: symmetry. In physics, the symmetry is defined such that the system, Lagrangian, remains unchanged when performing certain transformations. With various symmetries, which could come from experimental observation or just as a hypothesis, the Lagrangian can be fixed within a few possibilities.

i.3.1 Principle of Least Action and Noether's Theorem

Suppose we want to study a system with a field $\phi(x)$. If the Lagrangian density only depends on ϕ and its derivative, then the action will be

$$S[\phi] = \int \mathcal{L}(\phi(x), \partial_\mu \phi(x))\, d^4x \tag{i.1}$$

The classical **principle of least action** tells us that the system takes the extremum of S when it evolves from t_1 to t_2, i.e.

$$\delta S = 0\,.$$

From this condition, we can derive the Euler-Lagrange equation :

$$\frac{\delta \mathcal{L}}{\delta \phi} - \partial_\mu \frac{\delta \mathcal{L}}{\delta(\partial_\mu \phi)} = 0\,. \tag{i.2}$$

At the quantum level, the way of evolving from t_1 to t_2 is not unique but there are many permitted "paths" with different amplitudes.

If we impose a symmetry on the system, which means that the action S is unchanged when there is an infinitesimal change of the $\delta\phi$.

$$S[\phi + \delta\phi] = S[\phi] \tag{i.3}$$

or equivalently

$$\mathcal{L}(\phi + \delta\phi, \partial_\mu\phi + \delta\partial_\mu\phi) = \mathcal{L}(\phi, \partial_\mu\phi) \tag{i.4}$$

There is **Noether's theorem** which states: every differentiable symmetry of the action of a physical system has a corresponding conservation law. One example is Lorentz invariance that causes energy-momentum conservation in space-time. In particle physics, in addition to space-time symmetries, there are internal symmetries such as isospin and colour symmetry to describe the particle properties.

We can easily derive the conserved current of a Lagrangian

$$J^\mu = \frac{\delta\mathcal{L}}{\delta(\partial_\mu\phi)}\delta\phi\,, \tag{i.5}$$

and the conserved quantity (charge)

$$Q \equiv \int J^0 d^3\mathbf{x}\,. \tag{i.6}$$

i.3.2 Symmetry: Global vs Local

Generally, we can classify the symmetries as global or local symmetry, the latter often called gauge symmetry. One of the simplest examples of internal symmetry in particle physics is $U(1)$ symmetry. When this symmetry acts on a fermion field, the transform can be expressed as:

$$\psi \to \psi' = e^{i\alpha}\psi\,. \tag{i.7}$$

If α is a constant in space-time, i.e., it does not depend on the space-time coordinates $x = (\mathbf{x}, t)$, then we shall call it **global symmetry**. If α depends on x: $\alpha(x)$, then it is **local symmetry** or **gauge symmetry**. According to Noether's theorem, the global symmetry implies a conservation law, but the consequence of gauge symmetry is much more nontrivial.

The Lagrangian of a Dirac fermion is

$$\mathcal{L} = \bar{\psi}(i\gamma^\mu\partial_\mu - m)\psi\,, \tag{i.8}$$

which is invariant under the global $U(1)$ transformation. If we require that the Lagrangian in eq. (i.8) is invariant under the $U(1)$ gauge transformation,

then, because of the derivative on ψ', we have to add an extra piece into the Lagrangian:

$$\mathcal{L} = \bar{\psi}(i\gamma^\mu \partial_\mu - m)\psi - e\bar{\psi}\gamma^\mu A_\mu \psi \,. \tag{i.9}$$

Here A_μ is the photon field, and e is the coupling constant. The last term in eq. (*i*.9) thus is the interaction term between the fermion and photon. Under the $U(1)$ gauge symmetry, those two fields transform as

$$\psi \rightarrow \psi' = e^{-i\alpha(x)}\psi \,, \tag{i.10}$$

$$A_\mu(x) \rightarrow A'_\mu(x) = A_\mu(x) + \frac{1}{e}\partial_\mu \alpha(x) \,, \tag{i.11}$$

so the Lagrangian (*i*.9) can be invariant. When we add the kinetic term of the photon field into (*i*.9) , we get the Lagrangian of Quantum Electrodynamics (QED)

$$\mathcal{L} = \bar{\psi}(i\gamma^\mu D_\mu - m)\psi - \frac{1}{4}F_{\mu\nu}F^{\mu\nu} \tag{i.12}$$

$$D_\mu = \partial_\mu - ieA_\mu \,, \tag{i.13}$$

where D_μ is the covariant derivative, and $F_{\mu\nu}$ is the photon field strength $F_{\mu\nu} = \partial_\mu A_\nu - \partial_\nu A_\mu$.

From this example, we can see that *the gauge symmetry is the source of interactions*. This is one of the most profound discoveries of modern physics. It is also the foundation of the Standard Model of particle physics.

i.3.3 Symmetry Breaking: Explicit vs Spontaneous

A world with full symmetries is simple, since it is easy to study using mathematical tools. However this is not the case in nature, whose symmetries often break in some way to generate the complicated and beautiful real world.

There are two ways to break the symmetry. The most obvious way is **explicit symmetry breaking**. The symbol of Taiji from ancient Chinese philosophy in fig. *i*.2, shows how the rotation and reflection symmetries of the circle have been broken by painting two parts with different colours. In particle physics, if there are terms in the Lagrangian that are not invariant under certain transformations, the symmetry is broken explicitly. The consequence of explicit symmetry breaking is clear that the corresponding quantity is not conserved any more.

Another way to break symmetry is **spontaneous symmetry breaking** (SSB), which can generate highly nontrivial physics. One example is ferromagnetism. At high temperature, the atomic magnetic moments would point anywhere so that there is rotational symmetry (spatially invariant) on a macroscopic scale, see fig. *i*.3. When the system cools down to a certain temperature,

those atomic magnetic moment all point to one direction. The rotational symmetry is broken spontaneously. Another famous example is the cooper pair in the theory of superconductivity.

In particle physics, spontaneous symmetry breaking is most simply described by a scalar field potential. Suppose the Lagrangian of a complex scalar field $\phi(x)$ is

$$\mathcal{L} = \partial_\mu \phi^* \partial^\mu \phi - V(\phi)\,, \tag{i.14}$$

$$V(\phi) = -\mu^2 \phi^* \phi + \frac{1}{2}\lambda(\phi^* \phi)^2\,. \tag{i.15}$$

Obviously this Lagrangian has $U(1)$ symmetry

$$\phi \to \phi' = e^{-i\alpha}\phi\,.$$

From fig. i.4 we can see that the shape of the Mexican hat like potential $V(\phi)$ contains two kinds of extrema:

$$\phi_0 = \begin{cases} 0 & \text{(unstable)} \\ \sqrt{\frac{\mu^2}{\lambda}}\, e^{i\theta} & \text{(stable)} \end{cases} \tag{i.16}$$

The system always automatically goes down from the unstable extremum to one of the infinite number of stable minima at $\phi_0 = \sqrt{\frac{\mu^2}{\lambda}}\, e^{i\theta}$. In this case, the original symmetry $U(1)$ is spontaneously broken. In this case the condition for SSB is $-\mu^2 < 0$ and $\lambda > 0$.

Figure i.2: The symbol of Taiji in ancient Chinese philosophy showing the subtle symmetry and symmetry breaking.

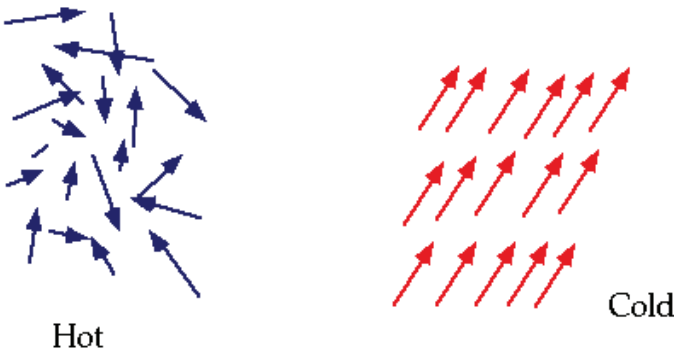

Figure *i*.3: The ferromagnetism is a perfect example of spontaneous symmetry breaking, the atomic magnetic moments automatically point to one direction when the temperature cooling down.

We also notice that moving from one place to another in the minima does not cost any energy, so that massless modes can be generated. There is a general **Nambu-Goldstone theorem** which states: if a physical system's symmetry is spontaneously broken to a lower symmetry due to the ground state (vacuum), there is one massless particle for each generator of the symmetry that is broken. These massless particles are called Nambu-Goldstone bosons (NGB). For example, when a system with $SU(N)$ symmetry, whose number of generators is N^2-1, spontaneously breaks to $SU(N-1)$ symmetry, whose number of generators is $(N-1)^2-1$, then the number of NGBs is $2N-1$.

Now let us connect spontaneous symmetry breaking to gauge symmetry. Suppose a complex scalar ϕ interacts with the photon field A_μ. The Lagrangian is

$$\begin{aligned} \mathcal{L} &= D_\mu\phi^* D^\mu\phi - \mu\phi^*\phi + \frac{1}{2}\lambda(\phi^*\phi)^2 - \frac{1}{4}F_{\mu\nu}F^{\mu\nu}\,, \\ D_\mu &= \partial_\mu - ieA_\mu\,. \end{aligned} \tag{i.17}$$

This Lagrangian is invariant under the $U(1)$ gauge transformation

$$\phi \rightarrow \phi' = e^{-i\alpha(x)}\phi\,, \tag{i.18}$$

$$A_\mu(x) \rightarrow A'_\mu(x) = A_\mu(x) + \frac{1}{e}\partial_\mu\alpha(x)\,. \tag{i.19}$$

The global $U(1)$ symmetry is still valid since it is a special case of gauge symmetry. As we have seen before, the global $U(1)$ symmetry is spontaneously broken because of the nonzero vacuum expectation value (vev) $\phi_0 = \langle 0|\phi|0\rangle$. If we write $\phi(x)$ with explicit real part and imaginary part, plus the vev

$$\phi(x) = \phi_0 + \frac{1}{\sqrt{2}}[\phi_1(x) + i\phi_2(x)]\,, \tag{i.20}$$

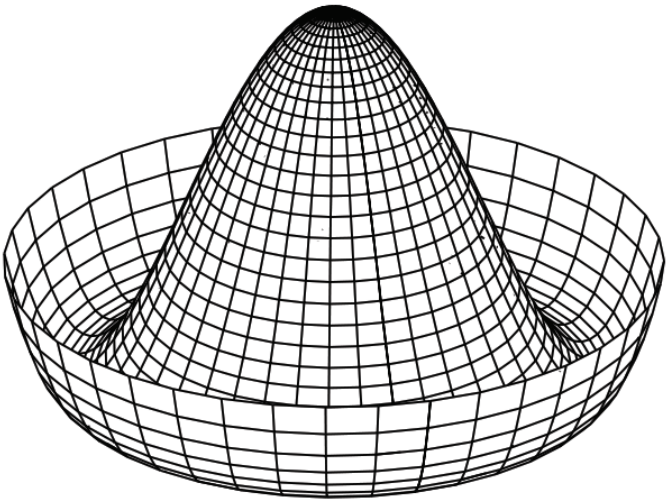

Figure *i*.4: The graph of Mexican hat like potential with unstable minimum at $\phi_0 = 0$.

the scalar potential becomes

$$V(\phi) \sim \text{constant} + \mu^2\phi_1^2 + \mathcal{O}(\phi_i^3) + \mathcal{O}(\phi_i^4)\,. \tag{i.21}$$

We can see that only the real scalar field ϕ_1 gets a mass with $m_{\phi_1} = \sqrt{2}\mu$, while ϕ_2 is massless. ϕ_2 is actually the Goldstone Boson. This is what we expected. Now let's put (*i*.20) into the covariant derivative term, it is

$$D_\mu\phi^* D^\mu\phi = \frac{1}{2}(\partial_\mu\phi_1)^2 + \frac{1}{2}(\partial_\mu\phi_2)^2 + \frac{e^2\mu^2}{\lambda}A_\mu A^\mu + \ldots\,. \tag{i.22}$$

Surprisingly, we've got an unexpected mass term for the photon

$$m_A^2 = \frac{2e^2\mu^2}{\lambda}\,, \tag{i.23}$$

which means the breakdown of the $U(1)$ gauge symmetry. It can be explained that the massless Nambu-Goldstone $\phi_2(x)$ Boson is "eaten" by the photon, or in other words, the NGB becomes the longitudinal mode of the photon to make the photon massive. If we choose the unitary gauge for $\phi(x)$, which we will explain later in section *i*.4.2, $\phi_2(x)$ disappears completely from the Lagrangian *i*.17.

Similarly, a massless fermion $\psi(x)$ also can get a mass term from the vev of

scalar field. The Yukawa coupling is

$$\begin{aligned}\mathcal{L}_{\psi\phi} &= -g\bar{\psi}\phi\psi \\ &= -g\sqrt{\frac{\mu^2}{\lambda}}\bar{\psi}\psi + ...\end{aligned}$$

The mass of fermion is $m_\psi = g\sqrt{\mu^2/\lambda}$. In this case the we don't have to put the mass of fermion as a free parameter in Lagrangian, but instead introduce the Yukawa coupling as the source of fermion mass through spontaneous symmetry breaking.

i.4 Standard Model of Particle Physics

i.4.1 Overview

The standard model of particle physics contains two parts: the electroweak theory (EW) whose gauge symmetry is $SU(2)_L \times U(1)_Y$, and Quantum Chromodynamics (QCD) whose gauge symmetry is $SU(3)_{\text{colour}}$. Fig. *i*.5 shows the

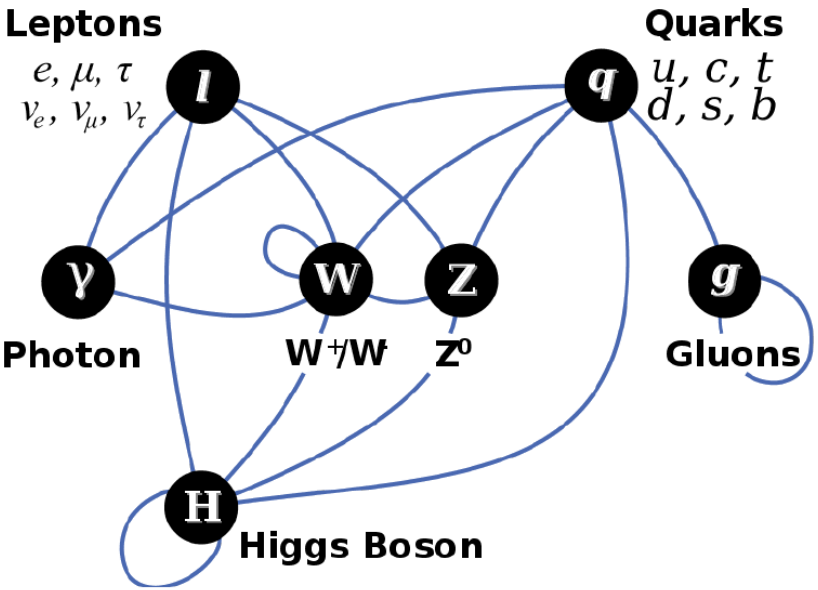

Figure *i*.5: The particles and interactions of Standard Model.

fundamental components of the Standard Model

- the fermions (spin $\frac{1}{2}$): quarks and leptons;
- the gauge bosons (spin 1): $W^{\pm}, Z^0$ (EW) and gluons g (QCD);
- the Higgs boson (spin 0);
- and their interactions.

Though we can write the symmetry of the Standard Model as $SU(3)_c \times SU(2)_L \times U(1)_Y$, the EW theory and QCD haven't been unified. All the particles in fig. *i*.5 have been found by experiments except the Higgs boson, which is one of the main reasons that people built the LHC.

i.4.2 Electroweak Theory

As we have mentioned before, gauge symmetry is the main source of interactions and is the foundation of modern particle physics. In early 1960s, Glashow proposed the $SU(2)_L \times U(1)_Y$ gauge symmetry to unify QED and the weak interaction. However gauge bosons should be massless like the photon in gauge theory, while the range of the weak interaction is very short implying that the weak gauge bosons are very massive. This problem was solved by Weinberg and Salam who incorporated the Higgs mechanism to give mass to the weak gauge bosons by spontaneous symmetry breaking.

Higgs Mechanism

The example shown in section *i*.3.3 is called Abelian gauge theory, in which the group members commute with each other. The symmetry of EW theory is $SU(2)_L \times U(1)_Y$, which is a non-Abelian gauge theory such that not all group members commute. But the idea of spontaneous symmetry breaking is the same.

We can write the scalar field, or Higgs field, as a complex doublet representation of $SU(2)_L$ with two complex components in the doublet

$$\Phi(x) = \begin{pmatrix} \phi^+(x) \\ \phi^0(x) \end{pmatrix},$$

The ϕ^+ is the charged scalar and ϕ^0 is the neutral scalar. The transformation under $SU(2)_L \times U(1)_Y$ gauge symmetry is

$$\Phi(x) \to \phi'(x) = e^{-i\tau^a \alpha(x)} e^{-\frac{i}{2}\beta(x)} \Phi(x), \qquad a = 1,2,3.$$

Here the τ^a are Pauli matrices, which are the generators of the $SU(2)$ symmetry. There are two gauge fields W^a_μ and B_μ corresponding to the $SU(2)_L$ weak isospin and $U(1)$ hypercharge gauge group respectively. The Lagrangian associated with gauge boson and Higgs doublet is

$$\begin{aligned} \mathcal{L}_{GH} &= (D_\mu \Phi)^\dagger (D^\mu \Phi) - V(\Phi), \\ V(\Phi) &= -\mu^2 \Phi^\dagger \Phi + \lambda (\Phi^\dagger \Phi)^2, \\ D_\mu &= \partial_\mu + i\frac{g_1}{2} Y_w B_\mu + i g_2 \frac{\tau^a}{2} W^a_\mu. \end{aligned} \tag{*i*.24}$$

The Higgs potential has nontrivial minima when the vacuum expect value of $\Phi(x)$ is

$$\Phi(x) = \frac{1}{\sqrt{2}} \begin{pmatrix} 0 \\ v \end{pmatrix} \quad \text{with } v = \sqrt{\frac{\mu^2}{\lambda}}.$$

Similar to eq. (*i*.20) we can rewrite the Higgs doublet as

$$\Phi(x) = \frac{1}{\sqrt{2}} \begin{pmatrix} \phi_3 + i\phi_4 \\ \phi_1 + i\phi_2 \end{pmatrix} + \frac{1}{\sqrt{2}} \begin{pmatrix} 0 \\ v \end{pmatrix}.$$

Inserting the above formula into $\mathcal{L}_{GH}$, we get the mass term for gauge bosons

$$\mathcal{L}_{Gmass} = \frac{1}{2}\frac{v^2}{4}\left\{ g_2^2\left[(W_\mu^1)^2 + (W_\mu^2)^2\right] + \left(-g_2 W_\mu^3 + g_1 B_\mu \right)^2 \right\}$$

Let us redefine the gauge boson to eliminate the mixing terms

$$W_\mu^\pm = \frac{1}{\sqrt{2}}(W_\mu^1 \mp i W_\mu^2), \tag{*i*.25}$$

$$Z_\mu^0 = \cos\theta_w W_\mu^3 - \sin\theta_w B_\mu, \tag{*i*.26}$$

$$A_\mu = \sin\theta_w W_\mu^3 + \cos\theta_w B_\mu, \tag{*i*.27}$$

where the Weinberg angle is defined as $\tan\theta_w = g_1/g_2$. Thus the masses of the gauge bosons are

$$m_W = \frac{v}{2} g_2, \quad m_Z = \frac{v}{2}\sqrt{g_1^2 + g_2^2}, \quad m_A = 0 \tag{*i*.28}$$

Now we realize that A_μ is the photon, and the original gauge symmetry $SU(2)_L \times U(1)_Y$ has been broken to $U(1)_{em}$ spontaneously.

Actually, before the symmetry breaking, we can use the global $SU(2) \times U(1)$ symmetry to rotate the $\Phi(x)$ into the ϕ_1 direction,

$$\Phi(x) = \frac{1}{\sqrt{2}} \begin{pmatrix} 0 \\ h + v \end{pmatrix}, \tag{*i*.29}$$

This is called unitary gauge. Under this gauge, ϕ_1 becomes the real physical Higgs boson h, while ϕ_2, ϕ_3 and ϕ_4 become the massless Goldstone Bosons. Those Goldstone bosons form the longitudinal modes of the W and Z bosons to make them massive.

Fermion Mass and CKM matrix

The quarks and leptons also can get mass from the Higgs field vev. We first define the left and right fermions according to their chirality

$$\psi_L = \frac{1 - \gamma_5}{2}\psi, \tag{*i*.30}$$

$$\psi_R = \frac{1 + \gamma_5}{2}\psi. \tag{*i*.31}$$

They are orthogonal to each other. The $SU(2)_L$ doublets for quarks and leptons are

$$Q'_L = \begin{pmatrix} U' \\ D' \end{pmatrix}_L \qquad U'_L = (u', c', t')_L, \quad D'_L = (d', s', b')_L \tag{i.32}$$

$$\ell'_L = \begin{pmatrix} \nu'_\ell \\ \ell' \end{pmatrix}_L \qquad (\nu'_\ell)_L = (\nu'_e, \nu'_\mu, \nu'_\tau)_L, \quad \ell'_L = (e', \mu', \tau')_L \tag{i.33}$$

and the singlets are

$$U'_R = (u', c', t')_R, \quad D'_R = (d', s', b')_R, \quad \ell'_R = (e', \mu', \tau')_R \,. \tag{i.34}$$

Though the neutrino masses have been confirmed a decade ago, their masses are very very small so that we can simply ignore the right handed neutrinos in this thesis. According to the $SU(2)_L \times U(1)_Y$ symmetry, the Yukawa coupling of the electroweak theory is

$$-\mathcal{L}_{HF} = f_u \bar{Q}'_L \tilde{\Phi} U'_R + f_d \bar{Q}'_L \Phi D'_R + f_e \bar{\ell}'_L \Phi \ell'_R + h.c., \tag{i.35}$$

where $\tilde{\Phi} = i\tau^2 \Phi^*$. That is because we need the opposite hypercharge of Φ to make the first term on the r.h.s. above invariant. Once we take the vev of the Higgs field

$$\Phi = \frac{1}{\sqrt{2}} \begin{pmatrix} 0 \\ v \end{pmatrix}. \tag{i.36}$$

The fermions get mass from the Yukawa couplings

$$M'_f = \frac{v}{\sqrt{2}} f_f \,, \tag{i.37}$$

which are general 3×3 matrices in the gauge basis of eq. (*i*.32-*i*.34). For the sake of experiment, which sees the propagating or mass eigenstates, we need to transform the Lagrangian to the mass basis.

The kinetic term of the fermion fields

$$\bar{\psi}_L i\gamma_\mu \partial^\mu \psi_L + \bar{\psi}_R i\gamma_\mu \partial^\mu \psi_R \tag{i.38}$$

has global $U(3)_L \times U(3)_R$ symmetry for up quarks and another global $U(3)_L \times U(3)_R$ symmetry for down quarks. This symmetry allows us to do unitary transformations on the fermions

$$\begin{aligned} U'_L &= V_L^U U_L \,, \quad U'_R = V_R^U U_R \,, \\ D'_L &= V_L^D D_L \,, \quad D'_R = V_R^D D_R \,, \\ \ell'_L &= V_L^\ell \ell_L \,, \quad \ell'_R = V_R^\ell \ell_R \,. \end{aligned} \tag{i.39}$$

and to diagonalize the fermion matrices

$$\begin{aligned} M^U &= V_L^{U\dagger} M'^U V_R^U \,, \\ M^D &= V_L^{D\dagger} M'^D V_R^U \,, \\ M^U &= V_L^{\ell\dagger} M'^\ell V_R^\ell \,. \end{aligned}$$

Apply this transformation to the other parts of the EW Lagrangian, we see that they have no effect on the neutral currents coupling to gauge bosons (γ, Z), because of the suppression by the GIM mechanism. But for the charged weak currents of quarks, the story is different

$$J^\mu_{\text{charge}} = 2\bar{U}'_L \gamma^\mu D'_L = 2\bar{U}_L \gamma^\mu (V_L^{U\dagger} V_L^D) D_L \,.$$

We define

$$V_{CKM} = V_L^{U\dagger} V_L^D = \begin{pmatrix} V_{ud} & V_{us} & V_{ub} \,, \\ V_{cd} & V_{cs} & V_{cb} \,, \\ V_{td} & V_{ts} & V_{tb} \,. \end{pmatrix} .$$

The 9 parameters of this general unitary matrix can be reduced to three mixing angles and one phase by redefining the quark mass eigenstates. A standard parametrization from the PDG [2] is

$$V_{CKM} = \begin{pmatrix} c_{12}c_{13} & s_{12}c_{13} & s_{12}e^{-i\delta} \\ -s_{12}c_{23} - c_{12}s_{13}e^{i\delta} & c_{12}s_{23} - s_{12}s_{23}s_{13}e^{i\delta} & s_{23}c_{13} \\ s_{12}c_{23} - c_{12}c_{23}s_{13}e^{i\delta} & -c_{12}s_{23} - s_{12}c_{23}s_{13}e^{i\delta} & c_{23}c_{13} \end{pmatrix} ,$$

where the complex phase $e^{i\delta}$ is the reason for the CP violation in the Standard Model.

i.4.3 Quantum Chromodynamics

QCD was built based on two experimental observations:

- **quark confinement**: there are no free quarks. The potential energy increases when the distance between the quarks in a hadron gets larger, so we need infinite energy to separate the quarks.
- **asymptotic freedom**: the interactions between quarks and gluons become weaker when the energy scale increases.

Confinement is dominant at low-energy scales while asymptotic freedom becomes dominant when the energy increases. The latter allows us to do perturbative calculations at high energy.

The gauge symmetry of QCD is $SU(3)_{\text{colour}}$. The quarks and antiquarks live in the fundamental representation **3** and $\mathbf{3}^*$ respectively, and the gluons live in the adjoint representation **8**. The Lagrangian of QCD is written as

$$\mathcal{L}_{QCD} = \sum_f \bar{q}_f^j \left(i\gamma_\mu D_{jk}^\mu - m_f \delta_{jk} \right) q_f^k - \frac{1}{4} G_a^{\mu\nu} G_{\mu\nu}^a$$

Where q is the quark field, $f = (u, d, s, c, b, t)$ is the flavour index, and (j, k)=(red, green, blue) are colour indices. $G_{\mu\nu}$ is the field strength of the gauge fields G_μ^a:

$$G_{\mu\nu}^a = \partial_\mu G_\nu^a - \partial_\nu G_\mu^a - g_3 f^{abc} G_\mu^b G_\nu^c \qquad a, b, c = 1, 2, ..., 8\,.$$

Here a is the index of different generators in the adjoint colour representation. The covariant derivative is

$$D_\mu = \partial_\mu + i g_3 \frac{\lambda^a}{2} G_\mu^a\,,$$

where λ^a is the 3×3 Gell-mann matrix, and g_3 is the strong coupling.

i.5 Chiral Perturbation Theory

As we mentioned before, quark confinement and asymptotic freedom somehow are like two end points of the seesaw. When the energy of a system moves down from a high scale to a low scale, QCD changes from the perturbative region to the non-perturbative region. Though there is no clear boundary between the two regions, once the energy scale is below some low value, e.g. 500 MeV, perturbative QCD completely fails. Things become difficult in this case because we are not very good at non-perturbative calculations.

The most promising non-perturbative method is lattice QCD which discretizes space-time and use Monte Carlo simulations to solve QCD numerically. This approach however is constrained by the power of computers, so the development strongly relies on computer science.

Some other approaches like the quark model use the global symmetry of QCD, and reduce the QCD colour interaction to classical or semi-classical level. The quark model was successful in explaining the hadron spectrum before QCD was established. However there are questions that remain unclear. For example, in the quark model the constituent quark mass is around 300 MeV . That cannot explain the mass of pions ($\sim$135 MeV) and kaons ($\sim$490 MeV) which are made by two quarks. The latter question was understood in the framework of **spontaneous breaking of chiral symmetry**, which is the third important feature of QCD besides confinement and asymptotic freedom. More extensive introduction to the subject of this section can be found in [3–9].

i.5.1 Effective Field Theory

In physics we do a lot of approximations as long as there are good reasons. When an intermediate state of a physical process is very heavy compared to the energy scale p, we can expand the propagator in term of p^2/M^2

$$1/(p^2 - M^2) \simeq -\frac{1}{M^2} - \frac{p^2}{M^4} + \dots . \tag{i.40}$$

In some cases, we are allowed to keep the first term only, with the condition $p^2 \ll M^2$. This approximation makes the theory much simpler to calculate, but one has to pay the price that some information is lost. However, as long as the energy of physical processes stays very small, this approximation is good enough in many cases.

One of the most well known examples is Fermi's theory for beta decay

$$\begin{aligned} n &\rightarrow p + e^- + \bar{\nu}_e \\ \mu^- &\rightarrow e^- + \bar{\nu}_e + \nu_\mu . \end{aligned} \tag{i.41}$$

Fermi's interaction is

$$\mathcal{L}_F = \frac{G_F}{\sqrt{2}} \bar{\psi}_a \gamma^\mu (1-\gamma_5) \psi_b \bar{\psi}_c \gamma_\mu (1-\gamma_5) \psi_d \,, \tag{*i*.42}$$

Where ψ is the fermion field, and a, b, c, d indicate the type of fermions in the processes (*i*.41). After the EW theory was established, people realized that Fermi's theory actually had taken the approximation

$$\frac{-g_{\mu\nu} + q_\mu q_\nu / M_W^2}{(p^2 - M_W^2)} \simeq \frac{g_{\mu\nu}}{M_W^2} \tag{*i*.43}$$

in the beta decay because $M_W^2 \gg p^2$. In this way we can also see that

$$\frac{G_F}{\sqrt{2}} = \frac{g^2}{8 M_W^2} \,. \tag{*i*.44}$$

Of course Fermi's theory didn't include the quark mixing matrix V_{CKM}, but that can be added easily. From this example we can learn the following things [3–9]:

- If the masses of degrees of freedom in the full theory are $M \gg \Lambda$ or $m \ll \Lambda$, we can integrate the heavy degree of freedom with $M \gg \Lambda$ out to simplify the theory. So the dynamics at low energy *decouples* from the dynamics at high energy.
- The *non-local* effects of heavy states are replaced by *local* (contact) non-renormalizable interactions.

Apart from the above points, there are other general properties for an EFT:

- The perturbative expansion can be described by E/Λ instead of an expansion in fundamental coupling constants. The system's energy E is associated with the momentum or derivative and its equivalent.
- In order to do have well defined high order calculations, one has to fix the power counting first which will be discussed in *i*.5.4.
- The low energy EFT should respect the original symmetries of the full theory.

i.5.2 Global Chiral Symmetry

Since the mass of light quarks are small, we could temporally ignore their mass terms and we can also neglect the effects of the heavy quarks c, b, t. Then the QCD Lagrangian is

$$\mathcal{L}^0_{QCD} = \bar{q}_L i \gamma_\mu D^\mu q_L + \bar{q}_R i \gamma_\mu D^\mu q_R - \frac{1}{4} G^{\mu\nu}_a G^a_{\mu\nu} \,. \tag{*i*.45}$$

The light quarks can be put into the column vector

$$q = \begin{pmatrix} u \\ d \\ s \end{pmatrix}, \tag{i.46}$$

The Lagrangian (*i*.45) is invariant under the chiral transformations

$$q_L \to q'_L = e^{-i\delta} e^{-i\sum_{a=1}^{8} \alpha_L^a T^a} q_L \tag{i.47}$$

$$q_R \to q'_R = e^{-i\gamma} e^{-i\sum_{a=1}^{8} \alpha_R^a T^a} q_R \tag{i.48}$$

which means it has a global $SU(3)_L \times U(1)_L \times SU(3)_R \times U(1)_R$ symmetry.

We can reorganize the $U(1)_L \times U(1)_R$ symmetry into $U(1)_V \times U(1)_A = e^{-i(\delta+\gamma)} \times e^{-i(\delta-\gamma)}$ by splitting them with different parity. The global $U(1)_V$ symmetry is connected to the conservation of baryon number. The global $U(1)_A$ symmetry is broken at the quantum level, which is called the QCD anomaly. In this thesis we will not talk about those two $U(1)$ symmetries.

Let us focus on the chiral $SU(3)_L \times SU(3)_R$ symmetry. We can rewrite the chiral transformation as

$$\begin{aligned} q_L \to q'_L &= g_L q_L \qquad g_L \in SU(3)_L\,, \\ q_R \to q'_R &= g_R q_R \qquad g_R \in SU(3)_R\,. \end{aligned} \tag{i.49}$$

According to many experimental and theoretical observations, the quark-antiquark operator has a nonzero value in the ground state or vacuum

$$\langle 0|\bar{q}q|0\rangle \neq 0$$

This non-vanishing vev forces $g_L = g_R$ in the chiral transformation in eq. (*i*.49), so that the original $SU(3)_L \times SU(3)_R$ symmetry is spontaneously broken to $SU(3)_V$. According to the Nambu-Goldstone theorem, 8 massless Goldstone bosons will be generated.

Now we add the mass term to $\mathcal{L}^0_{QCD}$

$$\mathcal{L}_{mass} = \bar{q}_L \mathcal{M} q_R + \bar{q}_R \mathcal{M} q_L \qquad \mathcal{M} = \begin{pmatrix} m_u & 0 & \\ 0 & m_d & 0 \\ 0 & 0 & m_s \end{pmatrix}.$$

We can see that the quark mass terms also break the $SU(3)_L \times SU(3)_R$ symmetry down to $SU(3)_V$ for $m_u = m_d = m_s$, but explicitly. In case of $m_u \neq m_d \neq m_s$, $SU(3)_V$ is also broken explicitly. In this way, the 8 Goldstone bosons acquire a mass from $\mathcal{M}$, so we should call them pseudo-Goldstone bosons (PGB) in-

stead. They are identified as the lowest lying (0^-) mesons in the hadron spectrum. We combine them in the matrix field

$$\phi(x) = \sum_{a=1}^{8} T^a \phi^a(x) = \begin{pmatrix} \frac{1}{\sqrt{2}}\pi^0 + \frac{1}{\sqrt{6}}\eta & \pi^+ & K^+ \\ \pi^- & -\frac{1}{\sqrt{2}}\pi^0 + \frac{1}{\sqrt{6}}\eta & K^0 \\ K^- & \overline{K^0} & -\frac{2}{\sqrt{6}}\eta \end{pmatrix}.$$

Throughout this paper we always use the convention

$$\begin{aligned} [T^a, T^b] &= i f^{abc} T^c, \\ \mathrm{Tr}(T^a T^b) &= \delta^{ab}. \end{aligned}$$

Now we want to find an effective theory to describe the pseudo-Goldstone bosons. The matrix

$$U = \exp\left(i\frac{\sqrt{2}}{F_0}\phi(x)\right)$$

parameterizes the PGB manifold $G/H{=}SU(3)_L \times SU(3)_R/SU(3)_V$ and transforms as $U \to g_R U g_L^\dagger$. Another building block is the quark matrix $\mathcal{M}$, which also transforms as $\mathcal{M} \to g_R \mathcal{M} g_L^\dagger$ under the $SU(3)_L \times SU(3)_R$ symmetry. So we can write down the Lagrangian which is invariant under the chiral symmetry

$$\begin{aligned} \mathcal{L}_2 &= \frac{F_0^2}{4}\mathrm{Tr}\left(\partial_\mu U \partial^\mu U^\dagger + \chi U^\dagger + \chi^\dagger U\right), \\ \chi &= 2B_0\mathcal{M} \end{aligned} \tag{*i*.50}$$

As we mentioned in section *i*.5.1, chiral perturbation theory (CHPT), as one of typical EFT, is expanded in term of $E/\Lambda_{\mathrm{CHPT}}$. We can easily see that the Lagrangian (*i*.50) is the lowest order in the expansion of energy, or momentum p^2. Here the low energy constant F_0 is the decay constant of PGB, and B_0 is related to the quark condensate. In principle they can be calculated from the QCD Lagrangian, but currently it's only possible to do this using the method of lattice QCD due to the complicated nonperturbative effects.

Using the Lagrangian (*i*.50), we can derive the mass of mesons in terms of quark masses, e.g.,

$$m_\pi^2 = (m_u + m_d)B_0. \tag{*i*.51}$$

The Lagrangian (*i*.50) can be used to study many processes involve PGBs only, e.g., pion-pion scattering.

i.5.3 Making the Chiral Symmetry Local

As we have seen the CHPT Lagrangian describes the interactions between the PGBs. Though the mesons are colourless, their interactions originate from the colour interaction of quarks and gluons. Because quarks are confined inside the meson, the residual colour interactions are very small. So we are able to describe the meson interaction perturbatively under the frame work of chiral symmetry breaking.

The quarks can also participate in the weak interactions, thus so do the mesons. In order to write down their interaction with gauge bosons, we shall make the global chiral symmetry local and introduce external sources. Let us start from the QCD Lagrangian with general external fields [10, 11]

$$\mathcal{L} = \mathcal{L}^0_{QCD} + \bar{q}_L \gamma^\mu l_\mu q_L + \bar{q}_R \gamma^\mu r_\mu q_R - \bar{q}_R (s + ip) q_L - \bar{q}_L (s - ip) q_R \,. \tag{i.52}$$

The l_μ, r_μ, s, p refer to left, right, scalar and pseudo-scalar external sources respectively. The above Lagrangian is invariant under $SU(3)_L \times SU(3)_R$ local symmetry if the quarks and source fields transform as

$$\begin{aligned}
q_L &\to q'_L = g_L q_L \\
q_R &\to q'_R = g_R q_R \\
r_\mu &\to r'_\mu = g_R r_\mu g_R^\dagger + i g_R \partial_\mu g_R^\dagger \\
l_\mu &\to l'_\mu = g_L l_\mu g_L^\dagger + i g_L \partial_\mu g_L^\dagger \\
s + ip &\to (s' + ip') = g_R (s + ip) g_L^\dagger
\end{aligned} \tag{i.53}$$

With respect to this symmetry, low energy CHPT can be written in terms of Goldstone matrix U and source fields

$$\begin{aligned}
\mathcal{L}_2(U, l_\mu, r_\mu, s, p) &= \frac{F_0^2}{4} \mathrm{Tr}\left(D_\mu U D^\mu U^\dagger + \chi U^\dagger + \chi^\dagger U \right), \\
\chi &= 2B_0 (s + ip) \\
D_\mu &= \partial_\mu U - i r_\mu U + i U l_\mu
\end{aligned} \tag{i.54}$$

Once we take $l_\mu = r_\mu = 0$ and $s + ip = \mathcal{M}$, we get CHPT for purely mesonic processes.

One of the typical applications is the weak decay of PGB. The PGB decay to leptons through $W^\pm$ boson exchange, e.g., $\pi^+ \to \mu^+ \nu_\mu$. The QCD part of its matrix element at the quark level is defined as

$$\begin{aligned}
\langle 0 | A^a_\mu | \phi^b \rangle &= \frac{i}{\sqrt{2}} \delta^{ab} F_\pi p_\mu \,, \\
A^a_\mu &= \bar{q} T^a \gamma_\mu \gamma_5 q \,.
\end{aligned} \tag{i.55}$$

The $\langle 0|$ on the left side means the QCD vacuum. This is a non-perturbative process. It's very hard to calculate the value of the pion decay constant F_π from

the QCD Lagrangian (also called a first principle QCD calculation), unless we go for lattice QCD. However, in the case of effective field theory, we put the source field $l_\mu^a = W_\mu^a$, and let it interact with the PGBs in $\mathcal{L}^{(2)}_{\rm CHPT}$. So the matrix element at meson level is

$$\langle 0|J_L^{\mu,a}|\phi^b\rangle = \frac{i}{\sqrt{2}}\delta^{ab}F_\pi p^\mu\,, \tag{i.56}$$

$$J_L^{\mu,a} = \frac{F_0}{2}\partial^\mu\phi^a + \mathcal{O}((\phi^a)^3)\,. \tag{i.57}$$

i.5.4 Power Counting

In the EW theory and QCD, the perturbative expansion is very clear, it is in powers of the coupling constants g_i. However in EFT, things are not that simple when loops are involved. We explain here the standard power-counting of EFT.

The general structure of energy(mass) dimension of the Lorenz-invariant matrix elements $\mathcal{M}$ can be written as

$$\mathcal{M} \sim M^{D_m}E^{D_E}H\left(\ln\frac{E}{m}\right)\,, \tag{i.58}$$

where D_m is the overall energy dimension of the coupling constants, D_E is the dimension coming from derivatives, and $H\left(\ln\frac{E}{m}\right)$ is the function of dimensionless quantities. Thus we have

$$D_{\mathcal{M}} = D_m + D_E = 4 - N_E\,, \tag{i.59}$$

where N_E is the number of external scalar fields. A general field theory analysis gives the relation between the momentum expansion and the loop expan-

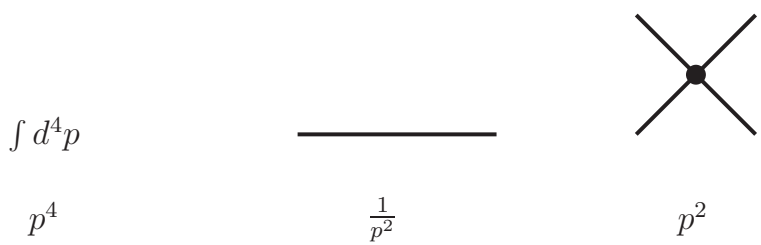

Figure *i*.6: The power counting in CHPT. The four momentum integral counts as p^4, the propagator counts as $1/p^2$ and the vertex counts could as p^2 at LO, p^4 at NLO, and p^6 at NNLO.

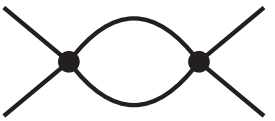

$$(p^2)^2 \times \left(\frac{1}{p^2}\right)^2 \times p^4 \;=\; p^2$$

Figure *i*.7: An example of power counting in CHPT. The contribution of momentum powers comes from two vertices, two pion propagators and a four momentum integal.

sion [12]

$$\begin{aligned} D_E &= 4 - N_E - D_m \\ &= \sum_n (d_n - 2) V_n + 2N_L + 2\,, \end{aligned} \tag{*i*.60}$$

where d_n is the dimension coming from derivatives, V_n is the number of vertices arising from the subset of the total lagrangian which contain d_n derivatives, and N_L is the number of loops.

This is Weinberg power counting which can give a systematic perturbative expansion for an EFT. We illustrate the power counting for CHPT (*i*.50) in fig. *i*.6. Fig. *i*.7 shows how to count the power of the expansion in momentum for a typical loop diagram of meson-meson scattering.

i.5.5 Beyond the Leading Order

The development of high precision measurements in experiment requires higher order theoretical calculations. On the another hand, the amplitudes at leading order are real, and some physical processes such as $\pi\pi$ scattering have nonzero imaginary parts because of unitarity. Therefore we need the results from higher orders.

The Effective Field Theory is not renormalizable, which means we have to introduce an infinite number of coupling constants to cancel the divergences in loops. Fortunately, according to the power counting rule, the divergences generated at one loop from the leading order CHPT Lagrangian can be absorbed by the coupling constants in the next-to leading order Lagrangian, and this generalizes to higher order of loops. So we are allowed to calculate any physical quantity order by order.

From (*i*.51) we can conclude

$$p^2 \sim m_\pi^2 \sim \mathcal{M}\,, \tag{*i*.61}$$

so the quark mass matrices are equivalent to a momentum squared in the momentum expansion.

Weinberg, Gasser and Leutwyler systematically developed CHPT beyond the leading order [10–12]. The Lagrangian for $SU(n_f)$ flavour symmetry at

next-to-leading order (or p^4) is written as

$$\begin{aligned}
\mathcal{L}_4 &= L_0 \mathrm{Tr}\left[D_\mu U (D_\nu U)^\dagger D^\mu U (D^\nu U)^\dagger\right] \\
&+ L_1 \left\{\mathrm{Tr}[D_\mu U (D^\mu U)^\dagger]\right\}^2 + L_2 \mathrm{Tr}\left[D_\mu U (D_\nu U)^\dagger\right] \mathrm{Tr}\left[D^\mu U (D^\nu U)^\dagger\right] \\
&+ L_3 \mathrm{Tr}\left[D_\mu U (D^\mu U)^\dagger D_\nu U (D^\nu U)^\dagger\right] + L_4 \mathrm{Tr}\left[D_\mu U (D^\mu U)^\dagger\right] \mathrm{Tr}\left(\chi U^\dagger + U \chi^\dagger\right) \\
&+ L_5 \mathrm{Tr}\left[D_\mu U (D^\mu U)^\dagger (\chi U^\dagger + U \chi^\dagger)\right] + L_6 \left[\mathrm{Tr}\left(\chi U^\dagger + U \chi^\dagger\right)\right]^2 \\
&+ L_7 \left[\mathrm{Tr}\left(\chi U^\dagger - U \chi^\dagger\right)\right]^2 + L_8 \mathrm{Tr}\left(U \chi^\dagger U \chi^\dagger + \chi U^\dagger \chi U^\dagger\right) \\
&- i L_9 \mathrm{Tr}\left[f_{\mu\nu}^R D^\mu U (D^\nu U)^\dagger + f_{\mu\nu}^L (D^\mu U)^\dagger D^\nu U\right] + L_{10} \mathrm{Tr}\left(U f_{\mu\nu}^L U^\dagger f_R^{\mu\nu}\right) \\
&+ H_1 \mathrm{Tr}\left(f_{\mu\nu}^R f_R^{\mu\nu} + f_{\mu\nu}^L f_L^{\mu\nu}\right) + H_2 \mathrm{Tr}\left(\chi \chi^\dagger\right) , \qquad (i.62)
\end{aligned}$$

where $L_1, \ldots, L_{10}$ and H_1, H_2 are coupling constants. The terms with H_1 and H_2 contain only external fields so they do not relate to physical processes including PGBs. Those coupling constants are designed to absorb the divergences from the loops of $\mathcal{L}_2$

$$\begin{aligned}
L_i &= (c\mu)^{d-4} \left[\frac{\Gamma_i}{16\pi^2 (d-4)} + L_i^r(\mu)\right] , \\
H_i &= (c\mu)^{d-4} \left[\frac{\Gamma_i}{16\pi^2 (d-4)} + H_i^r(\mu)\right] , \qquad (i.63)
\end{aligned}$$

where the space-time dimension is $d = 4 - 2\epsilon$, and

$$\ln c = -\frac{1}{2}[\ln 4\pi + \Gamma'(1) + 1] . \qquad (i.64)$$

According to the momentum expansion, those couplings constants should be order of $\mathcal{O}(10^{-2})$.

The next-to-next-to leading order (NNLO) (p^6) lagrangian for n_f flavours of quarks contains 112+3 terms [13,14]. The coupling constants at NNLO should be order of $\mathcal{O}(10^{-3})$.

i.6 Physics Beyond the Standard Model

And AC said: "LET THERE BE LIGHT!"
And there was light.
— Asimov 'The Last Question'

The Standard Model is very successful in particle physics. But besides the fact that the SM Higgs boson hasn't been observed, there are some problems from the theory itself as well:

- Triviality problem

  We have seen that the condition for SSB is $(-\mu^2 < 0, \lambda > 0)$ in (*i*.25). However the analysis of the running coupling constant λ shows

  $$\lambda(q^2, \Lambda) \xrightarrow{\Lambda \to \infty} 0$$

  which is not only in contradiction with the original requirement of $\lambda > 0 (\lambda \neq 0)$, but also make the Higgs theory trivial(no self interaction). That tells us the Standard Model will be valid up to a certain scale Λ_{SM} only.

- Unnaturalness/Hierarchy/Fine Tuning problem.

  The one-loop correction to the Higgs mass comes from three main intermediate states: top quark, EW gauge bosons and Higgs boson itself, see

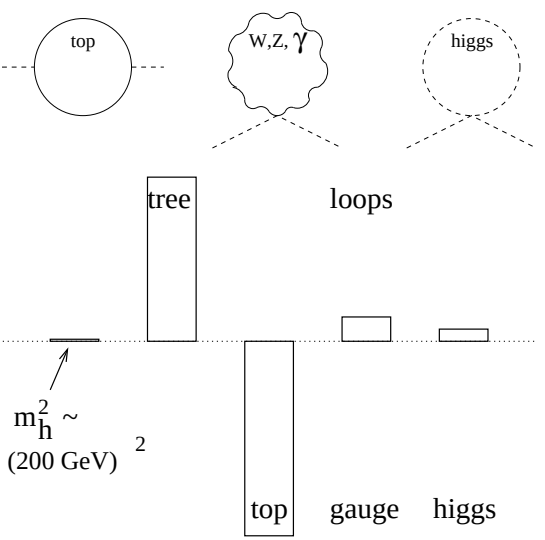

Figure *i*.8: The one loop corrections to Higgs mass.

fig. *i*.8. If we take the cut off scale at $\Lambda = 10$ TeV, their contribution to Higgs mass is, see e.g. [15],

$$\begin{aligned} \text{top loop} \quad & -\tfrac{3}{8\pi^2}\lambda_t^2\Lambda^2 \sim -(2\text{ TeV})^2, \\ SU(2)\text{ gauge boson loops} \quad & \tfrac{9}{64\pi^2}g^2\Lambda^2 \sim (700\text{ GeV})^2, \\ \text{Higgs loop} \quad & \tfrac{1}{16\pi^2}\lambda^2\Lambda^2 \sim (500\text{ GeV})^2. \end{aligned} \tag{*i*.65}$$

The SM Higgs mass is constrained to be a few hundred GeV, which means the tree and one loop contributions have to be fine tuned to obtain the physical Higgs mass. The problem gets much more acute when Λ is raised to the GUT or Plank scale, i.e., $10^{16} \sim 10^{19}$ GeV. The underlying reason is the quadratic divergence of the Higgs mass in (*i*.65).

- Too many parameters.

  The Standard Model contains 22 free parameters even without including the neutrino sector [2]. With so many free parameters, the Standard Model looks like an Effective Field Theory rather than a fundamental theory.

Apart from those problems, the EW theory and QCD is not a unified theory even though we write the symmetry of the SM as $SU(3)_c \times SU(2)_L \times U(1)_Y$.

There are many theories and models to explore the energy region at the TeV scale, like two Higgs doublet model, supersymmetry, technicolour, little Higgs, extra dimensions, etc.. In this chapter we will only give a very short introduction to the Two Higgs Doublet Model, Supersymmetry and Strong Dynamical electroweak symmetry breaking.

i.6.1 Two Higgs Doublet Model

In the Standard Model, there is only one Higgs doublet, that is why it is sometimes called the minimal Standard Model. Naturally, the minimal extension of SM is to add one more Higgs doublet. In general, this Two Higgs Doublet Model (2HDM) cannot solve the problems mentioned above, however many beyond the SM theories contain two or more Higgs doublets, such as Supersymmetry and Little Higgs Models. The problems of SM can be solved by special symmetries or other mechanisms in those more fundamental theories. The study of the general 2HDM can give some hints or constraints on beyond the SM theories, see the most recent review [16].

One standard convention to write the two Higgs doublets with the Gold-

[2] They are 3 gauge couplings (g_1, g_2, g_3), 12 fermion masses, 3 angle and one phase of the CKM matrix, 2 couplings (μ, λ) of the Higgs sector, and one angle θ_{QCD} from the QCD vacuum.

stone bosons is

$$\Phi_1 = \frac{1}{\sqrt{2}} \begin{pmatrix} \sqrt{2}\left(G^+ \cos\beta - H^+ \sin\beta\right) \\ v\cos\beta - h\sin\alpha + H\cos\alpha + \mathrm{i}\left(G^0\cos\beta - A\sin\beta\right) \end{pmatrix}, \quad (i.66)$$

$$\Phi_2 = \frac{1}{\sqrt{2}} \begin{pmatrix} \sqrt{2}\left(G^+ \sin\beta + H^+ \cos\beta\right) \\ v\sin\beta + h\cos\alpha + H\sin\alpha + \mathrm{i}\left(G^0\sin\beta + A\cos\beta\right) \end{pmatrix}. \quad (i.67)$$

Here $G^\pm$ and G^0 are the Goldstone bosons to be eaten by the EW gauge bosons during EW symmetry breaking. $H^\pm$ is the charged Higgs boson. The neutral Higgs scalar can be divided into CP even scalars (h, H) and CP odd pseudoscalar A. α is the mixing angle between h and H. Both doublets can have nonzero vevs

$$\langle\Phi_1\rangle_0 = \frac{1}{\sqrt{2}} \begin{pmatrix} 0 \\ v_1 \end{pmatrix} \qquad v_1 = v\cos\beta\,, \quad (i.68)$$

$$\langle\Phi_2\rangle_0 = \frac{1}{\sqrt{2}} e^{i\theta} \begin{pmatrix} 0 \\ v_2 \end{pmatrix} \qquad v_2 = v\sin\beta\,. \quad (i.69)$$

θ is the relative phase of $\langle\Phi_1\rangle_0$ and $\langle\Phi_2\rangle_0$, which can be a new source of CP violation if there are no any further constraints. Another choices is that only one doublet has a nonzero vev, this is called the Higgs basis. In this basis Φ_1 plays the role of the SM Higgs doublet in EW symmetry breaking and Φ_2 contains the charged Higgs $H^\pm$.

In the Yukawa sector, the two Higgs doublets introduce tree level flavour-changing-neutral-current (FCNC) couplings between quarks, which are absent in the SM. One of the possible solutions is to impose a Z_2 symmetry on the Lagrangian, and set one of the Φ_i and some of the right hand fermions to be Z_2 odd while the rest are Z_2 even. In this way, the up or down type of quarks only couple to one of the Φ_i, see the table IV.1 in paper IV. The four different ways to set the right hand fermions are called Type I, II, III(X) and IV(Y). A more general possibility is Yukawa alignment [17], which assumes that the Yukawa couplings with the two Φ_i are proportional to each other, so we can diagonalize them simultaneously. Thus all the 2HDM Z_2 types are just special cases of Yukawa alignment. Furthermore, there is the Cheng-Sher ansatz that allows tree level FCNC couplings but they are sufficiently small to avoid the current experimental bounds [18]. The hierarchy of their couplings are taken into account by the masses of the SM fermions. This is the most general option so far in that both the 2HDM Z_2 types and Yukawa alignment are special cases of the Cheng-Sher ansatz.

Depending on the parameters in the theory, the mass of the 5 Higgs scalar can vary from 100 GeV to several hundred GeV. The discovery of a charged Higgs in experiment could be the sign of two or more Higgs doublets.

i.6.2 Supersymmetry

Supersymmetry (SUSY) is one of the "mainstream" beyond the SM theories, an introduction is [19]. It assumes that every "fundamental" particle has their SUSY partner with different spin, i.e., the fermions have a spin zero SUSY partner, the bosons have their spin one half SUSY partner, and all the other particle properties should be the same. Those SUSY particles have not been observed, which means that they are heavier than the EW scale, so the SUSY must be broken in someway.

In order to cancel the anomaly and generate the mass of different fermions, all the SUSY models have to have even number of Higgs doublets. The minimal supersymmetric model (MSSM) contains two Higgs doublets, which happen to be the type II model of the general 2HDM. Thus SUSY is a major reason to study 2HDM.

One of the great features of SUSY is the cancelation of loop divergences: the contribution of SM particles in loop diagrams are canceled by its SUSY partner, see fig. *i*.9. In this way the fine tuning problem of the SM can be solved even if SUSY is broken softly. However SUSY introduces more free parameters than SM, which is not very satisfying from a theoretical point of view.

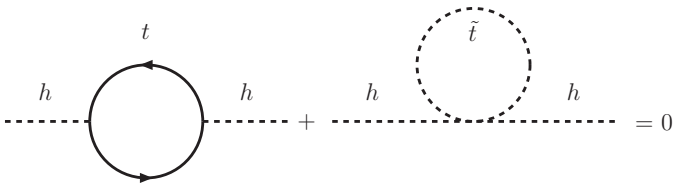

Figure *i*.9: The top-quark-mediated one loop divergence is canceled completely by its SUSY partner "stop" mediated loop, in the case when SUSY is not broken. In the case of softly broken SUSY, the quadratic divergences can still be canceled.

Another interesting aspect is that SUSY can give much more hope for grand unification theory which unifies the EW theory and QCD. In the Standard Model, the three running gauge coupling constants do not meet together anywhere, but in the MSSM they have all about the same value at an energy of 10^{16} GeV, i.e., the GUT scale.

i.6.3 Strong Dynamical Electroweak Symmetry Breaking

In chapter 3 we have shown that the EW $SU(2)_L \times U(1)_Y$ symmetry is broken by the nonzero Higgs vev. Actually this is not the whole truth. The quark-antiquark condensates also break the EW symmetry and offer a contribution to the mass of the EW gauge bosons. We know that QCD has the $SU(2)_L \times$

$SU(2)_R$ chiral symmetry for vanishing light quark masses m_u and m_d. When the energy scale is close to Λ_{QCD}, the quark condensates appear to break this symmetry spontaneously to the isospin symmetry

$$SU(2)_L \times SU(2)_R \to SU(2)_V \,.$$

Thus three Goldstone bosons associated with axial currents will be generated. When we include the EW theory without SSB, the gauge boson W^a_μ and B_μ couple to axial currents and get mass, as illustrated in fig. *i*.10. After diago-

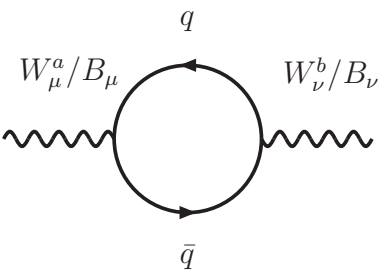

Figure *i*.10: EW symmetry broken dynamically by the $\bar{q}q$ condensates.

nalizing the gauge boson mass matrix, we get

$$m_W^2 = \frac{1}{2} g^2 F_\pi^2 \,, \tag{*i*.70}$$

$$m_Z^2 = \frac{1}{2}(g^2 + g'^2) F_\pi^2 \,, \tag{*i*.71}$$

$$m_A = 0 \,. \tag{*i*.72}$$

Where $F_\pi = 93$ MeV [3] is the decay constant of the pion, so the gauge boson mass is just $m_W \sim 30$ MeV, which is far smaller than the experimental result $m_W = 80$ GeV. So the quark condensates can break the $SU(2)_L \times U(1)_Y$ gauge symmetry, but not enough.

This idea initiated the Technicolour Theories (TC), which assume there is a new strong interaction other than QCD at the TeV scale, some reviews are [20, 21]. The condensates of techni-quarks $\bar{Q}Q$ spontaneously break the EW gauge symmetry, so there is no fundamental Higgs boson in the theory. In this way, the fine tuning problem automatically disappears.

However the simplest Technicolour model, which is just the scaling up of QCD, has been ruled out by the precision measurements from LEP using the analysis of oblique parameters. There are many variation of the simplest TC model, such as walking Technicolour.

[3] Some references, e.g. PDG [2], use another definition $f_\pi = \sqrt{2} F_\pi$.

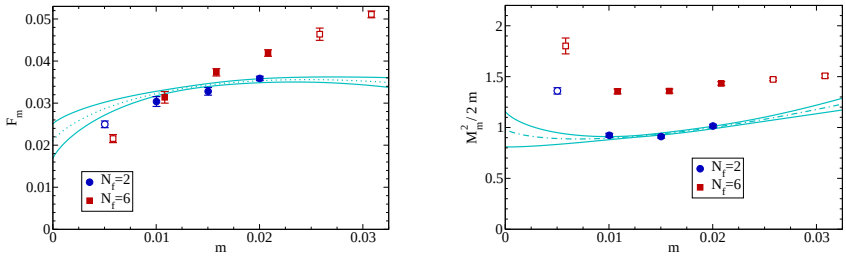

Figure *i*.11: The decay constant F_m and the slope of mass squared $M_m^2/2m$ of NGB, as a function of Techni-quark mass m. The dots come from the lattice simulation, the curves come from NLO CHPT. Plots from [22].

One of the practical problems of TC theories is the same as for low energy QCD: the interaction is very strong such that perturbative theory fails. Therefore effective field theory and lattice gauge theory become the main tools to make predictions.

We show the plots from one of the recent lattice gauge theory simulations of TC theories [22] in fig. *i*.11. The red and blue dots come from the lattice simulation from first principle of TC theory. However once the techni-quark mass gets close to the chiral limit $m = 0$, the need for computing power increases greatly. Therefore in lattice simulation people use result from Chiral Perturbation Theory to extrapolate the lattice data to the chiral limit. The main goal of paper I-III is to provide extrapolation formulas for the general TC theories.

There are other types of beyond SM theory based on strong dynamics, like Little Higgs Model, Twin Higgs Model, etc.. We do not discuss these theories here.

i.7 Introduction to the Papers

i.7.1 Paper I

In paper I we investigated three QCD-like theories and their effective field theories at low energy. For strong dynamics with a vector-like gauge group, they can be classified as three different cases: the quarks live in complex, real or pseudo-real representation of the gauge group. In the case of n_f degenerate flavours, those cases correspond to symmetry breaking patterns of $SU(n_f)_L \times SU(n_f)_R \to SU(n_f)_V$, $SU(2n_f) \to SO(2n_f)$ or $SU(2n_f) \to Sp(2n_f)$ respectively.

The complex case is very much like QCD, whose low energy EFT for pseudo-Goldstone bosons is Chiral Perturbation Theory for n_f flavours. We managed to write the EFT of the real and pseudo-real case very similar to CHPT, so one can use the techniques from CHPT to calculate many physical processes. We also obtained the coefficients of the NLO divergence structure and found a mathematical formula to perform traces of matrices for the real and pseudo-real case.

Based on the above work, we calculated the vacuum-expectation-value $\langle \bar{q}q \rangle$, the mass and decay constant of meson up to next-to-next-to-leading-order, i.e. two loop level in the effective field theory. These results can be used for chiral extrapolation in lattice calculation in the study of Technicolour Theory. This work might be also useful for research on finite baryon density.

i.7.2 Paper II

In paper II we studied the general meson-meson scattering in the EFT of QCD-like theories. Based on group theory, we analyzed the general structure of the scattering amplitude and possible intermediate channels for the three different QCD-like theories as the generalization of $\pi\pi$ scattering. Furthermore, we have derived the amplitude of various channels using the invariant functions: $B(s,t,u)$ and $C(s,t,u)$.

The function $B(s,t,u)$ and $C(s,t,u)$ have been calculated up to NNLO using the method of CHPT, and they are written in term of the physical meson mass M_{phys} and decay constant F_{phys}. Using the expressions of $B(s,t,u)$ and $C(s,t,u)$, we got the analytical results for the scattering lengths of the lowest partial wave for each channel. We presented some numerical results with chosen n_f for the purpose of illustration. We also discussed some relations between the different theories in the limit of large n_f.

We calculated analytic expressions for a number two loop vertex integrals with equal masses and tabulated them.

i.7.3 Paper III

In paper III we continued our work on QCD-like theories. We calculated the vector, axial-vector, scalar and pseudo-scalar two-point functions up to NNLO in the low-energy EFT of three different QCD-like theories. In addition, the pseudo-scalar decay constant G_M for all cases, which is similar the decay constant F_M, has also been calculated up to NNLO. We have written our analytic results of two point functions in term of physical meson mass M_M, decay constants F_M and G_M to reduce the lengthy expressions. Those expressions can be used to study the processes of pseudo-Goldstone bosons interacting with external sources, e.g., the gauge bosons.

Using the expression of the vector and axial-vector two point functions, we obtained analytic results for the S parameter of oblique corrections for the three different types of QCD-like theories. Their numerical estimates at the TeV scale were presented with the different flavour numbers n_f based on scaled up QCD.

i.7.4 Paper IV

In paper IV we study evolution of Yukawa couplings in the general Two Higgs Doublet Model. The general 2HDM can contain dangerous tree level flavour-changing-neutral-currents if there are no further constraints in the theory. The existing solutions for this problem can be classified as models with Z_2 symmetry, the Yukawa alignment model and the Cheng-Sher ansatz.

We wrote a computer program for the Renormalization-Group-Equation of Yukawa couplings to check what happens at high energy for those different schemes. With the most recent data, we investigated the place of Landau pole for models with Z_2 symmetry and Yukawa alignment. We also investigated the energy scale at which the nondiagonal FCNC Yukawa couplings get too large in these models. The constraints on the parameters λ^F in Cheng-Sher ansatz have also been updated with the most recent experimental and the theoretical input.

i.7.5 List of Contributions

The ideas of the first three papers were given by my supervisor, and the idea of the paper IV was given by Johan Rathsman.

- **paper I:** I did all the calculations separately. However, my calculations were heavily based on my supervisor's previous work, especially his old FORM programs.
- **paper II:** I did all the calculations independently, including the analytic derivations and the numerical estimates. I also wrote a small part of

the paper. Most of the analytic results were transformed from FORM expressions and organized by me.

- **paper III:** I did all the analytic and numerical calculations independently. I also wrote the first draft of the paper, which was modified and enriched by my supervisor. I drew all the Feynman diagrams in the paper.
- **paper IV:** I derived the mathematical formula and they were double checked by my supervisor later. I wrote the computer program independently. Almost all the results were triple checked by the three authors. The first draft was written by me, and it was changed and enriched by Johan Rathsman and my supervisor. I also made some plots in the paper.

Acknowledgments

First and foremost, I want to thank my supervisor Hans Bijnens for his patience and open mind to help me on the research. I have really learned a lot from you, not only the knowledge on physics but also the attitude to research.

I've got much help from the other faculty members at the high energy division of THEP: Gösta Gustafson who picked us from the station of Lund at the first day we arrived, Leif Lönnblad who helped us to borrow and move the furniture with his big green car, Torbjörn Sjöstrand who often invited us to his lovely summer house, Johan Rathsman who offered me the idea of the last project of my PhD study, and Bengt E Y Svensson who help me with the study plan every semester. I also want to thank all the administration staffs from THEP, HEP and Astronomy.

I have been very lucky to have many fellow PhD students starting together with me, also many others joined later. During the past five years, we had so much fun with each other on hiking, skiing, chatting and the party nights, etc.. I've learned a lot from many of you. Forgive me not to name you here simply because the list is too long. In the end, we have to find our own places somewhere in the world. But I will cherish our friendship no matter where we are.

At the last, I want to thank my wife who spent ten years of beautiful life with me and wish your good luck on fighting your own PhD. Many thanks to our daughter, Luffy, for bringing me numerous happy moments in the past two and a half years. Thanks to my parents for your support and love, especially for supporting me to do whatever I like, even if that means your only child will be ten thousands miles away from you.

i References

[1] http://ircamera.as.arizona.edu/NatSci102/NatSci102/images/extcosmo.htm. pages

[2] K. Nakamura *et al.* [Particle Data Group Collaboration], "Review of particle physics," *J. Phys. G* **37** (2010) 075021. pages

[3] A. Pich, "Effective field theory: Course," arXiv:hep-ph/9806303. Lectures at Les Houches Summer School in Theoretical Physics, Session 68: Probing the Standard Model of Particle Interactions, Les Houches, France, 28 Jul - 5 Sep 1997. pages

[4] S. Scherer, "Introduction to chiral perturbation theory," *Adv. Nucl. Phys.* **27** (2003) 277, arXiv:hep-ph/0210398. pages

[5] S. Scherer, "A Chiral perturbation theory primer," arXiv:hep-ph/0505265. pages

[6] G. Ecker, "Strong interactions of light flavors," arXiv:hep-ph/0011026. Lectures given at Advanced School on Quantum Chromodynamics (QCD 2000), Benasque, Huesca, Spain, 3-6 Jul 2000. pages

[7] J. Gasser, "Light-quark dynamics," in *Lect. Notes Phys.*, vol. 629, pp. 1–35. 2004. arXiv:hep-ph/0312367. Lectures given at 41st Internationale Universitaetswochen fuer Theoretische Physik (International University School of Theoretical Physics): Flavor Physics (IUTP 41), Schladming, Styria, Austria, 22-28 Feb 2003. pages

[8] H. Leutwyler, "Chiral dynamics," in *At the frontier of particle physics: Contribution to the Festschrift in honor of B.L. Ioffe*, M. Shifman, ed., vol. 1, pp. 271–316. 2000. arXiv:hep-ph/0008124. pages

[9] H. Leutwyler, "Principles of chiral perturbation theory," arXiv:hep-ph/9406283. lectures given at the Hadrons 94 Workshop, Gramado, Brazil, 10-14 Apr 1994. pages

[10] J. Gasser, H. Leutwyler, "Chiral Perturbation Theory To One Loop," *Annals Phys.* **158** (1984) 142. pages

[11] J. Gasser, H. Leutwyler, "Chiral Perturbation Theory: Expansions In The Mass Of The Strange Quark," *Nucl. Phys.* (1985) 465. pages

[12] S. Weinberg, "Phenomenological Lagrangians," *Physica A* **96** (1979) 327. pages

[13] J. Bijnens, G. Colangelo and G. Ecker, "The mesonic chiral Lagrangian of order p^6," *JHEP* **9902** (1999) 020, arXiv:hep-ph/9902437. pages

[14] J. Bijnens, G. Colangelo and G. Ecker, "Renormalization of chiral perturbation theory to order p^6," *Annals Phys.* **280** (2000) 100, arXiv:hep-ph/9907333. pages

[15] M. Schmaltz, "Physics beyond the standard model (Theory): Introducing the little Higgs," *Nucl. Phys. Proc. Suppl.* **117** (2003) 40, arXiv:hep-ph/0210415. pages

[16] G. C. Branco, P. M. Ferreira, L. Lavoura, M. N. Rebelo, M. Sher and J. P. Silva, "Theory and phenomenology of two-Higgs-doublet models," arXiv:1106.0034. pages

[17] A. Pich and P. Tuzon, "Yukawa Alignment in the Two-Higgs-Doublet Model," *Phys. Rev. D* **80** (2009) 091702, arXiv:0908.1554. pages

[18] T. P. Cheng and M. Sher, "Mass Matrix Ansatz and Flavor Nonconservation in Models with Multiple Higgs," *Phys. Rev. D* **35** (1987) 3484. pages

[19] S. P. Martin, "A Supersymmetry Primer," arXiv:hep-ph/9709356. pages

[20] C. T. Hill, E. H. Simmons, "Strong dynamics and electroweak symmetry breaking," *Phys. Rep.* **381** (2003) 235–402, arXiv:hep-ph/0203079. pages

[21] F. Sannino, "Conformal Dynamics for TeV Physics and Cosmology," *Acta Phys. Polon.* (2009) 3533–3743, arXiv:0911.0931. pages

[22] T. Appelquist, A. Avakian, R. Babich, R. C. Brower, M. Cheng, M. A. Clark, S. D. Cohen, G. T. Fleming *et al.*, "Toward TeV Conformality," *Phys. Rev. Lett.* **104** (2010) 071601, arXiv:0910.2224. pages

I

Technicolor and other QCD-like theories at next-to-next-to-leading order

Johan Bijnens and Jie Lu

Department of Theoretical Physics, Lund University,
Sölvegatan 14A, SE–223 62 Lund, Sweden
http://www.thep.lu.se/

Journal of High Energy Physics **0911** (2009) 116
arXiv:0910.5424 [hep-ph].

We calculate the vacuum-expectation-value, the meson mass and the meson decay constant to next-to-next-to-leading-order in the chiral expansion for QCD-like theories with general N_F degenerate flavours for the cases with a complex representation, a real and a pseudoreal representation, i.e. with global symmetry and breaking patters $SU(N_F)_L \times SU(N_F)_R \to SU(N_F)_V$, $SU(2N_F) \to SO(2N)$ and $SU(2N_F) \to Sp(2N_F)$. These calculations should be useful for lattice calculations for dynamical electroweak symmetry breaking and related cases.

I.1 Introduction

Chiral Perturbation Theory (ChPT) [1–3] as effective field theory (EFT) for QCD is a very well established method within strong interaction phenomenology. The same method can also be used for different symmetry pattern cases. These can be of interest for theories beyond the standard model. Early papers in this context are the technicolor variations discussed in [4–6]. Recently lattice calculations have started to explore some of these cases, some recent references are [7–11]. While one is primarily interested in these theories in the massless limit, lattice calculations are performed with finite masses and the results thus need to extrapolated to zero mass. For these extrapolations EFT is an excellent tool and it is heavily used in fitting results for the pseudoscalar meson octet in the QCD case. For high precision fits it is needed there to go to next-to-next-to-leading-order in the ChPT expansion.

When writing the EFT relevant for dynamical electroweak symmetry breaking one needs to consider different patterns of spontaneous breaking of the global symmetry than in QCD. The resulting set of Goldstone Bosons, or pseudo-Goldstone bosons in the presence of mass terms, is thus also different. The low-energy EFT is thus also different.

In this paper we only discuss cases where the underlying strong interaction is vectorlike and all fermions have the same mass. Here three main patterns of global symmetry show up. A thorough discussion of these cases at tree level or lowest order (LO) is [12]. With a gauge group with N_F fermions in a complex representation we have a global symmetry group $SU(N_F)_L \times SU(N_F)_R$ and we expect this to be spontaneously broken to the diagonal subgroup $SU(N_F)_V$. This is the direct extension of the QCD case. For N_F fermions in a real representation the global symmetry group becomes $SU(2N_F)$ and is expected to be spontaneously broken to $SO(2N_F)$. In the case of two colours and N_F fermions in the fundamental (pseudoreal) representation the global symmetry group is again $SU(2N_F)$ but here is expected to be spontaneously broken to an $Sp(2N_F)$ subgroup. Some earlier references are [13–15]. The complex case was treated to next-to-leading-order (NLO) in [3] in general and for the quantities considered here in [16]. The pseudo-real case has been done to NLO in [17]. We repeat here both calculations and also extend the third, real, case to NLO by calculating the full infinity structure for all three cases at NLO and giving the NLO Lagrangian.

In addition we also go to NNLO for three explicit quantities, the vacuum-expectation-value, the meson mass and the meson decay constant in the equal mass case. These formulas are our main result. We expect that the NNLO Lagrangian for all cases will be a simple generalization of the one for the complex case given in [18] but the calculation of the general divergence structure, though in principle similar to the one in [19], we have not performed.

In the remainder of this paper we refer to the complex representation case as QCD, the real representation case as adjoint and the pseudo-real case as two-colour or $N_c = 2$. We first discuss in Sect. I.2 the three different cases at the underlying fermion (quark) level. Here we introduce explicit external fields as done in [2, 3]. Sect. II.2 introduces the LO and NLO effective field theory and we do this using the general formalism derived in [20, 21]. This allows to see how similar the calculations for the three cases are. In Sect. I.4 we derive the divergent part at NLO and in Sect. II.4.3 we calculate the NNLO result for the meson mass, meson decay constant and vacuum expectation value. In Sect. II.6 we summarize our results.

I.2 Quark level

This section shortly introduces the quark-level Lagrangian giving the gauge groups and showing how the condensates can be written in the more general cases. A more extensive version of this discussion can be found in [12] and the earlier references [13, 15]. We remind the reader that we only consider cases with an underlying simple vector gauge group and we assume confinement and the formation of a condensate.

We use the notation q_R and q_L for the right- and left-handed fermions respectively. Gauge indices we usually suppress and flavour indices will be indicated when needed.

I.2.1 QCD

This is the usual case where the fermions are in a complex representation of the gauge group. With flavour indices i the fermion part of the Lagrangian enhanced by external fields is given by

$$\begin{aligned}\mathcal{L} &= \overline{q}_{Li} i\gamma^\mu D_\mu q_{Li} + \overline{q}_{Ri} i\gamma^\mu D_\mu q_{Ri} + \overline{q}_{Li}\gamma^\mu l_{\mu ij} q_{Lj} + \overline{q}_{Ri}\gamma^\mu r_{\mu ij} q_{Rj} \\ &\quad -\overline{q}_{Ri}\mathcal{M}_{ij} q_{Lj} - \overline{q}_{Li}\mathcal{M}^\dagger_{ij} q_{Rj}\,. \end{aligned} \tag{I.1}$$

The covariant derivative is given by $D_\mu q = \partial_\mu q - iG_\mu q$.

When the external fields vanish there is a $SU(N_F)_L \times SU(N_F)_R$ symmetry in the first two terms which is spontaneously broken to the diagonal subgroup $SU(N_F)_V$. This symmetry can be made local by adding the external fields with the transformations $g_L \times g_R \in SU(N_F)_L \times SU(N_F)_R$:

$$\begin{aligned} q_L &\to g_L q_L, \qquad q_R \to g_R q_R, \qquad \mathcal{M} \to g_R \mathcal{M} g_L^\dagger\,, \\ l_\mu &\to g_L l_\mu g_L^\dagger + i g_L \partial_\mu g_L^\dagger, \qquad r_\mu \to g_R r_\mu g_L^\dagger + i g_R \partial_\mu g_R^\dagger\,. \end{aligned} \tag{I.2}$$

We have here written q_L and q_R as column vectors in flavour and the external fields l_μ, r_μ and $\mathcal{M} = s - ip$ as matrices in flavour.

For later use, we define the big, $2N_F$, columnvector

$$\hat{q} = \begin{pmatrix} q_R \\ q_L \end{pmatrix} \tag{I.3}$$

and the big, $2N_F \times 2N_F$, matrices

$$\hat{V}_\mu = \begin{pmatrix} r_\mu & 0 \\ 0 & l_\mu \end{pmatrix} \qquad \hat{\mathcal{M}} = \begin{pmatrix} 0 & \mathcal{M} \\ \mathcal{M}^\dagger & 0 \end{pmatrix}, \qquad \hat{g} = \begin{pmatrix} g_R & 0 \\ 0 & g_L \end{pmatrix}. \tag{I.4}$$

In terms of these the symmetry transformation can be written as

$$\hat{q} \to \hat{g}\hat{q}\,, \qquad \hat{V}_\mu \to \hat{g}\hat{V}_\mu\hat{g}^\dagger + i\hat{g}\partial_\mu\hat{g}^\dagger\,, \qquad \hat{\mathcal{M}} \to \hat{g}\hat{\mathcal{M}}\hat{g}^\dagger\,. \tag{I.5}$$

Note that the symmetry group is not made larger since $\hat{q}$ contains objects that have different Lorentz properties.

The formation of a flavour neutral condensate $\langle\bar{q}q\rangle = \langle\bar{q}_R q_L\rangle + \text{h.c.}$ breaks the full symmetry spontaneously to the diagonal subgroup $SU(N_F)_V$

I.2.2 Adjoint

If the fermions are in the adjoint representations we can write down a similar Lagrangian as above

$$\begin{aligned}\mathcal{L} \;=\; & \text{tr}_c\left(\bar{q}_{Li} i\gamma^\mu D_\mu q_{Li}\right) + \text{tr}_c\left(\bar{q}_{Ri} i\gamma^\mu D_\mu q_{Ri}\right) + \text{tr}_c\left(\bar{q}_{Li}\gamma^\mu l_{\mu ij} q_{Lj}\right) + \text{tr}_c\left(\bar{q}_{Ri}\gamma^\mu r_{\mu ij} q_{Rj}\right) \\ & - \text{tr}_c\left(\bar{q}_{Ri}\mathcal{M}_{ij} q_{Lj}\right) - \text{tr}_c\left(\bar{q}_{Li}\mathcal{M}^\dagger_{ij} q_{Rj}\right).\end{aligned} \tag{I.6}$$

$\text{tr}_c\,(A)$ means a trace over the gauge group indices and the fermions are a matrix rather than a vector in the gauge group indices and $D_\mu q = \partial_\mu q - iG_\mu q + iqG_\mu$. Here we have the same transformation for the conjugated fermions, $D_\mu\bar{q} = \partial_\mu - iG_\mu\bar{q} + i\bar{q}G_\mu$ with $\bar{q} = q^\dagger\gamma^0$ and the Hermitian conjugate also means that the two gauge-indices are transposed. The symmetries discussed here exist in principle for any real representation for the fermions, not only the adjoint one.

We define the matrix $C = i\gamma^2\gamma^0$ and we can define a new fermion field

$$\tilde{q}_{Ri} \equiv C\bar{q}^T_{Li}\,. \tag{I.7}$$

The transpose in (I.7) works on the Dirac (and later also flavour) indices but not on the gauge indices. The field $\tilde{q}_{Ri}$ has the same transformation properties under the gauge group as q_R and is also a right-handed fermion.[1] In terms of

[1] We have chosen right-handed rather than left-handed in order to end up with transformations for fields that look most like those for the QCD case in [2,3].

the big matrices

$$\hat{q} = \begin{pmatrix} q_R \\ \tilde{q}_R \end{pmatrix}, \hat{V}_\mu = \begin{pmatrix} r_\mu & 0 \\ 0 & -l_\mu^T \end{pmatrix} \qquad \hat{\mathcal{M}} = \begin{pmatrix} 0 & \mathcal{M} \\ \mathcal{M}^T & 0 \end{pmatrix}. \tag{I.8}$$

The Lagrangian (I.6) becomes

$$\mathcal{L} = \mathrm{tr}_c \left(\bar{\hat{q}} i\gamma^\mu D_\mu \hat{q}\right) + \mathrm{tr}_c \left(\bar{\hat{q}}\gamma^\mu \hat{V}_\mu \hat{q}_j\right) - \frac{1}{2}\mathrm{tr}_c \left(\bar{\hat{q}} C \hat{\mathcal{M}} \bar{\hat{q}}^T\right) - \frac{1}{2}\mathrm{tr}_c \left(\hat{q}^T C \hat{\mathcal{M}}^\dagger \hat{q}\right). \tag{I.9}$$

The Lagrangian (I.9) has clearly a larger symmetry group, $SU(2N_F)$ as compared to QCD case above when we extend the external fields to the full matrices and have as symmetry transformations:

$$\hat{q} \to \hat{g}\hat{q}, \quad \hat{V}_\mu \to \hat{g}\hat{V}_\mu \hat{g}^\dagger + i\hat{g}\partial_\mu \hat{g}^\dagger, \quad \hat{\mathcal{M}} \to \hat{g}\hat{\mathcal{M}}\hat{g}^T. \tag{I.10}$$

The Vafa-Witten argument shows that also in this case the vector symmetries remain unbroken. We expect again a flavour neutral vacuum condensate $\langle \mathrm{tr}_c\,(\bar{q}q)\rangle$ which can be written as $\langle \mathrm{tr}_c\,(\hat{q}^T C J_S \hat{q})\rangle$ + h.c. with

$$J_S = \begin{pmatrix} 0 & \mathrm{I} \\ \mathrm{I} & 0 \end{pmatrix} \tag{I.11}$$

and I the $N_F \times N_F$ unit matrix. This condensate breaks the the symmetry group down to $SO(2N_F)$.

I.2.3 $N_c = 2$

The fundamental representation of $SU(2)$ is pseudo-real. The Lagrangian enhanced with external fields reads

$$\begin{aligned} \mathcal{L} \;=\; & \bar{q}_{Li} i\gamma^\mu D_\mu q_{Li} + \bar{q}_{Ri} i\gamma^\mu D_\mu q_{Ri} + \bar{q}_{Li}\gamma^\mu l_{\mu ij} q_{Lj} + \bar{q}_{Ri}\gamma^\mu r_{\mu ij} q_{Rj} \\ & - \bar{q}_{Ri}\mathcal{M}_{ij} q_{Lj} - \bar{q}_{Li}\mathcal{M}^\dagger_{ij} q_{Rj}. \end{aligned} \tag{I.12}$$

The covariant derivative is given by $D_\mu q = \partial_\mu q - iG_\mu q$.

We can define a field $\tilde{q}_R$ as in the previous section via

$$\tilde{q}_{R\alpha i} = \epsilon_{\alpha\beta} C \bar{q}^T_{L\beta i}, \tag{I.13}$$

with α, β gauge group indices, $\epsilon_{12} = -\epsilon_{21} = 1$, $\epsilon_{11} = \epsilon_{22} = 0$ and $C = i\gamma^2\gamma^0$ as defined before. The field $\tilde{q}_R$ is a right handed-handed fermion that transforms as the fundamental representation of $SU(2)$.

In terms of the big matrices

$$\hat{q} = \begin{pmatrix} q_R \\ \tilde{q}_R \end{pmatrix}, \hat{V}_\mu = \begin{pmatrix} r_\mu & 0 \\ 0 & -l_\mu^T \end{pmatrix} \qquad \hat{\mathcal{M}} = \begin{pmatrix} 0 & -\mathcal{M} \\ \mathcal{M}^T & 0 \end{pmatrix}. \tag{I.14}$$

The Lagrangian (I.12) becomes

$$\mathcal{L} = \bar{\hat{q}} i\gamma^\mu D_\mu \hat{q} + \bar{\hat{q}}\gamma^\mu \hat{V}_\mu \hat{q}_{Lj} - \frac{1}{2}\bar{\hat{q}}_\alpha C\epsilon_{\alpha\beta}\hat{\mathcal{M}}\bar{\hat{q}}_\beta^T - \frac{1}{2}\hat{q}_\alpha\epsilon_{\alpha\beta}C\hat{\mathcal{M}}^\dagger\hat{q}_\beta\,. \tag{I.15}$$

This has again much larger symmetry group, $SU(2N_F)$ as compared to QCD case above when we extend the external fields to the full matrices and have as symmetry transformations:

$$\hat{q} \to \hat{g}\hat{q}\,, \quad \hat{V}_\mu \to \hat{g}\hat{V}_\mu\hat{g}^\dagger + i\hat{g}\partial_\mu\hat{g}^\dagger\,, \quad \hat{\mathcal{M}} \to \hat{g}\hat{\mathcal{M}}\hat{g}^T\,. \tag{I.16}$$

The Vafa-Witten argument shows that also in this case the vector symmetries remain unbroken and we expect again a flavour neutral vacuum condensate $\langle\bar{q}q\rangle$ which can be written as $\langle\hat{q}_\alpha\epsilon_{\alpha\beta}CJ_A\hat{q}_\beta\rangle + \text{h.c.}$ with

$$J_A = \begin{pmatrix} 0 & -\mathrm{I} \\ \mathrm{I} & 0 \end{pmatrix} \tag{I.17}$$

and I the $N_F \times N_F$ unit matrix. This condensate breaks the the symmetry group down to $Sp(2N_F)$.

I.3 Effective field theory

In this section we will show how the three cases can be brought into an extremely similar form. That will allow to take over directly much of the technology developed for the QCD case to the other cases. We assume the reader to be familiar with ChPT and EFT. Introductions can be found in [22–28]. We will use the terminology LO, NLO and NNLO for the usual powercounting of order p^2, p^4 and p^6.

I.3.1 QCD

The Goldstone bosons from the spontaneous symmetry breakdown live in the space of possible vacua. For QCD and generalizations this is in the form of a nonzero vacuum condensate

$$\langle\bar{q}_{Lj}q_{Ri}\rangle = \frac{1}{2}\langle\bar{q}q\rangle\delta_{ij}\,. \tag{I.18}$$

This vacuum is left unchanged by the vector transformations with $g_L \times g_R \in SU(N_F)_L \times SU(N_F)_R$ and $g_L = g_R$. The unbroken symmetry is $SU(N_F)$. The broken symmetry part of the group are the axial transformations wit $g_R = g_L^\dagger \equiv u$, they rotate the vacuum into

$$\langle\bar{q}_{Lj}q_{Ri}\rangle_{\text{rotated}} = \frac{1}{2}\langle\bar{q}q\rangle U_{ij} \tag{I.19}$$

with $U = g_R g_L^\dagger = u^2$. The special unitary matrix U describes the space of possible vacua and varies under the symmetry as

$$U \to g_R U g_L^\dagger . \tag{I.20}$$

This matrix U can be used to construct the Lagrangians as was done in [3]. The covariant derivative on U is defined as

$$D_\mu U = \partial_\mu U - i r_\mu U + i U l_\mu . \tag{I.21}$$

The lowest order Lagrangian is

$$\mathcal{L} = \frac{F^2}{4} \langle D_\mu U D^\mu U^\dagger + \chi U^\dagger + U \chi^\dagger \rangle , \tag{I.22}$$

with $\chi = 2B_0 \mathcal{M}$ and $\langle A \rangle = \mathrm{tr}_F(A)$ This has the full global symmetry as can be checked using the transformations (I.2) and (I.20). In terms of the pion fields π^a the matrix u can be parametrized as

$$u = \exp\left(\frac{i}{\sqrt{2}\,F} \pi^a T^a \right) . \tag{I.23}$$

The T^a are the generators of $SU(N_F)$ and normalized as $\mathrm{tr}_F\left(T^a T^b\right) = \delta^{ab}$.

Let us now do the same analysis using the general formalism (CCWZ) [20,21]. We only look at the properties in the neighbourhood of the unit matrix here. For the perturbative treatment we do here that is sufficient. The global symmetry group G has generators T^a which are split up in a set of conserved generators Q^a and broken generators X^a. The Q^a generate the unbroken symmetry group H while the generators X^a generate in a sense the manifold of possible vacua, the quotient G/H . We must now find a way to parametrize the manifold G/H and define covariant derivatives in general. The manifold G/H and the group H we parametrize with

$$\hat{u} = \exp(i\phi^a X^a) \in G/H , \qquad \hat{h} = \exp(i\epsilon^a T^a) \in H \tag{I.24}$$

The symmetry transformation we define using the property that any group element $\hat{g}'$ can be written in the form

$$\hat{g}' = \hat{u}' \hat{h} , \tag{I.25}$$

where both $\hat{u}'$ and $\hat{h}$ are unique and of the form (I.24). The symmetry transformation on $\hat{u}$ by a group element $\hat{g} \in G$ is defined as

$$\hat{u} \to \hat{g} \hat{u} \hat{h}^\dagger \tag{I.26}$$

where $\hat{h}$ is the $\hat{h}$ of (II.12) needed to bring $\hat{g}' = \hat{g}\hat{u}$ in the standard form (II.12). Note that $\hat{h}$ is a nonlinear function of both $\hat{u}$ and $\hat{g}$. It is sometimes called the compensator.

The covariant derivatives are defined by using the fact that any variation $\hat{g}\delta\hat{g}^\dagger$ is an element of the Lie algebra and can be written as a linear combination of the generators. The same is true for $\hat{g}\left(\partial_\mu - i\hat{V}_\mu\right)\hat{g}^\dagger$ if we include external fields $\hat{V}_\mu$ transforming as $\hat{V}_\mu \to \hat{g}\hat{V}_\mu\hat{g}^\dagger + i\hat{g}\partial_\mu\hat{g}^\dagger$. We define [20,21]

$$\hat{u}^\dagger\left(\partial_\mu - i\hat{V}_\mu\right)\hat{u} \equiv \hat{\Gamma}_\mu - \frac{i}{2}\hat{u}_\mu\,, \qquad \hat{\Gamma}_\mu = \Gamma^a_\mu Q^a\,, \qquad \hat{u}_\mu = u^a_\mu X^a\,. \tag{I.27}$$

I.e. $\hat{\Gamma}_\mu$ is in the conserved part and $\hat{u}_\mu$ in the broken part of the Lie algebra. The transformation under the group G can be derived from (II.12) and is

$$\hat{\Gamma}_\mu \to \hat{h}\hat{\Gamma}_\mu\hat{h}^\dagger + \hat{h}\partial_\mu\hat{h}^\dagger\,, \qquad \hat{u}_\mu \to \hat{h}\hat{u}_\mu\hat{h}^\dagger\,. \tag{I.28}$$

$\hat{u}_\mu$ can be used to construct Lagrangians and covariant derivatives on objects ψ transforming as $\psi \to \hat{h}\psi$ are defined as

$$\hat{\nabla}_\mu\psi = \partial_\mu\psi + \hat{\Gamma}_\mu\psi\,. \tag{I.29}$$

It can be checked that $\hat{\nabla}_\mu\psi \to \hat{h}\hat{\nabla}_\mu\psi$. The external fields appear as (axial) vector fields $\hat{V}_\mu$ and (pseudo) scalar fields $\hat{\mathcal{M}}$. The external fields $\hat{V}_\mu$ show up in $\hat{u}_\mu$, covariant derivatives $\hat{\nabla}_\mu$ and field strengths $\hat{V}_{\mu\nu} \equiv \partial_\mu\hat{V}_\nu - \partial_\nu\hat{V}_\mu - i\left[\hat{V}_\mu, \hat{V}_\nu\right]$. The latter can be made to transform simpler by defining the objects

$$\hat{f}_{\mu\nu} \equiv \hat{u}^\dagger\hat{V}_{\mu\nu}\hat{u} \to \hat{h}\hat{f}_{\mu\nu}\hat{h}^\dagger\,. \tag{I.30}$$

$\hat{\mathcal{M}} \to \hat{g}\hat{\mathcal{M}}\hat{g}^\dagger$ can similarly be made into

$$\hat{\chi} \equiv \hat{u}^\dagger\hat{\mathcal{M}}\hat{u} \to \hat{h}\hat{\chi}\hat{h}^\dagger\,. \tag{I.31}$$

If there exists extra discrete symmetries like parity (P) that leave the unbroken part of the group invariant objects O like $\hat{f}_{\mu\nu}$ can be split into pieces that are independent via $O_\pm \equiv O \pm P(O)$.

In the effective field theory for QCD in terms of $N_F \times N_F$ matrices the notation usually used has the objects with the associated symmetry transformations:

$$\begin{aligned}
u &= \exp\left(\frac{i}{\sqrt{2}\,F}\pi^a T^a\right) \to g_R u h^\dagger = h u g_L^\dagger\,,\\
\Gamma_\mu &= \frac{1}{2}\left(u^\dagger(\partial_\mu - ir_\mu)u + u(\partial_\mu - l_\mu)u^\dagger\right) \to h\Gamma_\mu h^\dagger + ih\partial_\mu h^\dagger\,,\\
u_\mu &= i\left(u^\dagger(\partial_\mu - ir_\mu)u - u(\partial_\mu - l_\mu)u^\dagger\right) \to h u_\mu h^\dagger\,,\\
\nabla_\mu O &= \partial_\mu O + \Gamma_\mu O - O\Gamma_\mu \to h\nabla_\mu O h^\dagger \quad \text{for} \quad O \to hOh^\dagger\,,\\
\chi_\pm &= u^\dagger\chi u^\dagger \pm u\chi^\dagger u \to h\chi_\pm h^\dagger\,,\\
f_{\pm\mu\nu} &= u l_{\mu\nu} u^\dagger \pm u^\dagger r_{\mu\nu} u\,. \to h f_{\pm\mu\nu} h^\dagger
\end{aligned} \tag{I.32}$$

$l_{\mu\nu}$ and $r_{\mu\nu}$ are the field strengths from l_μ and r_μ. T^a are the $SU(N_F)$ generators. These can be related to the general objects defined in the CCWZ way via

$$\hat{u} = \begin{pmatrix} u & 0 \\ 0 & u^\dagger \end{pmatrix}, \qquad \hat{u}_\mu = \begin{pmatrix} u_\mu & 0 \\ 0 & -u_\mu \end{pmatrix}, \qquad \hat{\Gamma}_\mu = \begin{pmatrix} \Gamma_\mu & 0 \\ 0 & \Gamma_\mu \end{pmatrix} \cdots . \tag{I.33}$$

$\chi_\pm$ and $\hat{f}_{\pm\mu\nu}$ are constructed from $\hat{\chi}$ and $\hat{f}_{\mu\nu}$ using parity. These objects have been used to construct the NLO Lagrangian and the NNLO Lagrangian [18]. One of the nontrivial relations used there was

$$\nabla_\mu u_\nu - \nabla_\nu u_\mu = -f_{-\mu\nu} . \tag{I.34}$$

In this notation the lowest order Lagrangian is

$$\mathcal{L}_2 = \frac{F^2}{4} \langle u_\mu u^\mu + \chi_+ \rangle . \tag{I.35}$$

The NLO Lagrangian derived by [2] reads (here in the version for arbitrary N_F)

$$\begin{aligned} \mathcal{L}_4 \;=\; & L_0 \langle u^\mu u^\nu u_\mu u_\nu \rangle + L_1 \langle u^\mu u_\mu \rangle \langle u^\nu u_\nu \rangle + L_2 \langle u^\mu u^\nu \rangle \langle u_\mu u_\nu \rangle + L_3 \langle u^\mu u_\mu u^\nu u_\nu \rangle \\ & + L_4 \langle u^\mu u_\mu \rangle \langle \chi_+ \rangle + L_5 \langle u^\mu u_\mu \chi_+ \rangle + L_6 \langle \chi_+ \rangle^2 + L_7 \langle \chi_- \rangle^2 + \frac{1}{2} L_8 \langle \chi_+^2 + \chi_-^2 \rangle \\ & - i L_9 \langle f_{+\mu\nu} u^\mu u^\nu \rangle + \frac{1}{4} L_{10} \langle f_+^2 - f_-^2 \rangle + H_1 \langle l_{\mu\nu} l^{\mu\nu} + r_{\mu\nu} r^{\mu\nu} \rangle + H_2 \langle \chi \chi^\dagger \rangle \end{aligned} \tag{I.36}$$

I.3.2 Adjoint

The vacuum in this case can be characterized by the condensate

$$\langle \hat{q}_i^T C \hat{q}_j \rangle = \frac{1}{2} \langle \bar{q}_L q_R \rangle J_{Sij} . \tag{I.37}$$

Under the symmetry group $g \in SU(2N_F)$ this moves around as

$$J_S \to g J_S g^T . \tag{I.38}$$

The unbroken part of the group is given by the generators Q^a and the broken part by the generators X^a which satisfy

$$J_S Q^a = -Q^{aT} J_S , \qquad J_S X^a = X^{aT} J_S . \tag{I.39}$$

Just as in the QCD case we can now construct a rotated vacuum in general by using the broken part of the symmetry group on the vacuum. This leads to a matrix[2]

$$U = u J_S u^T \to g U g^T \qquad \text{with} \qquad u = \exp\left(\frac{i}{\sqrt{2}F} \pi^a X^a \right) . \tag{I.40}$$

[2] In Sect. I.3.1 we added a hat to many quantities to distinguish the $N_F \times N_F$ and $2N_F \times 2N_F$ matrices. This is not needed here and we only keep the hat explicitly on $\mathcal{M}$.

The matrix u transforms as in the general $CCWZ$ case as

$$u \to guh^\dagger \,. \tag{I.41}$$

The earlier work used the matrix U to describe the Lagrangian [12]. Here we will use the CCWZ scheme to obtain a notation that is formally identical to the QCD case. We add full $2N_F \times 2N_F$ matrices of external fields V_μ and $\hat{M}$. We need to obtain the Γ_μ and u_μ parts of $u^\dagger\left(\partial_\mu - iV_\mu\right)u$. Here several observations are useful. Eqs. (III.10) have as a consequence that matrices like u satisfy

$$uJ_S = J_S u^T \,, J_S u = u^T J_S \,. \tag{I.42}$$

A general matrix F can be split two parts, one behaving as the broken part, the other as the unbroken part of the group generators. I.e.

$$\begin{aligned} F &= \overline{F} + \tilde{F}\,, \\ \overline{F}J_S &= -J_S\overline{F}^T\,, \qquad \tilde{F}J_S = \tilde{F}^T J_S\,, \\ \overline{F} &= \frac{1}{2}\left(F - J_S F^T J_S\right)\,, \\ \tilde{F} &= \frac{1}{2}\left(F + J_S F^T J_S\right)\,. \end{aligned} \tag{I.43}$$

This means that we obtain

$$\begin{aligned} u_\mu &= i\left(u^\dagger(\partial_\mu - iV_\mu)u - u(\partial_\mu + iJ_S V_\mu^T J_S)u^\dagger\right)\,, \\ \Gamma_\mu &= \frac{1}{2}\left(u^\dagger(\partial_\mu - iV_\mu)u + u(\partial_\mu + iJ_S V_\mu^T J_S)u^\dagger\right)\,. \end{aligned} \tag{I.44}$$

Here we used the properties (I.42). With these quantities we can construct covariant derivatives and Lagrangians. The formal similarity to the QCD case is obviously there if we also use for the vector external fields

$$l_\mu = -J_S V_\mu^T J_S\,, \qquad r_\mu = V_\mu\,. \tag{I.45}$$

The analogy goes even further since $v_\mu = r_\mu + l_\mu$ corresponds to the currents from conserved generators and $a_\mu = r_\mu - l_\mu$ to the currents from the spontaneously broken generators. The equivalent quantities to the field strengths are

$$f_{\pm\mu\nu} = J_S u V_{\mu\nu} u^\dagger J_S \pm u V_{\mu\nu} u^\dagger \tag{I.46}$$

with $V_{\mu\nu} = \partial_\mu V_\nu - \partial_\nu V_\mu - i\left(V_\mu V_\nu - V_\nu V_\mu\right)$ and for the mass matrix

$$\begin{aligned} \chi_\pm &= u^\dagger \chi u^{\dagger T} J_S \pm J_S u^T \chi^\dagger u \\ &= u^\dagger \chi J_S u^\dagger \pm u J_S \chi^\dagger u\,, \end{aligned} \tag{I.47}$$

with $\chi = 2B_0\hat{\mathcal{M}}$. The Lagrangians at LO and NLO have exactly the same form as (III.7) and (I.36) but now with u_μ, $\chi_\pm$ and $f_{\pm\mu\nu}$ as defined in (III.12), (I.46) and (I.47).

I.3.3 Two colours

The vacuum in this case can be characterized by the condensate $\langle \hat{q}^T_{\alpha i} C\epsilon_{\alpha\beta}\hat{q}_{\beta j}\rangle = \frac{1}{2}\langle \bar{q}_L q_R\rangle J_{Aij}$. Under the symmetry group $g \in SU(2N_F)$ this moves around as $J_A \to gJ_Ag^T$ .The unbroken part of the group is given by the generators Q^a and the broken part by the generators X^a which satisfy $J_AQ^a = -Q^{aT}J_A$, $J_AX^a = X^{aT}J_A$. Just as in the QCD and the adjoint case we construct a rotated vacuum by using the broken part of the symmetry group on the vacuum. This leads to a matrix[3] $U = uJ_Au^T \to gUg^T$ with $u = \exp\left(\frac{i}{\sqrt{2}F}\pi^aX^a\right)$ .The matrix u transforms as $u \to guh^\dagger$ .Ref. [12] used the matrix U to describe the Lagrangian. Here we use the CCWZ scheme. We add full $2N_F \times 2N_F$ matrices of external fields V_μ and $\hat{\mathcal{M}}$ and then need to obtain the Γ_μ and u_μ parts of $u^\dagger\left(\partial_\mu - iV_\mu\right)u$. Matrices like u satisfy $uJ_A = J_Au^T$ and $J_Au = u^TJ_A$.

A general matrix F can be split two parts, one behaving as the broken part, the other as the unbroken part of the group generators. I.e.

$$\begin{aligned} F &= \overline{F} + \tilde{F}\,, \qquad \overline{F}J_A = -J_A\overline{F}^T\,, \qquad \tilde{F}J_A^T = \tilde{F}^TJ_A\,, \\ \overline{F} &= \frac{1}{2}\left(F - J_AF^TJ_A^T\right)\,, \qquad \tilde{F} = \frac{1}{2}\left(F + J_AF^TJ_A^T\right)\,. \end{aligned} \tag{I.48}$$

Using this, we obtain

$$\begin{aligned} u_\mu &= i\left(u^\dagger(\partial_\mu - iV_\mu)u - u(\partial_\mu + iJ_AV_\mu^TJ_A^T)u^\dagger\right)\,, \\ \Gamma_\mu &= \frac{1}{2}\left(u^\dagger(\partial_\mu - iV_\mu)u + u(\partial_\mu + iJ_AV_\mu^TJ_A^T)u^\dagger\right)\,. \end{aligned} \tag{I.49}$$

Covariant derivatives and Lagrangians are constructed as above. The formal similarity to the QCD case is once more obviously if we use for the vector external fields

$$l_\mu = -J_AV_\mu^TJ_A^T\,, \qquad r_\mu = V_\mu\,. \tag{I.50}$$

Again $v_\mu = r_\mu + l_\mu$ corresponds to the currents from conserved generators and $a_\mu = r_\mu - l_\mu$ to the currents from the spontaneously broken generators. The equivalent quantities to the field strengths are

$$f_{\pm\mu\nu} = J_AuV_{\mu\nu}u^\dagger J_A^T \pm uV_{\mu\nu}u^\dagger \tag{I.51}$$

with $V_{\mu\nu} = \partial_\mu V_\nu - \partial_\nu V_\mu - i\left(V_\mu V_\nu - V_\nu V_\mu\right)$ and for the mass matrix

$$\chi_\pm = u^\dagger\chi u^{\dagger T}J_A^T \pm J_Au^T\chi^\dagger u = u^\dagger\chi J_A^Tu^\dagger \pm uJ_A\chi^\dagger u\,, \tag{I.52}$$

with $\chi = 2B_0\hat{\mathcal{M}}$. The Lagrangians at LO and NLO have exactly the same form as (III.7) and (I.36) but with u_μ, $\chi_\pm$ and $f_{\pm\mu\nu}$ as defined in this subsection.

[3] The formulas in this subsection are almost identical with those in the previous subsection but $J_A^2 = -1$ while $J_S^2 = 1$. We have put in those by introducing J_A^T rather than J_A in a few places.

I.4 The divergence structure at NLO

When going beyond tree level renormalization becomes necessary. A thorough discussion of renormalization in ChPT at NNLO can be found in [**?**, 19]. We use here the same conventions and subtraction procedure. This means that the NLO LECs are replaced by

$$L_i = (c\mu)^{d-4}\left[\Gamma_i \Lambda + L_i^r(\mu)\right] , \tag{I.53}$$

with $\Lambda = 1/(16\pi^2(d-4))$ and $\ln c = -[\ln 4\pi + \Gamma'(1) + 1]/2$. The constants Γ_i were calculated for the *QCD* case in [3]. The same method can be generalized to the case here. The calculation is extremely similar for all three cases. The method is the same as the one in [3]. We split u in a classical and a quantum part

$$u = u_c e^{i\xi} \quad \text{with} \quad \xi = \sum_a \xi^a X^a . \tag{I.54}$$

The second variation w.r.t. ξ of the LO Lagrangian can be rewritten in the form

$$\mathcal{L} = \frac{F^2}{2}\left(d_\mu \xi^a d^\mu \xi^a - \xi^a \tilde{\sigma}^{ab}\xi^b\right) , \tag{I.55}$$

with $d_\mu \xi^a = \partial_\mu \xi^a + \tilde{\Gamma}_\mu^{ab}\xi^b$. The divergence at one-loop level is given by [3]

$$-\frac{1}{16\pi^2(d-4)}\left(\frac{1}{12}\tilde{\Gamma}_{\mu\nu}^{ab}\tilde{\Gamma}^{ba\mu\nu} + \frac{1}{2}\tilde{\sigma}^{ab}\tilde{\sigma}ba\right) . \tag{I.56}$$

Notice that the indices here run over the broken generators and $\tilde{\Gamma}_{\mu\nu}^{ab} = \partial_\mu \tilde{\Gamma}_\nu^{ab} - \partial_\nu \tilde{\Gamma}_\mu^{ab} + \tilde{\Gamma}_\mu^{ac}\tilde{\Gamma}_\nu^{cb} - \tilde{\Gamma}_\nu^{ac}\tilde{\Gamma}_\mu^{cb}$.

The expansion for all three cases is identical and leads to

$$\begin{aligned}
\tilde{\Gamma}_\mu^{ab} &= -\mathrm{tr}_F\left([X^a, X^b]\Gamma_\mu\right) , \\
\tilde{\sigma}^{ab} &= -\frac{1}{8}\mathrm{tr}_F\left(\{X^a, X^b\}\left(\chi_+ + u_\mu u^\mu\right)\right) + \frac{1}{2}\mathrm{tr}_F\left(X^a u_\mu X^b u^\mu\right) .
\end{aligned} \tag{I.57}$$

The difficulty in evaluating (I.56) is now rewriting the sums over broken generators into traces over the original matrices $u_\mu, \ldots$. In the QCD case, the X^a are $SU(N_F)$ generators and one can use the formulas with the $\mathrm{tr}_F(A)$ going from $1, \ldots, N_F$.

$$\begin{aligned}
&\text{QCD :} \\
\mathrm{tr}_F\left(X^a A X^a B\right) &= \mathrm{tr}_F(A)\,\mathrm{tr}_F(B) - \frac{1}{N_F}\mathrm{tr}_F(AB) , \\
\mathrm{tr}_F\left(X^a A\right)\mathrm{tr}_F\left(X^a B\right) &= \mathrm{tr}_F(AB) - \frac{1}{N_F}\mathrm{tr}_F(A)\,\mathrm{tr}_F(B) .
\end{aligned} \tag{I.58}$$

There exist similar formulas for the adjoint case now with $\mathrm{tr}_F(A)$ going from $1,\ldots,2N_F$.

$$\begin{aligned}
&\text{Adjoint :}\\
\mathrm{tr}_F\left(X^aAX^aB\right) &= \frac{1}{2}\mathrm{tr}_F(A)\,\mathrm{tr}_F(B)+\frac{1}{2}\mathrm{tr}_F\left(AJ_SB^TJ_S\right)-\frac{1}{2N_F}\mathrm{tr}_F(AB)\,,\\
\mathrm{tr}_F\left(X^aA\right)\mathrm{tr}_F\left(X^aB\right) &= \frac{1}{2}\mathrm{tr}_F(AB)+\frac{1}{2}\mathrm{tr}_F\left(AJ_SB^TJ_S\right)-\frac{1}{2N_F}\mathrm{tr}_F(A)\,\mathrm{tr}_F(B)
\end{aligned} \tag{I.59}$$

The equivalent formula for the two-colour case is [17], again with $\mathrm{tr}_F(A)$ going from $1,\ldots,2N_F$.

$$\begin{aligned}
&2-\text{colour :}\\
\mathrm{tr}_F\left(X^aAX^aB\right) &= \frac{1}{2}\mathrm{tr}_F(A)\,\mathrm{tr}_F(B)+\frac{1}{2}\mathrm{tr}_F\left(AJ_AB^TJ_A\right)-\frac{1}{2N_F}\mathrm{tr}_F(AB)\,,\\
\mathrm{tr}_F\left(X^aA\right)\mathrm{tr}_F\left(X^aB\right) &= \frac{1}{2}\mathrm{tr}_F(AB)-\frac{1}{2}\mathrm{tr}_F\left(AJ_AB^TJ_A\right)-\frac{1}{2N_F}\mathrm{tr}_F(A)\,\mathrm{tr}_F(B)
\end{aligned} \tag{I.60}$$

In all three cases these lead to

$$\tilde{\Gamma}^{ab}_{\mu\nu}=-\mathrm{tr}_F\left([X^a,X^b]\Gamma_{\mu\nu}\right)\,. \tag{I.61}$$

Repetitive use of these identities allows to rewrite (I.56) in the form of (I.36). These divergences are then absorbed into the redefinition of the NLO LECs (III.17). The needed constants Γ_i for the three cases are given in Tab. III.1. We agree with [3] for the QCD case, have a small discrepancy with [17] for the two-colour case, our coefficients for Γ_0 are Γ_3 are different. The adjoint case is obtained here for the first time.

I.5 The calculation: mass, decay constant and condensate

In this section we calculate the corrections to the vacuum expectation value, the meson mass and the decay constant. The calculations in the work on three-flavour ChPT were done using FORM [29] and in the loops an explicit sum over all possible particles was always implemented. For this work we have rewritten the flavour routines used in that work to use a general sum over the flavour indices and since we always calculate in the case where $\mathcal{M}=\mathrm{diag}(\hat{m},\ldots,\hat{m})$ we then use the trace formulas of the previous section to perform the sum.

We have checked that our calculations reproduce all the known results and for the QCD case that all infinities cancel when the NNLO divergence of [19]

i	QCD	Adjoint	2-colour
0	$N_F/48$	$(N_F+4)/48$	$(N_F-4)/48$
1	$1/16$	$1/32$	$1/32$
2	$1/8$	$1/16$	$1/16$
3	$N_F/24$	$(N_F-2)/24$	$(N_F+2)/24$
4	$1/8$	$1/16$	$1/16$
5	$N_F/8$	$N_F/8$	$N_F/8$
6	$(N_F^2+2)/(16N_F^2)$	$(N_F^2+1)/(32N_F^2)$	$(N_F^2+1)/(32N_F^2)$
7	0	0	0
8	$(N_F^2-4)/(16N_F)$	$(N_F^2+N_F-2)/(16N_F)$	$(N_F^2-N_F-2)/(16N_F)$
9	$N_F/12$	$(N_F+1)/2$	$(N_F-1)/2$
10	$-N_F/12$	$-(N_F+1)/2$	$-(N_F-1)/2$
1′	$-N_F/24$	$-(N_F+1)/4$	$-(N_F+1)/4$
2′	$(N_F^2-4)/(8N_F)$	$(N_F^2+N_F-2)/(8N_F)$	$(N_F^2-N_F-2)/(8N_F)$

Table I.1: The coefficients Γ_i for the three cases that are needed to absorb the divergences at NLO. The last two lines correspond to the terms with H_1 and H_2.

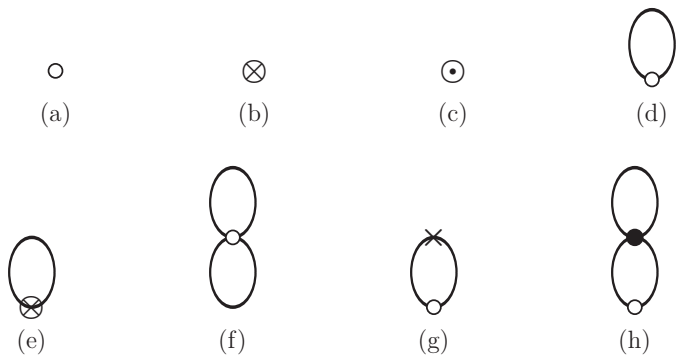

Figure I.1: The diagrams up to order p^6 for $\langle\bar{q}q\rangle$. The lines are meson propagators and the vertices are: $\circ$ a p^2 insertion of $\bar{q}q$, $\otimes$ a p^4 insertion of $\bar{q}q$, $\odot$ a p^6 insertion of $\bar{q}q$, $\bullet$ a p^2 vertex and $\times$ a p^4 vertex.

is used. For the adjoint and two-color case we observe that the nonlocal divergence cancels as it should.

The diagrams for the vacuum expectation value are shown in Fig. I.1. The

lowest order is the same for all three cases

$$\langle\bar{q}q\rangle_{\rm LO} \equiv \sum_{i=1,N_F} \langle\bar{q}_{Ri}q_{Li} + \bar{q}_{Li}q_{Ri}\rangle_{\rm LO} = -N_F B_0 F^2 \,. \tag{I.62}$$

We use M^2 as notation for the lowest order meson mass

$$M^2 = 2B_0\hat{m} \tag{I.63}$$

and in addition the function

$$\overline{A}(M^2) = -\frac{M^2}{16\pi^2}\log\frac{M^2}{\mu^2}\,. \tag{I.64}$$

The integrals needed at the two-loop level are evaluated with the methods of [30] and they can all be expressed in terms of $\overline{A}(M^2)$.

We express the final result as

$$\langle\bar{q}q\rangle = \langle\bar{q}q\rangle_{\rm LO} + \langle\bar{q}q\rangle_{\rm NLO} + \langle\bar{q}q\rangle_{\rm NNLO}\,. \tag{I.65}$$

The individual parts can be written in terms of logarithms and analytic contributions as

$$\begin{aligned}
\langle\bar{q}q\rangle_{\rm NLO} &= \langle\bar{q}q\rangle_{\rm LO}\left(a_V\frac{\overline{A}(M^2)}{F^2} + b_V\frac{M^2}{F^2}\right),\\
\langle\bar{q}q\rangle_{\rm NNLO} &= \langle\bar{q}q\rangle_{\rm LO}\left(c_V\frac{\overline{A}(M^2)^2}{F^4} + \frac{M^2\overline{A}(M^2)}{F^4}\left(d_V + \frac{e_V}{16\pi^2}\right)\right.\\
&\qquad \left. + \frac{M^4}{F^4}\left(f_V + \frac{g_V}{16\pi^2}\right)\right).
\end{aligned} \tag{I.66}$$

The coefficients for the three cases are given in Tab. I.2. Note that we use the same notation for the LECs in the three cases but they are different LECs and in addition different for different values of N_F. The infinite parts can be absorbed in the NNLO Lagrangian coefficients by writing

$$r_i = (c\mu)^{2(d-4)}\left(r_i^r - \Gamma_i^{(2)}\Lambda^2 - \left(\frac{1}{16\pi^2}\Gamma_i^{(1)} + \Gamma_i^{(L)}\right)\Lambda\right). \tag{I.67}$$

The subtractions needed for the QCD case have been derived in general before

	QCD
a_V	$N_F - \frac{1}{N_F}$
b_V	$16N_F L_6^r + 8L_8^r + 4H_2^r$
c_V	$\frac{3}{2}\left(-1 + \frac{1}{N_F^2}\right)$
d_V	$-24\left(N_F^2-1\right)\left(L_4^r - 2L_6^r + \frac{1}{N_F}(L_5^r - 2L_8^r)\right)$
e_V	$1 - \frac{1}{N_F^2}$
f_V	$48\left(K_{25}^r + N_F K_{26}^r + N_F^2 K_{27}^r\right)$
g_V	$8\left(N_F^2-1\right)\left(L_4^r - 2L_6^r + \frac{1}{N_F}(L_5^r - 2L_8^r)\right)$
	Adjoint
a_V	$N_F + \frac{1}{2} - \frac{1}{2N_F}$
b_V	$32N_F L_6^r + 8L_8^r + 4H_2^r$
c_V	$\frac{3}{8}\left(-1 + \frac{1}{N_F^2} - \frac{2}{N_F} + 2N_F\right)$
d_V	$-12\left(2N_F^2+N_F-1\right)\left(2L_4^r - 4L_6^r + \frac{1}{N_F}(L_5^r - 2L_8^r)\right)$
e_V	$\frac{1}{4}\left(1 - \frac{1}{N_F^2} + \frac{2}{N_F} - 2N_F\right)$
f_V	r_{VA}^r
g_V	$4\left(2N_F^2+N_F-1\right)\left(2L_4^r - 4L_6^r + \frac{1}{N_F}(L_5^r - 2L_8^r)\right)$
	2-colour
a_V	$N_F - \frac{1}{2} - \frac{1}{2N_F}$
b_V	$32N_F L_6^r + 8L_8^r + 4H_2^r$
c_V	$\frac{3}{8}\left(-1 + \frac{1}{N_F^2} + \frac{2}{N_F} - 2N_F\right)$
d_V	$-12\left(2N_F^2-N_F-1\right)\left(2L_4^r - 4L_6^r + \frac{1}{N_F}(L_5^r - 2L_8^r)\right)$
e_V	$\frac{1}{4}\left(1 - \frac{1}{N_F^2} - \frac{2}{N_F} + 2N_F\right)$
f_V	r_{VT}^r
g_V	$4\left(2N_F^2-N_F-1\right)\left(2L_4^r - 4L_6^r + \frac{1}{N_F}(L_5^r - 2L_8^r)\right)$

Table I.2: The coefficients $a_V, \ldots, g_V$ appearing in the expansion of the vacuum expectation value.

in [19]. The adjoint and two-colour case can be made finite by the following:

$$\begin{aligned}
\Gamma_{VA}^{(2)} &= \frac{3}{2}\left(1 - \frac{1}{N_F^2} + 2\frac{1}{N_F} - 2N_F\right), \\
\Gamma_{VA}^{(L)} &= 24\left(2N_F^2 + N_F - 1\right)\left(2L_4^r - 4L_6^r + \frac{1}{N_F}(L_5^r - 2L_8^r)\right), \\
\Gamma_{VA}^{(1)} &= 0,
\end{aligned}$$

$$\begin{aligned}
\Gamma^{(2)}_{VT} &= \frac{3}{2}\left(1-\frac{1}{N_F^2}-2\frac{1}{N_F}+2N_F\right), \\
\Gamma^{(L)}_{VT} &= 24\left(2N_F^2-N_F-1\right)\left(2L_4^r-4L_6^r+\frac{1}{N_F}(L_5^r-2L_8^r)\right), \\
\Gamma^{(1)}_{VT} &= 0\,. \qquad \text{(I.68)}
\end{aligned}$$

This result agrees at NLO with [16] for the QCD case and [17] [4] for the 2-colour case. It also agrees for $N_F = 3$ at NNLO with [31, 32]. The remaining results are new.

We perform the expansion of the physical meson mass to the same order. The physical mass can be written as

$$M^2_{\text{phys}} = M^2_{\text{LO}} + M^2_{\text{NLO}} + M^2_{\text{NNLO}}\,. \qquad \text{(I.69)}$$

The lowest order was already given in (I.63) and is the same for all three cases. The two higher order can be expanded in logarithms and analytical contributions via

$$\begin{aligned}
M^2_{\text{NLO}} &= M^2\left(a_M\frac{\overline{A}(M^2)}{F^2}+b_M\frac{M^2}{F^2}\right), \\
M^2_{\text{NNLO}} &= M^2\Bigg(c_M\frac{\overline{A}(M^2)^2}{F^4}+\frac{M^2\overline{A}(M^2)}{F^4}\left(d_M+\frac{e_M}{16\pi^2}\right) \\
&\quad +\frac{M^4}{F^4}\left(f_M+\frac{g_M}{16\pi^2}+\frac{h_M}{(16\pi^2)^2}\right)\Bigg). \qquad \text{(I.70)}
\end{aligned}$$

The mass can be calculated by finding the zeros of the inverse propagator, see e.g. the discussion [33]. The relevant one-particle irreducible diagrams are shown in Fig. I.2. The coefficients for the three cases are given in Tab. I.3. The subtractions needed for the QCD case have been derived in general before in [19]. The adjoint and two-colour case can be made finite by the following:

$$\begin{aligned}
\Gamma^{(2)}_{MA} &= \frac{1}{2}\left(1-\frac{9}{N_F^2}+\frac{12}{N_F}-7N_F-3N_F^2\right), \\
\Gamma^{(L)}_{MA} &= -8\Bigg[\left(3-\frac{3}{N_F}+2N\right)L_0^r+2\left(-1+2N_F+4N_F^2\right)L_1^r+\left(4+N_F+2N_F^2\right)L_2^r \\
&\quad +\left(3-\frac{3}{N_F}+5N_F\right)L_3^r+\frac{2}{N_F}(2-2N_F-3N_F^2)(2N_FL_4^r+L_5^r) \\
&\quad +4\left(-1+3N_F+4N_F^2\right)L_6^r+\left(10-\frac{10}{N_F}+12N_F\right)L_8^r)\Bigg],
\end{aligned}$$

[4] Those authors used a different normalization for F. Ours corresponds to $F_\pi \approx 93$ MeV for the QCD case and $N_c = 3$.

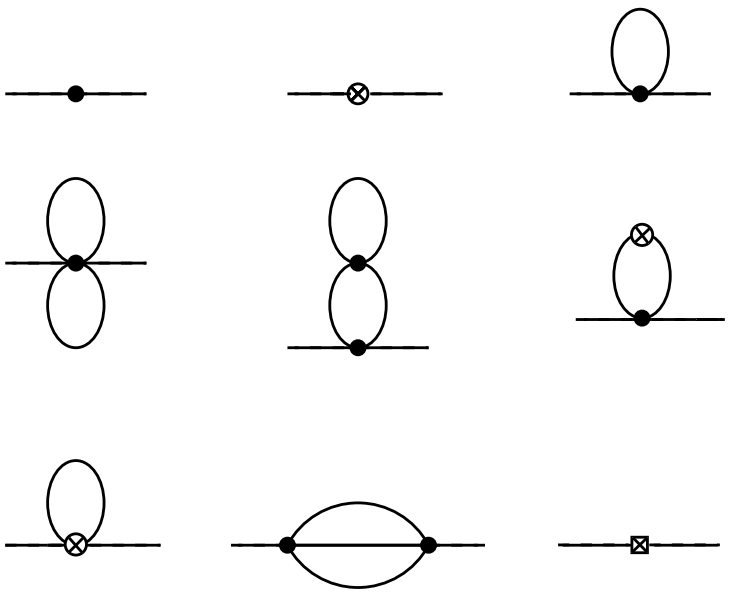

Figure I.2: The diagrams up to order p^6 for the meson self energy. The lines are meson propagators and the vertices are: • a p^2 vertex, $\times$ a p^4 vertex and a crossed box a p^6 vertex. The diagrams for the decay constant are the same with one external meson leg replaced by an axial current.

$$
\begin{aligned}
\Gamma^{(1)}_{MA} &= -\frac{1}{4}\left(-\frac{5}{3}+\frac{5}{N_F^2}-\frac{5}{N_F}+\frac{67}{12}N_F+\frac{47}{12}N_F^2\right), \\
\Gamma^{(2)}_{MT} &= \frac{1}{2}\left(1-\frac{9}{N_F^2}-\frac{12}{N_F}+7N_F-3N_F^2\right), \\
\Gamma^{(L)}_{MT} &= -8\Bigg[\left(-3-\frac{3}{N_F}+2N_F\right)L_0^r+2\left(-1-2N_F+4N_F^2\right)L_1^r+\left(4-N_F+2N_F^2\right)L_2^r \\
&\quad +\left(-3-\frac{3}{N_F}+5N_F\right)L_3^r+\frac{2}{N_F}(2+2N_F-3N_F^2)(2N_FL_4^r+L_5^r) \\
&\quad +4\left(-1-3N_F+4N_F^2\right)L_6^r+\left(-10-\frac{10}{N_F}+12N_F\right)L_8^r)\Bigg], \\
\Gamma^{(1)}_{MT} &= -\frac{1}{4}\left(-\frac{5}{3}+\frac{5}{N_F^2}+\frac{5}{N_F}-\frac{67}{12}N_F+\frac{47}{12}N_F^2\right). \qquad \text{(I.71)}
\end{aligned}
$$

This result agrees at NLO with [16] for the QCD case and [17] for the 2-colour case. It also agrees with the masses for two and three flavours in the QCD case

as calculated in [33–38]. The remaining results are new.

We perform the expansion of the physical decay constant to the same order. The decay constant can be written as

$$F_{\rm phys} = F_{\rm LO} + F_{\rm NLO} + F_{\rm NNLO}\,. \tag{I.72}$$

The lowest order is $F_{\rm LO} = F$ and is the same for all three cases. The two higher order can be expanded in logarithms and analytical contributions via

$$\begin{aligned} F_{\rm NLO} &= F\left(a_F \frac{\overline{A}(M^2)}{F^2} + b_F \frac{M^2}{F^2}\right), \\ F_{\rm NNLO} &= F\Bigg(c_F \frac{\overline{A}(M^2)^2}{F^4} + \frac{M^2\overline{A}(M^2)}{F^4}\left(d_F + \frac{e_F}{16\pi^2}\right) \\ &\quad + \frac{M^4}{F^4}\left(f_F + \frac{g_F}{16\pi^2} + \frac{h_F}{(16\pi^2)^2}\right)\Bigg). \end{aligned} \tag{I.73}$$

The decay constant can be calculated by computing the one-meson matrix element of the axial current. The diagrams for the wave-function renormalization are the same as those for the mass in Fig. I.2 and those for the bare matrix-element are again those of Fig. I.2 but with one external meson leg replaced by the axial current. The coefficients for the three cases are given in Tab. I.4. The subtractions needed for the QCD case have been derived in general before in [19]. The adjoint and two-colour case can be made finite by the following:

$$\begin{aligned} \Gamma^{(2)}_{FA} &= 1 - \frac{3}{4}N_F + \frac{1}{4}N_F^2, \\ \Gamma^{(L)}_{FA} &= -4\Bigg[\left(-3 + \frac{3}{N_F} - 2N_F\right)L_0^r + 2\left(1 - 2N_F - 4N_F^2\right)L_1^r + \left(-4 - N_F - 2N_F^2\right)L_2^r \\ &\quad + \left(-3 + \frac{3}{N_F} - 5N_F\right)L_3^r + \frac{1}{N_F}(N_F - 1)(2N_F L_4^r + L_5^r) + 8N_F^2 L_6^r + 4N_F L_8^r\Bigg], \\ \Gamma^{(1)}_{FA} &= -\frac{1}{8}\left(\frac{1}{3} - \frac{1}{N_F^2} + \frac{1}{N_F} - \frac{53}{12}N_F - \frac{49}{12}N_F^2\right), \\ \Gamma^{(2)}_{FT} &= 1 + \frac{3}{4}N_F + \frac{1}{4}N_F^2, \\ \Gamma^{(L)}_{FT} &= -4\Bigg[\left(3 + \frac{3}{N_F} - 2N_F\right)L_0^r + 2\left(1 + 2N_F - 4N_F^2\right)L_1^r + \left(-4 + N_F - 2N_F^2\right)L_2^r \\ &\quad + \left(3 + \frac{3}{N_F} - 5N_F\right)L_3^r - \frac{1}{N_F}(1 + N_F)(2N_F L_4^r + L_5^r) + 8N_F^2 L_6^r + 4N_F L_8^r\Bigg], \\ \Gamma^{(1)}_{FT} &= -\frac{1}{8}\left(\frac{1}{3} - \frac{1}{N_F^2} - \frac{1}{N_F} + \frac{53}{12}N_F - \frac{49}{12}N_F^2\right). \end{aligned} \tag{I.74}$$

This result agrees at NLO with [16] for the QCD case and [17] for the 2-colour case. It also agrees with the decay constant for two and three flavours in the QCD case as calculated in [33,34,36,38]. The remaining results are new.

The coefficient of the leading logarithm, $\overline{A}(M^2)^2$ is always determined but note that the coefficient of the subleading logarithm for the vacuum expectation value depends on LECs that can be determined from the masses.

The expansions (I.66), (I.70) and (I.73) have been written in terms of the lowest order mass and decay constant. It is possible to reorder the series in various ways. In particular one can rewrite the series in terms of the physical masses and decay constants instead. The logarithms come from physical particles propagating so the form in terms of physical masses might be preferable. There are some indications that in the case of two-flavour QCD this leads to a better convergence, see e.g. [39]. The physical mass and decay constant expansion is referred to there as the ξ expansion. We thus rewrite (I.66), (I.70) and (I.73) as

$$O_{\text{phys}} = O_{\text{LO}} + O_{\text{NLO}} + O_{\text{NNLO}}\,, \tag{I.75}$$

with

$$\begin{aligned} O_{\text{NLO}} &= O_{\text{LO}}\left(\alpha_O \frac{\overline{A}(M^2_{\text{phys}})}{F^2_{\text{phys}}} + \beta_O \frac{M^2_{\text{phys}}}{F^2_{\text{phys}}}\right), \\ O_{\text{NNLO}} &= O_{\text{LO}}\left(\gamma_O \frac{\overline{A}(M^2_{\text{phys}})^2}{F^4_{\text{phys}}} + \frac{M^2_{\text{phys}}\overline{A}(M^2_{\text{phys}})}{F^4_{\text{phys}}}\left(\delta_O + \frac{\epsilon_O}{16\pi^2}\right)\right. \\ &\qquad \left. + \frac{M^4_{\text{phys}}}{F^4_{\text{phys}}}\left(\zeta_O + \frac{\eta_O}{16\pi^2} + \frac{\theta_O}{(16\pi^2)^2}\right)\right). \end{aligned} \tag{I.76}$$

We do this for $O = V, M, F$ for the vacuum-expectation-value, mass and decay constant. The coefficients in the two expansions are related by

$$\begin{aligned} \alpha_O &= a_O\,, \qquad \beta_O = b_O\,, \qquad \gamma_O = c_O + (2a_F - a_M)a_O\,, \\ \delta_O &= d_O + (2b_F - b_M)a_O + (2a_F - a_M)b_O\,, \qquad \epsilon_O = e_O + a_M a_O\,, \\ \zeta_O &= f_O + (2b_F - b_M)b_O\,, \qquad \eta_O = g_O + b_M a_O\,, \qquad \theta_O = h_O\,. \end{aligned} \tag{I.77}$$

These can be easily evaluated using the results in Tabs. I.2 to I.4.

I.6 Conclusions

In this work we have calculated the vacuum expectation value, the meson mass and the meson decay constant in effective field theory to NNLO for the three cases with a simple underlying vector gauge groups and N_F equal mass

fermions in the same representation. We discussed the complex case (QCD), real representation (Adjoint) and pseudo-real representation (2-colour).

The three flavour cases have been calculated earlier at NNLO for the QCD case for the mass, decay constant [31, 38] and condensate [31]. For two flavour QCD the NNLO expressions exists for the mass and decay constants [18, 19, 30, 34, 35]. For the N_F flavour case the mass, decay constant and the condensate can be found in [16] to NLO. The NNLO expressions here are new. Note that the equal mass case considered here leads to considerably simpler expressions than those of [33, 38]. We have a slightly different NLO divergence structure for the two-colour case then [12] but agree with their explicit NLO expressions for the mass, decay constant and vacuum expectation value. Again the NNLO expressions here are new. The adjoint case we have extended to NLO in general and to NNLO for the mass, decay constant and vacuum expectation value. Notice that for all three cases the coefficient of the leading logarithm at NNLO is fully determined but that the coefficient of the subleading logarithm at NNLO for the vacuum expectation value depends on LECs that can be determined from the mass at NLO.

The main motivation behind this work is that these expressions should be useful for extrapolations to zero mass in lattice calculations for dynamical electroweak symmetry breaking.

Acknowledgements

This work is supported by the Marie Curie Early Stage Training program "HEP-EST" (contract number MEST-CT-2005-019626), European Commission RTN network, Contract MRTN-CT-2006-035482 (FLAVIAnet), European Community-Research Infrastructure Integrating Activity "Study of Strongly Interacting Matter" (HadronPhysics2, Grant Agreement n. 227431) and the Swedish Research Council.

	QCD
a_M	$-\frac{1}{N_F}$
b_M	$8N_F\left(2L_6^r - L_4^r\right) + 8\left(2L_8^r - L_5^r\right)$
c_M	$-\frac{1}{2} + \frac{9}{2N_F^2} + \frac{3}{8}N_F^2$
d_M	$8L_0^r(-\frac{3}{N_F} + N_F) + 8L_1^r(-1 + 2N_F^2) + 4L_2^r(4 + N_F^2) + L_3^r(-\frac{24}{N_F} + 20N_F)$
	$+L_4^r(40 - 16N_F^2) + L_5^r(\frac{40}{N_F} - 16N_F) + L_6^r(-16 + 16N_F^2) + L_8^r(-\frac{80}{N_F} + 32N_F)$
e_M	$-\frac{5}{3} + \frac{4}{N_F^2} + \frac{19}{16}N_F^2$
f_M	$-32K_{17}^r - 16K_{19}^r - 16K_{23}^r + 48K_{25}^r + 32K_{39}^r$
	$+N_F\left(-32K_{18}^r - 16K_{20}^r - 16K_{21}^r + 48K_{26}^r + 32K_{40}^r\right)$
	$+N_F^2\left(-16K_{22}^r + 48K_{27}^r\right) + 64(N_F L_4^r + L_5^r)(N_F L_4^r + L_5^r - 2N_F L_6^r - 2L_8^r)$
g_M	$-\frac{4}{N_F}(L_0^r + L_3^r) + 4L_1^r + 2N_F(2L_0^r + L_3^r) + 2N_F^2 L_2^r$
	$-8[L_4^r - 2L_6^r + \frac{1}{N_F}(L_5^r - 2L_8^r)]$
h_M	$-\frac{1}{4} + \frac{3}{4}\frac{1}{N_F^2} + \frac{169}{384}N_F^2$
	Adjoint
a_M	$\frac{1}{2} - \frac{1}{2N_F}$
b_M	$16N_F(2L_6^r - L_4^r) + 8(2L_8^r - L_5^r)$
c_M	$\frac{3}{8}\left(1 + \frac{3}{N_F^2} - \frac{4}{N_F} + N_F + N_F^2\right)$
d_M	$L_0^r(12 - 12\frac{1}{N_F} + 8N_F) + 8L_1^r(-1 + 2N_F + 4N_F^2)$
	$+4L_2^r(4 + N_F + 2N_F^2) + L_3^r(12 - \frac{12}{N_F} + 20N_F)$
	$+L_4^r(40 - 40N_F - 32N_F^2) + L_5^r(-20 + \frac{20}{N_F} - 16N_F)$
	$+16L_6^r(-1 + 3N_F + 2N_F^2) + L_8^r(40 - \frac{40}{N_F} + 32N_F)$
e_M	$-\frac{2}{3} + \frac{1}{N_F^2} - \frac{3}{4}\frac{1}{N_F} + \frac{77}{48}N_F + \frac{19}{16}N_F^2$
f_M	$r_{MA}^r + 64(2N_F L_4^r + L_5^r)(2N_F L_4^r + L_5^r - 4N_F L_6^r - 2L_8^r)$
g_M	$2L_0^r(1 - \frac{1}{N_F} + 2N_F) + 4L_1^r + 2N_F L_2^r(1 + 2N_F) + 2L_3^r(1 - \frac{1}{N_F} + N_F)$
	$-8(1 - N_F)(L_4^r - 2L_6^r) + 4(1 - \frac{1}{N_F})(L_5^r - 2L_8^r)$
h_M	$-\frac{1}{16} + \frac{3}{16}\frac{1}{N_F^2} - \frac{3}{16}\frac{1}{N_F} + \frac{193}{384}N_F + \frac{169}{384}N_F^2$
	2-colour
a_M	$-\frac{1}{2} - \frac{1}{2N_F}$
b_M	$16N_F(2L_6^r - L_4^r) + 8(2L_8^r - L_5^r)$
c_M	$\frac{3}{8}\left(1 + \frac{3}{N_F^2} + \frac{4}{N_F} - N_F + N_F^2\right)$
d_M	$L_0^r(-12 - 12\frac{1}{N_F} + 8N_F) + 8L_1^r(-1 - 2N_F + 4N_F^2)$
	$+4L_2^r(4 - N_F + 2N_F^2) + L_3^r(-12 - \frac{12}{N_F} + 20N_F)$
	$+L_4^r(40 + 40N_F - 32N_F^2) + L_5^r(20 + \frac{20}{N_F} - 16N_F)$
	$+16L_6^r(-1 - 3N_F + 2N_F^2) + L_8^r(-40 - \frac{40}{N_F} + 32N_F)$
e_M	$-\frac{2}{3} + \frac{1}{N_F^2} + \frac{3}{4}\frac{1}{N_F} - \frac{77}{48}N_F + \frac{19}{16}N_F^2$
f_M	$r_{MT}^r + 64(2N_F L_4^r + L_5^r)(2N_F L_4^r + L_5^r - 4N_F L_6^r - 2L_8^r)$
g_M	$-2L_0^r(1 + \frac{1}{N_F} - 2N_F) + 4L_1^r - 2N_F L_2^r(1 - 2N_F) - 2L_3^r(1 + \frac{1}{N_F} - N_F)$
	$-8(1 + N_F)(L_4^r - 2L_6^r) - 4(1 + \frac{1}{N_F})(L_5^r - 2L_8^r)$
h_M	$-\frac{1}{16} + \frac{3}{16}\frac{1}{N_F^2} + \frac{3}{16}\frac{1}{N_F} - \frac{193}{384}N_F + \frac{169}{384}N_F^2$

Table I.3: The coefficients $a_M, \ldots, g_M$ appearing in the expansion of the mass.

	QCD
a_F	$\frac{1}{2}N_F$
b_F	$4N_F L_4^r + 4L_5^r$
c_F	$-\frac{1}{2} - \frac{3}{16}N_F^2$
d_F	$\frac{4}{N_F}(3L_0^r + 3L_3^r - L_5^r) + 4L_1^r - 8L_2^r - 4L_4^r + N_F(-4L_0^r - 10L_3^r - 2L_5^r + 8L_8^r)$ $+2N_F^2(-4L_1^r - L_2^r - L_4^r + 4L_6^r)$
e_F	$\frac{2}{3} - \frac{1}{2N_F^2} - \frac{59}{96}N_F^2$
f_F	$-8\left(N_F L_4^r + L_5^r\right)^2 + 8(K_{19}^r + K_{23}^r) + 8N_F(K_{20}^r + K_{21}^r) + 8N_F^2 K_{22}^r$
g_F	$\frac{2}{N_F}(L_0^r + L_3^r) - 2L_1^r + N_F(-2L_0^r - L_3^r + 4L_5^r - 8L_8^r) + N_F^2(-L_2^r + 4L_4^r - 8L_6^r)$
h_F	$-\frac{7}{24} + \frac{7}{8N_F^2} + \frac{1}{768}N_F^2$
	Adjoint
a_F	$\frac{1}{2}N_F$
b_F	$8N_F L_4^r + 4L_5^r$
c_F	$-\frac{1}{4} + \frac{3}{16}N_F - \frac{3}{16}N_F^2$
d_F	$L_0^r(-6 + \frac{6}{N_F} - 4N_F) + 4L_1^r(1 - 2N_F - 4N_F^2) - 2L_2^r(4 + N_F + 2N_F^2)$ $+L_3^r(-6 + \frac{6}{N_F} - 10N_F) - 4L_4^r(1 - N_F + N_F^2) + 2L_5^r(1 - \frac{1}{N_F} - N_F)$ $+8N_F(2N_F L_6^r + L_8^r)$
e_F	$\frac{7}{24} - \frac{1}{8N_F^2} + \frac{1}{8N_F} - \frac{29}{32}N_F - \frac{59}{96}N_F^2$
f_F	$r_{FA}^r - 8(2N_F L_4^r + L_5^r)^2$
g_F	$L_0^r(-1 + \frac{1}{N_F} - 2N_F) - 2L_1^r + L_2^r(-N_F - 2N_F^2) + L_3^r(-1 + \frac{1}{N_F} - N_F)$ $8N_F^2(L_4^r - 2L_6^r) + 4N_F(L_5^r - 2L_8^r)$
h_F	$-\frac{7}{96} + \frac{7}{32}\frac{1}{N_F^2} - \frac{7}{32}\frac{1}{N_F} + \frac{19}{256}N_F + \frac{1}{768}N_F^2$
	2-colour
a_F	$\frac{1}{2}N_F$
b_F	$8N_F L_4^r + 4L_5^r$
c_F	$-\frac{1}{4} - \frac{3}{16}N_F - \frac{3}{16}N_F^2$
d_F	$L_0^r(6 + \frac{6}{N_F} - 4N_F) + 4L_1^r(1 + 2N_F - 4N_F^2) - 2L_2^r(4 - N_F + 2N_F^2)$ $+L_3^r(6 + \frac{6}{N_F} - 10N_F) - 4L_4^r(1 + N_F + N_F^2) - 2L_5^r(1 + \frac{1}{N_F} + N_F)$ $+8N_F(2N_F L_6^r + L_8^r)$
e_F	$\frac{7}{24} - \frac{1}{8N_F^2} - \frac{1}{8N_F} + \frac{29}{32}N_F - \frac{59}{96}N_F^2$
f_F	$r_{FT}^r - 8(2N_F L_4^r + L_5^r)^2$
g_F	$L_0^r(1 + \frac{1}{N_F} - 2N_F) - 2L_1^r + L_2^r(N_F - 2N_F^2) + L_3^r(1 + \frac{1}{N_F} - N_F)$ $8N_F^2(L_4^r - 2L_6^r) + 4N_F(L_5^r - 2L_8^r)$
h_F	$-\frac{7}{96} + \frac{7}{32}\frac{1}{N_F^2} + \frac{7}{32}\frac{1}{N_F} - \frac{19}{256}N_F + \frac{1}{768}N_F^2$

Table I.4: The coefficients $a_F, \ldots, g_F$ appearing in the expansion of the decay constant.

I References

[1] S. Weinberg, "Phenomenological Lagrangians," *Physica A* **96** (1979) 327. pages

[2] J. Gasser, H. Leutwyler, "Chiral Perturbation Theory To One Loop," *Annals Phys.* **158** (1984) 142. pages

[3] J. Gasser, H. Leutwyler, "Chiral Perturbation Theory: Expansions In The Mass Of The Strange Quark," *Nucl. Phys.* (1985) 465. pages

[4] M. E. Peskin, "The Alignment Of The Vacuum In Theories Of Technicolor," *Nucl. Phys.* (1980) 197. pages

[5] J. Preskill, "Subgroup Alignment In Hypercolor Theories," *Nucl. Phys.* (1981) 21. pages

[6] S. Dimopoulos, "Technicolored Signatures," *Nucl. Phys.* (1980) 69. pages

[7] T. Appelquist, A. Avakian, R. Babich, R. C. Brower, M. Cheng, M. A. Clark, S. D. Cohen, G. T. Fleming *et al.*, "Toward TeV Conformality," *Phys. Rev. Lett.* **104** (2010) 071601, arXiv:0910.2224. pages

[8] A. Deuzeman, M. P. Lombardo and E. Pallante, "The physics of eight flavours," *Phys. Lett.* (2008) 41, arXiv:0804.2905. pages

[9] C. Pica, L. Del Debbio, B. Lucini, A. Patella and A. Rago, "Technicolor on the Lattice," arXiv:0909.3178. pages

[10] T. DeGrand, Y. Shamir and B. Svetitsky, "Phase structure of SU(3) gauge theory with two flavors of symmetric-representation fermions," *Phys. Rev. D* **79** (2009) 034501, arXiv:0812.1427. pages

[11] S. Catterall, J. Giedt, F. Sannino and J. Schneible, "Phase diagram of SU(2) with 2 flavors of dynamical adjoint quarks," *JHEP* **0811** (2008) 009, arXiv:0807.0792. pages

[12] J. B. Kogut, M. A. Stephanov, D. Toublan, J. J. M. Verbaarschot and A. Zhitnitsky, "QCD-like theories at finite baryon density," *Nucl. Phys.* (2000) 477, arXiv:hep-ph/0001171. pages

[13] Y. I. Kogan, M. A. Shifman and M. I. Vysotsky, "Spontaneous Breaking Of Chiral Symmetry For Real Fermions And N=2 Susy Yang-Mills Theory," *Sov. J. Nucl. Phys.* **42** (1985) 318. pages

[14] H. Leutwyler and A. V. Smilga, "Spectrum of Dirac operator and role of winding number in QCD," *Phys. Rev. D* **46** (1992) 5607. pages

[15] A. V. Smilga and J. J. M. Verbaarschot, "Spectral Sum Rules And Finite Volume Partition Function In Gauge Theories With Real And Pseudoreal Fermions," *Phys. Rev. D* **51** (1995) 829, arXiv:hep-th/9404031. pages

[16] J. Gasser and H. Leutwyler, "Light Quarks at Low Temperatures," *Phys. Lett.* (1987) 83. pages

[17] K. Splittorff, D. Toublan and J. J. M. Verbaarschot, "Diquark condensate in QCD with two colors at next-to-leading order," *Nucl. Phys.* (2002) 290, arXiv:hep-ph/0108040. pages

[18] J. Bijnens, G. Colangelo and G. Ecker, "The mesonic chiral Lagrangian of order p^6," *JHEP* **9902** (1999) 020, arXiv:hep-ph/9902437. pages

[19] J. Bijnens, G. Colangelo and G. Ecker, "Renormalization of chiral perturbation theory to order p^6," *Annals Phys.* **280** (2000) 100, arXiv:hep-ph/9907333. pages

[20] S. R. Coleman, J. Wess and B. Zumino, "Structure of phenomenological Lagrangians. 1," *Phys. Rev.* **177** (1969) 2239. pages

[21] S. R. Coleman, J. Wess and B. Zumino, "Structure of phenomenological Lagrangians. 2," *Phys. Rev.* **177** (1969) 2247. pages

[22] A. Pich, "Effective field theory: Course," arXiv:hep-ph/9806303. Lectures at Les Houches Summer School in Theoretical Physics, Session 68: Probing the Standard Model of Particle Interactions, Les Houches, France, 28 Jul - 5 Sep 1997. pages

[23] S. Scherer, "Introduction to chiral perturbation theory," *Adv. Nucl. Phys.* **27** (2003) 277, arXiv:hep-ph/0210398. pages

[24] S. Scherer, "A Chiral perturbation theory primer," arXiv:hep-ph/0505265. pages

[25] G. Ecker, "Strong interactions of light flavors," arXiv:hep-ph/0011026. Lectures given at Advanced School on Quantum Chromodynamics (QCD 2000), Benasque, Huesca, Spain, 3-6 Jul 2000. pages

[26] J. Gasser, "Light-quark dynamics," in *Lect. Notes Phys.*, vol. 629, pp. 1–35. 2004. arXiv:hep-ph/0312367. Lectures given at 41st Internationale Universitaetswochen fuer Theoretische Physik (International University School of Theoretical Physics): Flavor Physics (IUTP 41), Schladming, Styria, Austria, 22-28 Feb 2003. pages

[27] H. Leutwyler, "Chiral dynamics," in *At the frontier of particle physics: Contribution to the Festschrift in honor of B.L. Ioffe*, M. Shifman, ed., vol. 1, pp. 271–316. 2000. arXiv:hep-ph/0008124. pages

[28] H. Leutwyler, "Principles of chiral perturbation theory," arXiv:hep-ph/9406283. lectures given at the Hadrons 94 Workshop, Gramado, Brazil, 10-14 Apr 1994. pages

[29] J. A. M. Vermaseren, "New features of FORM," arXiv:math-ph/0010025. pages

[30] J. Gasser, M. E. Sainio, "Two loop integrals in chiral perturbation theory," *Eur. Phys. J.* (1998) 297–306, arXiv:hep-ph/9803251. pages

[31] G. Amoros, J. Bijnens, P. Talavera, "K(lepton 4) form-factors and pi pi scattering," *Nucl. Phys.* (2000) 293–352, [Erratum-ibid. B 598 (2001) 665]:arXiv:hep-ph/0003258. pages

[32] J. Bijnens and K. Ghorbani, "Finite volume dependence of the quark-antiquark vacuum expectation value," *Phys. Lett.* (2006) 51–55, arXiv:hep-lat/0602019. pages

[33] G. Amoros, J. Bijnens, P. Talavera, "Two point functions at two loops in three flavor chiral perturbation theory," *Nucl. Phys.* (2000) 319–363, arXiv:hep-ph/9907264. pages

[34] U. Burgi, "Charged Pion Polarizabilities to two Loops," *Phys. Lett.* (1996) 147–152, arXiv:hep-ph/9602421. pages

[35] U. Burgi, "Charged pion pair production and pion polarizabilities to two loops," *Nucl. Phys.* (1996) 392–426, arXiv:hep-ph/9602429. pages

[36] J. Bijnens, G. Colangelo, G. Ecker, J. Gasser, M. E. Sainio, "Elastic pi pi scattering to two loops," *Phys. Lett.* (1996) 210–216, arXiv:hep-ph/9511397. pages

[37] J. Bijnens, G. Colangelo, G. Ecker, J. Gasser, M. E. Sainio, "Pion pion scattering at low-energy," *Nucl. Phys.* (1996) 210–216, arXiv:hep-ph/9511397. pages

[38] E. Golowich and J. Kambor, "Two loop analysis of axial vector current propagators in chiral perturbation theory," *Phys. Rev. D* **58** (1998) 036004, arXiv:hep-ph/9710214. pages

[39] J. Noaki *et al.* [JLQCD and TWQCD Collaboration], "Convergence of the chiral expansion in two-flavor lattice QCD," *Phys. Rev. Lett.* **101** (2008) 202004, arXiv:0806.0894. pages

II

Meson-meson Scattering in QCD-like Theories

Johan Bijnens and Jie Lu

Department of Astronomy and Theoretical Physics, Lund University,
Sölvegatan 14A, SE–223 62 Lund, Sweden
http://www.thep.lu.se/

Journal of High Energy Physics **1103** (2011) 028
arXiv:1102.0172 [hep-ph].

We discuss meson-meson scattering at next-to-next-to-leading order in the chiral expansion for QCD-like theories with general n degenerate flavours for the cases with a complex, real and pseudo-real representation. I.e. with global symmetry and breaking pattern $SU(n)_L \times SU(n)_R \to SU(n)_V$, $SU(2n) \to SO(2n)$ and $SU(2n) \to Sp(2n)$. We obtain fully analytical expressions for all these cases. We discuss the general structure of the amplitude and the structure of the possible intermediate channels for all three cases. We derive the expressions for the lowest partial wave scattering length in each channel and present some representative numerical results. We also show various relations between the different cases in the limit of large n.

II.1 Introduction

In an earlier paper [1] we started the phenomenology of QCD-like theories at next-to-next-to-leading (NNLO) order in the light mass expansion in their respective low-energy effective theories. The motivation for this work is that these theories are interesting as variations on QCD and could play some role as models for a nonperturbative Higgs sector. Early work in this context are the technicolor variations of [2–4]. Recent reviews of more modern developments are [5, 6]. Lattice calculations have started to explore these type of theories as well, some references are [7–13]. The main interest in these theories is in the massless limit but lattice simulations are necessarily performed at a finite fermion mass. In [1] we worked out a number of simple observables, the mass, decay constant and vacuum-expectation-value to NNLO in these theories. Here we work out the amplitude for meson-meson scattering to the same order. In lattice calculations the amplitude for meson-meson scattering is not directly accessible but the scattering lengths can be derived from the dependence on the volume of the lattice [14]. We therefore also provide explicit expressions for the scattering lengths.

The EFT relevant for dynamical electroweak symmetry breaking can have different patterns of spontaneous breaking of the global symmetry than QCD. The resulting Goldstone Bosons, or pseudo-Goldstone bosons in the presence of mass terms, are thus in different manifolds and the low-energy EFT is also different.

In this paper we only discuss the same cases as in [1] where the underlying strong interaction is vectorlike and all fermions have the same mass. Three main patterns of global symmetry show up. A thorough discussion tree level or lowest order (LO) is [15]. With n fermions[1] in a complex representation the global symmetry group is $SU(n)_L \times SU(n)_R$ and it is expected to be spontaneously broken to the diagonal subgroup $SU(n)_V$. This is the direct extension of the QCD case. For n fermions in a real representation the global symmetry group is $SU(2n)$ and it is expected to be spontaneously broken to $SO(2n)$. In the case of two colours and n fermions in the fundamental (pseudo-real) representation the global symmetry group is again $SU(2n)$ but here it is expected to be spontaneously broken to an $Sp(2n)$ subgroup. Earlier references are [16–18]. Some earlier work for the complex case and the pseudo-real case at NLO can be found in [19–21].

In the remainder of this paper we refer to the complex representation case as complex or QCD, the real representation case as adjoint or real and the pseudo-real representation case as two-colour or pseudo-real. In [1] we extended the construction of the general Lagrangian to NLO[2] including the di-

[1] We use n rather than N_F for the number of flavours since it makes the formulas shorter.

[2] References to some related work can be found in [6].

vergence structure. The NNLO for the QCD case is in [22] and the divergence structure in [23]. The Lagrangian constructed in [22] is with the changes discussed in [1] and in Sect. II.2 also a complete Lagrangian for the other two cases but we have not shown it to be minimal nor calculated the divergence structure.

We do not repeat the discussion of the three different cases at the underlying fermion (quark) level. This can be found in [15] and [1], Sect. 2. In Sect. II.2 we quote the structure of the effective field theories for the three cases but we again refer to [1] for more details. Sect. II.3 discusses in detail the general structure of the amplitude. The amplitude can be expressed in terms of two functions $B(s,t,u)$ and $C(s,t,u)$ which are generalizations of the amplitude $A(s,t,u)$ in $\pi\pi$-scattering [24]. We work out the possible intermediate states using the relevant group theory and using a projection operator formalism obtain the amplitudes in the different channels. The results for the amplitude are discussed in Sect. II.4 and for the scattering lengths in Sect. II.5. Here we present some representative numerical results for the scattering lengths as well as some large n relations between the different cases. The lengthier formulas at two-loop order are given in an appendix. This work needed a few more integrals at intermediate stages than [25, 26], these are given in App. III.1. In Sect. II.6 we summarize our results.

II.2 Effective Field Theory

II.2.1 Generators

The notation for the three cases can be brought in a very similar form. More details can be found in [1]. The Goldstone boson live on a manifold G/H where G is the full global symmetry group and H is the part that remains unbroken after spontaneous symmetry-breaking. We label the unbroken generators as T^a and the broken ones as X^a.

The space $SU(n) \times SU(n)/SU(n)$ is isomorphic to $SU(n)$ so we use the X^a as the generators of $SU(n)$ for the QCD case. They are traceless, hermitian $n \times n$ matrices.

The adjoint or real case has the generators in $SU(2n)/SO(2n)$ where the broken generators satisfy

$$J_S X^a = (X^a)^T J_S\,, \quad \text{with} \quad J_S = \begin{pmatrix} 0 & I \\ I & 0 \end{pmatrix}. \tag{II.1}$$

I is the $n \times n$ unit matrix and the superscript T indicates the transpose. The X^a are traceless, hermitian $2n \times 2n$ matrices in this case. Multiplying (II.1) with J_S

from left and right leads immediately to

$$X^a J_S = J_S \left(X^a\right)^T . \tag{II.2}$$

The two-colour or pseudo-real case has the generators in $SU(2n)/Sp(2n)$ where the broken generators satisfy

$$J_A X^a = \left(X^a\right)^T J_A , \quad \text{with} \quad J_A = \begin{pmatrix} 0 & -I \\ I & 0 \end{pmatrix} . \tag{II.3}$$

The X^a are traceless, hermitian $2n \times 2n$ matrices also in this case. Multiplying (II.3) with J_A similar to above gives

$$X^a J_A = J_A \left(X^a\right)^T . \tag{II.4}$$

The unbroken generators satisfy

$$\begin{aligned} SO(2n): &\qquad T^a J_S + J_S T^{aT} = 0 , \\ Sp(2n): &\qquad T^a J_S + J_S T^{aT} = 0 . \end{aligned} \tag{II.5}$$

This allows in both cases to derive using $J = J_S$ or $J = J_A$ respectively:

$$h^\dagger J = J h^T \quad \text{with} \quad h = \exp i h^a T^2 . \tag{II.6}$$

We always use generators normalized to one:

$$\langle T^a T^b \rangle = \langle X^a X^b \rangle = \delta^{ab} . \tag{II.7}$$

$\langle A \rangle = \mathrm{tr}_F(A)$, is the trace over the flavour indices. This is over n for the QCD case and $2n$ for the real and pseudo-real case.

During the course of the calculation, we often have to sum over the Goldstone Bosons. These sums can be easily performed using

$$\begin{aligned}
&\text{complex :} \\
\mathrm{tr}_F\left(X^a A X^a B\right) &= \mathrm{tr}_F(A)\,\mathrm{tr}_F(B) - \frac{1}{n}\mathrm{tr}_F(AB) , \\
\mathrm{tr}_F\left(X^a A\right)\mathrm{tr}_F\left(X^a B\right) &= \mathrm{tr}_F(AB) - \frac{1}{n}\mathrm{tr}_F(A)\,\mathrm{tr}_F(B) . \\
&\text{Real :} \\
\mathrm{tr}_F\left(X^a A X^a B\right) &= \frac{1}{2}\mathrm{tr}_F(A)\,\mathrm{tr}_F(B) + \frac{1}{2}\mathrm{tr}_F\left(A J_S B^T J_S\right) - \frac{1}{2n}\mathrm{tr}_F(AB) , \\
\mathrm{tr}_F\left(X^a A\right)\mathrm{tr}_F\left(X^a B\right) &= \frac{1}{2}\mathrm{tr}_F(AB) + \frac{1}{2}\mathrm{tr}_F\left(A J_S B^T J_S\right) - \frac{1}{2n}\mathrm{tr}_F(A)\,\mathrm{tr}_F(B) . \\
&\text{Pseudoreal :} \\
\mathrm{tr}_F\left(X^a A X^a B\right) &= \frac{1}{2}\mathrm{tr}_F(A)\,\mathrm{tr}_F(B) + \frac{1}{2}\mathrm{tr}_F\left(A J_A B^T J_A\right) - \frac{1}{2n}\mathrm{tr}_F(AB) , \\
\mathrm{tr}_F\left(X^a A\right)\mathrm{tr}_F\left(X^a B\right) &= \frac{1}{2}\mathrm{tr}_F(AB) - \frac{1}{2}\mathrm{tr}_F\left(A J_A B^T J_A\right) \\
&\quad - \frac{1}{2n}\mathrm{tr}_F(A)\,\mathrm{tr}_F(B) .
\end{aligned} \tag{II.8}$$

There is a relation that the broken generators satisfy for the real and pseudo-real case.

$$\mathrm{tr}_F\left(X^a X^b \dots X^k X^l\right) = \mathrm{tr}_F\left(X^l X^k \dots X^b X^a\right) . \tag{II.9}$$

The proof for the real case is

$$\begin{aligned}
\mathrm{tr}_F\left(X^a X^b \dots X^k X^l\right) &= \mathrm{tr}_F\left(X^a X^b \dots X^k X^l J_S^2\right) \\
&= \mathrm{tr}_F\left(X^a X^b \dots X^k J_S X^{lT} J_S\right) \\
&= \mathrm{tr}_F\left(X^a X^b \dots J_S X^{kT} X^{lT} J_S\right) \\
&= \mathrm{tr}_F\left(J_S X^{aT} X^{bT} \dots X^{kT} X^{lT} J_S\right) \\
&= \mathrm{tr}_F\left(X^{aT} X^{bT} \dots X^{kT} X^{lT}\right) \\
&= \mathrm{tr}_F\left(\left(X^l X^k \dots X^b X^a\right)^T\right) \\
&= \mathrm{tr}_F\left(X^l X^k \dots X^b X^a\right)
\end{aligned} \tag{II.10}$$

The pseudo-real case is proven by replacing J_S^2 by $-J_A^2$ and following the same steps. (II.9) is also the reason why the Lagrangian in [22] is not minimal for the real and pseudo-real case.

In the group theory references there is a conjecture mentioned that to get from $SO(2n)$ to $Sp(2n)$ it is sufficient to take $n \to -n$. This feature is indeed visible in most of our formulas.

II.2.2 Lagrangians

As described in more detail in [1] we can write the Lagrangians in the three cases in a very similar way. The Goldstone Boson manifold G/H is parametrized by

$$u = \exp\left(\frac{i}{\sqrt{2}F}\phi\right) , \quad \phi = \phi^a X^a . \tag{II.11}$$

These transform under the symmetry transformation in the QCD case for $g_L \times g_R \in SU(n)_L \times SU(n)_R$ as

$$u \to g_R u h(g_L, g_R, \phi)^\dagger = h(g_L, g_R, \phi) u g_L^\dagger . \tag{II.12}$$

h is the socalled compensator field and is defined by (II.12) and is also an $SU(n)$ matrix. This can be derived from the standard general formulation [27, 28] as done in [1]. For a transformation in the conserved part of the group we have that $g_L = g_R = g_V$ and $h = g_V$.

The notation for the other two cases is directly that of [27,28]. A symmetry transformation $g \in G = SU(2n)$ transforms u as

$$u \to g\, u\, h(g,\phi)^\dagger\,, \quad \text{with} \quad h = \exp\left(i h^a T^a\right)\,. \tag{II.13}$$

I.e. h is in the unbroken part H of the group. In case the transformation g is in the conserved part of the group, $g \in H$, we have that $h = g$.

We can now define the quantities

$$\begin{aligned} u_\mu &= i\left(u^\dagger \partial_\mu u - u \partial_\mu u^\dagger\right)\,, \\ \Gamma_\mu &= \frac{1}{2}\left(u^\dagger \partial_\mu u - u \partial_\mu u^\dagger\right)\,. \end{aligned} \tag{II.14}$$

Under the group transformation in all cases we have $u_\mu \to h u_\mu h^\dagger$ and Γ_μ can be used to define a covariant derivative.

$$\nabla_\mu u_\nu \equiv \partial_\mu u_\nu + \Gamma_\mu u_\nu - u_\nu \Gamma_\mu \to h \nabla_\mu u_\nu h^\dagger\,. \tag{II.15}$$

In [1] we also showed how the external fields can be included in a similar way as for the QCD case in [19,29]. In particular the quark masses can be put in a quantity $\chi_\pm$ that transforms as $\chi_\pm \to h \chi_\pm h^\dagger$.

The lowest order Lagrangian takes on the standard form

$$\mathcal{L}_{LO} = \frac{F^2}{4} \mathrm{tr}_F\left(u_\mu u^\mu + \chi_+\right) \tag{II.16}$$

for all three cases and the same is true for the NLO Lagrangian.

$$\begin{aligned} \mathcal{L}_{NLO} &= L_0 \langle u^\mu u^\nu u_\mu u_\nu\rangle + L_1 \langle u^\mu u_\mu\rangle\langle u^\nu u_\nu\rangle + L_2 \langle u^\mu u^\nu\rangle\langle u_\mu u_\nu\rangle \\ &\quad + L_3 \langle u^\mu u_\mu u^\nu u_\nu\rangle + L_4 \langle u^\mu u_\mu\rangle\langle \chi_+\rangle + L_5 \langle u^\mu u_\mu \chi_+\rangle + L_6 \langle \chi_+\rangle^2 \\ &\quad + L_7 \langle \chi_-\rangle^2 + \frac{1}{2} L_8 \langle \chi_+^2 + \chi_-^2\rangle\,. \end{aligned} \tag{II.17}$$

We have kept only the terms contributing to meson-meson scattering in (II.17).

The NNLO Lagrangian is known for the complex or QCD case [22] as well as its divergence structure [23]. The same Lagrangian with the changes mentioned above is complete for the other two cases but probably not minimal. We have nonetheless chosen to leave the contributions from those terms in the results quoted here.

II.2.3 Renormalization

We use the standard renormalization procedure in ChPT [19,29] with the extension to NNLO described in great detail in [23,26]. The divergences at NLO are canceled by the subtractions as calculated in [1]. At NNLO the divergences

for the QCD case are canceled by the subtractions calculated in [23]. The other two cases satisfy all the expected constraints. Nonlocal divergences fully cancel, the ϵ parts of the loop integrals as defined in App. III.1 always cancel and the double divergences satisfy the Weinberg relations [23].

As usual in ChPT we apply the $\overline{MS}$ scheme of dimensional regularization, in which the bare LECs L_i are defined as

$$L_i = (c\mu)^{d-4}\left[\Gamma_i \Lambda + L_i^r(\mu)\right] \tag{II.18}$$

Where the dimension $d = 4 - 2\epsilon$, and

$$\Lambda = \frac{1}{16\pi^2(d-4)}\,, \tag{II.19}$$

$$\ln c = -\frac{1}{2}[\ln 4\pi + \Gamma'(1) + 1]\,. \tag{II.20}$$

The coefficients Γ_i can be found in [1,29] for the complex and in [1] for the real and pseudo-real$Sp(2n)$ case.

The NNLO terms can be made finite with the subtractions

$$K_i = (c\mu)^{2(d-4)}\left[K_i^r - \Gamma_i^{(2)}\Lambda^2 - \left(\frac{1}{16\pi^2}\Gamma_i^{(1)} + \Gamma_i^{(L)}\right)\Lambda\right]\,. \tag{II.21}$$

The coefficients $\Gamma_i^{(2)}$, $\Gamma_i^{(1)}$ and $\Gamma_i^{(L)}$ for the complex case have been derived in [23]. For the real and pseudo-real case, the results do not exist. We have checked that all remaining divergences are local and can thus be subtracted.

II.3 General results for the amplitudes

II.3.1 $\pi\pi$ case

The $\pi\pi$ scattering amplitude, which correspond to the QCD case with $n = 2$ is well known. Due to crossing and the possible $SU(2)$ (isospin) invariants the amplitude can be written as [24,30]

$$M_{\pi\pi}(s,t,u) = \delta^{ab}\delta^{cd}A(s,t,u) + \delta^{ac}\delta^{bd}A(t,u,s) + \delta^{ad}\delta^{bc}A(u,s,t)\,. \tag{II.22}$$

The function $A(s,t,u)$ is symmetric under the interchange of t and u.

The possible states of two pions are isospin 0, 1 or 2. The amplitude for the three channels are given by [30]

$$\begin{aligned} T^0(s,t,u) &= 3A(s,t,u) + A(t,s,u) + A(u,t,s), \\ T^1(s,t,u) &= A(t,s,u) - A(u,s,t), \\ T^2(s,t,u) &= A(t,s,u) + A(u,s,t). \end{aligned} \tag{II.23}$$

Where I is isospin, and P_I is the projection operator on isospin I They satisfy the relation

$$M_{\pi\pi}(s,t,u) = \sum_{I=0,2} T^I(s,t,u) P_I. \tag{II.24}$$

and

$$T^I(s,t,u) P_I \text{ (no sum)} = P_I M_{\pi\pi}(s,t,u)\,. \tag{II.25}$$

In the remainder of this section we will generalize these results. (II.22) is generalized in terms of two functions in Sect. II.3.2. The possible intermediate states and the corresponding amplitudes are derived for the three cases separately in the last three subsections of this section.

II.3.2 General amplitude

The amplitude for meson-meson scattering is given by

$$\langle \phi^c(p_c)\phi^d(p_d)|\phi^a(p_a)\phi^b(p_d)\rangle = M(s,t,u)\,. \tag{II.26}$$

The Mandelstam variables s,t,u are defined by

$$s = (p_a+p_b)^2/M^2_{\text{phys}}\,, \qquad t = (p_a-p_c)^2/M^2_{\text{phys}}\,, \qquad u = (p_a-p_d)^2/M^2_{\text{phys}}\,. \tag{II.27}$$

These satisfy

$$s+t+u = 4\,. \tag{II.28}$$

We have chosen here to use the dimensionless versions in order to simplify later formulas.

The flavour structure of the amplitude for meson-meson scattering can be described by constructing all possible invariants from the four corresponding generator matrices X^e, $e = a,b,c,d$. Taking into account that $\text{tr}_F\,(X^e) = 0$ there are 9 invariants possible

$$\begin{aligned}
&\text{tr}_F\left(X^aX^bX^cX^d\right), \quad \text{tr}_F\left(X^aX^cX^dX^b\right), \quad \text{tr}_F\left(X^aX^dX^bX^c\right),\\
&\text{tr}_F\left(X^aX^dX^cX^b\right), \quad \text{tr}_F\left(X^aX^bX^dX^c\right), \quad \text{tr}_F\left(X^aX^cX^bX^d\right),\\
&\text{tr}_F\left(X^aX^b\right)\text{tr}_F\left(X^cX^d\right), \quad \text{tr}_F\left(X^aX^c\right)\text{tr}_F\left(X^bX^d\right), \quad \text{tr}_F\left(X^aX^d\right)\text{tr}_F\left(X^bX^c\right).
\end{aligned} \tag{II.29}$$

Under charge conjugation $X^a \longrightarrow X^{aT}$. This means that the amplitudes multiplying the first row in (II.29) must be the same as those multiplying the second row.[3] As a result the full amplitude can be written in terms of two invariant

[3] Alternatively use (II.9) for the real and pseudo-real case.

amplitudes $B(s,t,u)$ and $C(s,t,u)$.

$$\begin{aligned} M(s,t,u) &= \left[\mathrm{tr}_F\left(X^aX^bX^cX^d\right)+\mathrm{tr}_F\left(X^aX^dX^cX^b\right)\right]B(s,t,u) \\ &+\left[\mathrm{tr}_F\left(X^aX^cX^dX^b\right)+\mathrm{tr}_F\left(X^aX^bX^dX^c\right)\right]B(t,u,s) \\ &+\left[\mathrm{tr}_F\left(X^aX^dX^bX^c\right)+\mathrm{tr}_F\left(X^aX^cX^bX^d\right)\right]B(u,s,t) \\ &+\delta^{ab}\delta^{cd}C(s,t,u)+\delta^{ac}\delta^{bd}C(t,u,s)+\delta^{ad}\delta^{bc}C(u,s,t)\,. \end{aligned} \tag{II.30}$$

The flavour structure also implies that

$$B(s,t,u)=B(u,t,s) \qquad C(s,t,u)=C(s,u,t)\,. \tag{II.31}$$

For $n=3$ there is the Cayley-Hamilton relation

$$\sum_{6\text{ permutations}}\mathrm{tr}_F\left(X^aX^bX^cX^d\right)=\sum_{3\text{ permutations}}\mathrm{tr}_F\left(X^aX^b\right)\mathrm{tr}_F\left(X^cX^d\right)\,, \tag{II.32}$$

which allows for an ambiguity in the split of B and C. For $n=2$ we can perform all the traces with four matrices X^a in terms of Kronecker deltas.

The relation between the general amplitudes and the $\pi\pi$ scattering case (II.22) is

$$A(s,t,u)=C(s,t,u)+B(s,t,u)+B(t,u,s)-B(u,s,t)\,. \tag{II.33}$$

Note that the property (II.31) insures that $A(s,t,u)$ is symmetric under the interchange of t and u as it should be. The form (II.22) holds also for any set of pions. I.e., taking any $SU(2)$ subgroup of the unbroken group and any three of the pseudo Goldstone bosons that form a triplet under such a group, one can rewrite the general amplitude (II.30) into (II.22) using (II.33).

II.3.3 QCD case: channels and amplitudes

The Goldstone boson transform under the conserved part of the group, $SU(n)$, as

$$\phi \to h\phi h^\dagger\,. \tag{II.34}$$

This means that they are in the adjoint representation of $SU(n)$. For the $n=2,3$ case we have an isospin triplet under $SU(2)$ and an octet under $SU(3)$. The intermediate states for these are well known:

$$\begin{aligned} SU(2):\ 3\otimes 3 &= 1\oplus 3\oplus 5\ (\text{or } I=0,1,2)\,, \\ SU(3):\ 8\otimes 8 &= 1\oplus 8_S\oplus 8_A\oplus 10\oplus\overline{10}\oplus 27\,. \end{aligned} \tag{II.35}$$

The group theory for $SU(n)$ can be done in many ways. One is via Young diagrams and the second using tensor methods. We will do both. The $SU(n)$

case derived here was in fact known [31] and our results are in agreement with his. Young diagrams for $SU(n)$ are explained in [32] page 370. The Young diagrams for $SU(n)$ give

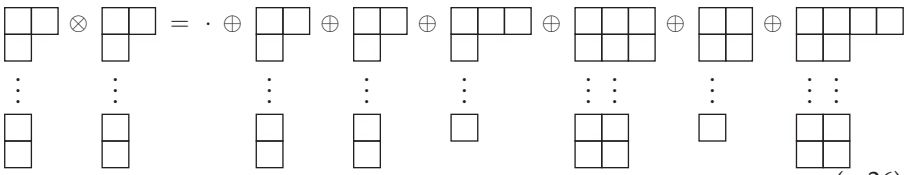

(II.36)

Note that the $\vdots$ stand for $n-5$ boxes. In terms of free indices the right hand side of (II.36) is no indices (singlet), twice one upper and one lower index (adjoint). The remaining four have all two lower and two upper indices, where the upper indices are produced from the columns with length $n-1$ and $n-2$ boxes using the Levi-Civita tensor $\epsilon^{i_1 \ldots i_n}$. For these we use the notation R_X^Y where $X = S, A$ indicate whether the lower indices are symmetric or antisymmetric and $Y = S, A$ the same for the upper indices. The decomposition (II.36) can thus be written as

$$Adj. \otimes Adj. = R_I \oplus R_S \oplus R_A \oplus + R_S^A \oplus R_A^S \oplus R_A^A \oplus R_S^S \tag{II.37}$$

The order of the irreducible representation on the right-hand side is the same in (II.36) and (II.37).

If we have a particular two-meson state $\phi^a(p_1)\phi^b(p_2)$ we have to write it in terms of states that belong to the irreducible multiplets to obtain the amplitudes for the different channels. We use a simplified notation below with $A = X^a, B = X^b, C = X^c$ and $D = X^d$ for many of the terms. All traces connecting a lower with an upper index must vanish.

- R_I: singlet representation. All indices should be contracted, so this must be proportional to $A_i^j B_j^i = \mathrm{tr}_F\,(AB)$. Summing over the n^2-1 states that are present tells us that the correct normalized state is

$$R_I = \frac{1}{\sqrt{n^2-1}} \sum_{a,b} \mathrm{tr}_F \left(X^a X^b \right) \phi^a \phi^b \,. \tag{II.38}$$

  A projection operator P_I^{abcd} that projects on the singlet component is

$$P_I^{abcd} = \frac{1}{n^2-1} \mathrm{tr}_F\,(AB)\,\mathrm{tr}_F\,(CD)\,. \tag{II.39}$$

  It can be checked that this is a projection operator

$$P_I^{abcd} P_I^{cdef} = P_I^{abef}\,, \tag{II.40}$$

  using (II.8) and $\sum_{a,b} \delta_{ab} = n^2 - 1$.

- R_S: adjoint symmetric representation. This needs in the end an upper and a lower index and must be traceless. We choose here to split up the two possible contractions of the indices of A and B in way that is symmetric under the interchange of A and B.

$$(R_S)^i_j = \sqrt{\frac{n}{2(n^2-4)}}\left[A^m_j B^i_m + B^m_j A^i_m - \frac{2}{n}\delta^i_j \mathrm{tr}_F\,(AB)\right]. \tag{II.41}$$

The last term is needed to make R_S traceless. The normalization can be worked out by checking the normalization of a particular state or by checking that the projection operator[4]

$$P_S = R_S(A,B)^i_j\, R_S(C,D)^j_i \tag{II.42}$$

has the correct normalization, its square is equal to itself. This leads finally to the projection operator

$$P_S = \frac{n}{2(n^2-4)}\left[\mathrm{tr}_F\left((AB+CD)(CD+DC)\right) - \frac{4}{n}\mathrm{tr}_F\,(AB)\,\mathrm{tr}_F\,(CD)\right]. \tag{II.43}$$

Suppressing the indices we get similar to (II.40) $P_S^2 = P_S$ and $P_S P_I = P_I P_S = 0$.

- R_A: adjoint anti-symmetric representation

$$(R_A)^i_j = \frac{1}{\sqrt{2n}}\left(A^m_j B^i{}_m - B^m_j A^i_m\right). \tag{II.44}$$

$R_A(A,B)$ is traceless and antisymmetric in A and B. The projection operator corresponding to this is

$$P_A = \frac{-1}{2n}\mathrm{tr}_F\left((AB-BA)(CD-DC)\right). \tag{II.45}$$

- R^A_S: symmetric for lower indices and antisymmetric for upper. A state here corresponds to

$$\begin{aligned}\left(R^A_S\right)^{ij}_{kl} &= \frac{1}{2}\left[A^i_k B^j_l + \frac{1}{n}\delta^i_k\left(A^j_m B^m_l - A^m_l B^j_m\right)\right] \\ &\quad -(i\leftrightarrow j)+(k\leftrightarrow l)-(i\leftrightarrow j, k\leftrightarrow l).\end{aligned} \tag{II.46}$$

The projection operator on this type of states is

$$\begin{aligned}P_{SA} &= \left(R^A_S(A,B)\right)^{ij}_{kl}\left(R^A_S(C,D)\right)^{kl}_{ij} \\ &= \frac{1}{4n}\Big[\mathrm{tr}_F\left((AB-BA)(CD-DC)\right) + n\Big(\mathrm{tr}_F\,(ACBD) \\ &\quad -\mathrm{tr}_F\,(ADBC)\Big) + n\Big(\mathrm{tr}_F\,(AC)\,\mathrm{tr}_F\,(BD) - \mathrm{tr}_F\,(AD)\,\mathrm{tr}_F\,(CD)\Big)\Big].\end{aligned} \tag{II.47}$$

[4] We suppress the superscript *abcd* from now on.

II

- R_A^S: antisymmetric for lower indices and symmetric for upper. A state here corresponds to

$$\left(R_A^S\right)_{kl}^{ij} = \frac{1}{2}\left[A_k^i B_l^j - \frac{1}{n}\delta_k^i\left(A_m^j B_l^m - A_l^m B_m^j\right)\right] + (i \leftrightarrow j) - (k \leftrightarrow l) - (i \leftrightarrow j, k \leftrightarrow l)\,. \tag{II.48}$$

The projection operator on this type of states is

$$P_{AS} = \frac{1}{4n}\Big[\mathrm{tr}_F\left((AB-BA)(CD-DC)\right) - n\Big(\mathrm{tr}_F\left(ACBD\right) - \mathrm{tr}_F\left(ADBC\right)\Big) + n\Big(\mathrm{tr}_F\left(AC\right)\mathrm{tr}_F\left(BD\right) - \mathrm{tr}_F\left(AD\right)\mathrm{tr}_F\left(CD\right)\Big)\Big]\,. \tag{II.49}$$

- R_S^S: symmetric for both upper index and lower index. The states are

$$(R_S^S)_{kl}^{ij} = \frac{1}{2}\left[A_k^i B_l^j - \frac{1}{n+2}\delta_k^i\left(A_l^m B_m^j + B_l^m A_m^j\right) + \frac{1}{(n+1)(n+2)}\delta_k^i\delta_l^j \mathrm{tr}_F\left(AB\right)\right] + (i \leftrightarrow j) + (k \leftrightarrow l) + (i \leftrightarrow j, k \leftrightarrow l) \tag{II.50}$$

and the projection operator is

$$P_{SS} = \frac{-1}{4(n+2)}\mathrm{tr}_F\left((AB+BA)(CD+DC)\right) + \frac{1}{4}\Big(\mathrm{tr}_F\left(ACBD\right) + \mathrm{tr}_F\left(ADBC\right)\Big) + \frac{1}{4}\Big(\mathrm{tr}_F\left(AC\right)\mathrm{tr}_F\left(BD\right) + \mathrm{tr}_F\left(AD\right)\mathrm{tr}_F\left(CD\right)\Big) + \frac{1}{2(n+1)(n+2)}\mathrm{tr}_F\left(AB\right)\mathrm{tr}_F\left(CD\right)\,. \tag{II.51}$$

- R_A^A: antisymmetric for both upper index and lower index. The states are

$$(R_A^A)_{kl}^{ij} = \frac{1}{2}\left[A_k^i B_l^j + \frac{1}{n-2}\delta_k^i\left(A_l^m B_m^j + B_l^m A_m^j\right) - \frac{1}{(n-1)(n-2)}\delta_k^i\delta_l^j \mathrm{tr}_F\left(AB\right)\right] - (i \leftrightarrow j) - (k \leftrightarrow l) + (i \leftrightarrow j, k \leftrightarrow l) \tag{II.52}$$

and the projection operator is

$$P_{AA} = \frac{-1}{4(n-2)}\mathrm{tr}_F\left((AB+BA)(CD+DC)\right) - \frac{1}{4}\Big(\mathrm{tr}_F\left(ACBD\right) + \mathrm{tr}_F\left(ADBC\right)\Big) + \frac{1}{4}\Big(\mathrm{tr}_F\left(AC\right)\mathrm{tr}_F\left(BD\right) + \mathrm{tr}_F\left(AD\right)\mathrm{tr}_F\left(CD\right)\Big) + \frac{1}{2(n-1)(n-2)}\mathrm{tr}_F\left(AB\right)\mathrm{tr}_F\left(CD\right)\,. \tag{II.53}$$

The projection operators agree with those of [31] and using (II.9) can be shown to satisfy $P_r P_{r'} = P_r \delta_{rr'}$ for r the various representations. One last check is that

$$\sum_r P_r = \mathrm{tr}_F\,(AC)\,\mathrm{tr}_F\,(BD)\ . \tag{II.54}$$

The right-hand side is the unit operator when acting on the product of two states in the adjoint representation. It can also be seen that R_I, R_S, R_A^A and R_S^S are symmetric under interchanging A and B while R_A, R_A^S and R_S^A are antisymmetric.

The amplitude in the different intermediate states can now be extracted from the general amplitude in two equivalent ways. We can pick a state R_r in a representation r and get it via

$$T_r = \langle R_r | M(s,t,u) | R_r \rangle\ , \tag{II.55}$$

or apply the projection operators on the full amplitude with

$$P_r T_r = P_r M(s,t,u)\ . \tag{II.56}$$

Both methods give as expected the same result but the second one is much easier to apply. For the first method it is best to choose a state where the terms with δ functions are not present. E.g. for the four index representations take a state R_r with $i=1, j=2, k=3, l=4$. For evaluating (II.56) one can use (II.8).

$$\begin{aligned}
T_I &= 2\left(n-\frac{1}{n}\right)[B(s,t,u)+B(t,u,s)] - \frac{2}{n}B(u,s,t) \\
&\quad +(n^2-1)C(s,t,u) + C(t,u,s) + C(u,s,t)\ , \\
T_S &= \left(n-\frac{4}{n}\right)[B(s,t,u)+B(t,u,s)] - \frac{4}{n}B(u,s,t) \\
&\quad +C(t,u,s) + C(u,s,t)\ , \\
T_A &= n[-B(s,t,u)+B(t,u,s)] + C(t,u,s) - C(u,s,t)\ , \\
T_{SA} &= C(t,u,s) - C(u,s,t)\ , \\
T_{AS} &= C(t,u,s) - C(u,s,t)\ , \\
T_{SS} &= 2B(u,s,t) + C(t,u,s) + C(u,s,t)\ , \\
T_{AA} &= -2B(u,s,t) + C(t,u,s) + C(u,s,t)\ .
\end{aligned} \tag{II.57}$$

They satisfy the relation similar to (II.24),

$$M(s,t,u) = \sum_r T_r(s,t,u) P_r\ . \tag{II.58}$$

One also notices that $T_{SA} = T_{AS}$ in general from (II.57).

II.3.4 Real case: channels and amplitudes

In this subsection we work out the possible two meson intermediate states for the case of $SU(2n)/SO(2n)$. One problem is that the mesons transform under $SO(2n)$ as $\phi \to h\phi h^\dagger$. The matrices $h \in SO(2n)$ in the embedding introduced here do not simply satisfy $hh^T = 1$ either. In our case the $SO(2n)$ is instead defined as $hJ_S h^T = J_S$. The easiest way to obtain objects that appear in the usual way is to note that using (II.6)

$$\phi J_S \to h\phi h^\dagger J_S = h\phi J_S h^T \tag{II.59}$$

and that an invariant trace on these object needs an extra factor of J_S. E.g.

$$(\phi^a J_S)J_S(\phi^b J_S) \to h(\phi^a J_S)h^T J_S h(\phi^b J_S)h^T = h(\phi^a J_S)J_S(\phi^b J_S)h^T\,. \tag{II.60}$$

Keeping that in mind we can use the standard way of dealing with $SO(2n)$. Note that $(\phi J_S)^T = J_S\phi^T = \phi J_S$ so the Goldstone bosons live in the symmetric representation of $SO(2n)$.

The method of Young tableaux has been generalized to $SO(2n)$ [33, 34]. Putting together two symmetric representations gives

(II.61)

We can write this in the form

$$Sym. \otimes Sym. = R_I \oplus R_A \oplus R_S \oplus R_{FS} \oplus R_{MA} \oplus R_{MS}\,. \tag{II.62}$$

The states are given in Tab. II.1. They are made traceless but remember that indices of $\phi^a J_S$ and $\phi^b J_S$ are always contracted with J_S.

As an example the singlet representation R_I is proportional to

$$(\phi^a J_S)_{ij} J_{Sik} J_{Sjl} (\phi^b J_S)kl = \mathrm{tr}_F\left(\phi^a \phi^b\right)\,.$$

The two-index antisymmetric representation R_A is, now using A, B for ϕ^a, ϕ^b,

$$(AJ_S)_{ik}(BJ_S)_{jl}J_{Skl} - (AJ_S)_{jk}(BJ_S)_{il}J_{Skl} = (ABJ - BAJ)_{ij} \tag{II.63}$$

where we heavily used $J_S^2 = 1$ and the fact that AJ_S and BJ_S are symmetric matrices. One can also easily check that the trace $(ABJ_S - BAJ_S)_{ij}J_{Sij}$ vanishes.

Then R_A and R_S are antisymmetric respectively symmetric both under $i \leftrightarrow j$ and $A \leftrightarrow B$. The remaining ones are the four-index representations. R_{FS} is fully symmetric in all indices and under $A \leftrightarrow B$. The two remaining representations have a mixed symmetry in the indices but are antisymmetric respectively symmetric under $A \leftrightarrow B$.

R_I	$\frac{1}{\sqrt{(2n-1)(n+1)}}\mathrm{tr}_F\,(AB)$
R_A	$(ABJ-BAJ)_{ij}$
R_S	$(ABJ+BAJ)_{ij}-\frac{1}{n}J_{ij}\langle AB\rangle$
R_{FS}	$(AJ)_{ij}\,(BJ)_{kl}-\frac{1}{n+2}\Big[J_{ij}(ABJ+BAJ)_{kl}\Big]+\frac{1}{2(n+2)(n+1)}J_{ij}J_{kl}\langle AB\rangle$ $+(ijkl\leftrightarrow ikjl)+(ijkl\leftrightarrow iljk)+(ijkl\leftrightarrow klij)$ $+(ijkl\leftrightarrow jlik)+(ijkl\leftrightarrow jkil)$
R_{MA}	$(AJ)_{ij}\,(BJ)_{kl}-(AJ)_{kl}\,(BJ)_{ij}-\frac{1}{2n+2}\Big[J_{ik}(ABJ-BAJ)_{jl}$ $+J_{jk}(ABJ-BAJ)_{il}+J_{il}(ABJ-BAJ)_{jk}+J_{jl}(ABJ-BAJ)_{ik}\Big]$
R_{MS}	$(AJ)_{ij}\,(BJ)_{kl}+(AJ)_{kl}\,(BJ)_{ij}-(AJ)_{ik}\,(BJ)_{jl}-(AJ)_{jl}\,(BJ)_{ik}$ $+\frac{1}{2(n-1)}\Big[J_{ij}(ABJ+BAJ)_{kl}+J_{kl}(ABJ+BAJ)_{ij}$ $-J_{ik}(ABJ+BAJ)_{jl}-J_{jl}(ABJ+BAJ)_{ik}\Big]$ $-\frac{1}{(n-1)(2n-1)}\Big(J_{ij}J_{kl}-J_{ik}J_{jl}\Big)\langle AB\rangle$

Table II.1: The intermediate states for the real or adjoint case, $SU(2n)/SO(2n)$. The notations A, B stands for ϕ^a and ϕ^b and J is J_S everywhere.

The corresponding projection operators are given in Tab. II.2. These can be obtained by contracting the indices with J_S of the states once with A, B and once with C, D.

We can now use Tabs. II.1 and II.2 to project out the amplitudes in the various channels using (II.55) or (II.56). The results are

$$\begin{aligned}
T_I &= \frac{1}{n}(2n-1)(n+1)[B(s,t,u)+B(t,u,s)]+\frac{1}{n}(n-1)B(u,s,t)\\
&\quad +(2n-1)(n+1)C(s,t,u)+C(t,u,s)+C(u,s,t)\,,\\
T_A &= -(1+n)[B(s,t,u)-B(t,u,s)]+C(t,u,s)-C(u,s,t)\,,\\
T_S &= \frac{1}{n}(n-1)(n+2)[B(s,t,u)+B(t,u,s)]+\frac{1}{n}(n-2)B(u,s,t)\\
&\quad +C(t,u,s)+C(u,s,t)\,,\\
T_{FS} &= 2B(u,s,t)+C(t,u,s)+C(u,s,t)\,,\\
T_{MA} &= C(t,u,s)-C(u,s,t)\,,\\
T_{MS} &= -B(u,s,t)+C(t,u,s)+C(u,s,t)\,.
\end{aligned} \tag{II.64}$$

P_I	$\frac{1}{(2n-1)(n+1)}\langle AB\rangle\langle CD\rangle$
P_A	$-\frac{1}{2(n+1)}\langle (AB-BA)(CD-DC)\rangle$
P_S	$\frac{n}{2(n-1)(n+2)}\Big(\langle (AB+BA)(CD+DC)\rangle - \frac{2}{n}\langle AB\rangle\langle CD\rangle\Big)$
P_{FS}	$\frac{1}{6}\Big[\frac{2}{(n+1)(n+2)}\langle AB\rangle\langle CD\rangle + \langle AC\rangle\langle BD\rangle + \langle AD\rangle\langle BC\rangle$ $+2\langle ACBD+ADBC\rangle - \frac{2}{n+2}\langle (AB+BA)(CD+DC)\rangle\Big]$
P_{MA}	$\frac{1}{2(n+1)}\langle (AB-BA)(CD-DC)\rangle + \frac{1}{2}(\langle AC\rangle\langle BD\rangle - \langle AD\rangle\langle BC\rangle)$
P_{MS}	$\frac{1}{6}\Big[\frac{2}{(n-1)(2n-1)}\langle AB\rangle\langle CD\rangle + 2\Big(\langle AC\rangle\langle BD\rangle + \langle AD\rangle\langle BC\rangle\Big)$ $-2\langle ADBC+ACBD\rangle - \frac{1}{n-1}\langle (AB+BA)(CD+DC)\rangle\Big]$

Table II.2: The projection operator for the different intermediate states for the real or adjoint case, $SU(2n)/SO(2n)$.

II.3.5 Pseudo-real case: channels and amplitudes

In this subsection we work out the possible two meson intermediate states for the case of $SU(2n)/Sp(2n)$. One problem is that the mesons transform under $Sp(2n)$ as in $\phi \to h\phi h^\dagger$. The easiest way to obtain objects that appear in the usual way is to note that using (II.6)

$$\phi J_A \to h\phi h^\dagger J_A = h\phi J_A h^T \tag{II.65}$$

and that an invariant trace on these object needs an extra factor of J_A. Keeping that in mind we can use the standard way of dealing with $Sp(2n)$. Note that $(\phi J_A)^T = J_A^T\phi^T = -J_A\phi^T = \phi J_S$ so the Goldstone bosons live in the antisymmetric representation of $Sp(2n)$.

The method of Young tableaux also is developed for $Sp(2n)$ [33,34]. Putting together two antisymmetric representations gives

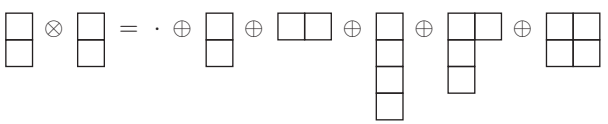

(II.66)

We can write this in the form

$$Asym. \otimes Asym. = R_I \oplus R_A \oplus R_S \oplus R_{FA} \oplus R_{MA} \oplus R_{MS}\,. \tag{II.67}$$

R_I	$\frac{1}{\sqrt{(2n+1)(n-1)}}\langle AB\rangle$
R_A	$(ABJ+BAJ)_{ij}-\frac{1}{n}J_{ij}\langle AB\rangle$
R_S	$(ABJ-BAJ)_{ij}$
R_{FA}	$(AJ)_{ij}\,(BJ)_{kl}+\frac{1}{n-2}J_{ij}(ABJ+BAJ)_{kl}-\frac{1}{2(n-1)(n-2)}J_{ij}J_{kl}\langle AB\rangle$ $-(ijkl\leftrightarrow ikjl)+(ijkl\leftrightarrow iljk)+(ijkl\leftrightarrow klij)$ $+(ijkl\leftrightarrow jlik)+(ijkl\leftrightarrow jkil)$
R_{MA}	$(AJ)_{ij}\,(BJ)_0kl-(AJ)_{kl}\,(BJ)_0ij-\frac{1}{2n-2}\Big[J_{ik}(ABJ-BAJ)_{jl}$ $+J_{jl}(ABJ-BAJ)_{ik}-J_{il}(ABJ-BAJ)_{jk}-J_{jk}(ABJ-BAJ)_{il}\Big]$
R_{MS}	$\Big\{(AJ)_{ij}\,(BJ)_{kl}+(AJ)_{ik}\,(BJ)_{jl}-\frac{1}{2(n+1)}\Big[J_{ij}(ABJ+BAJ)_{kl}$ $-J_{ik}(ABJ+BAJ)_{jl}\Big]+(ij\leftrightarrow kl)\Big\}$ $+\frac{1}{2(n+1)(2n-1)}\Big(J_{ij}J_{kl}-J_{ik}J_{jl}\Big)\langle AB\rangle$

Table II.3: The intermediate states for the pseudo-real or two-colour case, $SU(2n)/Sp(2n)$. J means J_A.

The states are given in Tab. II.1. They are made traceless but remember that indices of $\phi^a J_A$ and $\phi^b J_A$ are always contracted with J_A.

The representations are the singlet representation, symmetric under $A\leftrightarrow B$, R_A which is antisymmetric under the interchange $i\leftrightarrow j$ but symmetric under $A\leftrightarrow B$ and R_S which is symmetric under the interchange $i\leftrightarrow j$ but antisymmetric under $A\leftrightarrow B$ Let us show the latter on R_A The two-index antisymmetric representation R_A is, now using A,B for ϕ^a,ϕ^b,

$$\begin{aligned}&(AJ_A)_{ik}(BJ_A)_{jl}J_{Akl}-(AJ_A)_{jk}(BJ_A)_{il}J_{Akl}\\ &\quad=\quad-(AJ_A)_{ik}J_{Akl}(BJ_A)_{lj}J_{Akl}-(BJ_A)_{il}J_{Alk}(AJ_A)_{ki}\\ &\quad=\quad(ABJ+BAJ)_{ij}\,,\end{aligned}\tag{II.68}$$

where we used $J_A^2=-1$ and the fact that AJ_A, BJ_A and J_A are antisymmetric matrices.

The remaining ones are the four-index representations. R_{FA} is fully antisymmetric in all indices and symmetric under $A\leftrightarrow B$. The two remaining representations have a mixed symmetry in the indices but are antisymmetric respectively symmetric under $A\leftrightarrow B$. The states are give in Tab. II.3.

The projection operators can be constructed by contracting all indices with J_A of the states once with A,B and once with C,D. The results are given in Tab. II.4.

P_I	$\frac{1}{(2n+1)(n-1)}\langle AB\rangle\langle CD\rangle$
P_A	$\frac{n}{2(n+1)(n-2)}\Big(\langle(AB+BA)(CD+DC)\rangle - \frac{2}{n}\langle AB\rangle\langle CD\rangle\Big)$
P_S	$-\frac{1}{2(n-1)}\langle(AB-BA)(CD-DC)\rangle$
P_{FA}	$\frac{1}{6}\Big[\frac{2}{(n-1)(n-2)}\langle AB\rangle\langle CD\rangle + \langle AC\rangle\langle BD\rangle + \langle AD\rangle\langle BC\rangle$ $-2\langle ACBD+ADBC\rangle - \frac{2}{n-2}\langle(AB+BA)(CD+DC)\rangle\Big]$
P_{MA}	$\frac{1}{2(n-1)}\langle(AB-BA)(CD-DC)\rangle + \frac{1}{2}(\langle AC\rangle\langle BD\rangle - \langle AD\rangle\langle BC\rangle)$
P_{MS}	$\frac{1}{3}\Big[\frac{1}{(n+1)(2n+1)}\langle AB\rangle\langle CD\rangle + \langle AC\rangle\langle BD\rangle + \langle AD\rangle\langle BC\rangle$ $+\langle ACBD+ADBC\rangle - \frac{1}{2(n+1)}\langle(AB+BA)(CD+DC)\rangle\Big]$

Table II.4: The projection operator for the different channels for the pseudo-real or two-colour case, $SU(2n)/Sp(2n)$.

We can now use again (II.55) or (II.56) to obtain the amplitudes in the different channels. The results are very similar to the real case and read

$$\begin{aligned}
T_I &= \frac{1}{n}(2n+1)(n-1)[B(s,t,u)+B(t,u,s)] - \frac{1}{n}(n+1)B(u,s,t)\\
&\quad +(2n+1)(n-1)C(s,t,u) + C(t,u,s) + C(u,s,t)\,,\\
T_A &= \frac{1}{n}(n+1)(n-2)[B(s,t,u)+B(t,u,s)] - \frac{1}{n}(n+2)B(u,s,t)\\
&\quad +C(t,u,s) + C(u,s,t)\,,\\
T_S &= (1-n)[B(s,t,u)-B(t,u,s)] + C(t,u,s) - C(u,s,t)\,,\\
T_{FA} &= -2B(u,s,t) + C(t,u,s) + C(u,s,t)\,,\\
T_{MA} &= C(t,u,s) - C(u,s,t)\,.\\
T_{MS} &= B(u,s,t) + C(t,u,s) + C(u,s,t)\,,
\end{aligned} \tag{II.69}$$

II.4 Results for the amplitude $M(s,t,u)$

We have rewritten the amplitudes here in terms of the physical decay constant F_{phys} and mass M^2_{phys}. The relation of these to the lowest order results can be

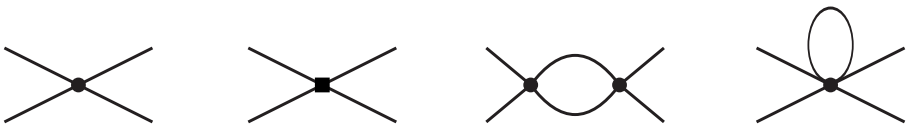

(1) (2) (3) (4)

Figure II.1: The leading order and next-to leading order for meson-meson scattering $\phi\phi \to \phi\phi$. The filled circle is a vertex from $\mathcal{L}_2$, and the filled square is a vertex from $\mathcal{L}_4$.

found in [1]. We also use the abbreviations

$$x_2 = \frac{M^2_{\text{phys}}}{F^2_{\text{phys}}}\,, \quad L = \frac{1}{16\pi^2}\ln\frac{M^2_{\text{phys}}}{\mu^2}\,, \quad \pi_{16} = \frac{1}{16\pi^2}. \tag{II.70}$$

In addition we have often used (II.28) to simplify the expressions.

II.4.1 Lowest order

The lowest order result comes from the simple tree-level diagram (1) of Fig. II.1.

$$B_{LO}(s,t,u) = x_2\left(-\frac{1}{2}t+1\right)\,, \qquad C_{LO}(s,t,u) = 0\,, \tag{II.71}$$

for all cases. This reproduces using the relation (II.33) Weinberg's result [24] for $\pi\pi$ scattering

$$A_{LO} = x_2\,(s-1)\,. \tag{II.72}$$

II.4.2 Next-to-leading order

The next-to-leading order contains the 3 diagrams (2-4) in Fig. II.1 in addition to wave-function-renormalization. The divergences from loop diagram (3) and (4) can be canceled by the bare low energy constants (LECs) of $\mathcal{L}_4$ in the diagram (2).

The functions $B(s,t,u)$ and $C(s,t,u)$ can be calculated from the one-loop graphs shown in Fig. II.1(2-4) and wave-function renormalization. It also contains terms from rewriting the lowest-order result in the physical mass and decay constant.

The functions $B(s,t,u)$ and $C(s,t,u)$ can be rewritten in the form

$$\begin{aligned} B(s,t,u) &= x_2^2\left[B_P(s,t,u) + B_S(s,t-u) + B_S(u,t-s) + B_T(t)\right]\,, \\ C(s,t,u) &= x_2^2\left[C_P(s,t,u) + C_S(s) + C_T(t) + C_T(u)\right]\,. \end{aligned} \tag{II.73}$$

$B_P(s,t,u)$ and $C_P(s,t,u)$ are the polynomial part, the remaining pieces are often called the unitarity correction. This can be proven using an extension of the methods of [35].

Using (II.28) we rewrite the polynomial part in its simplest form satisfying the symmetry constraints (II.31):

$$\begin{aligned} B_P(s,t,u) &= \alpha_1 + \alpha_2 t + \alpha_3 t^2 + \alpha_4 (s-u)^2 , \\ C_P(s,t,u) &= \beta_1 + \beta_2 s + \beta_3 s^2 + \beta_4 (t-u)^2 . \end{aligned} \tag{II.74}$$

The polynomial part for the three cases is give in Tab. II.5.

The unitarity correction is given in Tab.II.6. We noticed that the C functions for the $SO(2n)$ and $Sp(2n)$ case are the same.

II.4.3 Next-to-next-to-leading order

There are 13 diagrams at next-to-next-to-leading order shown in Fig. II.2. We have checked that the nonlocal divergence cancels for all three cases and that for the complex or QCD case the result is fully finite with the subtractions calculated in [23].

The diagrams (15) and (16) are often called the sunset and vertex or fish diagram respectively. These require the most difficult integrals. At intermediate stages we needed more integrals than those calculated for [25,26]. They were calculated with the methods of [36] and are given in App. III.1.

$$\begin{aligned} B(s,t,u) &= x_2^3 \left[B_P(s,t,u) + B_S(s,t-u) + B_S(u,t-s) + B_T(t) \right] , \\ C(s,t,u) &= x_2^3 \left[C_P(s,t,u) + C_S(s) + C_T(t) + C_T(u) \right] . \end{aligned} \tag{II.75}$$

The polynomial parts we rewrite using (II.28) in their simplest form satisfying the symmetry constraints (II.31):

$$\begin{aligned} B_P(s,t,u) &= \gamma_1 + \gamma_2 t + \gamma_3 t^2 + \gamma_4 (s-u)^2 + \gamma_5 t^3 + \gamma_6 t (s-u)^2 , \\ C_P(s,t,u) &= \delta_1 + \delta_2 s + \delta_3 s^2 + \delta_4 (t-u)^2 + \delta_5 s^3 + \delta_6 s (t-u)^2 . \end{aligned} \tag{II.76}$$

The coefficients in these polynomials as well as the functions in (II.75) are given in App. II.1. The FORM expressions can be downloaded from [37]. We stress once more that the result is fully analytical and expressed in terms of L and $\bar{J}$.

II.5 Scattering lengths

The threshold parameters of general meson meson scattering are defined similar to those of $\pi\pi$ scattering. First we calculate the amplitudes for the different

QCD: $SU(n) \times SU(n)/SU(n)$		
$B_P(s,t,u)$	α_1	$\frac{2}{n}L + \frac{2}{n}\pi_{16} + 16L_8^r + 16L_0^r - \frac{2}{3}nL - \frac{5}{9}n\pi_{16}$
	α_2	$-4L_5^r - 16L_0^r + \frac{5}{12}nL + \frac{11}{36}n\pi_{16}$
	α_3	$L_3^r + 4L_0^r - \frac{1}{16}nL - \frac{1}{24}n\pi_{16}$
	α_4	$L_3^r - \frac{1}{48}nL - \frac{1}{36}n\pi_{16}$
$C_P(s,t,u)$	β_1	$32(L_1^r - L_4^r + L_6^r) - \frac{2}{n^2}(L + \pi_{16})$
	β_2	$16L_4^r - 32\,L_1^r$
	β_3	$-\frac{3}{8}L + 2L_2^r + 8L_1^r - \frac{3}{8}\pi_{16}$
	β_4	$2L_2^r - \frac{1}{8}L - \frac{1}{8}\pi_{16}$
Adjoint: $SU(2n)/SO(2n)$		
$B_P(s,t,u)$	α_1	$16(L_0^r + L_8^r) - \left(\frac{7}{6} + \frac{2n}{3} - \frac{1}{n}\right)L - \left(\frac{19}{18} + \frac{5n}{9} - \frac{1}{n}\right)\pi_{16}$
	α_2	$-16L_0^r - 4L_5^r + \left(\frac{5n}{12} + \frac{2}{3}\right)L + \left(\frac{5}{9} + \frac{11n}{36}\right)\pi_{16}$
	α_3	$4L_0^r + L_3^r - \left(\frac{1}{8} + \frac{n}{16}\right)L - \left(\frac{5}{48} + \frac{n}{24}\right)\pi_{16}$
	α_4	$L_3^r + \left(\frac{1}{24} - \frac{n}{48}\right)L + \left(\frac{5}{144} - \frac{n}{36}\right)\pi_{16}$
$C_P(s,t,u)$	β_1	$32(L_1^r - L_4^r + L_6^r) - \frac{1}{2n^2}(L + \pi_{16})$
	β_2	$16\left(L_4^r - 2L_1^r\right)$
	β_3	$8L_1^r + 2L_2^r - \frac{3}{16}\pi_{16} - \frac{3}{16}L$
	β_4	$2L_2^r - \frac{1}{16}L - \frac{1}{16}\pi_{16}$
Two-colour: $SU(2N)/Sp(2N)$		
$B_P(s,t,u)$	α_1	$16(L_0^r + L_8^r) + \left(\frac{7}{6} + \frac{1}{n} - \frac{2n}{3}\right)L + \left(\frac{19}{18} - \frac{5n}{9} + \frac{1}{n}\right)\pi_{16}$
	α_2	$-16L_0^r - 4L_5^r + \left(\frac{5n}{12} - \frac{2}{3}\right)L + \left(\frac{5}{9} - \frac{11n}{36}\right)\pi_{16}$
	α_3	$4L_0^r + L_3^r + \left(\frac{1}{8} - \frac{n}{16}\right)L + \left(\frac{5}{48} - \frac{n}{24}\right)\pi_{16}$
	α_4	$L_3^r - \left(\frac{1}{24} + \frac{n}{48}\right)L - \left(\frac{5}{144} + \frac{n}{36}\right)\pi_{16}$
$C_P(s,t,u)$	β_1	$32(L_1^r - L_4^r + L_6^r) - \frac{1}{2n^2}(L + \pi_{16})$
	β_2	$16(L_4^r - 2L_1^r)$
	β_3	$8L_1^r + 2L_2^r - \frac{3}{16}\pi_{16} - \frac{3}{16}L$
	β_4	$2L_2^r - \frac{1}{16}L - \frac{1}{16}\pi_{16}$

Table II.5: The next-to-leading results for all three cases for the polynomial part. The coefficients are defined in (II.74).

channels using (II.57), (II.64) and (II.69) for each of the possible intermediate states of representation or channels I.

The scattering amplitude for each channel I can be projected out using the

QCD: $SU(n) \times SU(n)/SU(n)$	
$B_S(s,t-u)$	$\bar{J}(s)\left[-\frac{1}{n}+\frac{n}{16}s^2+\frac{n}{12}\left(1-\frac{s}{4}\right)(t-u)\right]$
$B_T(t)$	0
$C_S(s)$	$\bar{J}(s)\left(\frac{2}{n^2}+\frac{1}{4}s^2\right)$
$C_T(t)$	$\frac{1}{4}\bar{J}(t)\,(t-2)^2$
Adjoint: $SU(2n)/SO(2n)$	
$B_S(s,t-u)$	$\bar{J}(s)\left[-\frac{1}{2n}+\frac{s}{4}+\frac{1}{16}\,(n-1)\,s^2+\frac{1}{12}(n+1)\left(1-\frac{s}{4}\right)(t-u)\right]$
$B_T(t)$	$\frac{1}{8}\bar{J}(t)(t-2)^2$
$C_S(s)$	$\bar{J}(s)\left(\frac{1}{2n^2}+\frac{1}{8}s^2\right)$
$C_T(t)$	$\frac{1}{8}\bar{J}(t)(t-2)^2$
Two-colour: $SU(2N)/Sp(2N)$	
$B_S(s,t-u)$	$\bar{J}(s)\left[-\frac{1}{2n}-\frac{1}{4}s+\frac{1}{16}(n+1)s^2+\frac{1}{12}(n-1)\left(1-\frac{s}{4}\right)(t-u)\right]$
$B_T(t)$	$-\frac{1}{8}\bar{J}(t)(t-2)^2$
$C_S(s)$	$\bar{J}(s)\left(\frac{1}{2n^2}+\frac{1}{8}s^2\right)$
$C_T(t)$	$\frac{1}{8}\bar{J}(t)(t-2)^2$

Table II.6: The next-to-leading results for all three cases for the unitarity correction.

partial wave expansion

$$T_\ell^I(s)=\frac{1}{64\pi}\int_{-1}^{1}d(cos\theta)P_\ell(cos\theta)T_I(s,t,u)\,. \tag{II.77}$$

Near the threshold $s=4$, we can expand the amplitude above the threshold using $s=4(1+q^2/M_\pi^2)$ in the small three-momentum q.

$$\text{Re}\;T_\ell^I(s)=q^{2\ell}[a_\ell^I+q^2b_\ell^I+O(q^4)]\,, \tag{II.78}$$

where a_ℓ^I is the scattering length, and b_ℓ^I is the slope.

In App. II.3, we give the expressions of the lowest partial wave scattering length for each channel in all three cases. As mentioned in Sect. II.3, some channels are symmetric under $A\leftrightarrow B$, hence the lowest order partial wave is $\ell=0$. The other channels are antisymmetric under $A\leftrightarrow B$, so that the lowest order partial wave is $\ell=1$. A and B are the incoming mesons here using the notation of Sect. II.3.

For the purpose of illustration, we plot the scattering length for the singlet and the fully-symmetric (fully-antisymmetric) channels as a function of the physical meson mass M_{phys}^2. Since currently we do not have knowledge for

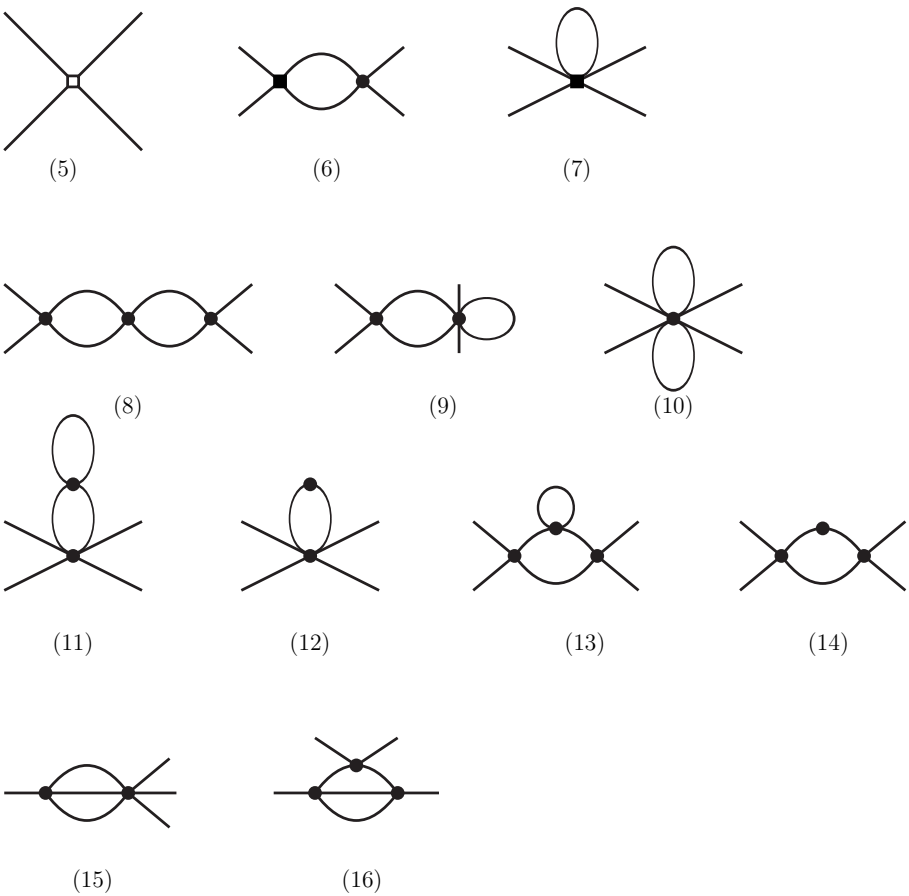

Figure II.2: The next-to-next-to leading order diagrams for $\pi\pi \to \pi\pi$. The filled circle a vertex from $\mathcal{L}_2$, The filled square is a vertex from $\mathcal{L}_4$, and the open square is a vertex from $\mathcal{L}_6$.

the values of the low energy constants for these, we take the values of the L_i^r of fit 10 of [38] for the complex or QCD case and half that for the other two as suggested by the large n relations discussed below. The values of the NNLO LECs we simply put to zero. We also choose the subtraction scale $\mu = 0.77$ GeV and the physical decay constant $F_{\text{phys}} = 0.0924$ GeV.

The singlet case for the complex case is shown in Fig. II.3. We have divided the scattering length by n to make the lowest order similar for all cases. Plotted are $n = 2, \ldots, 5$. One can see that for a given M^2_{phys} the convergence gets progressively worse for larger n. For $n = 2$ this corresponds to a_0^0.

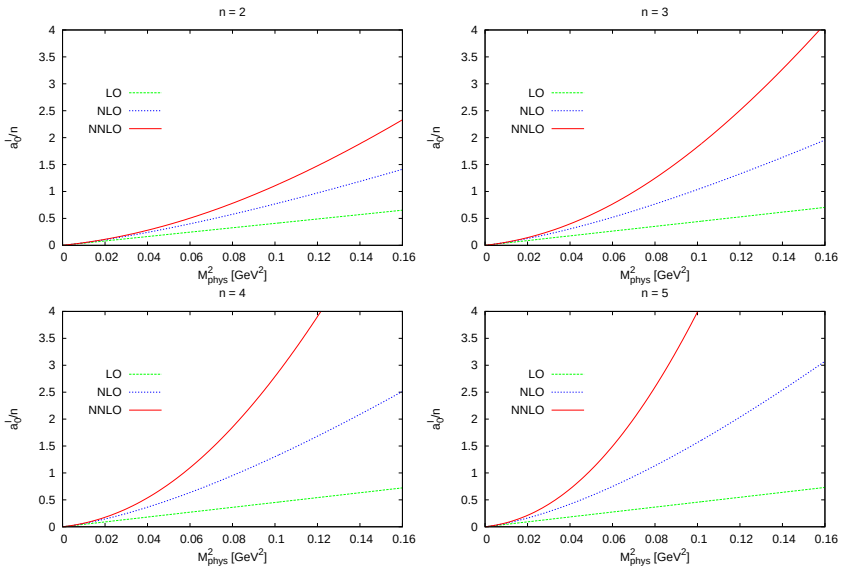

Figure II.3: Scattering length a_0^I/n for the complex or QCD case, $SU(n) \times SU(n)/SU(n)$.

The fully symmetric case case for the complex case is shown in Fig. II.4. Plotted are $n = 2, \ldots, 5$. One can see that for a given M^2_{phys} the convergence gets progressively worse for larger n. For $n = 2$ this corresponds to a_0^2. The lowest order is independent of n. The NLO order is only mildly dependent on n while the NNLO part grows fast with n.

II.5.1 Large n behaviour

Looking at the lowest order expressions in App. II.3 we notice immediately that the large n behaviour for the scattering lengths fall in three classes.

The scattering length is of order n for the singlet and symmetric and asymmetric representation and what is more they are clearly related for the three cases:

$$a_0^I|_{\text{complex}} = a_0^I|_{\text{real}} = a_0^I|_{\text{pseudoreal}} =_{LO} \frac{x_2}{\pi}\frac{n}{8}, \tag{II.79}$$

$$a_0^S|_{\text{complex}} = a_0^S|_{\text{real}} = a_0^A|_{\text{pseudoreal}} =_{LO} \frac{x_2}{\pi}\frac{n}{16}, \tag{II.80}$$

$$a_1^A|_{\text{complex}} = a_1^A|_{\text{real}} = a_1^S|_{\text{pseudoreal}} =_{LO} \frac{x_2}{\pi}\frac{n}{48}, \tag{II.81}$$

The symbol $=_{LO}$ means equality at lowest order. Do the relations (II.79-II.81)

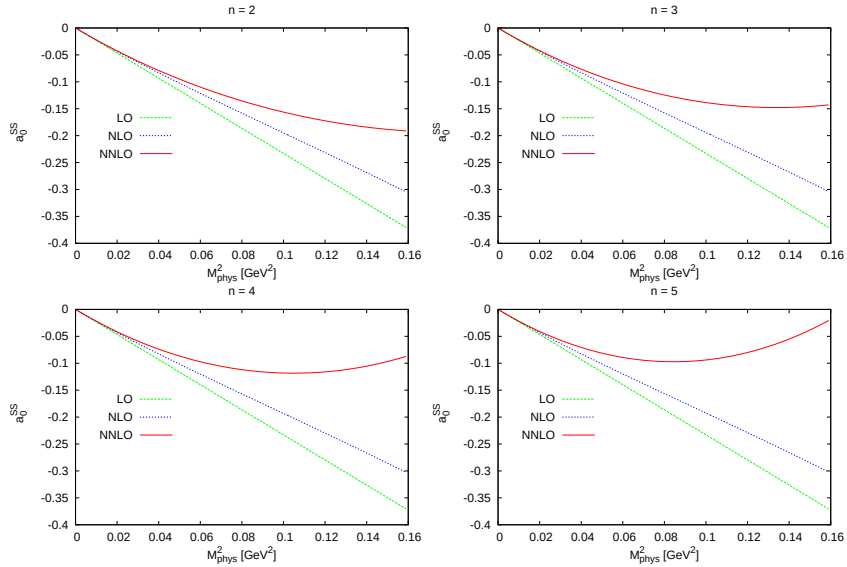

Figure II.4: Scattering length a_0^{SS} for the complex or QCD case, $SU(n) \times SU(n)/SU(n)$.

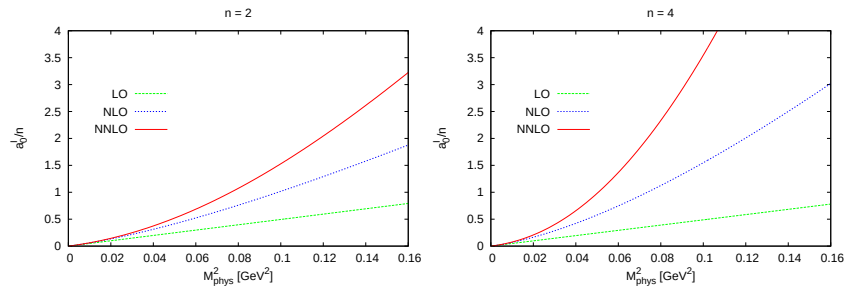

Figure II.5: Scattering length of a_0^I/n for the real or adjoint case, $SU(2n)/SO(2n)$.

remain valid at higher orders? If we choose $F^2_{\text{phys}} \propto n$ and M^2_{phys} independent of n, we find that it is indeed the case for (II.80,II.81). For (II.79) it is true, provided we set the NLO LECs L_i^r of the real and pseudoreal case to half those of the complex case and the NNLO coefficients K_i to $1/4$ the complex case. The contributions are nonzero at the three orders for all of them. The subleading orders in $1/n$ are different.

A second class is those which are order 1 in the coefficient of x_2/π at lowest

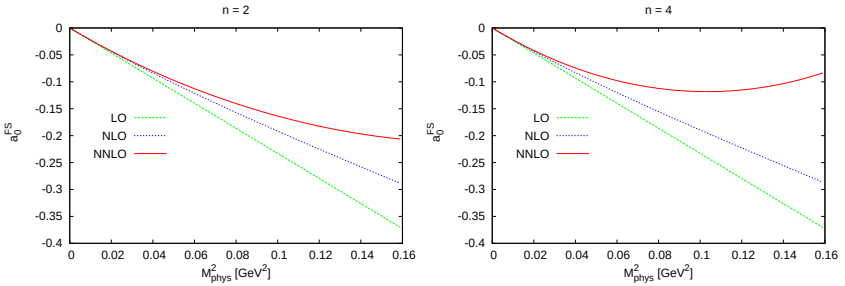

Figure II.6: Scattering length of a_0^{FS} for the real or adjoint case, $SU(2n)/SO(2n)$.

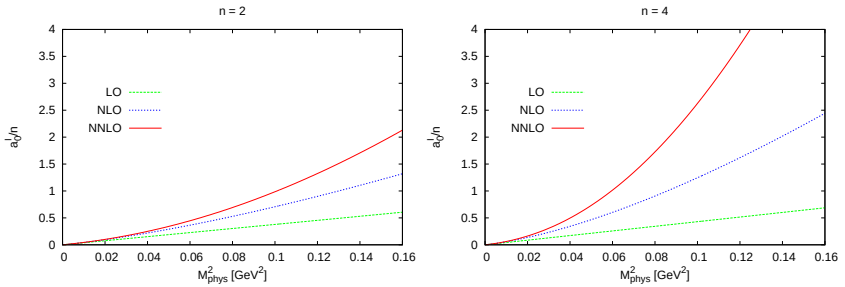

Figure II.7: Scattering length of a_0^I/n for the pseudoreal or two-colour case, $SU(2n)/Sp(2n)$.

order. For these we find

$$a_0^{SS}|_{\text{complex}} \quad = \quad a_0^{FS}|_{\text{real}} = 2a_0^{MS}|_{\text{pseudoreal}} =_{LO} \frac{x_2}{\pi}\frac{-1}{16}\,, \tag{II.82}$$

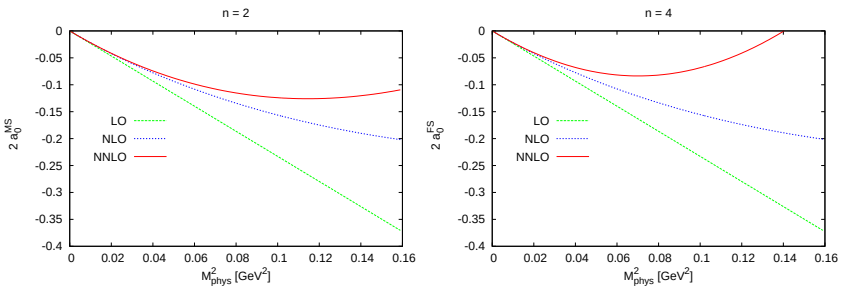

Figure II.8: Scattering length $2a_0^{MS}$ for the pseudoreal or two-colour case, $SU(2n)/Sp(2n)$. The factor of 2 included is because of the large n relation (II.82).

$$a_0^{AA}|_{\text{complex}} \quad = \quad 2a_0^{MS}|_{\text{real}} = a_0^{FA}|_{\text{pseudoreal}} =_{LO} \frac{x_2}{\pi}\frac{1}{16}\,. \tag{II.83}$$

We do indeed find that the relations are also satisfied at NLO and NNLO. In fact none of the scattering lengths in (II.82) has a leading n NLO correction to the lowest order result. This can be clearly seen in Fig. II.4 where the NLO result is very similar in all plots.

The third class is the amplitudes that vanish at lowest order

$$a_1^{SA}|_{\text{complex}} \quad = \quad a_1^{AS}|_{\text{complex}} = 2a_1^{MA}|_{\text{real}} = 2a_1^{MA}|_{\text{pseudoreal}} =_{LO} 0\,. \tag{II.84}$$

These are always suppressed by two powers of n compared to the first set of scattering lengths also at NLO and NNLO. The relations (II.84) are satisfied at NLO with same identifications of the LECs as above and almost at NNLO. The only terms that do not satisfy the relation are proportional to $L_4^r L_6^r$.

By comparing the plots shown one sees that the large n relations do predict the general behaviour but for $n = 2$ and $n = 4$ are not that accurate.

II.6 Conclusions

In this work we have presented the calculation of general meson-meson scattering for n flavours in a complex, real or pseudoreal representation of a strongly interaction gauge group. These are also referred to as QCD, Adjoint QCD and Two-color QCD and have as symmetry breaking patterns $SU(n) \times SU(n)/SU(n)$, $SU(2n)/SO(2n)$ and $SU(2n)/Sp(2n)$

We first reviewed the effective field theories of these three different cases. Those theories can be written in a very similar form as discussed earlier [1]. We have extended the methods used for $\pi\pi$ scattering in ChPT [26] to all the present cases. At intermediate stages some more integrals showed up, we have calculated them and they are tabulated in an appendix.

The amplitude can in general be written in terms of two invariant amplitudes which we called $B(s,t,u)$ and $C(s,t,u)$. These amplitudes can be written in terms of simpler functions and we have given their fully analytical expressions to NNLO.

Since the long term use of our work is the study of scattering on the lattice for these alternative theories we have discussed the group theory involved and all the possible intermediate channels. We have derived the amplitudes in all these channel as a function of the invariant B and C functions.

The expressions for the different channels we have not shown explicitly but we included expressions for scattering length of the lowest partial wave in all channels. We presented a few representative numerical results for the scattering lengths and discussed a series of relations between the different theories in the limit of a large number of flavours n.

Acknowledgements

This work is supported in part by the European Community-Research Infrastructure Integrating Activity "Study of Strongly Interacting Matter" (HadronPhysics2, Grant Agreement n. 227431) and the Swedish Research Council grants 621-2008-4074 and 621-2011-3326. This work heavily used FORM [39].

II.A Next-to-next-to leading order result

II.A.1 Complex or QCD

$$
\begin{aligned}
B_S(s,t-u) &= k_4(s)\left\{\frac{n_f^2}{12}+\frac{2}{n_f^2}\right\}(t-u)\\
&+k_3(s)\left\{\frac{s^2n_f^2}{48}-\frac{sn_f^2}{18}-\frac{1}{48}s(t-u)n_f^2+\frac{(t-u)n_f^2}{36}-\frac{(t-u)}{6}+\frac{1}{3}-\frac{s}{3n_f^2}\right.\\
&\qquad\left.+\frac{(t-u)}{3n_f^2}-\frac{8}{3n_f^2}\right\}\\
&+k_2(s)\left\{\frac{n_f^2s^3}{64}+\frac{s^3}{16}-\frac{1}{576}n_f^2(t-u)s^2-\frac{3s^2}{8}+\frac{1}{72}n_f^2(t-u)s-\frac{n_f^2(t-u)}{36}+\frac{2}{n_f^2}\right\}\\
&+k_1(s)\left\{\frac{n_f^2s^3}{576}+\frac{s^3}{24}-\frac{17n_f^2s^2}{288}+\frac{1}{576}n_f^2(t-u)s^2-\frac{s^2}{4}+\frac{n_f^2s}{12}-\frac{1}{96}n_f^2(t-u)s\right.\\
&\qquad\left.-\frac{(t-u)s}{24}+\frac{s}{2n_f^2}+\frac{7s}{12}-\frac{n_f^2(t-u)}{48}+\frac{(t-u)}{4}+\frac{4}{n_f^2}-\frac{1}{2}\right\}\\
&+\bar{J}(s)\left\{-\frac{5}{144}Ln_f^2s^3-\frac{5Ls^3}{24}+\frac{4L_1^rs^3}{3}+\frac{8L_2^rs^3}{3}+\frac{2}{3}L_0^rn_fs^3+\frac{4}{3}L_3^rn_fs^3\right.\\
&\qquad+\frac{17}{576}n_f^2\pi_{16}s^3+\frac{17\pi_{16}s^3}{72}+\frac{7}{144}Ln_f^2s^2+\frac{4Ls^2}{3}-\frac{8L_1^rs^2}{3}-\frac{28L_2^rs^2}{3}-4L_4^rs^2\\
&\qquad-\frac{4}{3}L_0^rn_fs^2-\frac{14}{3}L_3^rn_fs^2+L_5^rn_fs^2-\frac{35}{144}n_f^2\pi_{16}s^2-\frac{13\pi_{16}s^2}{9}+\frac{2}{3}L_1^r(t-u)s^2\\
&\qquad-\frac{1}{3}L_2^r(t-u)s^2-\frac{1}{3}L_0^rn_f(t-u)s^2+\frac{1}{6}L_3^rn_f(t-u)s^2-\frac{1}{432}n_f^2\pi_{16}(t-u)s^2\\
&\qquad-\frac{40L_0^rs^2}{3n_f}-\frac{40L_3^rs^2}{3n_f}-\frac{5}{36}Ln_f^2s-\frac{5Ls}{3}+\frac{16L_1^rs}{3}+\frac{32L_2^rs}{3}+16L_6^rs+\frac{8L_0^rn_fs}{3}\\
&\qquad\left.+\frac{16L_3^rn_fs}{3}-4L_5^rn_fs+8L_8^rn_fs+\frac{5}{12}n_f^2\pi_{16}s+\frac{2\pi_{16}s}{n_f^2}+\frac{65\pi_{16}s}{36}\right.
\end{aligned}
$$

$$
\begin{aligned}
&+\frac{1}{48}Ln_f^2(t-u)s+\frac{L(t-u)s}{12}-\frac{8L_1^r(t-u)s}{3}+\frac{4L_2^r(t-u)s}{3}-\frac{4L_4^r(t-u)s}{3}\\
&+\frac{4}{3}L_0^r n_f(t-u)s-\frac{2}{3}L_3^r n_f(t-u)s-\frac{1}{3}L_5^r n_f(t-u)s+\frac{17}{216}n_f^2\pi_{16}(t-u)s\\
&-\frac{5\pi_{16}(t-u)s}{72}+\frac{128L_0^r s}{3n_f}+\frac{128L_3^r s}{3n_f}-\frac{Ls}{n_f^2}+\frac{8L}{3}+\frac{20\pi_{16}}{n_f^2}-\frac{20\pi_{16}}{9}\\
&-\frac{1}{12}Ln_f^2(t-u)-\frac{L(t-u)}{3}+\frac{16L_4^r(t-u)}{3}+\frac{4L_5^r n_f(t-u)}{3}\\
&-\frac{11}{48}n_f^2\pi_{16}(t-u)-\frac{\pi_{16}(t-u)}{2n_f^2}+\frac{10\pi_{16}(t-u)}{9}-\frac{160L_0^r}{3n_f}-\frac{160L_3^r}{3n_f}+\frac{32L_5^r}{n_f}\\
&-\frac{96L_8^r}{n_f}-\frac{12L}{n_f^2}\Bigg\}
\end{aligned}
\tag{II.85}
$$

$$
\begin{aligned}
B_T(t)=\;&k_3(t)\left\{\frac{2t}{3n_f^2}+\frac{t}{3}-\frac{4}{3n_f^2}-\frac{2}{3}\right\}+k_2(t)\left\{-\frac{t^3}{8}+\frac{3t^2}{4}-\frac{3t}{2}+1\right\}\\
&+k_1(t)\left\{-\frac{t^3}{12}+\frac{t^2}{2}-\frac{t}{n_f^2}-\frac{7t}{6}+\frac{2}{n_f^2}+1\right\}\\
&+\bar{J}(t)\Bigg\{\frac{5Lt^3}{12}-\frac{8L_1^r t^3}{3}-\frac{16L_2^r t^3}{3}-\frac{17\pi_{16}t^3}{36}-\frac{8Lt^2}{3}+\frac{32L_1^r t^2}{3}+\frac{88L_2^r t^2}{3}+8L_4^r t^2\\
&+\frac{26\pi_{16}t^2}{9}+\frac{19Lt}{3}-\frac{64L_1^r t}{3}-\frac{176L_2^r t}{3}-16L_4^r t-32L_6^r t-\frac{4\pi_{16}t}{n_f^2}-\frac{64\pi_{16}t}{9}\\
&+\frac{2Lt}{n_f^2}-\frac{16L}{3}+\frac{64L_1^r}{3}+\frac{128L_2^r}{3}+64L_6^r+\frac{8\pi_{16}}{n_f^2}+\frac{58\pi_{16}}{9}-\frac{4L}{n_f^2}\Bigg\}
\end{aligned}
\tag{II.86}
$$

$$
\begin{aligned}
C_S(s)=\;&k_3(s)\left\{\frac{n_f s^2}{12}-\frac{5n_f s}{9}+\frac{2s}{3n_f}+\frac{16}{3n_f^3}\right\}\\
&+k_2(s)\left\{\frac{3n_f s^3}{16}-\frac{6}{n_f^3}\right\}+k_1(s)\left\{\frac{13n_f s^3}{144}-\frac{23n_f s^2}{72}+\frac{5n_f s}{6}-\frac{2s}{n_f}-\frac{8}{n_f^3}\right\}\\
&+\bar{J}(s)\Bigg\{\frac{8L_0^r s^3}{3}+\frac{16L_3^r s^3}{3}-\frac{5}{9}Ln_f s^3+8L_1^r n_f s^3+\frac{8}{3}L_2^r n_f s^3+\frac{85}{144}n_f\pi_{16}s^3\\
&-\frac{16L_0^r s^2}{3}-\frac{56L_3^r s^2}{3}+4L_5^r s^2+\frac{19}{36}Ln_f s^2-32L_1^r n_f s^2-\frac{16}{3}L_2^r n_f s^2\\
&+16L_4^r n_f s^2-\frac{7}{6}n_f\pi_{16}s^2-\frac{16L_1^r s^2}{n_f}-\frac{16L_2^r s^2}{3n_f}+\frac{80L_0^r s^2}{3n_f^2}+\frac{80L_3^r s^2}{3n_f^2}+\frac{32L_0^r s}{3}\\
&+\frac{64L_3^r s}{3}-16L_5^r s+32L_8^r s-\frac{11Ln_f s}{9}+32L_1^r n_f s+\frac{32L_2^r n_f s}{3}-32L_4^r n_f s
\end{aligned}
$$

$$+32L_6^r n_f s + \frac{35 n_f \pi_{16} s}{9} - \frac{7\pi_{16} s}{n_f} + \frac{4Ls}{n_f} + \frac{64L_1^r s}{n_f} + \frac{32L_2^r s}{3n_f} - \frac{32L_4^r s}{n_f}$$
$$- \frac{256L_0^r s}{3n_f^2} - \frac{256L_3^r s}{3n_f^2} - \frac{44\pi_{16}}{n_f^3} - \frac{4L}{n_f} - \frac{64L_1^r}{n_f} - \frac{64L_2^r}{3n_f} + \frac{64L_4^r}{n_f} - \frac{64L_6^r}{n_f}$$
$$+ \frac{320L_0^r}{3n_f^2} + \frac{320L_3^r}{3n_f^2} - \frac{64L_5^r}{n_f^2} + \frac{192L_8^r}{n_f^2} + \frac{28L}{n_f^3} \Bigg\} \qquad \text{(II.87)}$$

$$C_T(t) = k_3(t)\left\{ \frac{n_f t^2}{12} - \frac{2n_f t}{9} - \frac{2t}{3n_f} + \frac{n_f}{9} + \frac{4}{3n_f} \right\}$$
$$+k_1(t)\left\{ - \frac{5n_f t^3}{144} + \frac{n_f t^2}{8} - \frac{n_f t}{36} + \frac{t}{n_f} - \frac{n_f}{6} - \frac{2}{n_f} \right\}$$
$$+\bar{J}(t)\Bigg\{ - 4L_0^r t^3 - \frac{4L_3^r t^3}{3} + \frac{5}{72} L n_f t^3 - \frac{17}{144} n_f \pi_{16} t^3 + 24 L_0^r t^2 + \frac{16 L_3^r t^2}{3} + 4L_5^r t^2$$
$$- \frac{11}{18} L n_f t^2 + \frac{1}{9} n_f \pi_{16} t^2 - 48 L_0^r t - \frac{32 L_3^r t}{3} - 8L_5^r t - 16 L_8^r t + \frac{31 L n_f t}{18}$$
$$+ \frac{29 n_f \pi_{16} t}{36} + \frac{4\pi_{16} t}{n_f} - \frac{2Lt}{n_f} + 32L_0^r + \frac{32L_3^r}{3} + 32L_8^r - \frac{14 L n_f}{9} - \frac{10 n_f \pi_{16}}{9}$$
$$- \frac{8\pi_{16}}{n_f} + \frac{4L}{n_f} \Bigg\} \qquad \text{(II.88)}$$

II.A.2 Real or adjoint

$$B_S(s,t-u) = k_4(s)\left\{ \frac{(t-u)n^2}{12} - \frac{(t-u)n}{12} - \frac{(t-u)}{6} - \frac{(t-u)}{2n} + \frac{(t-u)}{2n^2} \right\}$$
$$+k_3(s)\Bigg\{ \frac{s^2 n^2}{48} - \frac{s n^2}{18} - \frac{1}{48} s(t-u) n^2 + \frac{(t-u)n^2}{36} - \frac{sn}{24} - \frac{s(t-u)n}{24} + \frac{(t-u)n}{72}$$
$$- \frac{n}{9} - \frac{s^2}{48} + \frac{s}{18} - \frac{s(t-u)}{48} - \frac{7(t-u)}{72} - \frac{1}{36} + \frac{s}{12n} - \frac{(t-u)}{12n} + \frac{1}{2n} - \frac{s}{12n^2}$$
$$+ \frac{(t-u)}{12n^2} - \frac{2}{3n^2} \Bigg\}$$
$$+k_2(s)\Bigg\{ \frac{n^2 s^3}{64} - \frac{n s^3}{64} + \frac{3s^3}{64} + \frac{3ns^2}{32} - \frac{1}{576} n^2 (t-u) s^2 - \frac{1}{288} n (t-u) s^2$$
$$- \frac{(t-u)s^2}{576} - \frac{9s^2}{32} + \frac{1}{72} n^2 (t-u) s + \frac{n(t-u)s}{36} + \frac{(t-u)s}{72} + \frac{3s}{16} - \frac{n^2 (t-u)}{36}$$

$$
\begin{aligned}
&-\frac{n(t-u)}{18}-\frac{(t-u)}{36}-\frac{1}{2n}+\frac{1}{2n^2}\Bigg\}\\
&+k_1(s)\Bigg\{\frac{n^2s^3}{576}+\frac{ns^3}{96}+\frac{11s^3}{576}-\frac{17n^2s^2}{288}-\frac{11ns^2}{288}+\frac{1}{576}n^2(t-u)s^2-\frac{1}{144}n(t-u)s^2\\
&-\frac{5(t-u)s^2}{576}-\frac{3s^2}{32}+\frac{n^2s}{12}+\frac{ns}{144}-\frac{1}{96}n^2(t-u)s+\frac{n(t-u)s}{32}+\frac{(t-u)s}{48}\\
&-\frac{s}{8n}+\frac{s}{8n^2}+\frac{31s}{144}+\frac{n}{6}-\frac{n^2(t-u)}{48}-\frac{n(t-u)}{24}+\frac{5(t-u)}{48}\\
&-\frac{3}{4n}+\frac{1}{n^2}+\frac{1}{24}\Bigg\}\\
&+\bar{J}(t)\Bigg\{-\frac{5}{144}Ln^2s^3-\frac{19Ls^3}{144}+L_0^rs^3+\frac{4L_1^rs^3}{3}+\frac{8L_2^rs^3}{3}+\frac{L_3^rs^3}{3}+\frac{1}{96}Lns^3\\
&+\frac{2}{3}L_0^rns^3+\frac{4}{3}L_3^rns^3+\frac{17}{576}n^2\pi_{16}s^3-\frac{1}{288}n\pi_{16}s^3+\frac{29\pi_{16}s^3}{192}+\frac{7}{144}Ln^2s^2\\
&+\frac{31Ls^2}{36}-\frac{8L_0^rs^2}{3}-\frac{8L_1^rs^2}{3}-\frac{28L_2^rs^2}{3}+2L_3^rs^2-4L_4^rs^2-L_5^rs^2-\frac{13}{144}Lns^2\\
&-\frac{4}{3}L_0^rns^2-\frac{14}{3}L_3^rns^2+L_5^rns^2-\frac{35}{144}n^2\pi_{16}s^2+\frac{19}{288}n\pi_{16}s^2-\frac{55\pi_{16}s^2}{72}\\
&+\frac{1}{48}L(t-u)s^2-\frac{1}{3}L_0^r(t-u)s^2+\frac{2}{3}L_1^r(t-u)s^2-\frac{1}{3}L_2^r(t-u)s^2\\
&+\frac{1}{6}L_3^r(t-u)s^2+\frac{1}{48}Ln(t-u)s^2-\frac{1}{3}L_0^rn(t-u)s^2+\frac{1}{6}L_3^rn(t-u)s^2\\
&-\frac{1}{432}n^2\pi_{16}(t-u)s^2-\frac{47n\pi_{16}(t-u)s^2}{1728}-\frac{43\pi_{16}(t-u)s^2}{1728}-\frac{20L_0^rs^2}{3n}\\
&-\frac{20L_3^rs^2}{3n}-\frac{5}{36}Ln^2s-\frac{97Ls}{72}+\frac{4L_0^rs}{3}+\frac{16L_1^rs}{3}+\frac{32L_2^rs}{3}-8L_3^rs+2L_5^rs\\
&+16L_6^rs+4L_8^rs-\frac{17Lns}{72}+\frac{8L_0^rns}{3}+\frac{16L_3^rns}{3}-4L_5^rns+8L_8^rns\\
&+\frac{5}{12}n^2\pi_{16}s+\frac{n\pi_{16}s}{24}-\frac{\pi_{16}s}{2n}+\frac{\pi_{16}s}{2n^2}+\frac{13\pi_{16}s}{16}+\frac{1}{48}Ln^2(t-u)s-\frac{L(t-u)s}{24}\\
&+\frac{4L_0^r(t-u)s}{3}-\frac{8L_1^r(t-u)s}{3}+\frac{4L_2^r(t-u)s}{3}-\frac{2L_3^r(t-u)s}{3}-\frac{4L_4^r(t-u)s}{3}\\
&-\frac{L_5^r(t-u)s}{3}-\frac{1}{16}Ln(t-u)s+\frac{4}{3}L_0^rn(t-u)s-\frac{2}{3}L_3^rn(t-u)s-\frac{1}{3}L_5^rn(t-u)s\\
&+\frac{17}{216}n^2\pi_{16}(t-u)s+\frac{253}{864}n\pi_{16}(t-u)s+\frac{155\pi_{16}(t-u)s}{864}+\frac{Ls}{4n}+\frac{64L_0^rs}{3n}\\
&+\frac{64L_3^rs}{3n}-\frac{Ls}{4n^2}+\frac{19L}{18}+\frac{16L_0^r}{3}+\frac{32L_3^r}{3}-8L_5^r+16L_8^r-\frac{5Ln}{18}+\frac{5n\pi_{16}}{6}\\
&-\frac{4\pi_{16}}{n}+\frac{5\pi_{16}}{n^2}+\frac{2\pi_{16}}{9}-\frac{1}{12}Ln^2(t-u)-\frac{L(t-u)}{6}+\frac{16L_4^r(t-u)}{3}
\end{aligned}
$$

II

$$+\frac{4L_5^r(t-u)}{3}-\frac{Ln(t-u)}{12}+\frac{4L_5^r n(t-u)}{3}-\frac{11}{48}n^2\pi_{16}(t-u)$$
$$-\frac{59n\pi_{16}(t-u)}{144}+\frac{\pi_{16}(t-u)}{8n}-\frac{\pi_{16}(t-u)}{8n^2}+\frac{3\pi_{16}(t-u)}{8}+\frac{5L}{2n}-\frac{80L_0^r}{3n}$$
$$-\frac{80L_3^r}{3n}+\frac{16L_5^r}{n}-\frac{48L_8^r}{n}-\frac{3L}{n^2}\Bigg\} \qquad \text{(II.89)}$$

$$B_T(t)=k_3(t)\left\{\frac{nt^2}{24}+\frac{t^2}{24}-\frac{nt}{9}-\frac{t}{6n}+\frac{t}{6n^2}+\frac{t}{18}+\frac{n}{18}+\frac{1}{3n}-\frac{1}{3n^2}-\frac{5}{18}\right\}$$
$$+k_2(t)\left\{-\frac{3t^3}{32}+\frac{9t^2}{16}-\frac{9t}{8}+\frac{3}{4}\right\}$$
$$+k_1(t)\left\{-\frac{5nt^3}{288}-\frac{11t^3}{288}+\frac{nt^2}{16}+\frac{3t^2}{16}-\frac{nt}{72}+\frac{t}{4n}-\frac{t}{4n^2}-\frac{31t}{72}-\frac{n}{12}-\frac{1}{2n}\right.$$
$$\left.+\frac{1}{2n^2}+\frac{5}{12}\right\}$$
$$+\bar{J}(t)\left\{\frac{19Lt^3}{72}-2L_0^r t^3-\frac{8L_1^r t^3}{3}-\frac{16L_2^r t^3}{3}-\frac{2L_3^r t^3}{3}+\frac{5}{144}Lnt^3-\frac{17}{288}n\pi_{16}t^3\right.$$
$$-\frac{29\pi_{16}t^3}{96}-\frac{31Lt^2}{18}+12L_0^r t^2+\frac{32L_1^r t^2}{3}+\frac{88L_2^r t^2}{3}+\frac{8L_3^r t^2}{3}+8L_4^r t^2+2L_5^r t^2$$
$$-\frac{11}{36}Lnt^2+\frac{1}{18}n\pi_{16}t^2+\frac{55\pi_{16}t^2}{36}+\frac{151Lt}{36}-24L_0^r t-\frac{64L_1^r t}{3}-\frac{176L_2^r t}{3}$$
$$-\frac{16L_3^r t}{3}-16L_4^r t-4L_5^r t-32L_6^r t-8L_8^r t+\frac{31Lnt}{36}+\frac{29n\pi_{16}t}{72}+\frac{\pi_{16}t}{n}-\frac{\pi_{16}t}{n^2}$$
$$-\frac{27\pi_{16}t}{8}-\frac{Lt}{2n}+\frac{Lt}{2n^2}-\frac{65L}{18}+16L_0^r+\frac{64L_1^r}{3}+\frac{128L_2^r}{3}+\frac{16L_3^r}{3}+64L_6^r$$
$$\left.+16L_8^r-\frac{7Ln}{9}-\frac{5n\pi_{16}}{9}-\frac{2\pi_{16}}{n}+\frac{2\pi_{16}}{n^2}+\frac{55\pi_{16}}{18}+\frac{L}{n}-\frac{L}{n^2}\right\} \qquad \text{(II.90)}$$

$$C_S(s)=k_3(s)\left\{\frac{ns^2}{24}+\frac{s^2}{24}-\frac{5ns}{18}+\frac{s}{6n}-\frac{7s}{36}-\frac{1}{3n^2}+\frac{2}{3n^3}-\frac{1}{6}\right\}$$
$$+k_2(s)\left\{\frac{3ns^3}{32}-\frac{s^3}{32}+\frac{3s^2}{16}+\frac{1}{2n^2}-\frac{3}{4n^3}\right\}$$
$$+k_1(s)\left\{\frac{13ns^3}{288}+\frac{s^3}{288}-\frac{23ns^2}{144}-\frac{s^2}{72}+\frac{5ns}{12}-\frac{s}{2n}+\frac{s}{4}+\frac{1}{2n^2}-\frac{1}{n^3}+\frac{1}{4}\right\}$$
$$+\bar{J}(s)\left\{\frac{Ls^3}{18}+\frac{4L_0^r s^3}{3}+\frac{8L_3^r s^3}{3}-\frac{5}{18}Lns^3+8L_1^r ns^3+\frac{8}{3}L_2^r ns^3+\frac{85}{288}n\pi_{16}s^3\right.$$

$$
\begin{aligned}
&-\frac{19\pi_{16}s^3}{288}-\frac{35Ls^2}{72}-\frac{8L_0^rs^2}{3}+8L_1^rs^2+\frac{8L_2^rs^2}{3}-\frac{28L_3^rs^2}{3}+2L_5^rs^2+\frac{19}{72}Lns^2\\
&-32L_1^rns^2-\frac{16}{3}L_2^rns^2+16L_4^rns^2-\frac{7}{12}n\pi_{16}s^2+\frac{3\pi_{16}s^2}{16}-\frac{8L_1^rs^2}{n}-\frac{8L_2^rs^2}{3n}\\
&+\frac{20L_0^rs^2}{3n^2}+\frac{20L_3^rs^2}{3n^2}-\frac{Ls}{9}+\frac{16L_0^rs}{3}-32L_1^rs-\frac{16L_2^rs}{3}+\frac{32L_3^rs}{3}+16L_4^rs\\
&-8L_5^rs+16L_8^rs-\frac{11Lns}{18}+32L_1^rns+\frac{32L_2^rns}{3}-32L_4^rns+32L_6^rns\\
&+\frac{35n\pi_{16}s}{18}-\frac{7\pi_{16}s}{4n}+\frac{89\pi_{16}s}{72}+\frac{Ls}{n}+\frac{32L_1^rs}{n}+\frac{16L_2^rs}{3n}-\frac{16L_4^rs}{n}-\frac{64L_0^rs}{3n^2}\\
&-\frac{64L_3^rs}{3n^2}-\frac{L}{3}+32L_1^r+\frac{32L_2^r}{3}-32L_4^r+32L_6^r+\frac{3\pi_{16}}{n^2}-\frac{11\pi_{16}}{2n^3}+\frac{10\pi_{16}}{9}\\
&-\frac{L}{n}-\frac{32L_1^r}{n}-\frac{32L_2^r}{3n}+\frac{32L_4^r}{n}-\frac{32L_6^r}{n}-\frac{2L}{n^2}+\frac{80L_0^r}{3n^2}+\frac{80L_3^r}{3n^2}-\frac{16L_5^r}{n^2}\\
&+\frac{48L_8^r}{n^2}+\frac{7L}{2n^3}\Bigg\}
\end{aligned}
\tag{II.91}
$$

$$
\begin{aligned}
C_T(t)=k_3(t)&\left\{\frac{nt^2}{24}+\frac{t^2}{24}-\frac{nt}{9}-\frac{t}{6n}-\frac{t}{9}+\frac{n}{18}+\frac{1}{3n}+\frac{1}{18}\right\}\\
+k_2(t)&\left\{-\frac{t^3}{32}+\frac{3t^2}{16}-\frac{3t}{8}+\frac{1}{4}\right\}\\
+k_1(t)&\left\{-\frac{5nt^3}{288}+\frac{t^3}{288}+\frac{nt^2}{16}-\frac{t^2}{16}-\frac{nt}{72}+\frac{t}{4n}+\frac{11t}{72}-\frac{n}{12}-\frac{1}{2n}-\frac{1}{12}\right\}\\
+\bar{J}(t)&\left\{\frac{Lt^3}{18}-2L_0^rt^3-\frac{2L_3^rt^3}{3}+\frac{5}{144}Lnt^3-\frac{17}{288}n\pi_{16}t^3-\frac{19\pi_{16}t^3}{288}-\frac{7Lt^2}{18}+12L_0^rt^2\right.\\
&+\frac{8L_3^rt^2}{3}+2L_5^rt^2-\frac{11}{36}Lnt^2+\frac{1}{18}n\pi_{16}t^2+\frac{\pi_{16}t^2}{12}+\frac{37Lt}{36}-24L_0^rt-\frac{16L_3^rt}{3}\\
&-4L_5^rt-8L_8^rt+\frac{31Lnt}{36}+\frac{29n\pi_{16}t}{72}+\frac{\pi_{16}t}{n}+\frac{13\pi_{16}t}{72}-\frac{Lt}{2n}-\frac{17L}{18}+16L_0^r\\
&\left.+\frac{16L_3^r}{3}+16L_8^r-\frac{7Ln}{9}-\frac{5n\pi_{16}}{9}-\frac{2\pi_{16}}{n}-\frac{\pi_{16}}{6}+\frac{L}{n}\right\}
\end{aligned}
\tag{II.92}
$$

II.A.3 Pseudo-real or two-colour

$$
\begin{aligned}
B_S(s,t-u)=k_4(s)&\left\{\frac{n^2}{12}+\frac{n}{12}-\frac{1}{6}+\frac{1}{2n}+\frac{1}{2n^2}\right\}(t-u)\\
+k_3(s)&\left\{\frac{s^2n^2}{48}-\frac{sn^2}{18}-\frac{1}{48}s(t-u)n^2+\frac{(t-u)n^2}{36}+\frac{sn}{24}+\frac{s(t-u)n}{24}\right.
\end{aligned}
\tag{II.93}
$$

II

$$
\begin{aligned}
&-\frac{(t-u)n}{72}+\frac{n}{9}-\frac{s^2}{48}+\frac{s}{18}-\frac{s(t-u)}{48}-\frac{7(t-u)}{72}-\frac{1}{36}-\frac{s}{12n}+\frac{(t-u)}{12n}\\
&-\frac{1}{2n}-\frac{s}{12n^2}+\frac{(t-u)}{12n^2}-\frac{2}{3n^2}\Bigg\}\\
&+k_2(s)\Bigg\{\frac{n^2s^3}{64}+\frac{ns^3}{64}+\frac{3s^3}{64}-\frac{3ns^2}{32}-\frac{1}{576}n^2(t-u)s^2+\frac{1}{288}n(t-u)s^2\\
&-\frac{(t-u)s^2}{576}-\frac{9s^2}{32}+\frac{1}{72}n^2(t-u)s-\frac{n(t-u)s}{36}+\frac{(t-u)s}{72}+\frac{3s}{16}-\frac{n^2(t-u)}{36}\\
&+\frac{n(t-u)}{18}-\frac{(t-u)}{36}+\frac{1}{2n}+\frac{1}{2n^2}\Bigg\}\\
&+k_1(s)\Bigg\{\frac{n^2s^3}{576}-\frac{ns^3}{96}+\frac{11s^3}{576}-\frac{17n^2s^2}{288}+\frac{11ns^2}{288}+\frac{1}{576}n^2(t-u)s^2\\
&+\frac{1}{144}n(t-u)s^2-\frac{5(t-u)s^2}{576}-\frac{3s^2}{32}+\frac{n^2s}{12}-\frac{ns}{144}-\frac{1}{96}n^2(t-u)s\\
&-\frac{n(t-u)s}{32}+\frac{(t-u)s}{48}+\frac{s}{8n}+\frac{s}{8n^2}+\frac{31s}{144}-\frac{n}{6}-\frac{n^2(t-u)}{48}\\
&+\frac{n(t-u)}{24}+\frac{5(t-u)}{48}+\frac{3}{4n}+\frac{1}{n^2}+\frac{1}{24}\Bigg\}\\
&+\bar{J}(s)\Bigg\{-\frac{5}{144}Ln^2s^3-\frac{19Ls^3}{144}-L_0^rs^3+\frac{4L_1^rs^3}{3}+\frac{8L_2^rs^3}{3}-\frac{L_3^rs^3}{3}-\frac{1}{96}Lns^3\\
&+\frac{2}{3}L_0^rns^3+\frac{4}{3}L_3^rns^3+\frac{17}{576}n^2\pi_{16}s^3+\frac{1}{288}n\pi_{16}s^3+\frac{29\pi_{16}s^3}{192}+\frac{7}{144}Ln^2s^2\\
&+\frac{31Ls^2}{36}+\frac{8L_0^rs^2}{3}-\frac{8L_1^rs^2}{3}-\frac{28L_2^rs^2}{3}-2L_3^rs^2-4L_4^rs^2+L_5^rs^2+\frac{13}{144}Lns^2\\
&-\frac{4}{3}L_0^rns^2-\frac{14}{3}L_3^rns^2+L_5^rns^2-\frac{35}{144}n^2\pi_{16}s^2-\frac{19}{288}n\pi_{16}s^2-\frac{55\pi_{16}s^2}{72}\\
&+\frac{1}{48}L(t-u)s^2+\frac{1}{3}L_0^r(t-u)s^2+\frac{2}{3}L_1^r(t-u)s^2-\frac{1}{3}L_2^r(t-u)s^2-\frac{1}{6}L_3^r(t-u)s^2\\
&-\frac{1}{48}Ln(t-u)s^2-\frac{1}{3}L_0^rn(t-u)s^2+\frac{1}{6}L_3^rn(t-u)s^2-\frac{1}{432}n^2\pi_{16}(t-u)s^2\\
&+\frac{47n\pi_{16}(t-u)s^2}{1728}-\frac{43\pi_{16}(t-u)s^2}{1728}-\frac{20L_0^rs^2}{3n}-\frac{20L_3^rs^2}{3n}-\frac{5}{36}Ln^2s-\frac{97Ls}{72}\\
&-\frac{4L_0^rs}{3}+\frac{16L_1^rs}{3}+\frac{32L_2^rs}{3}+8L_3^rs-2L_5^rs+16L_6^rs-4L_8^rs+\frac{17Lns}{72}+\frac{8L_0^rns}{3}\\
&+\frac{16L_3^rns}{3}-4L_5^rns+8L_8^rns+\frac{5}{12}n^2\pi_{16}s-\frac{n\pi_{16}s}{24}+\frac{\pi_{16}s}{2n}+\frac{\pi_{16}s}{2n^2}+\frac{13\pi_{16}s}{16}\\
&+\frac{1}{48}Ln^2(t-u)s-\frac{L(t-u)s}{24}-\frac{4L_0^r(t-u)s}{3}-\frac{8L_1^r(t-u)s}{3}+\frac{4L_2^r(t-u)s}{3}
\end{aligned}
$$

$$
\begin{aligned}
&+\frac{2L_3^r(t-u)s}{3}-\frac{4L_4^r(t-u)s}{3}+\frac{L_5^r(t-u)s}{3}+\frac{1}{16}Ln(t-u)s+\frac{4}{3}L_0^rn(t-u)s\\
&-\frac{2}{3}L_3^rn(t-u)s-\frac{1}{3}L_5^rn(t-u)s+\frac{17}{216}n^2\pi_{16}(t-u)s-\frac{253}{864}n\pi_{16}(t-u)s\\
&+\frac{155\pi_{16}(t-u)s}{864}-\frac{Ls}{4n}+\frac{64L_0^rs}{3n}+\frac{64L_3^rs}{3n}-\frac{Ls}{4n^2}+\frac{19L}{18}-\frac{16L_0^r}{3}-\frac{32L_3^r}{3}+8L_5^r\\
&-16L_8^r+\frac{5Ln}{18}-\frac{5n\pi_{16}}{6}+\frac{4\pi_{16}}{n}+\frac{5\pi_{16}}{n^2}+\frac{2\pi_{16}}{9}-\frac{1}{12}Ln^2(t-u)-\frac{L(t-u)}{6}\\
&+\frac{16L_4^r(t-u)}{3}-\frac{4L_5^r(t-u)}{3}+\frac{Ln(t-u)}{12}+\frac{4L_5^rn(t-u)}{3}-\frac{11}{48}n^2\pi_{16}(t-u)\\
&+\frac{59n\pi_{16}(t-u)}{144}-\frac{\pi_{16}(t-u)}{8n}-\frac{\pi_{16}(t-u)}{8n^2}+\frac{3\pi_{16}(t-u)}{8}-\frac{5L}{2n}-\frac{80L_0^r}{3n}-\frac{80L_3^r}{3n}\\
&+\frac{16L_5^r}{n}-\frac{48L_8^r}{n}-\frac{3L}{n^2}\Bigg\}
\end{aligned}
$$

$$
\begin{aligned}
B_T(t)=k_3(t)&\Bigg\{-\frac{nt^2}{24}+\frac{t^2}{24}+\frac{nt}{9}+\frac{t}{6n}+\frac{t}{6n^2}+\frac{t}{18}-\frac{n}{18}-\frac{1}{3n}-\frac{1}{3n^2}-\frac{5}{18}\Bigg\}\\
&+k_2(t)\Bigg\{-\frac{3t^3}{32}+\frac{9t^2}{16}-\frac{9t}{8}+\frac{3}{4}\Bigg\}\\
&+k_1(t)\Bigg\{\frac{5nt^3}{288}-\frac{11t^3}{288}-\frac{nt^2}{16}+\frac{3t^2}{16}+\frac{nt}{72}-\frac{t}{4n}-\frac{t}{4n^2}-\frac{31t}{72}+\frac{n}{12}\\
&\quad+\frac{1}{2n}+\frac{1}{2n^2}+\frac{5}{12}\Bigg\}\\
&+\bar{J}(t)\Bigg\{\frac{19Lt^3}{72}+2L_0^rt^3-\frac{8L_1^rt^3}{3}-\frac{16L_2^rt^3}{3}+\frac{2L_3^rt^3}{3}-\frac{5}{144}Lnt^3+\frac{17}{288}n\pi_{16}t^3\\
&\quad-\frac{29\pi_{16}t^3}{96}-\frac{31Lt^2}{18}-12L_0^rt^2+\frac{32L_1^rt^2}{3}+\frac{88L_2^rt^2}{3}-\frac{8L_3^rt^2}{3}+8L_4^rt^2-2L_5^rt^2\\
&\quad+\frac{11}{36}Lnt^2-\frac{1}{18}n\pi_{16}t^2+\frac{55\pi_{16}t^2}{36}+\frac{151Lt}{36}+24L_0^rt-\frac{64L_1^rt}{3}-\frac{176L_2^rt}{3}+\frac{16L_3^rt}{3}\\
&\quad-16L_4^rt+4L_5^rt-32L_6^rt+8L_8^rt-\frac{31Lnt}{36}-\frac{29n\pi_{16}t}{72}-\frac{\pi_{16}t}{n}-\frac{\pi_{16}t}{n^2}-\frac{27\pi_{16}t}{8}\\
&\quad+\frac{Lt}{2n}+\frac{Lt}{2n^2}-\frac{65L}{18}-16L_0^r+\frac{64L_1^r}{3}+\frac{128L_2^r}{3}-\frac{16L_3^r}{3}+64L_6^r-16L_8^r+\frac{7Ln}{9}\\
&\quad+\frac{5n\pi_{16}}{9}+\frac{2\pi_{16}}{n}+\frac{2\pi_{16}}{n^2}+\frac{55\pi_{16}}{18}-\frac{L}{n}-\frac{L}{n^2}\Bigg\}
\end{aligned}
\tag{II.94}
$$

$$
C_S(s)=k_3(s)\Bigg\{\frac{ns^2}{24}-\frac{s^2}{24}-\frac{5ns}{18}+\frac{s}{6n}+\frac{7s}{36}+\frac{1}{3n^2}+\frac{2}{3n^3}+\frac{1}{6}\Bigg\}
$$

$$
\begin{aligned}
&+k_2(s)\left\{\frac{3ns^3}{32}+\frac{s^3}{32}-\frac{3s^2}{16}-\frac{1}{2n^2}-\frac{3}{4n^3}\right\}\\
&+k_1(s)\left\{\frac{13ns^3}{288}-\frac{s^3}{288}-\frac{23ns^2}{144}+\frac{s^2}{72}+\frac{5ns}{12}-\frac{s}{2n}-\frac{s}{4}-\frac{1}{2n^2}-\frac{1}{n^3}-\frac{1}{4}\right\}\\
&+\bar{J}(s)\left\{-\frac{Ls^3}{18}+\frac{4L_0^rs^3}{3}+\frac{8L_3^rs^3}{3}-\frac{5}{18}Lns^3+8L_1^rns^3+\frac{8}{3}L_2^rns^3+\frac{85}{288}n\pi_{16}s^3\right.\\
&\quad+\frac{19\pi_{16}s^3}{288}+\frac{35Ls^2}{72}-\frac{8L_0^rs^2}{3}-8L_1^rs^2-\frac{8L_2^rs^2}{3}-\frac{28L_3^rs^2}{3}+2L_5^rs^2+\frac{19}{72}Lns^2\\
&\quad-32L_1^rns^2-\frac{16}{3}L_2^rns^2+16L_4^rns^2-\frac{7}{12}n\pi_{16}s^2-\frac{3\pi_{16}s^2}{16}-\frac{8L_1^rs^2}{n}-\frac{8L_2^rs^2}{3n}\\
&\quad+\frac{20L_0^rs^2}{3n^2}+\frac{20L_3^rs^2}{3n^2}+\frac{Ls}{9}+\frac{16L_0^rs}{3}+32L_1^rs+\frac{16L_2^rs}{3}+\frac{32L_3^rs}{3}-16L_4^rs-8L_5^rs\\
&\quad+16L_8^rs-\frac{11Lns}{18}+32L_1^rns+\frac{32L_2^rns}{3}-32L_4^rns+32L_6^rns+\frac{35n\pi_{16}s}{18}\\
&\quad-\frac{7\pi_{16}s}{4n}-\frac{89\pi_{16}s}{72}+\frac{Ls}{n}+\frac{32L_1^rs}{n}+\frac{16L_2^rs}{3n}-\frac{16L_4^rs}{n}-\frac{64L_0^rs}{3n^2}-\frac{64L_3^rs}{3n^2}+\frac{L}{3}-32L_1^r\\
&\quad-\frac{32L_2^r}{3}+32L_4^r-32L_6^r-\frac{3\pi_{16}}{n^2}-\frac{11\pi_{16}}{2n^3}-\frac{10\pi_{16}}{9}-\frac{L}{n}-\frac{32L_1^r}{n}-\frac{32L_2^r}{3n}\\
&\quad\left.+\frac{32L_4^r}{n}-\frac{32L_6^r}{n}+\frac{2L}{n^2}+\frac{80L_0^r}{3n^2}+\frac{80L_3^r}{3n^2}-\frac{16L_5^r}{n^2}+\frac{48L_8^r}{n^2}+\frac{7L}{2n^3}\right\}
\end{aligned}
\tag{II.95}
$$

$$
\begin{aligned}
C_T(t)=\;&k_3(t)\left\{\frac{nt^2}{24}-\frac{t^2}{24}-\frac{nt}{9}-\frac{t}{6n}+\frac{t}{9}+\frac{n}{18}+\frac{1}{3n}-\frac{1}{18}\right\}\\
&+k_2(t)\left\{\frac{t^3}{32}-\frac{3t^2}{16}+\frac{3t}{8}-\frac{1}{4}\right\}\\
&+k_1(t)\left\{-\frac{5nt^3}{288}-\frac{t^3}{288}+\frac{nt^2}{16}+\frac{t^2}{16}-\frac{nt}{72}+\frac{t}{4n}-\frac{11t}{72}-\frac{n}{12}-\frac{1}{2n}+\frac{1}{12}\right\}\\
&+\bar{J}(t)\left\{-\frac{Lt^3}{18}-2L_0^rt^3-\frac{2L_3^rt^3}{3}+\frac{5}{144}Lnt^3-\frac{17}{288}n\pi_{16}t^3+\frac{19\pi_{16}t^3}{288}+\frac{7Lt^2}{18}\right.\\
&\quad+12L_0^rt^2+\frac{8L_3^rt^2}{3}+2L_5^rt^2-\frac{11}{36}Lnt^2+\frac{1}{18}n\pi_{16}t^2-\frac{\pi_{16}t^2}{12}-\frac{37Lt}{36}-24L_0^rt\\
&\quad-\frac{16L_3^rt}{3}-4L_5^rt-8L_8^rt+\frac{31Lnt}{36}+\frac{29n\pi_{16}t}{72}+\frac{\pi_{16}t}{n}-\frac{13\pi_{16}t}{72}-\frac{Lt}{2n}\\
&\quad\left.+\frac{17L}{18}+16L_0^r+\frac{16L_3^r}{3}+16L_8^r-\frac{7Ln}{9}-\frac{5n\pi_{16}}{9}-\frac{2\pi_{16}}{n}+\frac{\pi_{16}}{6}+\frac{L}{n}\right\}
\end{aligned}
\tag{II.96}
$$

II.B Polynomial parts

Divergent parts can be put here.

II.B.1 Complex or QCD

The coefficients of polynomials part for B_P at NNLO.

$$
\begin{aligned}
\gamma_1 &= 32K_{13}^r + 32K_{14}^r n - 96K_{17}^r - 96K_{18}^r n + 96K_{25}^r + 32K_{26}^r n + 64K_3^r - 64K_{37}^r \\
&\quad + 96K_{39}^r + 32K_{40}^r n + \frac{29L^2n^2}{36} + \frac{19L^2}{n^2} + \frac{L^2}{3} - \frac{80LL_0^r n}{3} + \frac{64LL_0^r}{3n} - 64LL_1^r \\
&\quad - \frac{224LL_2^r}{3} - 8LL_3^r n + \frac{64LL_3^r}{3n} + \frac{64LL_4^r}{3} + \frac{40LL_5^r n}{3} - \frac{96LL_5^r}{n} - 160LL_6^r \\
&\quad - 32LL_7^r - 64LL_8^r n + \frac{224LL_8^r}{n} + 256L_4^r L_8^r n + 256L_5^r L_8^r - 512L_6^r L_8^r n - 512(L_8^r)^2 \\
&\quad + \pi_{16}^2 \left(\frac{n^2\pi^2}{27} + \frac{1645n^2}{1728} - \frac{35}{2n^2} + \frac{4\pi^2}{9} - \frac{181}{54} \right) \\
&\quad + \pi_{16} \left(\frac{229Ln^2}{216} + \frac{4L}{n^2} - \frac{26L}{9} - \frac{80L_0^r n}{9} + \frac{256L_0^r}{9n} - \frac{32L_1^r}{3} - \frac{368L_2^r}{9} \right. \\
&\quad \left. - \frac{8L_3^r n}{3} + \frac{256L_3^r}{9n} + \frac{256L_4^r}{9} + \frac{64L_5^r n}{9} - \frac{64L_5^r}{n} - 128L_6^r - 32L_8^r n + \frac{192L_8^r}{n} \right) \\
\gamma_2 &= -32K_{13}^r - 32K_{14}^r n + 64K_{17}^r + 64K_{18}^r n - 16K_{19}^r - 8K_{20}^r n - 16K_{23}^r - 32K_{28}^r \\
&\quad - 96K_3^r - 16K_{33}^r + 32K_{37}^r - \frac{17}{36}L^2n^2 - \frac{3L^2}{2n^2} - \frac{13L^2}{3} + 24LL_0^r n + \frac{16LL_0^r}{n} \\
&\quad + \frac{176LL_1^r}{3} + \frac{248LL_2^r}{3} + \frac{4LL_3^r n}{3} + \frac{16LL_3^r}{n} + \frac{32LL_4^r}{3} + \frac{20LL_5^r n}{3} + 48LL_6^r \\
&\quad + 8LL_8^r n - 32L_4^r L_5^r n - 32(L_5^r)^2 + 64L_5^r L_6^r n + 64L_5^r L_8^r \\
&\quad + \pi_{16} \left(- \frac{445Ln^2}{432} - \frac{37L}{36} + 8L_0^r n - \frac{16L_0^r}{n} + \frac{80L_1^r}{9} + \frac{512L_2^r}{9} + \frac{16L_3^r n}{9} \right. \\
&\quad \left. - \frac{16L_3^r}{n} + \frac{32L_4^r}{9} + \frac{8L_5^r n}{9} + 48L_6^r + 8L_8^r n \right) \\
&\quad + \pi_{16}^2 \left(- \frac{5}{72}n^2\pi^2 - \frac{3865n^2}{10368} + \frac{3}{n^2} - \frac{13\pi^2}{36} - \frac{25}{432} \right) \\
\gamma_3 &= 2K_{11}^r + 8K_{13}^r + 8K_{14}^r n - 16K_{17}^r - 12K_{18}^r n + 16K_{28}^r + 48K_3^r - 4K_{31}^r + 8K_5^r \\
&\quad + 2K_7^r + 2K_8^r n + \frac{29L^2n^2}{288} + \frac{27L^2}{16} - 8LL_0^r n + \frac{20LL_0^r}{3n} - \frac{56LL_1^r}{3} - 40LL_2^r \\
&\quad - \frac{8LL_3^r n}{3} + \frac{20LL_3^r}{3n} - 8LL_4^r - LL_5^r n
\end{aligned}
$$

$$
\begin{aligned}
&+\pi_{16}\left(\frac{49Ln^2}{216}+\frac{29L}{16}-\frac{7L_0^r n}{3}+\frac{56L_0^r}{9n}-\frac{62L_1^r}{9}-31L_2^r-\frac{25L_3^r n}{18}\right.\\
&\left.+\frac{56L_3^r}{9n}-\frac{20L_4^r}{3}-\frac{2L_5^r n}{3}\right)\\
&+\pi_{16}^2\left(\frac{n^2\pi^2}{72}+\frac{445n^2}{5184}+\frac{3\pi^2}{16}-\frac{23}{192}\right)\\
\gamma_4 \;=\;& 2K_{11}^r+4K_{18}^r n+4K_{31}^r+8K_5^r+2K_7^r+2K_8^r n+\frac{11L^2n^2}{288}-\frac{7L^2}{48}-\frac{4LL_0^r n}{3}\\
&+\frac{20LL_0^r}{3n}-\frac{4LL_2^r}{3}-2LL_3^r n+\frac{20LL_3^r}{3n}+\frac{8LL_4^r}{3}-\frac{LL_5^r n}{3}\\
&+\pi_{16}\left(\frac{29Ln^2}{216}+\frac{17L}{144}-\frac{13L_0^r n}{9}+\frac{56L_0^r}{9n}-\frac{10L_1^r}{3}-\frac{31L_2^r}{9}-\frac{11L_3^r n}{6}\right.\\
&\left.+\frac{56L_3^r}{9n}+\frac{20L_4^r}{9}-\frac{4L_5^r n}{9}\right)\\
&+\pi_{16}^2\left(-\frac{1}{108}n^2\pi^2+\frac{421n^2}{3456}-\frac{\pi^2}{144}-\frac{115}{1728}\right)\\
\gamma_5 \;=\;& K_1^r-8K_3^r-4K_5^r-\frac{5L^2n^2}{1152}-\frac{15L^2}{64}+\frac{5LL_0^r n}{12}+\frac{5LL_1^r}{2}+\frac{25LL_2^r}{4}+\frac{5LL_3^r n}{24}\\
&+\pi_{16}\left(-\frac{19Ln^2}{2304}-\frac{13L}{32}+\frac{2L_0^r n}{9}+\frac{7L_1^r}{3}+\frac{35L_2^r}{6}+\frac{5L_3^r n}{18}\right)\\
&+\pi_{16}^2\left(\frac{n^2\pi^2}{3456}-\frac{1015n^2}{165888}-\frac{\pi^2}{32}+\frac{23}{384}\right)\\
\gamma_6 \;=\;& 3K_1^r-4K_5^r-\frac{5}{384}L^2n^2-\frac{5L^2}{64}+\frac{7LL_0^r n}{12}+\frac{5LL_1^r}{6}+\frac{25LL_2^r}{12}+\frac{23LL_3^r n}{24}\\
&+\pi_{16}\left(-\frac{203Ln^2}{6912}-\frac{13L}{96}+\frac{4L_0^r n}{9}+\frac{7L_1^r}{9}+\frac{35L_2^r}{18}+\frac{17L_3^r n}{18}\right)\\
&+\pi_{16}^2\left(-\frac{n^2\pi^2}{3456}-\frac{1933n^2}{165888}-\frac{\pi^2}{96}+\frac{23}{1152}\right)
\end{aligned}
$$

The coefficients of polynomials part for C_P at NNLO.

$$
\begin{aligned}
\delta_1 \;=\;& 64K_{10}^r n-128K_{18}^r+128K_2^r-64K_{20}^r-128K_{21}^r-128K_{22}^r n+128K_{26}^r+192K_{27}^r n\\
&-128K_{35}^r+128K_{40}^r+64K_9^r-\frac{14L^2}{n^3}+\frac{2L^2}{n}-\frac{192LL_0^r}{n^2}-64LL_1^r n+\frac{128LL_1^r}{n}\\
&+\frac{32LL_2^r}{n}-\frac{192LL_3^r}{n^2}+64LL_4^r n-\frac{96LL_4^r}{n}+\frac{96LL_5^r}{n^2}+16LL_5^r-64LL_6^r n+\frac{64LL_6^r}{n}\\
&+\frac{64LL_7^r}{n}-\frac{192LL_8^r}{n^2}-32LL_8^r-256(L_4^r)^2 n-256L_4^r L_5^r+1024L_4^r L_6^r n+512L_4^r L_8^r\\
&+512L_5^r L_6^r-1024(L_6^r)^2 n-1024L_6^r L_8^r
\end{aligned}
$$

$$
\begin{aligned}
&+\pi_{16}\left(-\frac{12L}{n^3}+\frac{4L}{n}-\frac{64L_0^r}{n^2}+\frac{64L_1^r}{n}-\frac{64L_3^r}{n^2}-\frac{64L_4^r}{n}+\frac{64L_5^r}{n^2}+\frac{64L_6^r}{n}-\frac{192L_8^r}{n^2}\right)\\
&+\pi_{16}^2\left(\frac{10}{n^3}+\frac{3}{n}\right)\\
\delta_2 \;=\;& -64K_{10}^r n+128K_{18}^r-192K_2^r+32K_{20}^r+64K_{21}^r+64K_{22}^r n-32K_{32}^r+64K_{35}^r\\
&-32K_{38}^r-64K_9^r+\frac{37L^2n}{36}-\frac{3L^2}{n}+\frac{416LL_0^r}{3n^2}-16LL_0^r-\frac{96LL_1^r}{n}-16LL_2^r n\\
&-\frac{64LL_2^r}{3n}+\frac{416LL_3^r}{3n^2}-\frac{128LL_3^r}{3}+16LL_4^r n+\frac{32LL_4^r}{n}+24LL_5^r-32LL_6^r n\\
&-48LL_8^r+128(L_4^r)^2 n+128L_4^rL_5^r-256L_4^rL_6^r n-256L_4^rL_8^r\\
&+\pi_{16}\left(-\frac{31Ln}{12}-\frac{L}{n}+\frac{608L_0^r}{9n^2}-32L_1^r n-\frac{64L_1^r}{n}-\frac{16L_2^r}{9n}+\frac{608L_3^r}{9n^2}-\frac{176L_3^r}{9}\right.\\
&\left.+32L_4^r n+\frac{32L_4^r}{n}+24L_5^r-32L_6^r n-48L_8^r\right)\\
&+\pi_{16}^2\left(-\frac{2n\pi^2}{27}-\frac{373n}{1296}-\frac{\pi^2}{3n}+\frac{25}{4n}\right)\\
\delta_3 \;=\;& 16K_{10}^r n+4K_{15}^r+4K_{16}^r n-32K_{18}^r+96K_2^r-8K_{29}^r+16K_{32}^r+16K_9^r-\frac{13L^2n}{36}\\
&-\frac{80LL_0^r}{3n^2}+\frac{20LL_0^r}{3}+32LL_1^r n+\frac{16LL_1^r}{n}+\frac{20LL_2^r n}{3}+\frac{16LL_2^r}{3n}-\frac{80LL_3^r}{3n^2}+\frac{88LL_3^r}{3}\\
&-16LL_4^r n-6LL_5^r\\
&+\pi_{16}\left(\frac{11Ln}{12}-\frac{224L_0^r}{9n^2}+\frac{8L_0^r}{9}+32L_1^r n+\frac{16L_1^r}{n}+\frac{8L_2^r n}{9}+\frac{40L_2^r}{9n}\right.\\
&\left.-\frac{224L_3^r}{9n^2}+\frac{166L_3^r}{9}-16L_4^r n-6L_5^r\right)\\
&+\pi_{16}^2\left(\frac{625n}{1296}-\frac{25n\pi^2}{432}\right)\\
\delta_4 \;=\;& 4K_{15}^r+4K_{16}^r n+8K_{29}^r+\frac{5L^2n}{24}-4LL_0^r-4LL_2^r n-2LL_5^r\\
&+\pi_{16}\left(\frac{Ln}{8}+2L_3^r-2L_5^r\right)+\pi_{16}^2\left(\frac{n\pi^2}{144}+\frac{7n}{32}\right)\\
\delta_5 \;=\;& -16K_2^r+2K_4^r+2K_6^r+\frac{55L^2n}{192}-\frac{11LL_0^r}{3}-8LL_1^r n-\frac{8LL_2^r n}{3}-\frac{17LL_3^r}{3}\\
&+\pi_{16}\left(\frac{101Ln}{192}-\frac{29L_0^r}{9}-8L_1^r n-\frac{20L_2^r n}{9}-\frac{97L_3^r}{18}\right)+\pi_{16}^2\left(\frac{19n\pi^2}{576}-\frac{115n}{6912}\right)\\
\delta_6 \;=\;& 6K_4^r-2K_6^r+\frac{5L^2n}{192}-3LL_0^r-LL_3^r
\end{aligned}
$$

II

$$+\pi_{16}\left(\frac{Ln}{64}-3L_0^r-\frac{5L_3^r}{6}\right)+\pi_{16}^2\left(\frac{5n\pi^2}{576}-\frac{437n}{6912}\right)$$

II.B.2 Real or adjoint

The coefficients of polynomials part for B_P at NNLO.

$$\begin{aligned}
\gamma_1 &= 32K_{13}^r+64K_{14}^rn-96K_{17}^r-192K_{18}^rn+96K_{25}^r+64K_{26}^rn+64K_3^r-64K_{37}^r\\
&+96K_{39}^r+64K_{40}^rn+\frac{29L^2n^2}{36}+\frac{19L^2}{4n^2}+\frac{83L^2n}{36}-\frac{17L^2}{4n}+\frac{19L^2}{12}-\frac{80LL_0^rn}{3}\\
&+\frac{32LL_0^r}{3n}-\frac{80LL_0^r}{3}-64LL_1^r-\frac{224LL_2^r}{3}-8LL_3^rn+\frac{32LL_3^r}{3n}-\frac{56LL_3^r}{3}+\frac{64LL_4^r}{3}\\
&+\frac{40LL_5^rn}{3}-\frac{48LL_5^r}{n}+\frac{64LL_5^r}{3}-160LL_6^r-32LL_7^r-64LL_8^rn+\frac{112LL_8^r}{n}-80LL_8^r\\
&+512L_4^rL_8^rn+256L_5^rL_8^r-1024L_6^rL_8^rn-512(L_8^r)^2\\
&+\pi_{16}\left(\frac{229Ln^2}{216}+\frac{L}{n^2}+\frac{623Ln}{216}-\frac{L}{n}+\frac{155L}{108}-\frac{80L_0^rn}{9}+\frac{128L_0^r}{9n}-\frac{224L_0^r}{9}\right.\\
&-\frac{32L_1^r}{3}-\frac{368L_2^r}{9}-\frac{8L_3^rn}{3}+\frac{128L_3^r}{9n}-\frac{56L_3^r}{9}+\frac{256L_4^r}{9}+\frac{64L_5^rn}{9}-\frac{32L_5^r}{n}\\
&\left.+\frac{136L_5^r}{9}-128L_6^r-32L_8^rn+\frac{96L_8^r}{n}-64L_8^r\right)\\
&+\pi_{16}^2\left(\frac{n^2\pi^2}{27}+\frac{1645n^2}{1728}-\frac{35}{8n^2}+\frac{10763n}{5184}+\frac{27}{8n}+\frac{13\pi^2}{54}-\frac{2149}{1296}\right)\\
\gamma_2 &= -32K_{13}^r-64K_{14}^rn+64K_{17}^r+128K_{18}^rn-16K_{19}^r-16K_{20}^rn-16K_{23}^r-32K_{28}^r\\
&-96K_3^r-16K_{33}^r+32K_{37}^r-\frac{17}{36}L^2n^2-\frac{3L^2}{8n^2}-\frac{85L^2n}{72}+\frac{3L^2}{8n}-\frac{43L^2}{16}+24LL_0^rn\\
&+\frac{8LL_0^r}{n}+\frac{80LL_0^r}{3}+\frac{176LL_1^r}{3}+\frac{248LL_2^r}{3}+\frac{4LL_3^rn}{3}+\frac{8LL_3^r}{n}+\frac{32LL_3^r}{3}+\frac{32LL_4^r}{3}\\
&+\frac{20LL_5^rn}{3}+\frac{14LL_5^r}{3}+48LL_6^r+8LL_8^rn+12LL_8^r-64L_4^rL_5^rn-32(L_5^r)^2\\
&+128L_5^rL_6^rn+64L_5^rL_8^r\\
&+\pi_{16}\left(-\frac{445Ln^2}{432}-\frac{317Ln}{108}-\frac{743L}{216}+8L_0^rn-\frac{8L_0^r}{n}+\frac{272L_0^r}{9}+\frac{80L_1^r}{9}+\frac{512L_2^r}{9}\right.\\
&\left.+\frac{16L_3^rn}{9}-\frac{8L_3^r}{n}+\frac{38L_3^r}{9}+\frac{32L_4^r}{9}+\frac{8L_5^rn}{9}+\frac{26L_5^r}{9}+48L_6^r+8L_8^rn+12L_8^r\right)\\
&+\pi_{16}^2\left(-\frac{5}{72}n^2\pi^2-\frac{3865n^2}{10368}+\frac{3}{4n^2}-\frac{35n\pi^2}{216}-\frac{1837n}{3456}-\frac{3}{4n}-\frac{91\pi^2}{432}-\frac{853}{1296}\right)\\
\gamma_3 &= 2K_{11}^r+8K_{13}^r+16K_{14}^rn-16K_{17}^r-24K_{18}^rn+16K_{28}^r+48K_3^r-4K_{31}^r+8K_5^r
\end{aligned}$$

$$
\begin{aligned}
&+2K_7^r+4K_8^r n+\frac{29L^2n^2}{288}+\frac{23L^2n}{72}+\frac{101L^2}{96}-8LL_0^r n+\frac{10LL_0^r}{3n}-16LL_0^r\\
&-\frac{56LL_1^r}{3}-40LL_2^r-\frac{8LL_3^r n}{3}+\frac{10LL_3^r}{3n}-6LL_3^r-8LL_4^r-LL_5^r n-2LL_5^r\\
&+\pi_{16}\left(\frac{49Ln^2}{216}+\frac{503Ln}{864}+\frac{2867L}{1728}-\frac{7L_0^r n}{3}+\frac{28L_0^r}{9n}-\frac{43L_0^r}{3}-\frac{62L_1^r}{9}-31L_2^r\right.\\
&\left.-\frac{25L_3^r n}{18}+\frac{28L_3^r}{9n}-3L_3^r-\frac{20L_4^r}{3}-\frac{2L_5^r n}{3}-\frac{5L_5^r}{3}\right)\\
&+\pi_{16}^2\left(\frac{n^2\pi^2}{72}+\frac{445n^2}{5184}+\frac{67n\pi^2}{864}-\frac{59n}{288}+\frac{185\pi^2}{1728}+\frac{2705}{20736}\right)
\end{aligned}
$$

$$
\begin{aligned}
\gamma_4 \;=\;& 2K_{11}^r+8K_{18}^r n+4K_{31}^r+8K_5^r+2K_7^r+4K_8^r n+\frac{11L^2n^2}{288}-\frac{L^2n}{72}-\frac{7L^2}{96}-\frac{4LL_0^r n}{3}\\
&+\frac{10LL_0^r}{3n}-\frac{4LL_0^r}{3}-\frac{4LL_2^r}{3}-2LL_3^r n+\frac{10LL_3^r}{3n}-\frac{4LL_3^r}{3}+\frac{8LL_4^r}{3}-\frac{LL_5^r n}{3}+\frac{2LL_5^r}{3}\\
&+\pi_{16}\left(\frac{29Ln^2}{216}-\frac{23Ln}{864}-\frac{137L}{1728}-\frac{13L_0^r n}{9}+\frac{28L_0^r}{9n}-\frac{13L_0^r}{9}-\frac{10L_1^r}{3}-\frac{31L_2^r}{9}\right.\\
&\left.-\frac{11L_3^r n}{6}+\frac{28L_3^r}{9n}-\frac{19L_3^r}{9}+\frac{20L_4^r}{9}-\frac{4L_5^r n}{9}+\frac{5L_5^r}{9}\right)\\
&+\pi_{16}^2\left(-\frac{1}{108}n^2\pi^2+\frac{421n^2}{3456}-\frac{n\pi^2}{288}-\frac{289n}{10368}-\frac{11\pi^2}{1728}-\frac{1091}{20736}\right)
\end{aligned}
$$

$$
\begin{aligned}
\gamma_5 \;=\;& K_1^r-8K_3^r-4K_5^r-\frac{5L^2n^2}{1152}-\frac{55L^2n}{2304}-\frac{5L^2}{32}+\frac{5LL_0^r n}{12}+\frac{5LL_0^r}{2}+\frac{5LL_1^r}{2}\\
&+\frac{25LL_2^r}{4}+\frac{5LL_3^r n}{24}+\frac{5LL_3^r}{8}\\
&+\pi_{16}\left(-\frac{19Ln^2}{2304}-\frac{13Ln}{768}-\frac{307L}{1152}+\frac{2L_0^r n}{9}+\frac{7L_0^r}{3}+\frac{7L_1^r}{3}+\frac{35L_2^r}{6}+\frac{5L_3^r n}{18}+\frac{7L_3^r}{12}\right)\\
&+\pi_{16}^2\left(\frac{n^2\pi^2}{3456}-\frac{1015n^2}{165888}-\frac{29n\pi^2}{3456}+\frac{10313n}{165888}-\frac{19\pi^2}{1152}+\frac{71}{13824}\right)
\end{aligned}
$$

$$
\begin{aligned}
\gamma_6 \;=\;& 3K_1^r-4K_5^r-\frac{5}{384}L^2n^2+\frac{L^2n}{768}-\frac{5L^2}{96}+\frac{7LL_0^r n}{12}+\frac{5LL_0^r}{6}+\frac{5LL_1^r}{6}\\
&+\frac{25LL_2^r}{12}+\frac{23LL_3^r n}{24}+\frac{5LL_3^r}{24}\\
&+\pi_{16}\left(-\frac{203Ln^2}{6912}+\frac{65Ln}{6912}-\frac{307L}{3456}+\frac{4L_0^r n}{9}+\frac{7L_0^r}{9}+\frac{7L_1^r}{9}+\frac{35L_2^r}{18}+\frac{17L_3^r n}{18}+\frac{7L_3^r}{36}\right)\\
&+\pi_{16}^2\left(-\frac{n^2\pi^2}{3456}-\frac{1933n^2}{165888}-\frac{11n\pi^2}{3456}+\frac{5299n}{165888}-\frac{19\pi^2}{3456}+\frac{71}{41472}\right)
\end{aligned}
$$

The coefficients of polynomials part for C_P at NNLO.

$$
\delta_1 \;=\; 128K_{10}^r n-128K_{18}^r+128K_2^r-64K_{20}^r-128K_{21}^r-256K_{22}^r n+128K_{26}^r+384K_{27}^r n
$$

II

$$
\begin{aligned}
&-128K^r_{35}+128K^r_{40}+64K^r_9-\frac{7L^2}{4n^3}+\frac{L^2}{n^2}+\frac{L^2}{2n}+\frac{L^2}{2}-\frac{48LL^r_0}{n^2}-64LL^r_1n+\frac{64LL^r_1}{n}\\
&-64LL^r_1+\frac{16LL^r_2}{n}-16LL^r_2-\frac{48LL^r_3}{n^2}+64LL^r_4n-\frac{48LL^r_4}{n}+48LL^r_4+\frac{24LL^r_5}{n^2}\\
&+8LL^r_5-64LL^r_6n+\frac{32LL^r_6}{n}-32LL^r_6+\frac{32LL^r_7}{n}-\frac{48LL^r_8}{n^2}-16LL^r_8-512(L^r_4)^2n\\
&-256L^r_4L^r_5+2048L^r_4L^r_6n+512L^r_4L^r_8+512L^r_5L^r_6-2048(L^r_6)^2n-1024L^r_6L^r_8\\
&+\pi_{16}\Bigg(-\frac{3L}{2n^3}+\frac{L}{n^2}+\frac{L}{n}-L-\frac{16L^r_0}{n^2}+\frac{32L^r_1}{n}-32L^r_1-\frac{16L^r_3}{n^2}-\frac{32L^r_4}{n}+32L^r_4\\
&+\frac{16L^r_5}{n^2}+\frac{32L^r_6}{n}-32L^r_6-\frac{48L^r_8}{n^2}\Bigg)\\
&+\pi^2_{16}\left(\frac{5}{4n^3}-\frac{1}{2n^2}+\frac{3}{4n}-\frac{1}{6}\right)\\
\delta_2 \;=\;& -128K^r_{10}n+128K^r_{18}-192K^r_2+32K^r_{20}+64K^r_{21}+128K^r_{22}n-32K^r_{32}+64K^r_{35}\\
&-32K^r_{38}-64K^r_9+\frac{37L^2n}{72}-\frac{3L^2}{4n}-\frac{7L^2}{36}+\frac{104LL^r_0}{3n^2}-8LL^r_0-\frac{48LL^r_1}{n}+48LL^r_1\\
&-16LL^r_2n-\frac{32LL^r_2}{3n}+\frac{32LL^r_2}{3}+\frac{104LL^r_3}{3n^2}-\frac{64LL^r_3}{3}+16LL^r_4n+\frac{16LL^r_4}{n}-16LL^r_4\\
&+12LL^r_5-32LL^r_6n-24LL^r_8+256(L^r_4)^2n+128L^r_4L^r_5-512L^r_4L^r_6n-256L^r_4L^r_8\\
&+\pi_{16}\Bigg(-\frac{31Ln}{24}-\frac{L}{4n}-\frac{5L}{18}+\frac{152L^r_0}{9n^2}-32L^r_1n-\frac{32L^r_1}{n}+32L^r_1-\frac{8L^r_2}{9n}+\frac{8L^r_2}{9}\\
&+\frac{152L^r_3}{9n^2}-\frac{88L^r_3}{9}+32L^r_4n+\frac{16L^r_4}{n}-16L^r_4+12L^r_5-32L^r_6n-24L^r_8\Bigg)\\
&+\pi^2_{16}\left(-\frac{n\pi^2}{27}-\frac{\pi^2}{12n}-\frac{373n}{2592}+\frac{25}{16n}-\frac{5\pi^2}{216}-\frac{565}{648}\right)\\
\delta_3 \;=\;& 32K^r_{10}n+4K^r_{15}+8K^r_{16}n-32K^r_{18}+96K^r_2-8K^r_{29}+16K^r_{32}+16K^r_9-\frac{13L^2n}{72}\\
&+\frac{49L^2}{144}-\frac{20LL^r_0}{3n^2}+\frac{10LL^r_0}{3}+32LL^r_1n+\frac{8LL^r_1}{n}-8LL^r_1+\frac{20LL^r_2n}{3}+\frac{8LL^r_2}{3n}\\
&-\frac{8LL^r_2}{3}-\frac{20LL^r_3}{3n^2}+\frac{44LL^r_3}{3}-16LL^r_4n-3LL^r_5\\
&+\pi_{16}\Bigg(\frac{11Ln}{24}+\frac{115L}{144}-\frac{56L^r_0}{9n^2}+\frac{4L^r_0}{9}+32L^r_1n+\frac{8L^r_1}{n}-8L^r_1+\frac{8L^r_2n}{9}+\frac{20L^r_2}{9n}\\
&-\frac{20L^r_2}{9}-\frac{56L^r_3}{9n^2}+\frac{83L^r_3}{9}-16L^r_4n-3L^r_5\Bigg)\\
&+\pi^2_{16}\left(-\frac{25n\pi^2}{864}+\frac{625n}{2592}+\frac{17\pi^2}{864}+\frac{1451}{5184}\right)
\end{aligned}
$$

$$
\begin{aligned}
\delta_4 &= 4K_{15}^r + 8K_{16}^r n + 8K_{29}^r + \frac{5L^2 n}{48} + \frac{L^2}{24} - 2LL_0^r - 4LL_2^r n - LL_5^r \\
&\quad + \pi_{16}\left(\frac{Ln}{16} + \frac{7L}{48} + L_3^r - L_5^r\right) \\
&\quad + \pi_{16}^2\left(\frac{n\pi^2}{288} + \frac{7n}{64} + \frac{\pi^2}{288} + \frac{11}{192}\right) \\
\delta_5 &= -16K_2^r + 2K_4^r + 2K_6^r + \frac{55L^2 n}{384} - \frac{L^2}{48} - \frac{11LL_0^r}{6} - 8LL_1^r n - \frac{8LL_2^r n}{3} - \frac{17LL_3^r}{6} \\
&\quad + \pi_{16}\left(\frac{101Ln}{384} - \frac{13L}{384} - \frac{29L_0^r}{18} - 8L_1^r n - \frac{20L_2^r n}{9} - \frac{97L_3^r}{36}\right) \\
&\quad + \pi_{16}^2\left(\frac{19n\pi^2}{1152} - \frac{115n}{13824} + \frac{\pi^2}{1152} - \frac{349}{13824}\right) \\
\delta_6 &= 6K_4^r - 2K_6^r + \frac{5L^2 n}{384} + \frac{L^2}{48} - \frac{3LL_0^r}{2} - \frac{LL_3^r}{2} \\
&\quad + \pi_{16}\left(\frac{Ln}{128} + \frac{13L}{384} - \frac{3L_0^r}{2} - \frac{5L_3^r}{12}\right) \\
&\quad + \pi_{16}^2\left(\frac{5n\pi^2}{1152} - \frac{437n}{13824} - \frac{\pi^2}{1152} + \frac{349}{13824}\right)
\end{aligned}
$$

II.B.3 Pseudo-real or two-colour

The coefficients of polynomials part for B_P at NNLO.

$$
\begin{aligned}
\gamma_1 &= 32K_{13}^r + 64K_{14}^r n - 96K_{17}^r - 192K_{18}^r n + 96K_{25}^r + 64K_{26}^r n + 64K_3^r - 64K_{37}^r \\
&\quad + 96K_{39}^r + 64K_{40}^r n + \frac{29L^2 n^2}{36} - \frac{83L^2 n}{36} + \frac{19L^2}{4n^2} + \frac{17L^2}{4n} + \frac{19L^2}{12} - \frac{80LL_0^r n}{3} \\
&\quad + \frac{32LL_0^r}{3n} + \frac{80LL_0^r}{3} - 64LL_1^r - \frac{224LL_2^r}{3} - 8LL_3^r n + \frac{32LL_3^r}{3n} + \frac{56LL_3^r}{3} + \frac{64LL_4^r}{3} \\
&\quad + \frac{40LL_5^r n}{3} - \frac{48LL_5^r}{n} - \frac{64LL_5^r}{3} - 160LL_6^r - 32LL_7^r - 64LL_8^r n + \frac{112LL_8^r}{n} \\
&\quad + 80LL_8^r + 512L_4^r L_8^r n + 256L_5^r L_8^r - 1024L_6^r L_8^r n - 512(L_8^r)^2 \\
&\quad + \pi_{16}\left(\frac{229Ln^2}{216} - \frac{623Ln}{216} + \frac{L}{n^2} + \frac{L}{n} + \frac{155L}{108} - \frac{80L_0^r n}{9} + \frac{128L_0^r}{9n} + \frac{224L_0^r}{9}\right. \\
&\quad - \frac{32L_1^r}{3} - \frac{368L_2^r}{9} - \frac{8L_3^r n}{3} + \frac{128L_3^r}{9n} + \frac{56L_3^r}{9} + \frac{256L_4^r}{9} + \frac{64L_5^r n}{9} \\
&\quad \left. - \frac{32L_5^r}{n} - \frac{136L_5^r}{9} - 128L_6^r - 32L_8^r n + \frac{96L_8^r}{n} + 64L_8^r\right) \\
&\quad + \pi_{16}^2\left(\frac{n^2\pi^2}{27} + \frac{1645n^2}{1728} - \frac{10763n}{5184} - \frac{35}{8n^2} - \frac{27}{8n} + \frac{13\pi^2}{54} - \frac{2149}{1296}\right) \\
\gamma_2 &= -32K_{13}^r - 64K_{14}^r n + 64K_{17}^r + 128K_{18}^r n - 16K_{19}^r - 16K_{20}^r n - 16K_{23}^r - 32K_{28}^r
\end{aligned}
$$

$$
\begin{aligned}
&-96K_3^r - 16K_{33}^r + 32K_{37}^r - \frac{17}{36}L^2n^2 + \frac{85L^2n}{72} - \frac{3L^2}{8n^2} - \frac{3L^2}{8n} - \frac{43L^2}{16} + 24LL_0^rn \\
&+\frac{8LL_0^r}{n} - \frac{80LL_0^r}{3} + \frac{176LL_1^r}{3} + \frac{248LL_2^r}{3} + \frac{4LL_3^rn}{3} + \frac{8LL_3^r}{n} - \frac{32LL_3^r}{3} + \frac{32LL_4^r}{3} \\
&+\frac{20LL_5^rn}{3} - \frac{14LL_5^r}{3} + 48LL_6^r + 8LL_8^rn - 12LL_8^r - 64L_4^rL_5^rn \\
&-32(L_5^r)^2 + 128L_5^rL_6^rn + 64L_5^rL_8^r \\
&+\pi_{16}\Bigg(- \frac{445Ln^2}{432} + \frac{317Ln}{108} - \frac{743L}{216} + 8L_0^rn - \frac{8L_0^r}{n} - \frac{272L_0^r}{9} + \frac{80L_1^r}{9} \\
&+\frac{512L_2^r}{9} + \frac{16L_3^rn}{9} - \frac{8L_3^r}{n} - \frac{38L_3^r}{9} + \frac{32L_4^r}{9} + \frac{8L_5^rn}{9} - \frac{26L_5^r}{9} + 48L_6^r + 8L_8^rn - 12L_8^r\Bigg) \\
&+\pi_{16}^2\left(-\frac{5}{72}n^2\pi^2 - \frac{3865n^2}{10368} + \frac{35n\pi^2}{216} + \frac{1837n}{3456} + \frac{3}{4n^2} + \frac{3}{4n} - \frac{91\pi^2}{432} - \frac{853}{1296}\right)
\end{aligned}
$$

$$
\begin{aligned}
\gamma_3 \;=\;& 2K_{11}^r + 8K_{13}^r + 16K_{14}^rn - 16K_{17}^r - 24K_{18}^rn + 16K_{28}^r + 48K_3^r - 4K_{31}^r + 8K_5^r \\
&+2K_7^r + 4K_8^rn + \frac{29L^2n^2}{288} - \frac{23L^2n}{72} + \frac{101L^2}{96} - 8LL_0^rn + \frac{10LL_0^r}{3n} + 16LL_0^r \\
&-\frac{56LL_1^r}{3} - 40LL_2^r - \frac{8LL_3^rn}{3} + \frac{10LL_3^r}{3n} + 6LL_3^r - 8LL_4^r - LL_5^rn + 2LL_5^r \\
&+\pi_{16}\Bigg(\frac{49Ln^2}{216} - \frac{503Ln}{864} + \frac{2867L}{1728} - \frac{7L_0^rn}{3} + \frac{28L_0^r}{9n} + \frac{43L_0^r}{3} - \frac{62L_1^r}{9} - 31L_2^r \\
&-\frac{25L_3^rn}{18} + \frac{28L_3^r}{9n} + 3L_3^r - \frac{20L_4^r}{3} - \frac{2L_5^rn}{3} + \frac{5L_5^r}{3}\Bigg) \\
&+\pi_{16}^2\left(\frac{n^2\pi^2}{72} + \frac{445n^2}{5184} - \frac{67n\pi^2}{864} + \frac{59n}{288} + \frac{185\pi^2}{1728} + \frac{2705}{20736}\right)
\end{aligned}
$$

$$
\begin{aligned}
\gamma_4 \;=\;& 2K_{11}^r + 8K_{18}^rn + 4K_{31}^r + 8K_5^r + 2K_7^r + 4K_8^rn + \frac{11L^2n^2}{288} + \frac{L^2n}{72} - \frac{7L^2}{96} - \frac{4LL_0^rn}{3} \\
&+\frac{10LL_0^r}{3n} + \frac{4LL_0^r}{3} - \frac{4LL_2^r}{3} - 2LL_3^rn + \frac{10LL_3^r}{3n} + \frac{4LL_3^r}{3} + \frac{8LL_4^r}{3} - \frac{LL_5^rn}{3} - \frac{2LL_5^r}{3} \\
&+\pi_{16}\Bigg(\frac{29Ln^2}{216} + \frac{23Ln}{864} - \frac{137L}{1728} - \frac{13L_0^rn}{9} + \frac{28L_0^r}{9n} + \frac{13L_0^r}{9} - \frac{10L_1^r}{3} - \frac{31L_2^r}{9} \\
&-\frac{11L_3^rn}{6} + \frac{28L_3^r}{9n} + \frac{19L_3^r}{9} + \frac{20L_4^r}{9} - \frac{4L_5^rn}{9} - \frac{5L_5^r}{9}\Bigg) \\
&+\pi_{16}^2\left(-\frac{1}{108}n^2\pi^2 + \frac{421n^2}{3456} + \frac{n\pi^2}{288} + \frac{289n}{10368} - \frac{11\pi^2}{1728} - \frac{1091}{20736}\right)
\end{aligned}
$$

$$
\begin{aligned}
\gamma_5 \;=\;& K_1^r - 8K_3^r - 4K_5^r - \frac{5L^2n^2}{1152} + \frac{55L^2n}{2304} - \frac{5L^2}{32} + \frac{5LL_0^rn}{12} - \frac{5LL_0^r}{2} \\
&+\frac{5LL_1^r}{2} + \frac{25LL_2^r}{4} + \frac{5LL_3^rn}{24} - \frac{5LL_3^r}{8}
\end{aligned}
$$

$$
\begin{aligned}
&+\pi_{16}\left(-\frac{19Ln^2}{2304}+\frac{13Ln}{768}-\frac{307L}{1152}+\frac{2L_0^r n}{9}-\frac{7L_0^r}{3}+\frac{7L_1^r}{3}+\frac{35L_2^r}{6}+\frac{5L_3^r n}{18}-\frac{7L_3^r}{12}\right)\\
&+\pi_{16}^2\left(\frac{n^2\pi^2}{3456}-\frac{1015n^2}{165888}+\frac{29n\pi^2}{3456}-\frac{10313n}{165888}-\frac{19\pi^2}{1152}+\frac{71}{13824}\right)\\
\gamma_6 \;=\;& 3K_1^r-4K_5^r-\frac{5}{384}L^2n^2-\frac{L^2n}{768}-\frac{5L^2}{96}+\frac{7LL_0^r n}{12}-\frac{5LL_0^r}{6}+\frac{5LL_1^r}{6}\\
&+\frac{25LL_2^r}{12}+\frac{23LL_3^r n}{24}-\frac{5LL_3^r}{24}\\
&+\pi_{16}\left(-\frac{203Ln^2}{6912}-\frac{65Ln}{6912}-\frac{307L}{3456}+\frac{4L_0^r n}{9}-\frac{7L_0^r}{9}+\frac{7L_1^r}{9}+\frac{35L_2^r}{18}+\frac{17L_3^r n}{18}-\frac{7L_3^r}{36}\right)\\
&+\pi_{16}^2\left(-\frac{n^2\pi^2}{3456}-\frac{1933n^2}{165888}+\frac{11n\pi^2}{3456}-\frac{5299n}{165888}-\frac{19\pi^2}{3456}+\frac{71}{41472}\right)
\end{aligned}
$$

The coefficients of polynomials part for C_P at NNLO.

$$
\begin{aligned}
\delta_1 \;=\;& 128K_{10}^r n-128K_{18}^r+128K_2^r-64K_{20}^r-128K_{21}^r-256K_{22}^r n+128K_{26}^r\\
&+384K_{27}^r n-128K_{35}^r+128K_{40}^r+64K_9^r-\frac{7L^2}{4n^3}-\frac{L^2}{n^2}+\frac{L^2}{2n}-\frac{L^2}{2}-\frac{48LL_0^r}{n^2}\\
&-64LL_1^r n+\frac{64LL_1^r}{n}+64LL_1^r+\frac{16LL_2^r}{n}+16LL_2^r-\frac{48LL_3^r}{n^2}+64LL_4^r n\\
&-\frac{48LL_4^r}{n}-48LL_4^r+\frac{24LL_5^r}{n^2}+8LL_5^r-64LL_6^r n+\frac{32LL_6^r}{n}+32LL_6^r+\frac{32LL_7^r}{n}\\
&-\frac{48LL_8^r}{n^2}-16LL_8^r-512(L_4^r)^2n-256L_4^rL_5^r+2048L_4^rL_6^r n+512L_4^rL_8^r\\
&+512L_5^rL_6^r-2048(L_6^r)^2n-1024L_6^rL_8^r\\
&+\pi_{16}\left(-\frac{3L}{2n^3}-\frac{L}{n^2}+\frac{L}{n}+L-\frac{16L_0^r}{n^2}+\frac{32L_1^r}{n}+32L_1^r-\frac{16L_3^r}{n^2}-\frac{32L_4^r}{n}\right.\\
&\left.-32L_4^r+\frac{16L_5^r}{n^2}+\frac{32L_6^r}{n}+32L_6^r-\frac{48L_8^r}{n^2}\right)\\
&+\left(\frac{5}{4n^3}+\frac{1}{2n^2}+\frac{3}{4n}+\frac{1}{6}\right)\pi_{16}^2\\
\delta_2 \;=\;& -128K_{10}^r n+128K_{18}^r-192K_2^r+32K_{20}^r+64K_{21}^r+128K_{22}^r n-32K_{32}^r+64K_{35}^r\\
&-32K_{38}^r-64K_9^r+\frac{37L^2n}{72}-\frac{3L^2}{4n}+\frac{7L^2}{36}+\frac{104LL_0^r}{3n^2}-8LL_0^r-\frac{48LL_1^r}{n}-48LL_1^r\\
&-16LL_2^r n-\frac{32LL_2^r}{3n}-\frac{32LL_2^r}{3}+\frac{104LL_3^r}{3n^2}-\frac{64LL_3^r}{3}+16LL_4^r n+\frac{16LL_4^r}{n}+16LL_4^r\\
&+12LL_5^r-32LL_6^r n-24LL_8^r+256(L_4^r)^2n+128L_4^rL_5^r-512L_4^rL_6^r n-256L_4^rL_8^r\\
&+\pi_{16}\left(-\frac{31Ln}{24}-\frac{L}{4n}+\frac{5L}{18}+\frac{152L_0^r}{9n^2}-32L_1^r n-\frac{32L_1^r}{n}-32L_1^r-\frac{8L_2^r}{9n}\right.
\end{aligned}
$$

II

$$
\begin{aligned}
&-\frac{8L_2^r}{9}+\frac{152L_3^r}{9n^2}-\frac{88L_3^r}{9}+32L_4^r n+\frac{16L_4^r}{n}+16L_4^r+12L_5^r-32L_6^r n-24L_8^r\Bigg)\\
&+\pi_{16}^2\left(-\frac{n\pi^2}{27}-\frac{373n}{2592}-\frac{\pi^2}{12n}+\frac{25}{16n}+\frac{5\pi^2}{216}+\frac{565}{648}\right)\\
\delta_3 \;=\;& 32K_{10}^r n+4K_{15}^r+8K_{16}^r n-32K_{18}^r+96K_2^r-8K_{29}^r+16K_{32}^r+16K_9^r-\frac{13L^2n}{72}\\
&-\frac{49L^2}{144}-\frac{20LL_0^r}{3n^2}+\frac{10LL_0^r}{3}+32LL_1^r n+\frac{8LL_1^r}{n}+8LL_1^r+\frac{20LL_2^r n}{3}\\
&+\frac{8LL_2^r}{3n}+\frac{8LL_2^r}{3}-\frac{20LL_3^r}{3n^2}+\frac{44LL_3^r}{3}-16LL_4^r n-3LL_5^r\\
&+\pi_{16}\Bigg(\frac{11Ln}{24}-\frac{115L}{144}-\frac{56L_0^r}{9n^2}+\frac{4L_0^r}{9}+32L_1^r n+\frac{8L_1^r}{n}+8L_1^r+\frac{8L_2^r n}{9}+\frac{20L_2^r}{9n}\\
&+\frac{20L_2^r}{9}-\frac{56L_3^r}{9n^2}+\frac{83L_3^r}{9}-16L_4^r n-3L_5^r\Bigg)\\
&+\pi_{16}^2\left(-\frac{25n\pi^2}{864}+\frac{625n}{2592}-\frac{17\pi^2}{864}-\frac{1451}{5184}\right)\\
\delta_4 \;=\;& 4K_{15}^r+8K_{16}^r n+8K_{29}^r+\frac{5L^2n}{48}-\frac{L^2}{24}-2LL_0^r-4LL_2^r n-LL_5^r\\
&+\pi_{16}\left(\frac{Ln}{16}-\frac{7L}{48}+L_3^r-L_5^r\right)+\pi_{16}^2\left(\frac{n\pi^2}{288}+\frac{7n}{64}-\frac{\pi^2}{288}-\frac{11}{192}\right)\\
\delta_5 \;=\;& -16K_2^r+2K_4^r+2K_6^r+\frac{55L^2n}{384}+\frac{L^2}{48}-\frac{11LL_0^r}{6}-8LL_1^r n-\frac{8LL_2^r n}{3}-\frac{17LL_3^r}{6}\\
&+\pi_{16}\left(\frac{101Ln}{384}+\frac{13L}{384}-\frac{29L_0^r}{18}-8L_1^r n-\frac{20L_2^r n}{9}-\frac{97L_3^r}{36}\right)\\
&+\pi_{16}^2\left(\frac{19n\pi^2}{1152}-\frac{115n}{13824}-\frac{\pi^2}{1152}+\frac{349}{13824}\right)\\
\delta_6 \;=\;& 6K_4^r-2K_6^r+\frac{5L^2n}{384}-\frac{L^2}{48}-\frac{3LL_0^r}{2}-\frac{LL_3^r}{2}\\
&+\pi_{16}\left(\frac{Ln}{128}-\frac{13L}{384}-\frac{3L_0^r}{2}-\frac{5L_3^r}{12}\right)\\
&+\pi_{16}^2\left(\frac{5n\pi^2}{1152}-\frac{437n}{13824}+\frac{\pi^2}{1152}-\frac{349}{13824}\right)
\end{aligned}
$$

II.C Scattering lengths

II.C.1 Complex or QCD case

$$
\begin{aligned}
\pi a_0^I = {} & x_2 \left(-\frac{1}{16n} + \frac{n}{8} \right) \\
& + x_2^2 \left(-\frac{2}{n}\,\alpha_4 - \frac{1}{n}\,\alpha_3 - \frac{1}{4n}\,\alpha_2 - \frac{3}{16n}\,\alpha_1 + \beta_4 - \frac{1}{2}\,\beta_3 - \frac{1}{8}\,\beta_2 + \frac{1}{32}\,\beta_1 \right. \\
& \qquad \left. + 2\,n\,\alpha_4 + \frac{n}{8}\,\alpha_1 + \frac{n^2}{2}\,\beta_3 + \frac{n^2}{8}\,\beta_2 + \frac{n^2}{32}\,\beta_1 \right) \\
& + \pi_{16}\, x_2^2 \left(-\frac{1}{2} + \frac{1}{8n^2} + \frac{n^2}{2} \right) \\
& + x_2^3 \left(-\frac{4}{n}\,\gamma_5 - \frac{2}{n}\,\gamma_4 - \frac{1}{n}\,\gamma_3 - \frac{1}{4n}\,\gamma_2 - \frac{3}{16n}\,\gamma_1 - 2\,\delta_5 + \delta_4 - \frac{1}{2}\,\delta_3 - \frac{1}{8}\,\delta_2 \right. \\
& \qquad \left. + \frac{1}{32}\,\delta_1 + 2\,n\,\gamma_4 + \frac{n}{8}\,\gamma_1 + 2\,n^2\,\delta_5 + \frac{n^2}{2}\,\delta_3 + \frac{n^2}{8}\,\delta_2 + \frac{n^2}{32}\,\delta_1 \right) \\
& + \pi_{16}\, x_2^3 \left(\frac{7}{4n^3}\,L + \frac{12}{n^2}\,L_8^r - \frac{4}{n^2}\,L_5^r + \frac{12}{n^2}\,L_3^r + \frac{12}{n^2}\,L_0^r - \frac{5}{n}\,L - \frac{4}{n}\,L_6^r \right. \\
& \qquad + \frac{12}{n}\,L_4^r - \frac{4}{n}\,L_2^r - \frac{4}{n}\,L_1^r - 32\,L_8^r + 8\,L_5^r - 32\,L_3^r - 32\,L_0^r + \frac{17n}{4}\,L \\
& \qquad + 4\,n\,L_6^r - 28\,n\,L_4^r + 4\,n\,L_2^r + 4\,n\,L_1^r + 16\,n^2\,L_8^r + 16\,n^2\,L_3^r \\
& \qquad \left. + 16\,n^2\,L_0^r - \frac{5n^3}{2}\,L + 8\,n^3\,L_6^r + 8\,n^3\,L_4^r + 8\,n^3\,L_2^r + 8\,n^3\,L_1^r \right) \\
& + \pi_{16}^2\, x_2^3 \left[-\frac{3}{n^3} + \frac{7}{n} - \frac{49n}{24} + \frac{n^3}{12} + \pi^2 \left(\frac{1}{2n^3} - \frac{7}{6n} + \frac{53n}{144} - \frac{5n^3}{72} \right) \right], \qquad \text{(II.97)} \\
\pi a_0^S = {} & + x_2 \left(-\frac{1}{8n} + \frac{n}{16} \right) \\
& + x_2^2 \left(-\frac{4}{n}\,\alpha_4 - \frac{2}{n}\,\alpha_3 - \frac{1}{2n}\,\alpha_2 - \frac{3}{8n}\,\alpha_1 + \beta_4 + \frac{1}{16}\,\beta_1 + n\,\alpha_4 + \frac{n}{16}\,\alpha_1 \right) \\
& + \pi_{16}\, x_2^2 \left(-\frac{1}{2} + \frac{1}{2n^2} + \frac{n^2}{8} \right) \\
& + x_2^3 \left(-\frac{8}{n}\,\gamma_5 - \frac{4}{n}\,\gamma_4 - \frac{2}{n}\,\gamma_3 - \frac{1}{2n}\,\gamma_2 - \frac{3}{8n}\,\gamma_1 + \delta_4 + \frac{1}{16}\,\delta_1 + n\,\gamma_4 + \frac{n}{16}\,\gamma_1 \right)
\end{aligned}
$$

$$
\begin{aligned}
&+\pi_{16}\,x_2^3\left(\frac{7}{n^3}\,L+\frac{48}{n^2}\,L_8^r-\frac{16}{n^2}\,L_5^r+\frac{48}{n^2}\,L_3^r+\frac{48}{n^2}\,L_0^r-\frac{11}{2n}\,L-\frac{16}{n}\,L_6^r\right.\\
&\qquad+\frac{16}{n}\,L_4^r-\frac{16}{n}\,L_2^r-\frac{16}{n}\,L_1^r-32\,L_8^r+8\,L_5^r-32\,L_3^r-32\,L_0^r+\frac{3n}{2}\,L\\
&\qquad+8\,n\,L_6^r-8\,n\,L_4^r+8\,n\,L_2^r+8\,n\,L_1^r+4\,n^2\,L_8^r+4\,n^2\,L_3^r+4\,n^2\,L_0^r\\
&\qquad\left.-\frac{n^3}{4}\,L\right)\\
&+\pi_{16}^2\,x_2^3\left[-\frac{10}{n^3}+\frac{9}{2n}+\frac{5n}{6}-\frac{7n^3}{24}+\pi^2\left(\frac{5}{3n^3}-\frac{3}{4n}-\frac{n}{9}+\frac{5n^3}{144}\right)\right], \qquad \text{(II.98)}\\
\pi a_1^A &= +x_2\left(\frac{n}{48}\right)\\
&+x_2^2\left(\frac{1}{3}\,\beta_4+\frac{1}{24}\,\beta_2-\frac{n}{3}\,\alpha_4-\frac{n}{24}\,\alpha_2\right)\\
&+\pi_{16}\,x_2^2\left(-\frac{1}{72}+\frac{1}{72n^2}-\frac{n^2}{432}\right)\\
&+x_2^3\left(\frac{2}{3}\,\delta_6+\frac{1}{3}\,\delta_4+\frac{1}{24}\,\delta_2-\frac{2n}{3}\,\gamma_6-\frac{n}{3}\,\gamma_4-\frac{n}{24}\,\gamma_2\right)\\
&+\pi_{16}\,x_2^3\left(\frac{7}{36n^3}\,L+\frac{4}{3n^2}\,L_8^r-\frac{4}{9n^2}\,L_5^r+\frac{20}{27n^2}\,L_3^r+\frac{20}{27n^2}\,L_0^r-\frac{1}{9n}\,L\right.\\
&\qquad-\frac{4}{9n}\,L_6^r+\frac{4}{9n}\,L_4^r-\frac{4}{27n}\,L_2^r-\frac{4}{9n}\,L_1^r-\frac{8}{9}\,L_8^r+\frac{2}{9}\,L_5^r-\frac{4}{9}\,L_3^r-\frac{16}{27}\,L_0^r\\
&\qquad\left.+\frac{49n}{648}\,L-\frac{4n}{9}\,L_6^r-\frac{4n}{27}\,L_4^r-\frac{8n}{27}\,L_2^r-\frac{4n}{27}\,L_1^r-\frac{n^2}{27}\,L_5^r+\frac{n^3}{432}\,L\right) \qquad \text{(II.99)}\\
&+\pi_{16}^2\,x_2^3\left[\frac{1}{12n^3}+\frac{1}{8n}-\frac{7n}{54}-\frac{25n^3}{5184}+\pi^2\left(\frac{1}{54n^3}-\frac{5}{216n}+\frac{25n}{1296}-\frac{n^3}{1296}\right)\right],\\
\pi a_1^{SA} &= +x_2^2\left(\frac{1}{3}\,\beta_4+\frac{1}{24}\,\beta_2\right)+\pi_{16}\,x_2^2\left(-\frac{1}{144}+\frac{1}{72n^2}\right)\\
&+x_2^3\left(\frac{2}{3}\,\delta_6+\frac{1}{3}\,\delta_4+\frac{1}{24}\,\delta_2\right)\\
&+\pi_{16}\,x_2^3\left(\frac{7}{36n^3}\,L+\frac{4}{3n^2}\,L_8^r-\frac{4}{9n^2}\,L_5^r+\frac{20}{27n^2}\,L_3^r+\frac{20}{27n^2}\,L_0^r-\frac{1}{18n}\,L\right.\\
&\qquad\left.-\frac{4}{9n}\,L_6^r+\frac{4}{9n}\,L_4^r-\frac{4}{27n}\,L_2^r-\frac{4}{9n}\,L_1^r-\frac{2}{9}\,L_8^r-\frac{2}{27}\,L_3^r-\frac{2}{9}\,L_0^r+\frac{7n}{648}\,L\right)
\end{aligned}
$$

$$+\pi_{16}^2\,x_2^3\left(\frac{1}{12n^3}+\frac{n}{324}\right)+\pi^2\,\pi_{16}^2\,x_2^3\left(\frac{1}{54n^3}-\frac{1}{216n}-\frac{n}{2592}\right), \tag{II.100}$$

$$\pi a_1^{AS}=\pi a_1^{SA} \tag{II.101}$$

$$\begin{aligned}\pi a_0^{SS}=&-\frac{1}{16}x_2\\&+x_2^2\left(\alpha_3+\frac{1}{4}\,\alpha_2+\frac{1}{16}\,\alpha_1+\beta_4+\frac{1}{16}\,\beta_1+\frac{1}{8}\pi_{16}\right)\\&+x_2^3\left(\delta_4+\frac{1}{16}\,\delta_1+4\,\gamma_5+\gamma_3+\frac{1}{4}\,\gamma_2+\frac{1}{16}\,\gamma_1\right)\\&+\pi_{16}\,x_2^3\left(\frac{1}{2n^2}\,L-\frac{1}{2n}\,L+\frac{1}{2}\,L-4\,L_8^r-8\,L_6^r+4\,L_5^r+8\,L_4^r-4\,L_3^r\right.\\&\qquad\left.-8\,L_2^r-8\,L_1^r-4\,L_0^r\right)\\&+\pi_{16}^2\,x_2^3\left[-\frac{1}{2}-\frac{1}{n^2}+\frac{1}{n}-\frac{n}{24}+\pi^2\left(\frac{1}{12}+\frac{1}{6n^2}-\frac{1}{6n}+\frac{7n}{144}\right)\right],\end{aligned} \tag{II.102}$$

$$\begin{aligned}\pi a_0^{AA}=&+\frac{1}{16}x_2\\&+x_2^2\left(-\alpha_3-\frac{1}{4}\,\alpha_2-\frac{1}{16}\,\alpha_1+\beta_4+\frac{1}{16}\,\beta_1+\frac{\pi_{16}}{8}\right)\\&+x_2^3\left(\delta_4+\frac{1}{16}\,\delta_1-4\,\gamma_5-\gamma_3-\frac{1}{4}\,\gamma_2-\frac{1}{16}\,\gamma_1\right)\\&+\pi_{16}\,x_2^3\left(-\frac{1}{2n^2}\,L-\frac{1}{2n}\,L-\frac{1}{2}\,L-4\,L_8^r+8\,L_6^r+4\,L_5^r-8\,L_4^r-4\,L_3^r\right.\\&\qquad\left.+8\,L_2^r+8\,L_1^r-4\,L_0^r\right)\\&+\pi_{16}^2\,x_2^3\left[\frac{1}{2}+\frac{1}{n^2}+\frac{1}{n}-\frac{n}{24}+\pi^2\left(-\frac{1}{12}-\frac{1}{6n^2}-\frac{1}{6n}+\frac{7n}{144}\right)\right].\end{aligned} \tag{II.103}$$

II.C.2 Real or adjoint case

$$\begin{aligned}\pi a_0^{I}=&+x_2\left(\frac{1}{32}-\frac{1}{32n}+\frac{n}{8}\right)\\&+x_2^2\left(-\frac{1}{n}\,\alpha_4-\frac{1}{2n}\,\alpha_3-\frac{1}{8n}\,\alpha_2-\frac{3}{32n}\,\alpha_1+\alpha_4+\frac{1}{2}\,\alpha_3+\frac{1}{8}\,\alpha_2+\frac{3}{32}\,\alpha_1\right.\end{aligned}$$

II

$$
\begin{aligned}
&+\beta_4 - \frac{1}{2}\,\beta_3 - \frac{1}{8}\,\beta_2 + \frac{1}{32}\,\beta_1 + 2\,n\,\alpha_4 + \frac{n}{8}\,\alpha_1 + \frac{n}{2}\,\beta_3 + \frac{n}{8}\,\beta_2 + \frac{n}{32}\,\beta_1 \\
&+n^2\,\beta_3 + \frac{n^2}{4}\,\beta_2 + \frac{n^2}{16}\,\beta_1\Big) \\
&+\pi_{16}\,x_2^2\left(-\frac{7}{32} + \frac{1}{32n^2} - \frac{1}{16n} + \frac{n}{4} + \frac{n^2}{2}\right) \\
&+x_2^3\left(-\frac{2}{n}\,\gamma_5 - \frac{1}{n}\,\gamma_4 - \frac{1}{2n}\,\gamma_3 - \frac{1}{8n}\,\gamma_2 - \frac{3}{32n}\,\gamma_1 - 2\,\delta_5 + \delta_4 - \frac{1}{2}\,\delta_3 - \frac{1}{8}\,\delta_2\right. \\
&+\frac{1}{32}\,\delta_1 + 2\,\gamma_5 + \gamma_4 + \frac{1}{2}\,\gamma_3 + \frac{1}{8}\,\gamma_2 + \frac{3}{32}\,\gamma_1 + 2\,n\,\delta_5 + \frac{n}{2}\,\delta_3 + \frac{n}{8}\,\delta_2 \\
&\left.+\frac{n}{32}\,\delta_1 + 2\,n\,\gamma_4 + \frac{n}{8}\,\gamma_1 + 4\,n^2\,\delta_5 + n^2\,\delta_3 + \frac{n^2}{4}\,\delta_2 + \frac{n^2}{16}\,\delta_1\right) \\
&+\pi_{16}\,x_2^3\left(\frac{7}{32n^3}\,L - \frac{15}{32n^2}\,L + \frac{3}{n^2}\,L_8^r - \frac{1}{n^2}\,L_5^r + \frac{3}{n^2}\,L_3^r + \frac{3}{n^2}\,L_0^r\right. \\
&-\frac{29}{32n}\,L - \frac{6}{n}\,L_8^r - \frac{2}{n}\,L_6^r + \frac{2}{n}\,L_5^r + \frac{6}{n}\,L_4^r - \frac{6}{n}\,L_3^r - \frac{2}{n}\,L_2^r - \frac{2}{n}\,L_1^r \\
&-\frac{6}{n}\,L_0^r + \frac{55}{32}\,L - 13\,L_8^r + 3\,L_5^r - 8\,L_4^r - 13\,L_3^r - 13\,L_0^r + \frac{21n}{16}\,L \\
&+16\,n\,L_8^r + 6\,n\,L_6^r - 4\,n\,L_5^r - 26\,n\,L_4^r + 16\,n\,L_3^r + 6\,n\,L_2^r + 6\,n\,L_1^r \\
&+16\,n\,L_0^r - \frac{19n^2}{8}\,L + 16\,n^2\,L_8^r + 12\,n^2\,L_6^r + 12\,n^2\,L_4^r + 16\,n^2\,L_3^r \\
&+12\,n^2\,L_2^r + 12\,n^2\,L_1^r + 16\,n^2\,L_0^r - \frac{5n^3}{2}\,L + 16\,n^3\,L_6^r + 16\,n^3\,L_4^r \\
&\left.+16\,n^3\,L_2^r + 16\,n^3\,L_1^r\right) \\
&+\pi_{16}^2\,x_2^3\left(-\frac{85}{48} - \frac{3}{8n^3} + \frac{3}{4n^2} + \frac{5}{4n} - \frac{3n}{8} + \frac{29n^2}{48} + \frac{n^3}{12}\right) \\
&+\pi^2\,\pi_{16}^2\,x_2^3\left(\frac{89}{288} + \frac{1}{16n^3} - \frac{1}{8n^2} - \frac{5}{24n} + \frac{n}{16} - \frac{49n^2}{288} - \frac{5n^3}{72}\right), \qquad \text{(II.104)}
\end{aligned}
$$

$$
\begin{aligned}
\pi a_1^A &= +x_2\left(\frac{1}{48} + \frac{n}{48}\right) \\
&+x_2^2\left(-\frac{1}{3}\,\alpha_4 - \frac{1}{24}\,\alpha_2 + \frac{1}{3}\,\beta_4 + \frac{1}{24}\,\beta_2 - \frac{n}{3}\,\alpha_4 - \frac{n}{24}\,\alpha_2\right) \\
&+\pi_{16}\,x_2^2\left(-\frac{11}{864} + \frac{1}{288n^2} - \frac{1}{288n} - \frac{7n}{864} - \frac{n^2}{432}\right)
\end{aligned}
$$

$$
\begin{aligned}
&+x_2^3\left(\frac{2}{3}\,\delta_6+\frac{1}{3}\,\delta_4+\frac{1}{24}\,\delta_2-\frac{2}{3}\,\gamma_6-\frac{1}{3}\,\gamma_4-\frac{1}{24}\,\gamma_2-\frac{2n}{3}\,\gamma_6-\frac{n}{3}\,\gamma_4-\frac{n}{24}\,\gamma_2\right)\\
&+\pi_{16}\,x_2^3\left(\frac{7}{288n^3}\,L-\frac{1}{36n^2}\,L+\frac{1}{3n^2}\,L_8^r-\frac{1}{9n^2}\,L_5^r+\frac{5}{27n^2}\,L_3^r+\frac{5}{27n^2}\,L_0^r\right.\\
&\quad-\frac{5}{288n}\,L-\frac{1}{3n}\,L_8^r-\frac{2}{9n}\,L_6^r+\frac{1}{9n}\,L_5^r+\frac{2}{9n}\,L_4^r-\frac{5}{27n}\,L_3^r-\frac{2}{27n}\,L_2^r\\
&\quad-\frac{2}{9n}\,L_1^r-\frac{5}{27n}\,L_0^r+\frac{67}{1296}\,L-\frac{4}{9}\,L_8^r-\frac{2}{9}\,L_6^r+\frac{1}{54}\,L_5^r-\frac{10}{27}\,L_4^r\\
&\quad-\frac{5}{27}\,L_3^r-\frac{2}{9}\,L_2^r+\frac{2}{27}\,L_1^r-\frac{10}{27}\,L_0^r+\frac{125n}{2592}\,L-\frac{4n}{9}\,L_6^r-\frac{7n}{54}\,L_5^r\\
&\quad-\frac{4n}{27}\,L_4^r+\frac{n}{27}\,L_3^r-\frac{8n}{27}\,L_2^r-\frac{4n}{27}\,L_1^r-\frac{2n}{27}\,L_0^r+\frac{7n^2}{864}\,L-\frac{n^2}{27}\,L_5^r\\
&\quad\left.+\frac{n^3}{432}\,L\right)\\
&+\pi_{16}^2\,x_2^3\left(-\frac{13}{96}+\frac{1}{96n^3}+\frac{7}{288n^2}-\frac{281n}{1728}-\frac{151n^2}{2592}-\frac{25n^3}{5184}\right)\\
&+\pi^2\,\pi_{16}^2\,x_2^3\left(\frac{173}{10368}+\frac{1}{432n^3}-\frac{5}{864n^2}-\frac{1}{576n}+\frac{169n}{10368}+\frac{n^2}{432}-\frac{n^3}{1296}\right),
\end{aligned}
\tag{II.105}
$$

$$
\begin{aligned}
\pi a_0^S &= +x_2\left(\frac{1}{32}-\frac{1}{16n}+\frac{n}{16}\right)\\
&+x_2^2\left(-\frac{2}{n}\,\alpha_4-\frac{1}{n}\,\alpha_3-\frac{1}{4n}\,\alpha_2-\frac{3}{16n}\,\alpha_1+\alpha_4+\frac{1}{2}\,\alpha_3+\frac{1}{8}\,\alpha_2+\frac{3}{32}\,\alpha_1\right.\\
&\quad\left.+\beta_4+\frac{1}{16}\,\beta_1+n\,\alpha_4+\frac{n}{16}\,\alpha_1\right)\\
&+\pi_{16}\,x_2^2\left(-\frac{7}{32}+\frac{1}{8n^2}-\frac{1}{8n}+\frac{n}{8}+\frac{n^2}{8}\right)\\
&+x_2^3\left(-\frac{4}{n}\,\gamma_5-\frac{2}{n}\,\gamma_4-\frac{1}{n}\,\gamma_3-\frac{1}{4n}\,\gamma_2-\frac{3}{16n}\,\gamma_1+\delta_4+\frac{1}{16}\,\delta_1+2\,\gamma_5\right.\\
&\quad\left.+\gamma_4+\frac{1}{2}\,\gamma_3+\frac{1}{8}\,\gamma_2+\frac{3}{32}\,\gamma_1+n\,\gamma_4+\frac{n}{16}\,\gamma_1\right)\\
&+\pi_{16}\,x_2^3\left(+\frac{7}{8n^3}\,L-\frac{19}{16n^2}\,L+\frac{12}{n^2}\,L_8^r-\frac{4}{n^2}\,L_5^r+\frac{12}{n^2}\,L_3^r+\frac{12}{n^2}\,L_0^r-\frac{13}{16n}\,L\right.\\
&\quad\left.-\frac{12}{n}\,L_8^r-\frac{8}{n}\,L_6^r+\frac{4}{n}\,L_5^r+\frac{8}{n}\,L_4^r-\frac{12}{n}\,L_3^r-\frac{8}{n}\,L_2^r-\frac{8}{n}\,L_1^r-\frac{12}{n}\,L_0^r\right.
\end{aligned}
$$

II

$$
\begin{aligned}
&+\frac{41}{32}\,L-13\,L_8^r+4\,L_6^r+3\,L_5^r-4\,L_4^r-13\,L_3^r+4\,L_2^r+4\,L_1^r-13\,L_0^r\\
&+\frac{3n}{8}\,L+8\,n\,L_8^r+8\,n\,L_6^r-2\,n\,L_5^r-8\,n\,L_4^r+8\,n\,L_3^r+8\,n\,L_2^r\\
&+8\,n\,L_1^r+8\,n\,L_0^r-\frac{n^2}{2}\,L+4\,n^2\,L_8^r+4\,n^2\,L_3^r+4\,n^2\,L_0^r-\frac{n^3}{4}\,L\Bigg)\\
&+\pi_{16}^2\,x_2^3\left(-\frac{37}{48}-\frac{5}{4n^3}+\frac{13}{8n^2}+\frac{3}{8n}+\frac{31n}{48}-\frac{3n^2}{16}-\frac{7n^3}{24}\right)\\
&+\pi^2\,\pi_{16}^2\,x_2^3\left(\frac{41}{288}+\frac{5}{24n^3}-\frac{13}{48n^2}-\frac{1}{16n}-\frac{29n}{288}+\frac{n^2}{96}+\frac{5n^3}{144}\right),
\end{aligned}
\tag{II.106}
$$

$$
\begin{aligned}
\pi a_0^{FS} &= +x_2\left(-\frac{1}{16}\right)\\
&+x_2^2\left(\alpha_3+\frac{1}{4}\,\alpha_2+\frac{1}{16}\,\alpha_1+\beta_4+\frac{1}{16}\,\beta_1\right)+\frac{1}{8}\pi_{16}\,x_2^2\\
&+x_2^3\left(+\delta_4+\frac{1}{16}\,\delta_1+4\,\gamma_5+\gamma_3+\frac{1}{4}\,\gamma_2+\frac{1}{16}\,\gamma_1\right)\\
&+\pi_{16}\,x_2^3\left(\frac{1}{8n^2}\,L-\frac{1}{4n}\,L+\frac{3}{8}\,L-4\,L_8^r-8\,L_6^r+4\,L_5^r+8\,L_4^r-4\,L_3^r\right.\\
&\qquad\left.-8\,L_2^r-8\,L_1^r-4\,L_0^r\right)\\
&+\pi_{16}^2\,x_2^3\left[-\frac{17}{24}-\frac{1}{4n^2}+\frac{1}{2n}-\frac{n}{24}+\pi^2\left(\frac{13}{144}+\frac{1}{24n^2}-\frac{1}{12n}+\frac{7n}{144}\right)\right]
\end{aligned}
\tag{II.107}
$$

$$
\begin{aligned}
\pi a_1^{MA} &= +x_2^2\left[\frac{1}{3}\,\beta_4+\frac{1}{24}\,\beta_2+\pi_{16}\left(-\frac{1}{288}+\frac{1}{288n^2}\right)\right]\\
&+x_2^3\left(\frac{2}{3}\,\delta_6+\frac{1}{3}\,\delta_4+\frac{1}{24}\,\delta_2\right)\\
&+\pi_{16}\,x_2^3\left(\frac{7}{288n^3}\,L-\frac{1}{72n^2}\,L+\frac{1}{3n^2}\,L_8^r-\frac{1}{9n^2}\,L_5^r+\frac{5}{27n^2}\,L_3^r+\frac{5}{27n^2}\,L_0^r\right.\\
&\qquad-\frac{1}{72n}\,L-\frac{2}{9n}\,L_6^r+\frac{2}{9n}\,L_4^r-\frac{2}{27n}\,L_2^r-\frac{2}{9n}\,L_1^r+\frac{11}{2592}\,L-\frac{1}{9}\,L_8^r\\
&\qquad\left.+\frac{2}{9}\,L_6^r-\frac{2}{9}\,L_4^r-\frac{1}{27}\,L_3^r+\frac{2}{27}\,L_2^r+\frac{2}{9}\,L_1^r-\frac{1}{9}\,L_0^r+\frac{7n}{1296}\,L\right)\\
&+\pi_{16}^2\,x_2^3\left(\frac{17}{2592}+\frac{1}{96n^3}-\frac{1}{144n^2}+\frac{n}{648}\right)
\end{aligned}
$$

$$+\pi^2\,\pi_{16}^2\,x_2^3\left(-\frac{1}{1296}+\frac{1}{432n^3}-\frac{1}{864n^2}-\frac{1}{864n}-\frac{n}{5184}\right), \tag{II.108}$$

$$\begin{aligned}\pi a_0^{MS} &= +\frac{1}{32}x_2\\ &+x_2^2\left(-\frac{1}{2}\,\alpha_3-\frac{1}{8}\,\alpha_2-\frac{1}{32}\,\alpha_1+\beta_4+\frac{1}{16}\,\beta_1+\frac{1}{32}\,\pi_{16}\right)\\ &+x_2^3\left(\delta_4+\frac{1}{16}\,\delta_1-2\,\gamma_5-\frac{1}{2}\,\gamma_3-\frac{1}{8}\,\gamma_2-\frac{1}{32}\,\gamma_1\right)\\ &+\pi_{16}\,x_2^3\left(-\frac{1}{16n^2}\,L-\frac{1}{16n}\,L-\frac{3}{32}\,L-L_8^r+4\,L_6^r+L_5^r-4\,L_4^r-L_3^r\right.\\ &\qquad\left.+4\,L_2^r+4\,L_1^r-L_0^r\right)\\ &+\pi_{16}^2\,x_2^3\left[\frac{1}{96}+\frac{1}{8n^2}+\frac{1}{8n}-\frac{n}{96}+\pi^2\left(-\frac{5}{576}-\frac{1}{48n^2}-\frac{1}{48n}+\frac{7n}{576}\right)\right]\end{aligned} \tag{II.109}$$

II.C.3 Pseudo-real or two-colour case

$$\begin{aligned}\pi a_0^I &= +x_2\left(-\frac{1}{32}-\frac{1}{32n}+\frac{n}{8}\right)\\ &+x_2^2\left(-\frac{1}{n}\,\alpha_4-\frac{1}{2n}\,\alpha_3-\frac{1}{8n}\,\alpha_2-\frac{3}{32n}\,\alpha_1-\alpha_4-\frac{1}{2}\,\alpha_3-\frac{1}{8}\,\alpha_2-\frac{3}{32}\,\alpha_1\right.\\ &\qquad+\beta_4-\frac{1}{2}\,\beta_3-\frac{1}{8}\,\beta_2+\frac{1}{32}\,\beta_1+2\,n\,\alpha_4+\frac{n}{8}\,\alpha_1-\frac{n}{2}\,\beta_3-\frac{n}{8}\,\beta_2-\frac{n}{32}\,\beta_1\\ &\qquad\left.+n^2\,\beta_3+\frac{n^2}{4}\,\beta_2+\frac{n^2}{16}\,\beta_1\right)\\ &+\pi_{16}\,x_2^2\left(-\frac{7}{32}+\frac{1}{32n^2}+\frac{1}{16n}-\frac{n}{4}+\frac{n^2}{2}\right)\\ &+x_2^3\left(-\frac{2}{n}\,\gamma_5-\frac{1}{n}\,\gamma_4-\frac{1}{2n}\,\gamma_3-\frac{1}{8n}\,\gamma_2-\frac{3}{32n}\,\gamma_1-2\,\delta_5+\delta_4-\frac{1}{2}\,\delta_3-\frac{1}{8}\,\delta_2\right.\\ &\qquad+\frac{1}{32}\,\delta_1-2\,\gamma_5-\gamma_4-\frac{1}{2}\,\gamma_3-\frac{1}{8}\,\gamma_2-\frac{3}{32}\,\gamma_1-2\,n\,\delta_5-\frac{n}{2}\,\delta_3-\frac{n}{8}\,\delta_2\\ &\qquad\left.-\frac{n}{32}\,\delta_1+2\,n\,\gamma_4+\frac{n}{8}\,\gamma_1+4\,n^2\,\delta_5+n^2\,\delta_3+\frac{n^2}{4}\,\delta_2+\frac{n^2}{16}\,\delta_1\right)\\ &+\pi_{16}\,x_2^3\left(\frac{7}{32n^3}\,L+\frac{15}{32n^2}\,L+\frac{3}{n^2}\,L_8^r-\frac{1}{n^2}\,L_5^r+\frac{3}{n^2}\,L_3^r+\frac{3}{n^2}\,L_0^r-\frac{29}{32n}\,L\right.\end{aligned}$$

II

$$
\begin{aligned}
&+\frac{6}{n}\,L_8^r-\frac{2}{n}\,L_6^r-\frac{2}{n}\,L_5^r+\frac{6}{n}\,L_4^r+\frac{6}{n}\,L_3^r-\frac{2}{n}\,L_2^r-\frac{2}{n}\,L_1^r+\frac{6}{n}\,L_0^r\\
&-\frac{55}{32}\,L-13\,L_8^r+3\,L_5^r+8\,L_4^r-13\,L_3^r-13\,L_0^r+\frac{21n}{16}\,L-16\,n\,L_8^r\\
&+6\,n\,L_6^r+4\,n\,L_5^r-26\,n\,L_4^r-16\,n\,L_3^r+6\,n\,L_2^r+6\,n\,L_1^r-16\,n\,L_0^r\\
&+\frac{19n^2}{8}\,L+16\,n^2\,L_8^r-12\,n^2\,L_6^r-12\,n^2\,L_4^r+16\,n^2\,L_3^r-12\,n^2\,L_2^r\\
&-12\,n^2\,L_1^r+16\,n^2\,L_0^r-\frac{5n^3}{2}\,L+16\,n^3\,L_6^r+16\,n^3\,L_4^r+16\,n^3\,L_2^r\\
&+16\,n^3\,L_1^r\Bigg)\\
&+\pi_{16}^2\,x_2^3\left(\frac{85}{48}-\frac{3}{8n^3}-\frac{3}{4n^2}+\frac{5}{4n}-\frac{3n}{8}-\frac{29n^2}{48}+\frac{n^3}{12}\right)\\
&+\pi^2\,\pi_{16}^2\,x_2^3\left(-\frac{89}{288}+\frac{1}{16n^3}+\frac{1}{8n^2}-\frac{5}{24n}+\frac{n}{16}+\frac{49n^2}{288}-\frac{5n^3}{72}\right),
\end{aligned}
\tag{II.110}
$$

$$
\begin{aligned}
\pi a_0^A &= +x_2\left(-\frac{1}{32}-\frac{1}{16n}+\frac{n}{16}\right)\\
&+x_2^2\left(-\frac{2}{n}\,\alpha_4-\frac{1}{n}\,\alpha_3-\frac{1}{4n}\,\alpha_2-\frac{3}{16n}\,\alpha_1-\alpha_4-\frac{1}{2}\,\alpha_3-\frac{1}{8}\,\alpha_2-\frac{3}{32}\,\alpha_1\right.\\
&\left.+\beta_4+\frac{1}{16}\,\beta_1+n\,\alpha_4+\frac{n}{16}\,\alpha_1\right)\\
&+\pi_{16}\,x_2^2\left(-\frac{7}{32}+\frac{1}{8n^2}+\frac{1}{8n}-\frac{n}{8}+\frac{n^2}{8}\right)\\
&+x_2^3\left(-\frac{4}{n}\,\gamma_5-\frac{2}{n}\,\gamma_4-\frac{1}{n}\,\gamma_3-\frac{1}{4n}\,\gamma_2-\frac{3}{16n}\,\gamma_1+\delta_4+\frac{1}{16}\,\delta_1-2\,\gamma_5-\gamma_4\right.\\
&\left.-\frac{1}{2}\,\gamma_3-\frac{1}{8}\,\gamma_2-\frac{3}{32}\,\gamma_1+n\,\gamma_4+\frac{n}{16}\,\gamma_1\right)\\
&+\pi_{16}\,x_2^3\left(\frac{7}{8n^3}\,L+\frac{19}{16n^2}\,L+\frac{12}{n^2}\,L_8^r-\frac{4}{n^2}\,L_5^r+\frac{12}{n^2}\,L_3^r+\frac{12}{n^2}\,L_0^r-\frac{13}{16n}\,L\right.\\
&+\frac{12}{n}\,L_8^r-\frac{8}{n}\,L_6^r-\frac{4}{n}\,L_5^r+\frac{8}{n}\,L_4^r+\frac{12}{n}\,L_3^r-\frac{8}{n}\,L_2^r-\frac{8}{n}\,L_1^r+\frac{12}{n}\,L_0^r\\
&-\frac{41}{32}\,L-13\,L_8^r-4\,L_6^r+3\,L_5^r+4\,L_4^r-13\,L_3^r-4\,L_2^r-4\,L_1^r-13\,L_0^r\\
&\left.+\frac{3n}{8}\,L-8\,n\,L_8^r+8\,n\,L_6^r+2\,n\,L_5^r-8\,n\,L_4^r-8\,n\,L_3^r+8\,n\,L_2^r\right)
\end{aligned}
$$

$$
\begin{aligned}
&+8\,n\,L_1^r - 8\,n\,L_0^r + \frac{n^2}{2}\,L + 4\,n^2\,L_8^r + 4\,n^2\,L_3^r + 4\,n^2\,L_0^r - \frac{n^3}{4}\,L\Bigg) \\
&+\pi_{16}^2\,x_2^3\left(\frac{37}{48} - \frac{5}{4n^3} - \frac{13}{8n^2} + \frac{3}{8n} + \frac{31n}{48} + \frac{3n^2}{16} - \frac{7n^3}{24}\right) \\
&+\pi^2\,\pi_{16}^2\,x_2^3\left(-\frac{41}{288} + \frac{5}{24n^3} + \frac{13}{48n^2} - \frac{1}{16n} - \frac{29n}{288} - \frac{n^2}{96} + \frac{5n^3}{144}\right), \qquad \text{(II.111)} \\
\pi a_1^S &= +x_2\left(-\frac{1}{48} + \frac{n}{48}\right) \\
&+x_2^2\left(\frac{1}{3}\,\alpha_4 + \frac{1}{24}\,\alpha_2 + \frac{1}{3}\,\beta_4 + \frac{1}{24}\,\beta_2 - \frac{n}{3}\,\alpha_4 - \frac{n}{24}\,\alpha_2\right) \\
&+\pi_{16}\,x_2^2\left(-\frac{11}{864} + \frac{1}{288n^2} + \frac{1}{288n} + \frac{7n}{864} - \frac{n^2}{432}\right) \\
&+x_2^3\left(\frac{2}{3}\,\delta_6 + \frac{1}{3}\,\delta_4 + \frac{1}{24}\,\delta_2 + \frac{2}{3}\,\gamma_6 + \frac{1}{3}\,\gamma_4 + \frac{1}{24}\,\gamma_2 - \frac{2n}{3}\,\gamma_6 - \frac{n}{3}\,\gamma_4\right. \\
&\qquad \left.-\frac{n}{24}\,\gamma_2\right) \\
&+\pi_{16}\,x_2^3\left(\frac{7}{288n^3}\,L + \frac{1}{36n^2}\,L + \frac{1}{3n^2}\,L_8^r - \frac{1}{9n^2}\,L_5^r + \frac{5}{27n^2}\,L_3^r + \frac{5}{27n^2}\,L_0^r\right. \\
&\qquad -\frac{5}{288n}\,L + \frac{1}{3n}\,L_8^r - \frac{2}{9n}\,L_6^r - \frac{1}{9n}\,L_5^r + \frac{2}{9n}\,L_4^r + \frac{5}{27n}\,L_3^r - \frac{2}{27n}\,L_2^r \\
&\qquad -\frac{2}{9n}\,L_1^r + \frac{5}{27n}\,L_0^r - \frac{67}{1296}\,L - \frac{4}{9}\,L_8^r + \frac{2}{9}\,L_6^r + \frac{1}{54}\,L_5^r + \frac{10}{27}\,L_4^r \\
&\qquad -\frac{5}{27}\,L_3^r + \frac{2}{9}\,L_2^r - \frac{2}{27}\,L_1^r - \frac{10}{27}\,L_0^r + \frac{125n}{2592}\,L - \frac{4n}{9}\,L_6^r + \frac{7n}{54}\,L_5^r \\
&\qquad -\frac{4n}{27}\,L_4^r - \frac{n}{27}\,L_3^r - \frac{8n}{27}\,L_2^r - \frac{4n}{27}\,L_1^r + \frac{2n}{27}\,L_0^r - \frac{7n^2}{864}\,L - \frac{n^2}{27}\,L_5^r \\
&\qquad \left.+\frac{n^3}{432}\,L\right) \\
&+\pi_{16}^2\,x_2^3\left(\frac{13}{96} + \frac{1}{96n^3} - \frac{7}{288n^2} - \frac{281n}{1728} + \frac{151n^2}{2592} - \frac{25n^3}{5184}\right) \\
&+\pi^2\,\pi_{16}^2\,x_2^3\left(-\frac{173}{10368} + \frac{1}{432n^3} + \frac{5}{864n^2} - \frac{1}{576n} + \frac{169n}{10368} - \frac{n^2}{432}\right. \\
&\qquad \left.-\frac{n^3}{1296}\right), \qquad \text{(II.112)}
\end{aligned}
$$

II

$$
\begin{aligned}
\pi a_0^{FA} = &+\frac{1}{16}x_2 \\
&+x_2^2\left(-\alpha_3-\frac{1}{4}\alpha_2-\frac{1}{16}\alpha_1+\beta_4+\frac{1}{16}\beta_1+\frac{1}{8}\pi_{16}\right) \\
&+x_2^3\left(\delta_4+\frac{1}{16}\delta_1-4\gamma_5-\gamma_3-\frac{1}{4}\gamma_2-\frac{1}{16}\gamma_1\right) \\
&+\pi_{16}x_2^3\left(-\frac{1}{8n^2}L-\frac{1}{4n}L-\frac{3}{8}L-4L_8^r+8L_6^r+4L_5^r-8L_4^r-4L_3^r\right. \\
&\qquad\left.+8L_2^r+8L_1^r-4L_0^r\right) \\
&+\pi_{16}^2x_2^3\left[\frac{17}{24}+\frac{1}{4n^2}+\frac{1}{2n}-\frac{n}{24}+\pi^2\left(\frac{7n}{144}-\frac{13}{144}-\frac{1}{24n^2}-\frac{1}{12n}\right)\right], \qquad \text{(II.113)} \\
\pi a_1^{MA} = &+x_2^2\left[\frac{1}{3}\beta_4+\frac{1}{24}\beta_2+\pi_{16}\left(-\frac{1}{288}+\frac{1}{288n^2}\right)\right] \\
&+x_2^3\left(\frac{2}{3}\delta_6+\frac{1}{3}\delta_4+\frac{1}{24}\delta_2\right) \\
&+\pi_{16}x_2^3\left(\frac{7}{288n^3}L+\frac{1}{72n^2}L+\frac{1}{3n^2}L_8^r-\frac{1}{9n^2}L_5^r+\frac{5}{27n^2}L_3^r+\frac{5}{27n^2}L_0^r\right. \\
&\qquad-\frac{1}{72n}L-\frac{2}{9n}L_6^r+\frac{2}{9n}L_4^r-\frac{2}{27n}L_2^r-\frac{2}{9n}L_1^r-\frac{11}{2592}L-\frac{1}{9}L_8^r \\
&\qquad\left.-\frac{2}{9}L_6^r+\frac{2}{9}L_4^r-\frac{1}{27}L_3^r-\frac{2}{27}L_2^r-\frac{2}{9}L_1^r-\frac{1}{9}L_0^r+\frac{7n}{1296}L\right) \\
&+\pi_{16}^2x_2^3\left(-\frac{17}{2592}+\frac{1}{96n^3}+\frac{1}{144n^2}+\frac{n}{648}\right) \\
&+\pi^2\pi_{16}^2x_2^3\left(\frac{1}{1296}+\frac{1}{432n^3}+\frac{1}{864n^2}-\frac{1}{864n}-\frac{n}{5184}\right), \qquad \text{(II.114)} \\
\pi a_0^{MS} = &-\frac{1}{32}x_2 \\
&+x_2^2\left(\frac{1}{2}\alpha_3+\frac{1}{8}\alpha_2+\frac{1}{32}\alpha_1+\beta_4+\frac{1}{16}\beta_1+\frac{1}{32}\pi_{16}\right) \\
&+x_2^3\left(+\delta_4+\frac{1}{16}\delta_1+2\gamma_5+\frac{1}{2}\gamma_3+\frac{1}{8}\gamma_2+\frac{1}{32}\gamma_1\right) \\
&+\pi_{16}x_2^3\left(+\frac{1}{16n^2}L-\frac{1}{16n}L+\frac{3}{32}L-L_8^r-4L_6^r+L_5^r+4L_4^r-L_3^r\right.
\end{aligned}
$$

$$-4\,L_2^r - 4\,L_1^r - L_0^r\Big)$$
$$+\pi_{16}^2\,x_2^3\left[\frac{1}{8n} - \frac{1}{96} - \frac{1}{8n^2} - \frac{11n}{96} + \pi^2\left(\frac{5}{576} + \frac{1}{48n^2} - \frac{1}{48n} + \frac{7n}{576}\right)\right] \quad \text{(II.115)}$$

II.D Loop integrals

II.D.1 One-loop integrals

We use dimensional regularization here throughout in d dimensions with $d = 4 - 2\epsilon$. We need integrals with one, two and three propagators in principle. These one propagator integral is

$$A(m^2) = \frac{1}{i}\int \frac{d^dq}{(2\pi)^d}\frac{1}{q^2 - m^2}\,. \quad \text{(II.116)}$$

The two propagator integrals we encountered are

$$\begin{aligned}
B(m_1^2, m_2^2, p^2) &= \frac{1}{i}\int \frac{d^dq}{(2\pi)^d}\frac{1}{(q^2 - m_1^2)((q-p)^2 - m_2^2)}\,,\\
B_\mu(m_1^2, m_2^2, p) &= \frac{1}{i}\int \frac{d^dq}{(2\pi)^d}\frac{q_\mu}{(q^2 - m_1^2)((q-p)^2 - m_2^2)}\\
&= p_\mu B_1(m_1^2, m_2^2, p^2)\,,\\
B_{\mu\nu}(m_1^2, m_2^2, p) &= \frac{1}{i}\int \frac{d^dq}{(2\pi)^d}\frac{q_\mu q_\nu}{(q^2 - m_1^2)((q-p)^2 - m_2^2)}\\
&= p_\mu p_\nu B_{21}(m_1^2, m_2^2, p^2) + g_{\mu\nu}B_{22}(m_1^2, m_2^2, p^2)\,. \quad \text{(II.117)}
\end{aligned}$$

All the cases with three propagator integrals that show up can be absorbed into the two-propagator ones by moving to the real masses rather than the lowest order masses. This provides a consistency check on the calculations.

The explicit expressions are well known

$$\begin{aligned}
A(m^2) &= \frac{m^2}{16\pi^2}\left\{\lambda_0 - \ln(m^2) + \epsilon\Big(\frac{C^2}{2} + \frac{1}{2} + \frac{\pi^2}{12} + \frac{1}{2}\ln^2(m^2)\right.\\
&\qquad \left.-C\ln(m^2)\Big)\right\} + \mathcal{O}(\epsilon^2)\,,\\
B(m_1^2, m_2^2, p^2) &= \frac{1}{16\pi^2}\left(\lambda_0 - \frac{m_1^2\ln(m_1^2) - m_2^2\ln(m_2^2)}{m_1^2 - m_2^2}\right) + \bar{J}(m_1^2, m_2^2, p^2) + \mathcal{O}(\epsilon)\,,\\
\bar{J}(m_1^2, m_2^2, p^2) &= -\frac{1}{16\pi^2}\int_0^1 dx \ln\left(\frac{m_1^2 x + m_2^2(1-x) - x(1-x)p^2}{m_1^2 x + m_2^2(1-x)}\right)\,, \quad \text{(II.118)}
\end{aligned}$$

II

$C = \ln(4\pi) + 1 - \gamma$ and $\lambda_0 = 1/\epsilon + C$. The function $\bar{J}(m_1^2, m_2^2, p^2)$ develops an imaginary part for $p^2 \geq (m_1 + m_2)^2$. Using $\Delta = m_1^2 - m_2^2$, $\Sigma = m_1^2 + m_2^2$ and $\nu^2 = p^4 + m_1^4 + m_2^4 - 2p^2m_1^2 - 2p^2m_2^2 - 2m_1^2m_2^2$ it is given by

$$(32\pi^2)\bar{J}(m_1^2, m_2^2, p^2) = 2 + \left(-\frac{\Delta}{p^2} + \frac{\Sigma}{\Delta}\right)\ln\frac{m_1^2}{m_2^2} - \frac{\nu}{p^2}\ln\frac{(p^2+\nu)^2 - \Delta^2}{(p^2-\nu)^2 - \Delta^2}\,. \quad \text{(II.119)}$$

The two-propagator integrals can all be reduced to B and A via

$$\begin{aligned}
B_1(m_1^2, m_2^2, p^2) &= -\frac{1}{2p^2}\left(A(m_1^2) - A(m_2^2) + (m_2^2 - m_1^2 - p^2)B(m_1^2, m_2^2, p^2)\right)\,,\\
B_{22}(m_1^2, m_2^2, p^2) &= \frac{1}{2(d-1)}\Big(A(m_2^2) + 2m_1^2B(m_1^2, m_2^2, p^2)\\
&\quad + (m_2^2 - m_1^2 - p^2)B_1(m_1^2, m_2^2, p^2)\Big)\,,\\
B_{21}(m_1^2, m_2^2, p^2) &= \frac{1}{p^2}\left(A(m_2^2) + m_1^2B(m_1^2, m_2^2, p^2) - dB_{22}(m_1^2, m_2^2, p^2)\right)\,. \quad \text{(II.120)}
\end{aligned}$$

The basic method used here is the one from Passarino and Veltman [40].

II.D.2 Sunset integrals

Sunset integrals have been treated in many places already, in general and for various special cases. We use here a method that is a hybrid of various other approaches. We only cite the literature actually used. We define

$$\langle\langle X\rangle\rangle = \frac{1}{i^2}\int\frac{d^dq}{(2\pi)^d}\frac{d^dr}{(2\pi)^d}\frac{X}{\left(q^2 - m_1^2\right)\left(r^2 - m_2^2\right)\left((q+r-p)^2 - m_3^2\right)}\,, \quad \text{(II.121)}$$

$$\begin{aligned}
H(m_1^2, m_2^2, m_3^2; p^2) &= \langle\langle 1\rangle\rangle\,,\\
H_\mu(m_1^2, m_2^2, m_3^2; p^2) &= \langle\langle q_\mu\rangle\rangle = p_\mu H_1(m_1^2, m_2^2, m_3^2; p^2)\,,\\
H_{\mu\nu}(m_1^2, m_2^2, m_3^2; p^2) &= \langle\langle q_\mu q_\nu\rangle\rangle\\
&= p_\mu p_\nu H_{21}(m_1^2, m_2^2, m_3^2; p^2) + g_{\mu\nu}H_{22}(m_1^2, m_2^2, m_3^2; p^2)\,.
\end{aligned} \quad \text{(II.122)}$$

By redefining momenta the others can be simply related to the above three:

$$\begin{aligned}
\langle\langle r_\mu\rangle\rangle &= p_\mu H_1(m_2^2, m_1^2, m_3^2; p^2)\,,\\
\langle\langle r_\mu r_\nu\rangle\rangle &= p_\mu p_\nu H_{21}(m_2^2, m_1^2, m_3^2; p^2) + g_{\mu\nu}H_{22}(m_2^2, m_1^2, m_3^2; p^2)\,,\\
\langle\langle q_\mu r_\nu\rangle\rangle &= \langle\langle r_\mu q_\nu\rangle\rangle\,,\\
\langle\langle q_\mu r_\nu\rangle\rangle &= p_\mu p_\nu H_{23}(m_1^2, m_2^2, m_3^2; p^2) + g_{\mu\nu}H_{24}(m_1^2, m_2^2, m_3^2; p^2)\,, \quad \text{(II.123)}
\end{aligned}$$

with

$$\begin{aligned} 2H_{23}(m_1^2,m_2^2,m_3^2;p^2) &= -H_{21}(m_1^2,m_2^2,m_3^2;p^2) - H_{21}(m_2^2,m_1^2,m_3^2;p^2) \\ &\quad +H_{21}(m_3^2,m_1^2,m_2^2;p^2) + 2H_1(m_1^2,m_2^2,m_3^2;p^2) \\ &\quad +2H_1(m_2^2,m_1^2,m_3^2;p^2) - H(m_1^2,m_2^2,m_3^2;p^2)\,, \\ 2H_{24}(m_1^2,m_2^2,m_3^2;p^2) &= -H_{22}(m_1^2,m_2^2,m_3^2;p^2) - H_{22}(m_2^2,m_1^2,m_3^2;p^2) \\ &\quad +H_{22}(m_3^2,m_1^2,m_2^2;p^2)\,. \end{aligned} \tag{II.124}$$

The first two follow from interchanging q and r and the third from the fact that it is proportional to $g_{\mu\nu}$ or $p_\mu p_\nu$, which are both symmetric in μ and ν. The last one is deribed using

$$\begin{aligned} (q_\mu r_\nu + r_\mu q_\nu) &= (q_\mu + r_\mu - p_\mu)\,(q_\nu + r_\nu - p_\nu) - q_\mu q_\nu - r_\mu r_\nu - p_\mu p_\nu \\ &\quad +2p_\mu\,(q_\nu + r_\nu) + 2p_\nu\,(q_\mu + r_\mu) \end{aligned} \tag{II.125}$$

and redefining momenta and masses on the r.h.s.. In addition we have the relation

$$\begin{aligned} p^2 H_{21}(m_1^2,m_2^2,m_3^2;p^2) + dH_{22}(m_1^2,m_2^2,m_3^2;p^2) = \\ m_1^2 H(m_1^2,m_2^2,m_3^2;p^2) + A(m_2^2)A(m_3^2)\,. \end{aligned} \tag{II.126}$$

which allows to express H_{22} in a simple way in terms of H_{21}. There is also a relation between H_1 and H

$$\begin{aligned} H_1(m_1^2,m_2^2,m_3^2;p^2) + H_1(m_2^2,m_1^2,m_3^2;p^2) + H_1(m_3^2,m_1^2,m_2^2;p^2) = \\ H(m_1^2,m_2^2,m_3^2;p^2)\,, \end{aligned} \tag{II.127}$$

which allows to write $H_1(m^2,m^2,m^2;p^2) = 1/3\ H(m^2,m^2,m^2;p^2)$ in the case of equal masses. The function H is fully symmetric in m_1^2, m_2^2 and m_3^2, while H_1, H_{21} and H_{22} are symmetric under the interchange of m_2^2 and m_3^2.

We only need the sunset integrals at $p^2 = m_1^2 = m_2^2 = m_3^2$ and their derivatives w.r.t. p^2. These have been calculated using the methods of [36]. With $H_{id} = \frac{\partial}{\partial p^2} H_i$ we obtain

$$\begin{aligned} H &= \lambda_1 m^2 \left(\frac{5\pi_{16}^2}{4} - 3L\pi_{16}\right) + \frac{3}{2}\lambda_2 m^2 \pi_{16}^2 \\ &\quad +m^2 \left(3L^2 - \frac{5}{2}L\pi_{16} + \frac{1}{4}\pi^2\pi_{16}^2 + \frac{15\pi_{16}^2}{8}\right) \end{aligned} \tag{II.128}$$

$$\begin{aligned} H_{21} &= \lambda_1 m^2 \left(\frac{11\pi_{16}^2}{72} - \frac{2}{3}L\pi_{16}\right) + \frac{1}{3}\lambda_2 m^2 \pi_{16}^2 \\ &\quad +m^2 \left(-\frac{11}{36}L\pi_{16} + \frac{1}{18}\pi^2\pi_{16}^2 + \frac{493\pi_{16}^2}{864}\right) \end{aligned} \tag{II.129}$$

II

$$
\begin{aligned}
H_{22} &= \lambda_1 m^4 \left(\frac{157\pi_{16}^2}{288} - \frac{13}{12} L\pi_{16} \right) + \frac{13}{24}\lambda_2 m^4 \pi_{16}^2 \\
&\quad + m^4 \left(-\frac{157}{144} L\pi_{16} + \frac{13L^24}{12} + \frac{13}{144}\pi^2\pi_{16}^2 + \frac{2933\pi_{16}^2}{3456} \right) \qquad \text{(II.130)} \\
H_d &= \frac{L\pi_{16}}{2} - \frac{\lambda_1 \pi_{16}^2}{4} + \frac{7\pi_{16}^2}{8} \qquad \text{(II.131)} \\
H_{21d} &= \frac{L\pi_{16}}{12} - \frac{\lambda_1 \pi_{16}^2}{24} + \frac{43\pi_{16}^2}{288} \qquad \text{(II.132)} \\
H_{22d} &= \frac{5}{48} L m^2 \pi_{16} - \frac{5}{96}\lambda_1 m^2 \pi_{16}^2 + \frac{179\pi_{16}^2}{1152} m^2 \qquad \text{(II.133)}
\end{aligned}
$$

H_1 and H_{1d} follow immmediately using (III.86).

II.D.3 Vertex integrals

The vertex diagram (16) in Fig. II.2 is the most difficult two-loop diagram in $\phi\phi$ scattering, and it can also appear in other process. The two loop integral for the equal mass case can be written as

$$
\langle\langle X \rangle\rangle = \frac{\mu^{4\epsilon}}{i^2} \int\int dr ds \frac{X}{(r^2 - m^2)\cdot[(r-q)^2 - m^2]\cdot(s^2 - m^2)\cdot[(s+r-p)^2 - m^2]} \qquad \text{(II.134)}
$$

The Lorentz decompositions of the vertex integrals are [41]

$$
\begin{aligned}
\langle\langle 1 \rangle\rangle &= V\,, \\
\langle\langle r_\mu \rangle\rangle &= p_\mu V_{11} + q_\mu V_{12}\,, \\
\langle\langle s_\mu \rangle\rangle &= p_\mu V_{13} + q_\mu V_{14}\,, \\
\langle\langle r_\mu r_\nu \rangle\rangle &= g_{\mu\nu} V_{21} + p_\mu p_\nu V_{22} + q_\mu q_\nu V_{23} + (p_\mu q_\nu + q_\mu p_\nu) V_{24}\,, \\
\langle\langle r_\mu s_\nu \rangle\rangle &= g_{\mu\nu} V_{25} + p_\mu p_\nu V_{26} + q_\mu q_\nu V_{27} + q_\mu p_\nu V_{28} + p_\mu q_\nu V_{29}\,, \\
\langle\langle s_\mu s_\nu \rangle\rangle &= g_{\mu\nu} V_{210} + p_\mu p_\nu V_{211} + q_\mu q_\nu V_{212} + (q_\mu p_\nu + p_\mu q_\nu) V_{213}\,, \\
\langle\langle r_\mu r_\nu r_\alpha \rangle\rangle &= (g_{\mu\nu} p_\alpha + g_{\mu\alpha} p_\nu + g_{\nu\alpha} p_\mu) V_{31} + (g_{\mu\nu} q_\alpha + g_{\mu\alpha} q_\nu + g_{\nu\alpha} q_\mu) V_{32} \\
&\quad + p_\mu p_\nu p_\alpha V_{33} + q_\mu q_\nu q_\alpha V_{34} \\
&\quad + (p_\mu p_\nu q_\alpha + p_\mu q_\nu p_\alpha + q_\mu p_\nu p_\alpha) V_{35} + (q_\mu q_\nu p_\alpha + q_\mu p_\nu q_\alpha + p_\mu q_\nu q_\alpha) V_{36}\,, \\
\langle\langle r_\mu r_\nu s_\alpha \rangle\rangle &= g_{\mu\nu} p_\alpha V_{37} + g_{\mu\nu} q_\alpha V_{38} + (g_{\mu\alpha} p_\nu + g_{\nu\alpha} p_\mu) V_{39} + (g_{\mu\alpha} q_\nu + g_{\nu\alpha} q_\mu) V_{310} \\
&\quad + p_\mu p_\nu p_\alpha V_{311} + q_\mu q_\nu q_\alpha V_{312} + p_\mu p_\nu q_\alpha V_{313} + q_\mu q_\nu p_\alpha V_{314} \\
&\quad + (p_\mu q_\nu + q_\mu p_\nu) p_\alpha V_{315} + (p_\mu q_\nu + q_\mu p_\nu) q_\alpha V_{316}\,, \\
\langle\langle r_\mu s_\nu s_\alpha \rangle\rangle &= p_\mu g_{\nu\alpha} V_{317} + q_\mu g_{\nu\alpha} V_{318} + (g_{\mu\nu} p_\alpha + g_{\mu\alpha} p_\nu) V_{319} + (g_{\mu\nu} q_\alpha + g_{\mu\alpha} q_\nu) V_{320} \\
&\quad + p_\mu p_\nu p_\alpha V_{321} + q_\mu q_\nu q_\alpha V_{322} + p_\mu q_\nu q_\alpha V_{323} + q_\mu p_\nu p_\alpha V_{324} \\
&\quad + p_\mu (p_\nu q_\alpha + q_\nu p_\alpha) V_{325} + q_\mu (p_\nu q_\alpha + q_\nu p_\alpha) V_{326}\,. \qquad \text{(II.135)}
\end{aligned}
$$

The $\langle\langle s_\mu s_\nu s_\alpha \rangle\rangle$ does not show up in $\phi\phi$ scattering. Most of those V_i functions have been calculated analytically in [26] except the $\langle\langle s_\mu s_\nu \rangle\rangle$ and $\langle\langle r_\mu s_\nu s_\alpha \rangle\rangle$. We have calculated the rest of them in this work, which are $V_{210} - V_{213}$ and $V_{317} - V_{326}$. Again, the methods of [36] were used here, somewhat extended to the cases at hand. We have compared our results with the numerical evaluation for general masses described in [41]. The quantity B^ϵ is the next term in the expansion of B in (III.80) but these terms always cancel in the final result.

$$
\begin{aligned}
V_0 &= \lambda_1\left(\pi_{16}\bar{B} + \frac{\pi_{16}^2}{2}\right) + \lambda_2\frac{\pi_{16}^2}{2} + \pi_{16}B^\epsilon \\
&\quad + \bar{J}(2\pi_{16} - L) + \frac{k_1}{2} - \frac{k_3}{3} + \frac{L^2}{2} - \pi_{16}^2 \\
V_{11} &= \lambda_1\frac{\pi_{16}^2}{4} + \frac{1}{2}\pi_{16}\bar{J} - \frac{1}{3}k_3 - 2k_4 - \frac{L\pi_{16}}{2} - \frac{7\pi_{16}^2}{8} \\
V_{12} &= \lambda_1\left(\frac{1}{2}\pi_{16}\bar{B} + \frac{\pi_{16}^2}{8}\right) + \lambda_2\frac{\pi_{16}^2}{4} + \frac{1}{2}\pi_{16}B^\epsilon \\
&\quad + \bar{J}\left(\frac{3\pi_{16}}{4} - \frac{L}{2}\right) + \frac{k_1}{4} + k_4 + \frac{L^2}{4} + \frac{L\pi_{16}}{4} - \frac{\pi_{16}^2}{16} \\
V_{13} &= \lambda_1\left(\frac{1}{2}\pi_{16}\bar{B} + \frac{\pi_{16}^2}{8}\right) + \lambda_2\frac{\pi_{16}^2}{4} + \frac{1}{2}\pi_{16}B^\epsilon \\
&\quad + \bar{J}\left(\frac{3\pi_{16}}{4} - \frac{L}{2}\right) + \frac{k_1}{4} + k_4 + \frac{L^2}{4} + \frac{L\pi_{16}}{4} - \frac{\pi_{16}^2}{16} \\
V_{14} &= -\lambda_1\left(\frac{1}{4}\pi_{16}\bar{B} + \frac{\pi_{16}^2}{16}\right) - \lambda_2\frac{\pi_{16}^2}{8} - \frac{1}{4}\pi_{16}B^\epsilon \\
&\quad + \bar{J}\left(\frac{L}{4} - \frac{3\pi_{16}}{8}\right) - \frac{k_1}{8} - \frac{k_4}{2} - \frac{L^2}{8} - \frac{L\pi_{16}}{8} + \frac{\pi_{16}^2}{32} \\
V_{21} &= \frac{1}{2}\lambda_1\left\{\pi_{16}\left[s\bar{B}_{21} + \bar{B}\left(m^2 - \frac{1}{2}s\right) - Lm^2\right] + \pi_{16}^2\left(\frac{11m^2}{6} - \frac{13s}{72}\right)\right\} \\
&\quad + \frac{1}{2}\lambda_2\pi_{16}^2\left(m^2 - \frac{s}{12}\right) + B^\epsilon\pi_{16}\left(\frac{m^2}{3} - \frac{s}{12}\right) \\
&\quad + \bar{J}\left(\frac{Ls}{12} - \frac{Lm^2}{3} + \frac{5m^2\pi_{16}}{12} - \frac{5\pi_{16}s}{24}\right) - \frac{m^2}{6}k_1 - \frac{s}{24}k_2 - \frac{m^2}{6}k_3 - m^2k_4 \\
&\quad + \frac{5L^2m^2}{6} - \frac{L^2s}{24} + \pi_{16}L\left(\frac{s}{24} - \frac{7m^2}{6}\right) + \pi_{16}^2\left(\frac{m^2\pi^2}{18} + \frac{11m^2}{24} - \frac{\pi^2 s}{72} - \frac{5s}{96}\right) \\
V_{22} &= \lambda_1\frac{\pi_{16}^2}{12} + \frac{1}{6}\pi_{16}\bar{J} - \frac{k_3}{3} - 6k_4 - 12k_5 - \frac{L\pi_{16}}{6} - \frac{7\pi_{16}^2}{24} \\
V_{23} &= \lambda_1\left(\pi_{16}\bar{B}_{21} + \frac{\pi_{16}^2}{36}\right) + \lambda_2\frac{\pi_{16}^2}{6} + B^\epsilon\pi_{16}\left(\frac{1}{3} - \frac{m^2}{3s}\right)
\end{aligned}
$$

II

$$
\begin{aligned}
&+\bar{J}\left(\frac{Lm^2}{3s}-\frac{L}{3}-\frac{2m^2\pi_{16}}{3s}+\frac{\pi_{16}}{2}\right)+\frac{3k_1}{16}-\frac{k_2}{48}-\frac{k_4}{4}-3k_5+\frac{k_9}{12}\\
&+\frac{L^2m^2}{6s}+\frac{L^2}{6}+\pi_{16}L\left(\frac{m^2}{3s}+\frac{1}{6}\right)+\pi_{16}^2\left(\frac{m^2\pi^2}{36s}+\frac{m^2}{6s}+\frac{5}{24}\right)\\
V_{24} &= \lambda_1\frac{\pi_{16}^2}{12}+\frac{1}{6}\pi_{16}\bar{J}+2k_4+6k_5-\frac{L\pi_{16}}{6}-\frac{7\pi_{16}^2}{24}\\
V_{25} &= \frac{1}{4}\lambda_1\left\{\pi_{16}\left[-s\bar{B}_{21}+\bar{B}\left(\frac{s}{2}-m^2\right)+Lm^2\right]+\pi_{16}^2\left(\frac{13s}{72}-\frac{11}{6}m^2\right)\right\}\\
&+\frac{1}{4}\lambda_2\pi_{16}^2\left(\frac{s}{12}-m^2\right)+B^\epsilon\pi_{16}\left(\frac{s}{24}-\frac{m^2}{6}\right)\\
&+\bar{J}\left(\frac{Lm^2}{6}-\frac{Ls}{24}-\frac{5m^2\pi_{16}}{24}+\frac{5\pi_{16}s}{48}\right)+\frac{m^2}{12}k_1+\frac{s}{48}k_2+\frac{m^2}{12}k_3+\frac{m^2}{2}k_4\\
&-\frac{5L^2m^2}{12}+\frac{L^2s}{48}+L\pi_{16}\left(\frac{7m^2}{12}-\frac{s}{48}\right)+\pi_{16}^2\left(\frac{\pi^2s}{144}+\frac{5s}{192}-\frac{m^2\pi^2}{36}-\frac{11m^2}{48}\right)\\
V_{26} &= \lambda_1\frac{\pi_{16}^2}{12}+\frac{1}{6}\pi_{16}\bar{J}+2k_4+6k_5-\frac{L\pi_{16}}{6}-\frac{7\pi_{16}^2}{24}\\
V_{27} &= -\frac{1}{2}\lambda_1\left(\pi_{16}\bar{B}_{21}+\frac{\pi_{16}^2}{36}\right)-\lambda_2\frac{\pi_{16}^2}{12}+B^\epsilon\pi_{16}\left(\frac{m^2}{6s}-\frac{1}{6}\right)\\
&+\bar{J}\left(\frac{L}{6}-\frac{Lm^2}{6s}+\frac{m^2\pi_{16}}{3s}-\frac{\pi_{16}}{4}\right)-\frac{3k_1}{32}+\frac{k_2}{96}+\frac{k_4}{8}+\frac{3k_5}{2}-\frac{k_9}{24}\\
&-\frac{L^2m^2}{12s}-\frac{L^2}{12}-L\pi_{16}\left(\frac{m^2}{6s}+\frac{1}{12}\right)-\pi_{16}^2\left(\frac{m^2\pi^2}{72s}+\frac{m^2}{12s}+\frac{5}{48}\right)\\
V_{28} &= \frac{1}{4}\lambda_1\left(\pi_{16}\bar{B}+\frac{\pi_{16}^2}{12}\right)+\lambda_2\frac{\pi_{16}^2}{8}+\frac{1}{4}\pi_{16}B^\epsilon\\
&+\bar{J}\left(\frac{7\pi_{16}}{24}-\frac{L}{4}\right)+\frac{k_1}{8}-\frac{k_4}{2}-3k_5+\frac{L^2}{8}+\frac{5L\pi_{16}}{24}+\frac{11\pi_{16}^2}{96}\\
V_{29} &= -\lambda_1\frac{\pi_{16}^2}{24}-\frac{1}{12}\pi_{16}\bar{J}-k_4-3k_5+\frac{L\pi_{16}}{12}+\frac{7\pi_{16}^2}{48}\\
V_{210} &= \lambda_1\left\{\frac{1}{4}\pi_{16}\left[-\frac{s}{3}\bar{B}_{21}+\bar{B}\left(\frac{5m^2}{3}+\frac{s}{6}\right)-Lm^2\right]+5\pi_{16}^2\left(\frac{m^2}{18}+\frac{s}{864}\right)\right\}\\
&+\lambda_2\pi_{16}^2\left(\frac{m^2}{3}+\frac{s}{144}\right)+B^\epsilon\pi_{16}\left(\frac{4m^2}{9}+\frac{s}{72}\right)\\
&+\bar{J}\left(\frac{499m^2\pi_{16}}{864}+\frac{7\pi_{16}s}{432}-\frac{4Lm^2}{9}-\frac{Ls}{72}\right)\\
&+k_1\left(\frac{17m^2}{288}+\frac{s}{96}\right)-\frac{s}{288}k_2-\frac{m^2}{12}k_3-\frac{m^2}{24}k_4+k_5\left(\frac{m^2}{2}-\frac{s}{8}\right)\\
&+\frac{4L^2m^2}{9}+\frac{L^2s}{144}+\pi_{16}L\left(\frac{5s}{432}-\frac{m^2}{6}\right)+\pi_{16}^2\left(\frac{m^2\pi^2}{54}-\frac{47m^2}{216}-\frac{\pi^2s}{864}-\frac{11s}{1296}\right)
\end{aligned}
$$

$$
\begin{aligned}
V_{211} &= \lambda_1\left(\frac{1}{3}\pi_{16}\bar{B}+\frac{\pi_{16}^2}{18}\right)+\lambda_2\frac{\pi_{16}^2}{6}+\frac{1}{3}\pi_{16}B^\epsilon \\
&\quad +\bar{J}\left(\frac{4\pi_{16}}{9}-\frac{L}{3}\right)+\frac{k_1}{6}-2k_5+\frac{L^2}{6}+\frac{2L\pi_{16}}{9}+\frac{\pi_{16}^2}{27} \\
V_{212} &= \lambda_1\left(\frac{1}{3}\pi_{16}\bar{B}_{21}+\frac{\pi_{16}^2}{54}\right)+\lambda_2\frac{\pi_{16}^2}{18}+B^\epsilon\pi_{16}\left(\frac{1}{9}-\frac{m^2}{9s}\right) \\
&\quad +\bar{J}\left(\frac{Lm^2}{9s}-\frac{L}{9}+\frac{m^2\pi_{16}}{54s}+\frac{5\pi_{16}}{27}\right)+\frac{k_1}{24}+\frac{k_2}{72}-\frac{k_5}{2}+\frac{k_8}{6} \\
&\quad +\frac{L^2}{18}\left(\frac{m^2}{s}+1\right)+L\pi_{16}\left(\frac{m^2}{9s}+\frac{1}{27}\right)+\pi_{16}^2\left(\frac{m^2\pi^2}{108s}+\frac{m^2}{18s}-\frac{1}{108}\right) \\
V_{213} &= -\lambda_1\left(\frac{1}{6}\pi_{16}\bar{B}+\frac{\pi_{16}^2}{36}\right)-\lambda_2\frac{\pi_{16}^2}{12}-\frac{1}{6}\pi_{16}B^\epsilon \\
&\quad +\bar{J}\left(\frac{L}{6}-\frac{2\pi_{16}}{9}\right)-\frac{k_1}{12}+k_5-\frac{L^2}{12}-\frac{L\pi_{16}}{9}-\frac{\pi_{16}^2}{54} \\
V_{31} &= \lambda_1\left(\frac{19m^2\pi_{16}^2}{144}-\frac{1}{6}Lm^2\pi_{16}-\frac{\pi_{16}^2 s}{96}\right)+\frac{1}{12}\lambda_2 m^2\pi_{16}^2 \\
&\quad -\bar{J}\left(\frac{2m^2\pi_{16}}{9}+\frac{\pi_{16}s}{48}\right)-\frac{1}{12}m^2k_1-\frac{1}{6}m^2k_3-3m^2k_4-5m^2k_5 \\
&\quad +\frac{L^2m^2}{6}-\frac{19Lm^2\pi_{16}}{72}+\frac{L\pi_{16}s}{48}+\pi_{16}^2\left(\frac{m^2\pi^2}{72}+\frac{47m^2}{1728}-\frac{s}{384}\right) \\
V_{32} &= \frac{1}{2}\lambda_1\left[\pi_{16}\left(s\bar{B}_{31}-s\bar{B}_{21}+\frac{1}{2}m^2\bar{B}-\frac{1}{3}Lm^2\right)+\pi_{16}^2\left(\frac{113m^2}{144}-\frac{23s}{288}\right)\right] \\
&\quad +\lambda_2\pi_{16}^2\left(\frac{5m^2}{24}-\frac{s}{48}\right)+B^\epsilon\pi_{16}\left(\frac{m^2}{6}-\frac{s}{24}\right) \\
&\quad +\bar{J}\left(\frac{Ls}{24}-\frac{Lm^2}{6}+\frac{23m^2\pi_{16}}{72}-\frac{3\pi_{16}s}{32}\right)-\frac{m^2}{24}k_1-\frac{s}{48}k_2+m^2k_4+\frac{5m^2}{2}k_5 \\
&\quad +\frac{L^2m^2}{3}-\frac{L^2s}{48}+L\pi_{16}\left(\frac{s}{96}-\frac{65m^2}{144}\right)+\pi_{16}^2\left(\frac{m^2\pi^2}{48}+\frac{745m^2}{3456}-\frac{\pi^2 s}{144}-\frac{19s}{768}\right) \\
V_{33} &= \lambda_1\frac{\pi_{16}^2}{24}+\frac{1}{12}\pi_{16}\bar{J}-\frac{k_3}{3}-12k_4-60k_5-20k_6-\frac{L\pi_{16}}{12}-\frac{43\pi_{16}^2}{288} \\
V_{34} &= \lambda_1\left(\pi_{16}\bar{B}_{31}-\frac{\pi_{16}^2}{96}\right)+\lambda_2\frac{\pi_{16}^2}{8}+B^\epsilon\pi_{16}\left(\frac{1}{4}-\frac{m^2}{2s}\right) \\
&\quad +\bar{J}\left(\frac{Lm^2}{2s}-\frac{L}{4}-\frac{5m^2\pi_{16}}{6s}+\frac{19\pi_{16}}{48}\right) \\
&\quad +\frac{19k_1}{128}-\frac{3k_2}{128}-\frac{9k_4}{32}+\frac{9k_5}{8}+\frac{5k_6}{2}+\frac{3k_9}{32}
\end{aligned}
$$

$$
\begin{aligned}
&+\frac{L^2m^2}{4s}+\frac{L^2}{8}+\pi_{16}L\left(\frac{m^2}{2s}+\frac{5}{48}\right)+\pi_{16}^2\left(\frac{m^2\pi^2}{24s}+\frac{m^2}{4s}+\frac{323}{1152}\right)\\
V_{35} &= \lambda_1\frac{\pi_{16}^2}{48}+\frac{1}{24}\pi_{16}\bar{J}+3k_4+24k_5+10k_6-\frac{L\pi_{16}}{24}-\frac{41\pi_{16}^2}{576}\\
V_{36} &= \lambda_1\frac{\pi_{16}^2}{24}-\frac{L\pi_{16}}{12}-\frac{37\pi_{16}^2}{288}\\
&+\bar{J}\left(\frac{\pi_{16}}{12}-\frac{m^2\pi_{16}}{9s}\right)+\frac{k_1}{192}-\frac{k_2}{192}-\frac{k_4}{16}-\frac{31k_5}{4}-5k_6+\frac{k_9}{48}\\
V_{37} &= \lambda_1\left\{\frac{1}{4}\pi_{16}\left[s\bar{B}_{21}+\bar{B}\left(m^2-\frac{1}{2}s\right)-\frac{2}{3}Lm^2\right]+\pi_{16}^2\left(\frac{113m^2}{288}-\frac{23s}{576}\right)\right\}\\
&+\lambda_2\pi_{16}^2\left(\frac{5m^2}{24}-\frac{s}{48}\right)+B^\epsilon\pi_{16}\left(\frac{m^2}{6}-\frac{s}{24}\right)\\
&+\bar{J}\left(\frac{Ls}{24}-\frac{Lm^2}{6}+\frac{23m^2\pi_{16}}{72}-\frac{3\pi_{16}s}{32}\right)-\frac{m^2}{24}k_1-\frac{s}{48}k_2+m^2k_4+\frac{5m^2}{2}k_5\\
&+\frac{L^2m^2}{3}-\frac{L^2s}{48}-\frac{65Lm^2\pi_{16}}{144}+\frac{L\pi_{16}s}{96}+\pi_{16}^2\left(\frac{m^2\pi^2}{48}+\frac{745m^2}{3456}-\frac{\pi^2s}{144}-\frac{19s}{768}\right)\\
V_{38} &= \lambda_1\left[\frac{1}{4}\pi_{16}\left(s\bar{B}_{21}-s\bar{B}_{31}-\frac{m^2}{2}\bar{B}+\frac{Lm^2}{3}\right)+\pi_{16}^2\left(\frac{23s}{1152}-\frac{113}{576}m^2\right)\right]\\
&+\lambda_2\pi_{16}^2\left(\frac{s}{96}-\frac{5m^2}{48}\right)+B^\epsilon\pi_{16}\left(\frac{s}{48}-\frac{m^2}{12}\right)\\
&+\bar{J}\left(\frac{Lm^2}{12}-\frac{Ls}{48}-\frac{23m^2\pi_{16}}{144}+\frac{3\pi_{16}s}{64}\right)+\frac{m^2}{48}k_1+\frac{s}{96}k_2-\frac{m^2}{2}k_4-\frac{5m^2}{4}k_5\\
&-\frac{L^2m^2}{6}+\frac{L^2s}{96}+\frac{65Lm^2\pi_{16}}{288}-\frac{L\pi_{16}s}{192}+\pi_{16}^2\left(\frac{\pi^2s}{288}+\frac{19s}{1536}-\frac{m^2\pi^2}{96}-\frac{745m^2}{6912}\right)\\
V_{39} &= \lambda_1\left(\frac{1}{12}Lm^2\pi_{16}-\frac{19}{288}m^2\pi_{16}^2+\frac{\pi_{16}^2s}{192}\right)-\frac{1}{24}\lambda_2m^2\pi_{16}^2\\
&+\bar{J}\left(\frac{m^2\pi_{16}}{9}+\frac{\pi_{16}s}{96}\right)+\frac{1}{24}m^2k_1+\frac{1}{12}m^2k_3+\frac{3}{2}m^2k_4+\frac{5}{2}m^2k_5\\
&-\frac{L^2m^2}{12}+\frac{19Lm^2\pi_{16}}{144}-\frac{L\pi_{16}s}{96}+\pi_{16}^2\left(\frac{s}{768}-\frac{m^2\pi^2}{144}-\frac{47m^2}{3456}\right)\\
V_{310} &= \lambda_1\left[\frac{1}{4}\pi_{16}\left(s\bar{B}_{21}-s\bar{B}_{31}-\frac{1}{2}m^2\bar{B}+\frac{1}{3}Lm^2\right)+\pi_{16}^2\left(\frac{23s}{1152}-\frac{113}{576}m^2\right)\right]\\
&+\lambda_2\left(\frac{\pi_{16}^2s}{96}-\frac{5m^2\pi_{16}^2}{48}\right)+B^\epsilon\pi_{16}\left(\frac{s}{48}-\frac{m^2}{12}\right)\\
&+\bar{J}\left(\frac{Lm^2}{12}-\frac{Ls}{48}-\frac{23m^2\pi_{16}}{144}+\frac{3\pi_{16}s}{64}\right)+\frac{m^2}{48}k_1+\frac{s}{96}k_2-\frac{m^2}{2}k_4-\frac{m^2}{4}k_5\\
&-\frac{L^2m^2}{6}+\frac{L^2s}{96}+\frac{65Lm^2\pi_{16}}{288}-\frac{L\pi_{16}s}{192}+\pi_{16}^2\left(\frac{\pi^2s}{288}+\frac{19s}{1536}-\frac{m^2\pi^2}{96}-\frac{745m^2}{6912}\right)
\end{aligned}
$$

$$
\begin{aligned}
V_{311} &= \lambda_1 \frac{\pi_{16}^2}{48} + \frac{1}{24}\pi_{16}\bar{J} + 3k_4 + 24k_5 + 10k_6 - \frac{L\pi_{16}}{24} - \frac{41\pi_{16}^2}{576} \\
V_{312} &= \lambda_1 \left(\frac{\pi_{16}^2}{192} - \frac{1}{2}\pi_{16}\bar{B}_{31} \right) - \lambda_2 \frac{\pi_{16}^2}{16} + B^\epsilon \pi_{16} \left(\frac{m^2}{4s} - \frac{1}{8} \right) \\
&\quad + \bar{J} \left(\frac{L}{8} - \frac{Lm^2}{4s} + \frac{5m^2\pi_{16}}{12s} - \frac{19\pi_{16}}{96} \right) - \frac{19k_1}{256} + \frac{3k_2}{256} + \frac{9k_4}{64} - \frac{9k_5}{16} - \frac{5k_6}{4} - \frac{3k_9}{64} \\
&\quad - \frac{L^2m^2}{8s} - \frac{L^2}{16} - \frac{Lm^2\pi_{16}}{4s} - \frac{5L\pi_{16}}{96} - \pi_{16}^2 \left(\frac{m^2\pi^2}{48s} + \frac{m^2}{8s} + \frac{323}{2304} \right) \\
V_{313} &= -\lambda_1 \frac{\pi_{16}^2}{96} - \frac{1}{48}\pi_{16}\bar{J} - \frac{3k_4}{2} - 12k_5 - 5k_6 + \frac{L\pi_{16}}{48} + \frac{41\pi_{16}^2}{1152} \\
V_{314} &= \lambda_1 \left(\frac{1}{2}\pi_{16}\bar{B}_{21} - \frac{\pi_{16}^2}{144} \right) + \lambda_2 \frac{\pi_{16}^2}{12} + B^\epsilon \pi_{16} \left(\frac{1}{6} - \frac{m^2}{6s} \right) \\
&\quad + \bar{J} \left(\frac{Lm^2}{6s} - \frac{L}{6} - \frac{5m^2\pi_{16}}{18s} + \frac{5\pi_{16}}{24} \right) + \frac{35k_1}{384} - \frac{k_2}{128} - \frac{3k_4}{32} + \frac{19k_5}{8} + \frac{5k_6}{2} + \frac{k_9}{32} \\
&\quad + \frac{L^2m^2}{12s} + \frac{L^2}{12} + \frac{Lm^2\pi_{16}}{6s} + \frac{L\pi_{16}}{8} + \pi_{16}^2 \left(\frac{m^2\pi^2}{72s} + \frac{m^2}{12s} + \frac{97}{576} \right) \\
V_{315} &= \lambda_1 \frac{\pi_{16}^2}{32} + \frac{1}{16}\pi_{16}\bar{J} - \frac{k_4}{2} - 9k_5 - 5k_6 - \frac{L\pi_{16}}{16} - \frac{127\pi_{16}^2}{1152} \\
V_{316} &= -\lambda_1 \frac{\pi_{16}^2}{48} + \bar{J} \left(\frac{m^2\pi_{16}}{18s} - \frac{\pi_{16}}{24} \right) \\
&\quad - \frac{k_1}{384} + \frac{k_2}{384} + \frac{k_4}{32} + \frac{31k_5}{8} + \frac{5k_6}{2} - \frac{k_9}{96} + \frac{L\pi_{16}}{24} + \frac{37\pi_{16}^2}{576} \\
V_{317} &= \lambda_1 \left[\frac{1}{12}\pi_{16} \left(s\bar{B}_{21} + m^2\bar{B} - \frac{1}{2}s\bar{B} - Lm^2 \right) + \pi_{16}^2 \left(\frac{31m^2}{144} - \frac{7s}{432} \right) \right] \\
&\quad + \lambda_2 \pi_{16}^2 \left(\frac{m^2}{12} - \frac{s}{144} \right) + B^\epsilon \pi_{16} \left(\frac{m^2}{18} - \frac{s}{72} \right) \\
&\quad + \bar{J} \left(\frac{Ls}{72} - \frac{Lm^2}{18} + \frac{101m^2\pi_{16}}{864} - \frac{\pi_{16}s}{27} \right) - \frac{11}{288}m^2k_1 - \frac{1}{144}sk_2 - \frac{1}{12}m^2k_3 \\
&\quad - \frac{11}{24}m^2k_4 + k_5 \left(\frac{7m^2}{4} - \frac{3s}{8} \right) + k_6 \left(m^2 - \frac{s}{4} \right) \\
&\quad + \frac{5L^2m^2}{36} - \frac{L^2s}{144} - \frac{23Lm^2\pi_{16}}{72} + \frac{L\pi_{16}s}{108} + \pi_{16}^2 \left(\frac{m^2\pi^2}{108} - \frac{m^2}{1728} - \frac{\pi^2 s}{432} - \frac{173s}{10368} \right) \\
V_{318} &= \lambda_1 \left[\frac{1}{6}\pi_{16} \left(s\bar{B}_{21} - s\bar{B}_{31} + m^2\bar{B} - \frac{1}{2}Lm^2 \right) + \pi_{16}^2 \left(\frac{m^2}{32} + \frac{19s}{1728} \right) \right] \\
&\quad + \lambda_2 \pi_{16}^2 \left(\frac{m^2}{8} + \frac{s}{144} \right) + B^\epsilon \pi_{16} \left(\frac{7m^2}{36} + \frac{s}{72} \right) \\
&\quad + \bar{J} \left(-\frac{7Lm^2}{36} - \frac{Ls}{72} + \frac{199m^2\pi_{16}}{864} + \frac{23\pi_{16}s}{864} \right)
\end{aligned}
$$

II

$$
\begin{aligned}
&+k_1\left(\frac{7m^2}{144}+\frac{s}{192}\right)+\frac{s}{576}k_2+\frac{5m^2}{24}k_4+k_5\left(\frac{s}{8}-\frac{5m^2}{8}\right)+k_6\left(\frac{s}{8}-\frac{m^2}{2}\right)\\
&+\frac{11L^2m^2}{72}+\frac{L^2s}{144}+\frac{11Lm^2\pi_{16}}{144}+\frac{L\pi_{16}s}{864}+\pi_{16}^2\left(\frac{m^2\pi^2}{216}-\frac{125m^2}{1152}+\frac{\pi^2s}{1728}+\frac{85s}{20736}\right)\\
V_{319} &= \lambda_1\left\{\frac{1}{6}\pi_{16}\left[-s\bar{B}_{21}+\bar{B}\left(\frac{1}{2}s-m^2\right)+Lm^2\right]+\pi_{16}^2\left(\frac{25s}{864}-\frac{35}{144}m^2\right)\right\}\\
&+\lambda_2\pi_{16}^2\left(\frac{s}{72}-\frac{m^2}{6}\right)+B^\epsilon\pi_{16}\left(\frac{s}{36}-\frac{m^2}{9}\right)\\
&+\bar{J}\left(\frac{Lm^2}{9}-\frac{Ls}{36}-\frac{2m^2\pi_{16}}{27}+\frac{29\pi_{16}s}{432}\right)+\frac{1}{18}m^2k_1+\frac{1}{72}sk_2-\frac{1}{3}m^2k_4-m^2k_5\\
&-\frac{5L^2m^2}{18}+\frac{L^2s}{72}+\frac{19Lm^2\pi_{16}}{72}-\frac{5L\pi_{16}s}{432}+\pi_{16}^2\left(\frac{\pi^2s}{216}+\frac{169s}{10368}-\frac{m^2\pi^2}{54}-\frac{397m^2}{1728}\right)\\
V_{320} &= \lambda_1\left[\frac{1}{6}\pi_{16}\left(-s\bar{B}_{21}+s\bar{B}_{31}+\frac{1}{2}m^2\bar{B}-\frac{1}{2}Lm^2\right)+\pi_{16}^2\left(\frac{35m^2}{288}-\frac{25s}{1728}\right)\right]\\
&+\lambda_2\pi_{16}^2\left(\frac{m^2}{12}-\frac{s}{144}\right)+B^\epsilon\pi_{16}\left(\frac{m^2}{18}-\frac{s}{72}\right)\\
&+\bar{J}\left(\frac{Ls}{72}-\frac{Lm^2}{18}+\frac{m^2\pi_{16}}{27}-\frac{29\pi_{16}s}{864}\right)-\frac{m^2}{36}k_1-\frac{s}{144}k_2+\frac{m^2}{6}k_4+\frac{m^2}{2}k_5\\
&+\frac{5L^2m^2}{36}-\frac{L^2s}{144}-\frac{19Lm^2\pi_{16}}{144}+\frac{5L\pi_{16}s}{864}+\pi_{16}^2\left(\frac{m^2\pi^2}{108}+\frac{397m^2}{3456}-\frac{\pi^2s}{432}-\frac{169s}{20736}\right)\\
V_{321} &= \lambda_1\frac{\pi_{16}^2}{24}+\frac{1}{12}\pi_{16}\bar{J}-6k_5-4k_6-\frac{L\pi_{16}}{12}-\frac{43\pi_{16}^2}{288}\\
V_{322} &= \lambda_1\left(\frac{1}{3}\pi_{16}\bar{B}_{31}+\frac{\pi_{16}^2}{288}\right)+\lambda_2\frac{\pi_{16}^2}{24}+B^\epsilon\pi_{16}\left(\frac{1}{12}-\frac{m^2}{6s}\right)\\
&+\bar{J}\left(\frac{Lm^2}{6s}-\frac{L}{12}+\frac{m^2\pi_{16}}{36s}+\frac{7\pi_{16}}{48}\right)+\frac{k_1}{48}+\frac{k_2}{48}+\frac{k_5}{2}+\frac{k_6}{2}-\frac{3k_7}{2}+\frac{k_8}{4}\\
&+\frac{L^2m^2}{12s}+\frac{L^2}{24}+\frac{Lm^2\pi_{16}}{6s}+\frac{L\pi_{16}}{48}+\pi_{16}^2\left(\frac{m^2\pi^2}{72s}+\frac{m^2}{12s}+\frac{49}{3456}\right)\\
V_{323} &= \lambda_1\frac{\pi_{16}^2}{72}+\frac{1}{36}\pi_{16}\bar{J}-\frac{3k_5}{2}-k_6+k_7-\frac{L\pi_{16}}{36}-\frac{43\pi_{16}^2}{864}\\
V_{324} &= \lambda_1\left(\frac{1}{6}\pi_{16}\bar{B}+\frac{\pi_{16}^2}{144}\right)+\lambda_2\frac{\pi_{16}^2}{12}+\frac{1}{6}\pi_{16}B^\epsilon\\
&+\bar{J}\left(\frac{13\pi_{16}}{72}-\frac{L}{6}\right)+\frac{k_1}{12}+2k_5+2k_6+\frac{L^2}{12}+\frac{11L\pi_{16}}{72}+\frac{161\pi_{16}^2}{1728}\\
V_{325} &= -\lambda_1\frac{\pi_{16}^2}{48}-\frac{1}{24}\pi_{16}\bar{J}+3k_5+2k_6+\frac{L\pi_{16}}{24}+\frac{43\pi_{16}^2}{576}\\
V_{326} &= -\lambda_1\left(\frac{1}{3}\pi_{16}\bar{B}_{21}+\frac{\pi_{16}^2}{216}\right)-\lambda_2\frac{\pi_{16}^2}{18}+B^\epsilon\pi_{16}\left(\frac{m^2}{9s}-\frac{1}{9}\right)
\end{aligned}
$$

$$+\bar{J}\left(\frac{L}{9}-\frac{Lm^2}{9s}-\frac{m^2\pi_{16}}{54s}-\frac{17\pi_{16}}{108}\right)-\frac{k_1}{24}-\frac{k_2}{72}-k_5-k_6+k_7-\frac{k_8}{6}$$
$$-\frac{L^2m^2}{18s}-\frac{L^2}{18}-\frac{Lm^2\pi_{16}}{9s}-\pi_{16}^2\left(\frac{m^2\pi^2}{108s}+\frac{m^2}{18s}+\frac{35}{864}\right)$$

Where the $\bar{J}$ and k_i function are defined as

$$\begin{aligned}
\sigma &= \sqrt{1-\frac{4}{s}},\\
h &= \frac{1}{\sigma}\ln\frac{\sigma-1}{\sigma+1}\\
\bar{J} &= \pi_{16}(\sigma^2 h+2)\\
k_1 &= \pi_{16}^2\sigma^2h^2\\
k_2 &= \pi_{16}^2(\sigma^4h^2-4)\\
k_3 &= \frac{1}{(16\pi^2)^2}\left[\frac{\sigma^2}{s}h^3+\pi^2\frac{1}{s}h-\frac{\pi^2}{2}\right]\\
k_4 &= \frac{1}{s\sigma^2}\left[\frac{1}{2}k_1+\frac{1}{3}k_3+\pi_{16}\bar{J}+\frac{\pi_{16}^2}{12}(\pi^2-6)s\right].\\
k_5 &= \frac{1}{s\sigma^2}\left[k_4-\frac{1}{12}k_1-\frac{\pi_{16}}{12}\bar{J}+\pi_{16}^2\left(\frac{5}{6}-\frac{\pi^2}{9}\right)\right]+\frac{\pi_{16}^2}{12}\left(\frac{5}{2}-\frac{1}{3}pi^2\right)\\
k_6 &= \frac{1}{s\sigma^2}\left[5k_5+\frac{1}{12}k_1+\frac{\pi_{16}}{18}\bar{J}+\frac{\pi_{16}^2}{6}\left(\pi^2-\frac{49}{6}\right)\right]+\frac{1}{24}\pi_{16}^2\left(\pi^2-\frac{49}{6}\right)\\
k_7 &= \frac{1}{s}\left(k_5+\frac{1}{2}k_4+\frac{1}{24}k_1+\frac{5}{24}\pi_{16}\bar{J}\right)+\frac{1}{72}\pi_{16}^2\\
k_8 &= \frac{1}{s}\left(k_4+\frac{7}{12}k_1+\frac{25}{36}\pi_{16}\bar{J}\right)+\pi_{16}^2\left(\frac{47}{216}+\frac{1}{36}\pi^2\right)\\
k_9 &= \frac{1}{s}\left(k_3-\frac{5}{2}k_1\right)-\pi_{16}^2\left(2+\frac{\pi^2}{12}\right)
\end{aligned}$$

The $\bar{J}$ and k_i vanish at $s=0$ and are well behaved for $s\to\infty$. They have discontinuities in the derivative at threshold but there no poles there. The functions k_i are constructed using the arguments and methods of [42].

All the k_i above show up at intermediate stages of the calulations but in the final result $k_5(s),\ldots,k_9(s)$ always appear multiplied by powers of s and can thus be removed.

Finally, to get the scattering lengths we need to expand these functions around $t,u=0$ and $s=4$. The expansion using $s=4(1+q^2)$ around $s=4$ reads up to order q^4.

$$\bar{J}(s) = \pi_{16}\left(2-2q^2+\frac{4}{3}q^4\right)$$

$$
\begin{aligned}
k_1(s) &= \pi_{16}^2 \left(-\pi^2 + 4q^2 - \frac{4}{3}q^4\right) \\
k_2(s) &= \pi_{16}^2 \left(-4 - \pi^2 q^2 + (4+\pi^2)q^4\right) \\
k_3(s) &= \pi_{16}^2 \left(\frac{1}{2}\pi^2 - \left(2 + \frac{2}{3}\pi^2\right) q^2 + \left(2 + \frac{8}{15}\pi^2\right) q^4\right) \\
k_4(s) &= \pi_{16}^2 \left(-\frac{2}{3} + \frac{1}{36}\pi^2 + \left(\frac{1}{3} + \frac{2}{45}\pi^2\right) q^2 - \left(\frac{1}{3} + \frac{4}{105}\pi^2\right) q^4\right) \quad \text{(II.136)}
\end{aligned}
$$

The expansion around $t = 0$ up to order t^2 are

$$
\begin{aligned}
\bar{J}(t) &= \pi_{16} \left(\frac{1}{6}t + \frac{1}{60}t^2\right), \\
k_1(t) &= \pi_{16}^2 \left(-t - \frac{1}{12}t^2\right) \\
k_2(t) &= \pi_{16}^2 \left(-\frac{2}{3}t - \frac{7}{180}t^2\right) \\
k_3(t) &= \pi_{16}^2 \left(\left(-\frac{1}{2} + \frac{1}{12}\pi^2\right) t + \left(-\frac{1}{8} + \frac{1}{60}\pi^2\right) t^2\right) \\
k_4(t) &= \pi_{16}^2 \left(\left(\frac{1}{4} - \frac{1}{36}\pi^2\right) t + \left(\frac{19}{240} - \frac{1}{120}\pi^2\right) t^2\right). \quad \text{(II.137)}
\end{aligned}
$$

II References

[1] J. Bijnens, J. Lu, "Technicolor and other QCD-like theories at next-to-next-to-leading order," *JHEP* **0911** (2009) 116, arXiv:0910.5424. pages

[2] M. E. Peskin, "The Alignment Of The Vacuum In Theories Of Technicolor," *Nucl. Phys.* (1980) 197. pages

[3] J. Preskill, "Subgroup Alignment In Hypercolor Theories," *Nucl. Phys.* (1981) 21. pages

[4] S. Dimopoulos, "Technicolored Signatures," *Nucl. Phys.* (1980) 69. pages

[5] C. T. Hill, E. H. Simmons, "Strong dynamics and electroweak symmetry breaking," *Phys. Rep.* **381** (2003) 235–402, arXiv:hep-ph/0203079. pages

[6] F. Sannino, "Conformal Dynamics for TeV Physics and Cosmology," *Acta Phys. Polon.* (2009) 3533–3743, arXiv:0911.0931. pages

[7] T. Appelquist, A. Avakian, R. Babich, R. C. Brower, M. Cheng, M. A. Clark, S. D. Cohen, G. T. Fleming *et al.*, "Toward TeV Conformality," *Phys. Rev. Lett.* **104** (2010) 071601, arXiv:0910.2224. pages

[8] A. Deuzeman, M. P. Lombardo and E. Pallante, "The physics of eight flavours," *Phys. Lett.* (2008) 41, arXiv:0804.2905. pages

[9] C. Pica, L. Del Debbio, B. Lucini, A. Patella and A. Rago, "Technicolor on the Lattice," arXiv:0909.3178. pages

[10] T. DeGrand, Y. Shamir and B. Svetitsky, "Phase structure of SU(3) gauge theory with two flavors of symmetric-representation fermions," *Phys. Rev. D* **79** (2009) 034501, arXiv:0812.1427. pages

[11] S. Catterall, J. Giedt, F. Sannino and J. Schneible, "Phase diagram of SU(2) with 2 flavors of dynamical adjoint quarks," *JHEP* **0811** (2008) 009, arXiv:0807.0792. pages

[12] S. Catterall, F. Sannino, "Minimal walking on the lattice," *Phys. Rev. D* **76** (2007) 034504, arXiv:0705.1664. pages

[13] L. Del Debbio, B. Lucini, A. Patella, C. Pica, A. Rago, "The infrared dynamics of Minimal Walking Technicolor," *Phys. Rev. D* **82** (2010) 014510, arXiv:0705.1664. pages

[14] M. Luscher, "Volume Dependence of the Energy Spectrum in Massive Quantum Field Theories. 2. Scattering States," *Commun. Math. Phys.* **105** (1986) 153–188. pages

[15] J. B. Kogut, M. A. Stephanov, D. Toublan, J. J. M. Verbaarschot and A. Zhitnitsky, "QCD-like theories at finite baryon density," *Nucl. Phys.* (2000) 477, arXiv:hep-ph/0001171. pages

[16] Y. I. Kogan, M. A. Shifman and M. I. Vysotsky, "Spontaneous Breaking Of Chiral Symmetry For Real Fermions And N=2 Susy Yang-Mills Theory," *Sov. J. Nucl. Phys.* **42** (1985) 318. pages

[17] H. Leutwyler and A. V. Smilga, "Spectrum of Dirac operator and role of winding number in QCD," *Phys. Rev. D* **46** (1992) 5607. pages

[18] A. V. Smilga and J. J. M. Verbaarschot, "Spectral Sum Rules And Finite Volume Partition Function In Gauge Theories With Real And Pseudoreal Fermions," *Phys. Rev. D* **51** (1995) 829, arXiv:hep-th/9404031. pages

[19] J. Gasser, H. Leutwyler, "Chiral Perturbation Theory: Expansions In The Mass Of The Strange Quark," *Nucl. Phys.* (1985) 465. pages

[20] J. Gasser and H. Leutwyler, "Light Quarks at Low Temperatures," *Phys. Lett.* (1987) 83. pages

[21] K. Splittorff, D. Toublan and J. J. M. Verbaarschot, "Diquark condensate in QCD with two colors at next-to-leading order," *Nucl. Phys.* (2002) 290, arXiv:hep-ph/0108040. pages

[22] J. Bijnens, G. Colangelo and G. Ecker, "The mesonic chiral Lagrangian of order p^6," *JHEP* **9902** (1999) 020, arXiv:hep-ph/9902437. pages

[23] J. Bijnens, G. Colangelo and G. Ecker, "Renormalization of chiral perturbation theory to order p^6," *Annals Phys.* **280** (2000) 100, arXiv:hep-ph/9907333. pages

[24] S. Weinberg, "Pion scattering lengths," *Phys. Rev. Lett.* **17** (1966) 616–621. pages

[25] J. Bijnens, G. Colangelo, G. Ecker, J. Gasser, M. E. Sainio, "Elastic pi pi scattering to two loops," *Phys. Lett.* (1996) 210–216, arXiv:hep-ph/9511397. pages

[26] J. Bijnens, G. Colangelo, G. Ecker, J. Gasser, M. E. Sainio, "Pion pion scattering at low-energy," *Nucl. Phys.* (1996) 210–216, arXiv:hep-ph/9511397. pages

[27] S. R. Coleman, J. Wess and B. Zumino, "Structure of phenomenological Lagrangians. 1," *Phys. Rev.* **177** (1969) 2239. pages

[28] S. R. Coleman, J. Wess and B. Zumino, "Structure of phenomenological Lagrangians. 2," *Phys. Rev.* **177** (1969) 2247. pages

[29] J. Gasser, H. Leutwyler, "Chiral Perturbation Theory To One Loop," *Annals Phys.* **158** (1984) 142. pages

[30] G. F. Chew, S. Mandelstam, "Theory of low-energy pion pion interactions," *Phys. Rev.* **119** (1960) 467–477. pages

[31] D. E. Neville, "Elastic Scattering of Pseudosscalar Mesons and SU_n Symmetry," *Phys. Rev.* **132** (1963) 844. pages

[32] K. Nakamura *et al.* [Particle Data Group Collaboration], "Review of particle physics," *J. Phys. G* **37** (2010) 075021. pages

[33] G. Girardi, A. Sciarrino, P. Sorba, "KRONECKER PRODUCTS FOR SO(2p) REPRESENTATIONS," *J. Phys. A* **15** (1982) 1119. pages

[34] G. Girardi, A. Sciarrino, P. Sorba, "KRONECKER PRODUCT OF Sp(2n) REPRESENTATIONS USING GENERALIZED YOUNG TABLEAUX," *J. Phys. A* **16** (1983) 2609. pages

[35] J. Stern, H. Sazdjian, N. H. Fuchs, "What pi - pi scattering tells us about chiral perturbation theory," *Phys. Rev. D* **47** (1993) 3814–3838, `arXiv:hep-ph/9301244`. pages

[36] J. Gasser, M. E. Sainio, "Two loop integrals in chiral perturbation theory," *Eur. Phys. J.* (1998) 297–306, `arXiv:hep-ph/9803251`. pages

[37] `http://www.thep.lu.se/~bijnens/chpt.html`. pages

[38] G. Amoros, J. Bijnens, P. Talavera, "QCD isospin breaking in meson masses, decay constants and quark mass ratios," *Nucl. Phys.* (2001) 87–108, `arXiv:hep-ph/0101127`. pages

[39] J. A. M. Vermaseren, "New features of FORM," `arXiv:math-ph/0010025`. pages

[40] G. Passarino, M. J. G. Veltman, "One Loop Corrections for e+ e- Annihilation Into mu+ mu- in the Weinberg Model," *Nucl. Phys.* (1979) 151. pages

[41] J. Bijnens and P. Talavera, "Pion and kaon electromagnetic form-factors," *JHEP* **0203** (2002) 046, `arXiv:hep-ph/0203049`. pages

[42] M. Knecht, B. Moussallam, J. Stern, N. H. Fuchs, "The Low-energy pi pi amplitude to one and two loops," *Nucl. Phys.* (1995) 513–576, arXiv:hep-ph/9507319. pages

III

Two-Point Functions and S-Parameter in QCD-like Theories

Johan Bijnens and Jie Lu

Department of Astronomy and Theoretical Physics, Lund University,
Sölvegatan 14A, SE–223 62 Lund, Sweden
http://www.thep.lu.se/complex/

Submitted to *Journal of High Energy Physics*
arXiv:1111.1886 [hep-ph]

We calculated the vector, axial-vector, scalar and pseudo-scalar two-point functions up to two-loop level in the low-energy effective field theory for three different QCD-like theories. In addition we also calculated the pseudo-scalar decay constant G_M. The QCD-like theories we used are those with fermions in a complex, real or pseudo-real representation with in general n flavours. These case correspond to global symmetry breaking pattern of $SU(n)_L \times SU(n)_R \to SU(n)_V$, $SU(2n) \to SO(2n)$ or $SU(2n) \to Sp(2n)$. We also estimated the S parameter for those different theories.

III.1 Introduction

The different global symmetry breaking patterns of QCD-like theories with a vector-like gauge group have been summarized in [1–3] around 30 years ago. The global symmetry and its spontaneous breaking depend on whether the fermions live in a complex, real and pseudo-real representation of the gauge group. For n identical fermions this corresponds to the symmetry breaking pattern $SU(n)_L \times SU(n)_R \to SU(n)_V$, $SU(2n) \to SO(2n)$ and $SU(2n) \to Sp(2n)$ respectively. These theories can be used to characterize some of technicolor models with vector-like gauge bosons. QCD-like theories are also important in the theory of finite baryon density. Here the real and pseudo-real case allow to investigate the mechanism of diquark condensate and finite density without the sign problem. A main nonperturbative tool in studying strongly interacting theories is lattice gauge theory. Numerical calculations are performed at finite fermion mass and need in general to be extrapolated to the zero mass limit. In the case of QCD Chiral Perturbation Theory (ChPT) is used to help with this extrapolation. Our work has the intention of providing similar formulas for the QCD-like theories using the effective field theory (EFT) appropriate for the alternative global symmetry patterns.

These EFT have been used at lowest order (LO) [4] with earlier work to be found in [5–7] and some studies at next-to-leading order (NLO) have also appeared [8–10]. The former two are the usual QCD case with n flavours. In our earlier papers [11, 12] we have systematically studied the effective field theory of these three different QCD-like theories to next-to-next-to-leading order (NNLO). We managed to write the EFT of these cases in an extremely similar form. We calculated the quark-antiquark condensates, the mass and decay constant of the pseudo-Goldstone bosons [11], and meson-meson scattering [12]. In this paper we extend the analysis to two-point correlation functions. We obtain expressions for the vector, axial-vector, scalar and pseudo-scalar two-point functions as well as the pion pseudo-scalar coupling G_M to NNLO[1] or order p^6.

In our earlier work [11,12], we called the three different cases QCD or complex, adjoint or real and two-colour or pseudo-real. In this paper we use only the latter, more general, terminology.

One motivation for this set of work was the study of strongly interacting Higgs sectors, reviews are [13, 14]. For any model beyond the Standard Model, passing the test of oblique corrections, or precision LEP observables, is crucial [15, 16]. Over the years, the impact of the oblique corrections in those models have been studied quite intensively but in strongly interacting cases mainly an analogy with QCD has been invoked. Lattice gauge theory

[1]We use LO, NLO and NNLO as synomyms for order p^2, order p^4 and order p^6 calculations even if the order p^2 vanishes.

methods allow to study strongly interacting models from first principles. The contributions from these theories to the S-parameter can be calculated using the two-point functions studied here and our formulas are useful to perform the extrapolation to the massless case. This was in fact the major motivation for the present work but we included the other two-point functions for completeness.

The paper is organized as follows. In Section III.2 we give a brief introduction to EFT for the three different cases. Section III.3 is the main part of the paper. We define the fermion currents and the two-point functions in Section III.3.1. In Sections III.3.2 to III.3.5, we present the calculation of vector, axial-vector, scalar, pseudo-scalar two-point functions. In Section III.4, we discuss the oblique corrections and the S-parameter. Section III.5 summarizes our main results and we present the definition.

III.2 Effective Field Theory

In this section we briefly review the EFT of QCD-like theories, the details can be found in the earlier paper [11]. The basic methods are those of Chiral Perturbation Theory [17,18]. The counting of orders is in all cases the same as in ChPT, we count momenta as order p and the fermion mass m as order p^2.

III.2.1 Complex representation: QCD and CHPT

The case of n fermions in a complex representation is essentially like QCD. The Lagrangian with external left and right vector, scalar and pseudos-calar external sources, l_μ, r_μ, s and p, is

$$\begin{aligned}\mathcal{L} &= \bar{q}_{Li} i\gamma^\mu D_\mu q_{Li} + \bar{q}_{Ri} i\gamma^\mu D_\mu q_{Ri} + \bar{q}_{Li}\gamma^\mu l_{\mu ij} q_{Lj} + \bar{q}_{Ri}\gamma^\mu r_{\mu ij} q_{Rj} \\ &\quad -\bar{q}_{Ri}\mathcal{M}_{ij} q_{Lj} - \bar{q}_{Li}\mathcal{M}^\dagger_{ij} q_{Rj} \qquad\qquad i,j = 1,2,...,n\,. \end{aligned} \tag{III.1}$$

The covariant derivative is given by $D_\mu q = \partial_\mu q - iG_\mu q$, and the mass matrix $\mathcal{M} = s - ip$. The sums shown are over the flavour index. The sums over gauge group indices are implicit.

The Lagrangian (III.1) has a symmetry $SU(n)_L \times SU(n)_R$ which is made local by the external sources [8,18]. The quark-anti-quark condensate $\langle\bar{q}q\rangle$ breaks $SU(n)_L \times SU(n)_R$ spontaneously to the diagonal subgroup $SU(n)_V$. According to the Nambu-Goldstone theorem, $n^2 - 1$ Goldstone Bosons will thus be generated. We add a small fermion mass m explicitly by setting $s = m + s$. This mass term explicitly breaks the symmetry $SU(n)_L \times SU(n)_R$ down to $SU(n)_V$ as well and gives the Goldstone bosons a small mass.

The Goldstone boson manifold $SU(n)_L \times SU(n)_R/SU(n)_V$ can be parametrized by

$$u = \exp\left(\frac{i}{\sqrt{2}\,F}\pi^a T^a\right) \qquad a = 1, 2, ..., n^2 - 1\,. \tag{III.2}$$

The T^a are the generators of $SU(n)$ normalized to $\langle T^a T^b\rangle = \delta^{ab}$. The notation $\langle A\rangle$ stands for the trace over flavour indices. u transforms under $g_L \times g_R \in SU(n)_L \times SU(n)_R$ as $u \to g_R u h^\dagger = h u g_L^\dagger$ where h is the "compensator" and is a function of u, g_L and g_R. The methods are those of [19, 20], but we use the notation of [21, 22]. We can construct quantities which transform under the unbroken group H as : $O \to hOh^\dagger$

$$\begin{aligned} u_\mu &= i[u^\dagger(\partial_\mu - ir_\mu)u - u(\partial_\mu - l_\mu)u^\dagger]\,, \\ \nabla_\mu O &= \partial_\mu O + \Gamma_\mu O - O\Gamma_\mu\,, \\ \chi_\pm &= u^\dagger\chi u^\dagger \pm u\chi^\dagger u\,, \\ f_{\pm\mu\nu} &= u l_{\mu\nu} u^\dagger \pm u^\dagger r_{\mu\nu} u\,. \end{aligned} \tag{III.3}$$

The field strengths $l_{\mu\nu}$ and $r_{\mu\nu}$ are

$$\begin{aligned} l_{\mu\nu} &= \partial_\mu l_\nu - \partial_\nu l_\mu - i[l_\mu, l_\nu]\,, \\ r_{\mu\nu} &= \partial_\mu r_\nu - \partial_\nu r_\mu - i[r_\mu, r_\nu]\,. \end{aligned} \tag{III.4}$$

The covariant derivative ∇_μ contains

$$\Gamma_\mu = \frac{1}{2}[u^\dagger(\partial_\mu - ir_\mu)u + u(\partial_\mu - l_\mu)u^\dagger]\,. \tag{III.5}$$

χ contains the matrix $\mathcal{M}$, which is the combination of scalar and pseudo-scalar sources

$$\chi = 2B_0\mathcal{M} = 2B_0(s - ip). \tag{III.6}$$

Using the quantities in (III.3), we can find the leading order, p^2, Lagrangian which is invariant under Lorentz and chiral symmetry:

$$\mathcal{L}_2 = \frac{F^2}{4}\langle u_\mu u^\mu + \chi_+\rangle\,. \tag{III.7}$$

The subscript "2" stands for the order of p^2. The p^4 and p^6 Lagrangian will be explained in Section III.2.3.

III.2.2 Real and Pseudo-Real representation

The case of n fermions in a real or pseudo-real representation of the gauge group we can treat in a similar way as the complex case. In the real case,

the global symmetry breaking pattern is $SU(2n) \to SO(2n)$, and the number of generated Goldstone bosons is $2n^2 + n - 1$. In the pseudo-real case, the symmetry breaking is $SU(2n) \to Sp(2n)$, and the number of generated Goldstone is $2n^2 - n - 1$. In both cases anti-fermions are in the same representation of the gauge group and can be put together in a $2n$ vector $\hat{q}$, see [11] for more details.

The condensate can now be a diquark condensate as well as a quark-antiquark condensate. Our choice of vacuum corresponds to a quark-antiquark condensate. In terms of the $2n$ fermion vector $\hat{q}$ they can be written as

$$\text{Real}: \qquad \langle \hat{q}^T C J_S \hat{q} \rangle + \text{h.c.} \qquad J_S = \begin{pmatrix} 0 & \mathrm{I} \\ \mathrm{I} & 0 \end{pmatrix}, \tag{III.8}$$

$$\text{Pseudo}-\text{Real}: \quad \langle \hat{q}_\alpha \epsilon_{\alpha\beta} C J_A \hat{q}_\beta \rangle + \text{h.c.} \qquad J_A = \begin{pmatrix} 0 & -\mathrm{I} \\ \mathrm{I} & 0 \end{pmatrix}. \tag{III.9}$$

Here C is the charge conjugation operator. J_S and J_A are symmetric and anti-symmetric $2n \times 2n$ matrices, I is the $n \times n$ unit matrix. Since J_S and J_A often appear in the same way in the expressions, we use J for both cases unless a distinction is needed.

The generators, T^a, of the global symmetry group $SU(2n)$ can be separated into belonging to the broken, X^a, or unbroken part, Q^a. They satisfy the following relations with J:

$$JQ^a = -Q^{aT} J\,, \qquad JX^a = X^{aT} J\,, \tag{III.10}$$

The Goldstone boson manifold can be parametrized with

$$U = uJu^T \to gUg^T\,, \qquad \text{with} \qquad u = \exp\left(\frac{i}{\sqrt{2}\,F}\pi^a X^a\right). \tag{III.11}$$

where $J = J_S$ and a runs from 1 to $2n^2 + n - 1$ for the real case and $J = J_A$ and a runs from 1 to $2n^2 - n - 1$ for the pseudo-real case.

In our earlier paper [11], we constructed quantities similar to those in (III.3–III.5)

$$\begin{aligned} u_\mu &= i[u^\dagger(\partial_\mu - iV_\mu)u - u(\partial_\mu + iJV_\mu^T J)u^\dagger]\,, \\ \Gamma_\mu &= \frac{1}{2}[u^\dagger(\partial_\mu - iV_\mu)u + u(\partial_\mu + iJV_\mu^T J)u^\dagger]\,. \\ f_{\pm\mu\nu} &= JuV_{\mu\nu}u^\dagger J \pm uV_{\mu\nu}u^\dagger\,, \\ \chi_\pm &= u^\dagger \chi J u^\dagger \pm u J \chi^\dagger u\,. \end{aligned} \tag{III.12}$$

The $2n \times 2n$ matrix V_μ includes the left and right-handed external sources

$$V_\mu = \begin{pmatrix} r_\mu & 0 \\ 0 & -l_\mu^T \end{pmatrix} \tag{III.13}$$

and $V_{\mu\nu}$ is the field strength

$$V_{\mu\nu} = \partial_\mu V_\nu - \partial_\nu V_\mu - i\left(V_\mu V_\nu - V_\nu V_\mu\right) . \tag{III.14}$$

χ include the matrix $\hat{\mathcal{M}}$ via $\chi = 2B_0\hat{\mathcal{M}}$ [11]. Those quantities behave similarly as those (III.3) if we take

$$-JV_\mu^T J \to l_\mu , \qquad V_\mu \to r_\mu . \tag{III.15}$$

With this correspondence, the Lagrangian of the real and pseudo-real case has the same form as the complex one. However one has to remember there are differences in the generators, external sources, coupling constants,.... Anyway, now we can use the techniques of ChPT to perform the calculations.

III.2.3 High Order Lagrangians and Renormalization

Using Lorentz and chiral invariance, we can write down the p^4 EFT lagrangian [18] for all three cases using the quantities listed in (III.3) and (III.12):

$$\begin{aligned}\mathcal{L}_4 \;=\;& L_0\langle u^\mu u^\nu u_\mu u_\nu\rangle + L_1\langle u^\mu u_\mu\rangle\langle u^\nu u_\nu\rangle + L_2\langle u^\mu u^\nu\rangle\langle u_\mu u_\nu\rangle + L_3\langle u^\mu u_\mu u^\nu u_\nu\rangle \\ &+ L_4\langle u^\mu u_\mu\rangle\langle\chi_+\rangle + L_5\langle u^\mu u_\mu\chi_+\rangle + L_6\langle\chi_+\rangle^2 + L_7\langle\chi_-\rangle^2 + \frac{1}{2}L_8\langle\chi_+^2+\chi_-^2\rangle \\ &- iL_9\langle f_{+\mu\nu}u^\mu u^\nu\rangle + \frac{1}{4}L_{10}\langle f_+^2 - f_-^2\rangle + H_1\langle l_{\mu\nu}l^{\mu\nu} + r_{\mu\nu}r^{\mu\nu}\rangle + H_2\langle\chi\chi^\dagger\rangle .\end{aligned} \tag{III.16}$$

To do the renormalization, we use the ChPT $\overline{\text{MS}}$ scheme with dimensional regularization [8, 18, 22]. The bare coupling constants L_i are defined as

$$L_i = (c\mu)^{d-4}\left[\Gamma_i\Lambda + L_i^r(\mu)\right] , \tag{III.17}$$

where the dimension $d = 4 - 2\epsilon$, and

$$\Lambda \;=\; \frac{1}{16\pi^2(d-4)} , \tag{III.18}$$

$$\ln c \;=\; -\frac{1}{2}[\ln 4\pi + \Gamma'(1) + 1] . \tag{III.19}$$

The coefficients Γ_i for the complex case have been obtained in [8], for the real and pseudo-real case we have calculated them earlier in [11]. However, there are mistakes in the coefficients of L_9, L_{10} and H_1 in the Table 1 of [11]. These mistakes had no effects on our previous calculations. We therefore list all the coefficients here again in Table III.1.

The p^6 Lagrangian for the complex case and general n has been obtained in [21], it contains 112+3 terms. The divergence structure of the bare coupling

i	complex	real	pseudo-real
0	$n/48$	$(n+4)/48$	$(n-4)/48$
1	$1/16$	$1/32$	$1/32$
2	$1/8$	$1/16$	$1/16$
3	$n/24$	$(n-2)/24$	$(n+2)/24$
4	$1/8$	$1/16$	$1/16$
5	$n/8$	$n/8$	$n/8$
6	$(n^2+2)/(16n^2)$	$(n^2+1)/(32n^2)$	$(n^2+1)/(32n^2)$
7	0	0	0
8	$(n^2-4)/(16n)$	$(n^2+n-2)/(16n)$	$(n^2-n-2)/(16n)$
9	$n/12$	$(n+1)/12$	$(n-1)/12$
10	$-n/12$	$-(n+1)/12$	$-(n-1)/12$
1′	$-n/24$	$-(n+1)/24$	$-(n-1)/24$
2′	$(n^2-4)/(8n)$	$(n^2+n-2)/(8n)$	$(n^2-n-2)/(8n)$

Table III.1: The coefficients Γ_i for the three cases that are needed to absorb the divergences at NLO. The last two lines correspond to the terms with H_1 and H_2. This is the same as Table 1 in [11] but with the error for L_9, L_{10} and H_1 corrected.

constants K_i in the p^6 can be written as[2]

$$K_i = (c\mu)^{2(d-4)}\left[K_i^r - \Gamma_i^{(2)}\Lambda^2 - \left(\frac{1}{16\pi^2}\Gamma_i^{(1)} + \Gamma_i^{(L)}\right)\Lambda\right]. \qquad \text{(III.20)}$$

The coefficients $\Gamma_i^{(2)}$, $\Gamma_i^{(1)}$ and $\Gamma_i^{(L)}$ for the complex case have been obtained in [22].

For the real and pseudo-real case, the p^6 Lagrangian has the same form as in the complex case but some terms might be redundant. The divergence structure as given in (III.20) still holds but the coefficients are not known. One check on our results that remains is that all the non-local divergences cancel.

III.3 Two-Point Functions

III.3.1 Definition

The effective action of the fermion level theory with external sources is

$$\exp\{iZ(l_\mu, r_\mu, s, p)\} = \int \mathcal{D}q\mathcal{D}\bar{q}\mathcal{D}G_\mu \exp\left\{i\int d^4x \mathcal{L}_{QCD}(q, \bar{q}, G_\mu, l_\mu, r_\mu, s, p)\right\} \qquad \text{(III.21)}$$

[2]The K_i have been made dimensionless by including a factor of $1/F^2$ explicitly in the order p^6 Lagrangian.

At low energies, i.e. below 1 GeV in QCD, the effective action can be obtained also from the low-energy effective theory

$$\exp\{iZ(l_\mu, r_\mu, s, p)\} = \int \mathcal{D}U \, \exp\left\{ i \int d^4x \mathcal{L}_{eff}(U, l_\mu, r_\mu, s, p) \right\}. \tag{III.22}$$

With this effective action, the n-point Green functions can be easily derived by taking the functional derivative w.r.t. the external sources of $Z(J)$

$$G^{(n)}(x_1, \ldots, x_n) = \frac{\delta^n}{i^n \delta j(x_1) \ldots \delta j(x_n)} Z[J]\Big|_{J=0}. \tag{III.23}$$

Here j stands for any of the external sources l_μ, r_μ, s, p and J for the whole set of them.

The vector current v_μ and axial-vector current a_μ are included via

$$l_\mu = v_\mu - a_\mu\,, \qquad r_\mu = v_\mu + a_\mu\,. \tag{III.24}$$

In this paper we will calculate the two-point functions of vector, axial-vector, scalar and pseudo-scalar currents. The fermion currents in the complex case are defined as

$$V^a_\mu(x) = \bar{q}_i T^a_{ij} \gamma_\mu q_j\,, \tag{III.25}$$
$$A^a_\mu(x) = \bar{q}_i T^a_{ij} \gamma_\mu \gamma_5 q_j\,, \tag{III.26}$$
$$S^a(x) = -\bar{q}_i T^a_{ij} q_j\,, \tag{III.27}$$
$$P^a(x) = i\bar{q}_i T^a_{ij} \gamma_5 q_j\,. \tag{III.28}$$

T^a is an $SU(n)$ generator[3] or in addition for the singlet scalar and pseudo-scalar current the unit matrix which we label by T^0. These currents also exist the for real and pseudo-real case. In this case also currents with two fermions or two anti-fermions exist. These can be combined with those above. The generators can then become $SU(2n)$ generators. All conserved generators are like the vector or scalar case while the broken generators are like the axial-vecor or pseudo-scalar case. All those cases are related to the ones with the currents of (III.25)-(III.28) via transformations under the unbroken part of the symmetry group.

[3]We have defined here the current with fermion-anti-fermion operators, hence the $SU(n)$ for n fermions. For the real and pseudo-real case, the unbroken symmetry relates them also to difermion ot dianti-fermmion operators.

The definitions of the two-point functions are

$$\begin{aligned}
\Pi_{Va\mu\nu}(q) &\equiv i\int d^4x\, e^{iq\cdot x}\, \langle 0|T(V^a_\mu(x)V^a_\nu(0))^\dagger|0\rangle\,,\\
\Pi_{Aa\mu\nu}(q) &\equiv i\int d^4x\, e^{iq\cdot x}\, \langle 0|T(A^a_\mu(x)A^a_\nu(0))^\dagger|0\rangle\,,\\
\Pi_{SMa\mu}(q) &\equiv i\int d^4x\, e^{iq\cdot x}\, \langle 0|T(V^a_\mu(x)S^a(0))^\dagger|0\rangle\,,\\
\Pi_{PMa\mu}(q) &\equiv i\int d^4x\, e^{iq\cdot x}\, \langle 0|T(A^a_\mu(x)P^a(0))^\dagger|0\rangle\,,\\
\Pi_{Sa}(q) &\equiv i\int d^4x\, e^{iq\cdot x}\, \langle 0|T(S^a(x)S^a(0))^\dagger|0\rangle\,,\\
\Pi_{Pa}(q) &\equiv i\int d^4x\, e^{iq\cdot x}\, \langle 0|T(P^a(x)P^a(0))^\dagger|0\rangle\,.
\end{aligned} \tag{III.29}$$

Using Lorentz invariance the two-point functions with vectors and axial-vectors can be decomposed in scalar functions

$$\Pi_{Va\mu\nu} = (q_\mu q_\nu - q^2 g_{\mu\nu})\Pi^{(1)}_{Va}(q^2) + q_\mu q_\nu \Pi^{(0)}_{Va}(q^2)\,. \tag{III.30}$$

where $\Pi^{(1)}_{Va}(q^2)$ is the transverse part and $\Pi^{(0)}_{Va}(q^2)$ is the longitudinal part or alternatively the spin one and spin 0 part. The same definition holds for the axial-vector two-point functions. The mixed functions can be decomposed as

$$\begin{aligned}
\Pi_{SMa\mu} &= q_\mu \Pi_{SMa}\,,\\
\Pi_{PMa\mu} &= iq_\mu \Pi_{PMa}\,.
\end{aligned} \tag{III.31}$$

Using the divergence of fermion currents and equal time commutation relations, we find that some two-point functions are related to each other by Ward identities. In the equal mass case considered here, they are

$$\begin{aligned}
\Pi^{(0)}_{Va} &= \Pi_{SMa} = 0\,,\\
q^2\Pi^{(0)}_{Aa} &= 2m\Pi_{PMa}\,,\\
q^4\Pi^{(0)}_{Aa} &= 4m^2\Pi_{Pa} + 4m\langle\bar{q}q\rangle\,.
\end{aligned} \tag{III.32}$$

The vacuum expectation value is the single quark-anti-quark one. We will use the last relation to double check our results of axial-vector and pseudo-scalar two-point functions.

The mixed two-point functions, Π_{SMa} and Π_{PMa} we do not discuss further since they are fully given by the Ward identities.

III.3.2 The Vector Two-Point Function

The vector two-point function is defined in (III.29). The longitudinal part vanishes for all three cases because of the Ward identities.

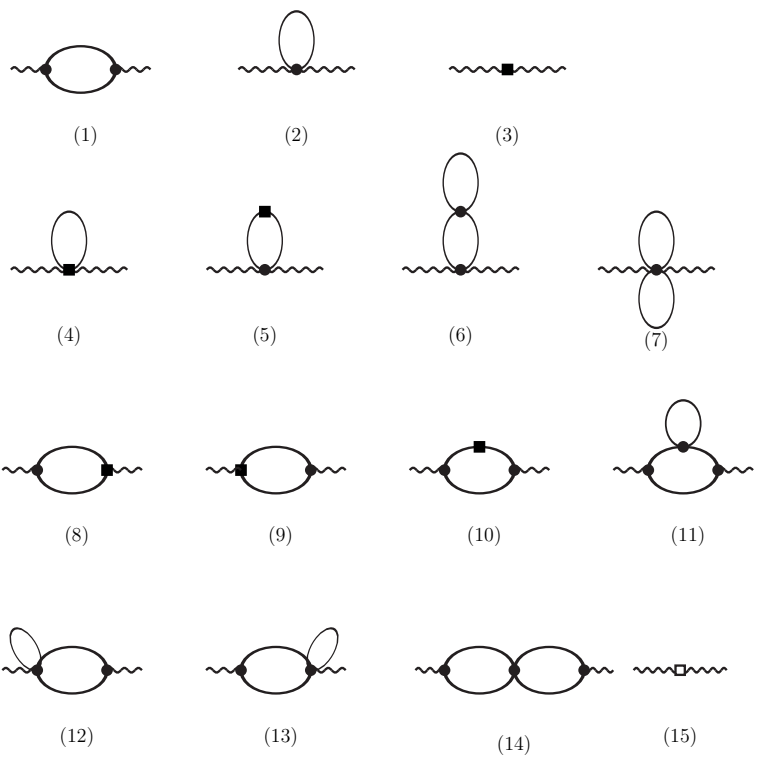

Figure III.1: The diagrams for the vector two-point function. A filled circle is a vertex from $\mathcal{L}_2$, a filled square a vertex from $\mathcal{L}_4$, and an open square a vertex from $\mathcal{L}_6$. The top line is order p^4. The remaining ones are order p^6.

The Feynman diagrams for the vector two-point function are listed in Fig. III.1. There is no diagram at lowest order. The diagrams at NLO are (1–3) in Fig. III.1. The NNLO diagrams are (4–15). The 3-flavour QCD case is known to NNLO [23, 24].

We have rewritten the results in terms of the physical mass and decay constant. For these we use the notation M_M and F_M rather than the M_{phys} and F_{phys} used in [11, 12]. Their expression in terms of the lowest order quantities F and $M^2 = 2B_0 m$ can be found in [11]. We also use the quantities

$$L = \frac{1}{16\pi^2} \log \frac{M_M^2}{\mu^2} \quad \text{and} \quad \pi_{16} = \frac{1}{16\pi^2}\,. \tag{III.33}$$

The loop integral $\overline{B}_{22}$ is defined in Appendix III.1.1.

The results up to NNLO for three different cases are listed below, where

the first line in each case is the NLO contributions, the rest are NNLO contributions.

Complex

$$\begin{aligned}\Pi_{VV}^{(1)} &= -\frac{n}{q^2}\left[4\overline{B}_{22}(M_M^2,M_M^2,q^2)+2LM_M^2\right]-4L_{10}^r-8H_1^r\\ &+\frac{1}{F_M^2}\left\{\left(\frac{4M_M^2}{q^2}Ln^2-16L_9^r n\right)\overline{B}_{22}(M_M^2,M_M^2,q^2)+\frac{4n^2}{q^2}[\overline{B}_{22}(M_M^2,M_M^2,q^2)]^2\right.\\ &\left.+\frac{M_M^4}{q^2}L^2n^2-8q^2K_{115}^r+8M_M^2(LL_{10}^r n-4K_{81}^r-4K_{82}^r n)\right\}, \qquad \text{(III.34)}\end{aligned}$$

Real

$$\begin{aligned}\Pi_{VV}^{(1)} &= -\frac{1}{q^2}(n+1)\left[4\overline{B}_{22}(M_M^2,M_M^2,q^2)+2M_M^2L\right]-4L_{10}^r-8H_1^r\\ &+\frac{1}{F_M^2}\left\{\left[\frac{4M_M^2}{q^2}L(n+1)^2-16(n+1)L_9^r\right]\overline{B}_{22}(M_M^2,M_M^2,q^2)\right.\\ &+\frac{4}{q^2}(n+1)^2[\overline{B}_{22}(M_M^2,M_M^2,q^2)]^2+\frac{M_M^4}{q^2}L^2(n+1)^2\\ &\left.-8q^2K_{115}^r+8M_M^2[LL_{10}^r(n+1)-4K_{81}^r-8K_{82}^r n]\right\}, \qquad \text{(III.35)}\end{aligned}$$

Pseudo − Real

$$\begin{aligned}\Pi_{VV}^{(1)} &= -\frac{1}{q^2}(n-1)\left[4\overline{B}_{22}(M_M^2,M_M^2,q^2)+2M_M^2L\right]-4L_{10}^r-8H_1^r\\ &+\frac{1}{F_M^2}\left\{\left[\frac{4M_M^2}{q^2}L(n-1)^2-16L_9^r(n-1)\right]\overline{B}_{22}(M_M^2,M_M^2,q^2)\right.\\ &+\frac{4}{q^2}(n-1)^2[\overline{B}_{22}(M_M^2,M_M^2,q^2)]^2+\frac{M_M^4}{q^2}L^2(n-1)^2\\ &\left.-8q^2K_{115}^r+8M_M^2[LL_{10}^r(n-1)-4K_{81}^r-8K_{82}^r n]\right\}. \qquad \text{(III.36)}\end{aligned}$$

The complex result with $n=3$ agrees with [23] when the masses there are set equal.

III.3.3 The Axial-Vector Two-Point Function

The axial-vector two-point function is defined in (III.29). Similar to the vector two-point function, it also can be decomposed in a transverse and longitudinal part.

$$\Pi_{AA}^{\mu\nu}=(q^\mu q^\nu-q^2g^{\mu\nu})\Pi_{AA}^{(1)}(q^2)+q^\mu q^\nu\Pi_{AA}^{(0)}(q^2)\,. \qquad \text{(III.37)}$$

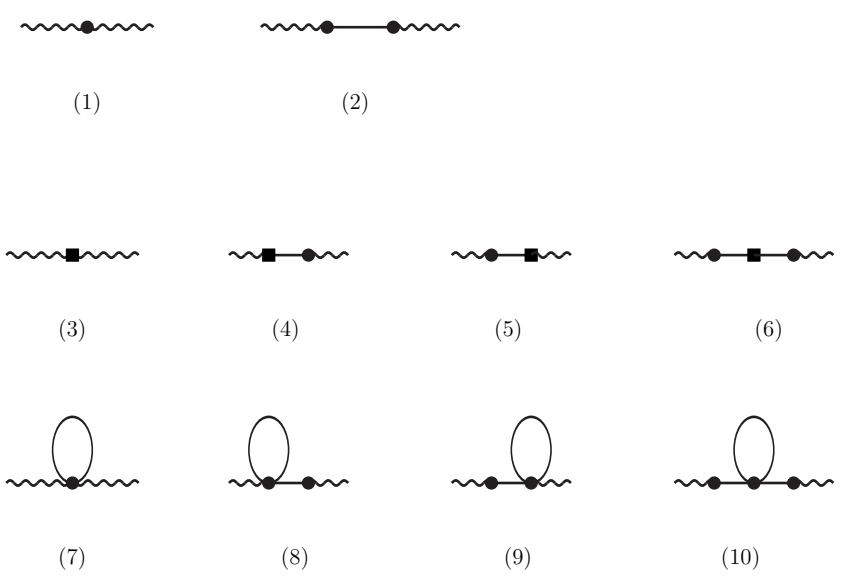

Figure III.2: The axial-vector two-point function at LO and NLO. The filled circle is a vertex from $\mathcal{L}_2$, The filled square is a vertex from $\mathcal{L}_4$, and the open square is a vertex from $\mathcal{L}_6$.

.

The diagrams contributing at LO are shown in (1–2) in Fig. III.2. The LO results are the same for all three cases. The result is

$$\Pi^{\mu\nu}_{AA}(q^2) = 2F\left(g^{\mu\nu} - q^\mu q^\nu \frac{1}{q^2 - M^2}\right) . \tag{III.38}$$

F and M are the LO decay constant and mass respectively. Note that in the massless limit this has only a transverse part as follows from the Ward identities.

The diagrams at NLO are (3–10) in Fig. III.2 and the NNLO diagrams are (11–48) in Fig. III.3.

Many of the diagrams are one-particle-reducible and at first sight have double and triple poles at $q^2 = M^2$. From general properties of field theory these should be resummable in into a single pole at the physical mass, $q^2 = M_M^2$ and a nonsingular part that only has cuts. The residue at the pole is the decay constant squared. We must thus find contributions that allow for the last term in (III.38) the lowest order F^2, M^2 to be replaced by F_M^2, M_M^2. It turns out to be advantageous to also do this in the first term. Most of the corrections are already included in this way.

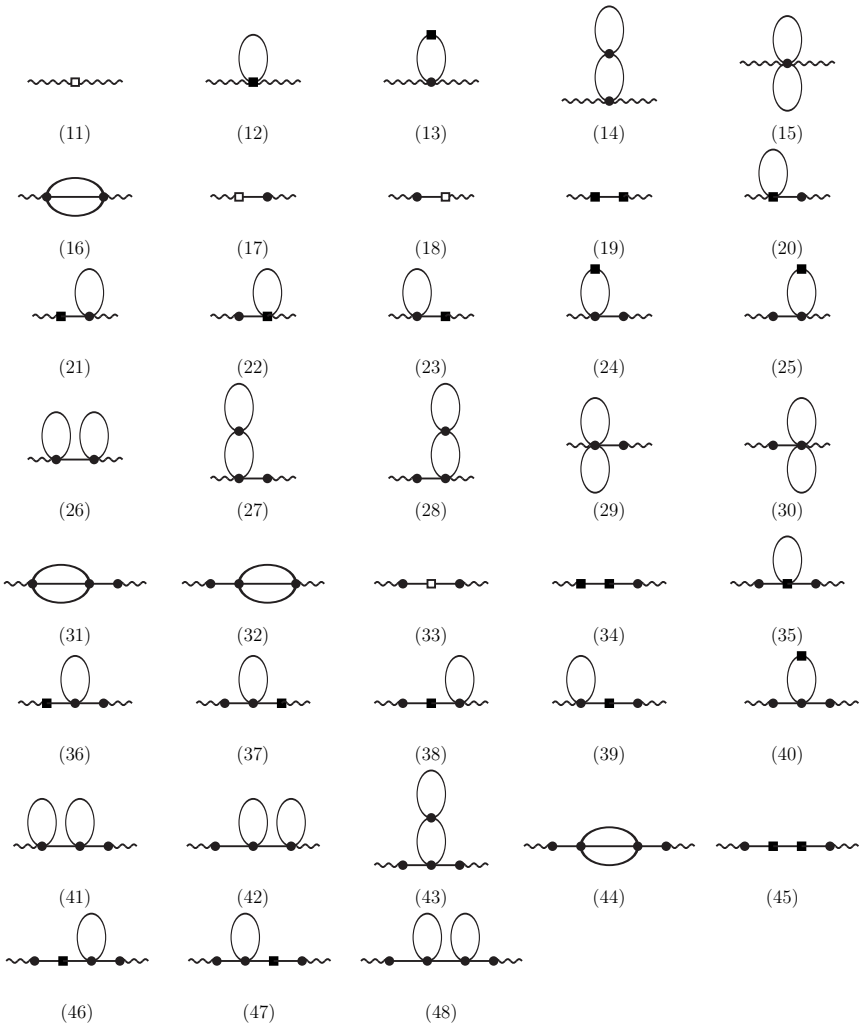

Figure III.3: The axial-vector two-point function at NNLO. The filled circle is a vertex from $\mathcal{L}_2$, the filled square is a vertex from $\mathcal{L}_4$, and the open square is a vertex from $\mathcal{L}_6$

At NLO the remaining part is only from the tree level diagram (3) in Fig. III.2 and is

$$\Pi_{AA}^{(1)} = 4L_{10}^r - 8H_1^r\,, \qquad \Pi_{AA}^{(0)} = 0\,. \tag{III.39}$$

So we can express our result up to NNLO as

$$\begin{aligned}\Pi^{\mu\nu}_{AA}(q^2) &= 2F_M^2\left(g^{\mu\nu}-q^\mu q^\nu\frac{1}{q^2-M_M^2}\right)+(q^\mu q^\nu-q^2g^{\mu\nu})(4L^r_{10}-8H^r_1)\\ &\quad+\frac{1}{F_M^2}\left[(q^\mu q^\nu-q^2g^{\mu\nu})\hat{\Pi}^{(1)}_{AA}(q^2)+q^\mu q^\nu\hat{\Pi}^{(0)}_{AA}(q^2)\right]. \qquad \text{(III.40)}\end{aligned}$$

The $\hat{\Pi}^{(0)}_{AA}(q^2)$ and $\hat{\Pi}^{(1)}_{AA}(q^2)$ are the remainders at NNLO and have no singularity at $q^2=M_M^2$.

The transverse part can be obtained from the part containing $g_{\mu\nu}$ as an overall factor. So the transverse part cannot come from the one-particle reducible diagrams and only gets contributions from diagrams (11–16) at NNLO. The sunset integrals H^F and H^F_{21} appearing in the results are defined in Appendix III.1.2.

The longitudinal part gets at NNLO contributions from all diagrams shown in Fig III.3. In order to rewrite the results into the single pole we need to expand the integrals around the mass. This introduces derivatives of the sunsetintegrals. These always show up in the combinations H^M and H^M_{21} defined in Appendix III.1.2.

Complex

$$\begin{aligned}\hat{\Pi}^{(1)}_{AA}(q^2) &= \frac{n^2}{2}\left[\frac{M_M^2}{q^2}H^F(M_M^2,M_M^2,M_M^2,q^2)-H^F_{21}(M_M^2,M_M^2,M_M^2,q^2)\right]\\ &\quad+M_M^2\left[\frac{L^2n^2}{6}-8nLL^r_{10}-32\,(K^r_{102}+K^r_{103}n+K^r_{17}+K^r_{18}n)\right]\\ &\quad-q^2(16K^r_{109}+8K^r_{115})-\frac{M_M^4}{q^2}\left(8K^r_{113}+\frac{3}{2}n^2L^2\right)\\ &\quad+\pi_{16}L\left[\frac{M_M^4}{q^2}\left(\frac{13n^2}{8}+\frac{2}{n^2}-\frac{2}{3}\right)+\frac{M_M^2}{6}n^2\right]\\ &\quad+\pi_{16}^2\left[\frac{M_M^4}{q^2}\left(\frac{7}{2n^2}-\frac{1}{8}n^2\pi^2-\frac{17n^2}{64}-\frac{7}{6}\right)\right.\\ &\quad\left.+M_M^2n^2\left(\frac{\pi^2}{36}+\frac{1}{72}\right)+\frac{n^2}{96}q^2\right], \qquad \text{(III.41)}\\ \hat{\Pi}^{(0)}_{AA}(q^2) &= \left[M_M^4\left(\frac{4}{3}-\frac{4}{n^2}\right)-\frac{M_M^6}{2q^2}n^2\right]H^M(M_M^2,M_M^2,M_M^2,q^2)\\ &\quad-\frac{3M_M^4}{2}n^2H^M_{21}(M_M^2,M_M^2,M_M^2,q^2)+\frac{8M_M^4}{q^2}K^r_{113}\end{aligned}$$

$$+\frac{M_M^4}{q^2}\left[\pi_{16}L\left(\frac{2}{3}-\frac{n^2}{8}-\frac{2}{n^2}\right)+\pi_{16}^2\left(\frac{7}{6}-\frac{15n^2}{64}-\frac{7}{2n^2}\right)\right], \quad \text{(III.42)}$$

Real

$$\begin{aligned}
\hat{\Pi}_{AA}^{(1)}(q^2) &= \frac{n}{2}(n+1)\left[\frac{M_M^2}{q^2}H^F(M_M^2,M_M^2,M_M^2,q^2)-H_{21}^F(M_M^2,M_M^2,M_M^2,q^2)\right]\\
&+M_M^2\left[\frac{L^2}{6}n(n+1)-8nLL_{10}^r-32(K_{102}^r+2nK_{103}^r+K_{17}^r+2nK_{18}^r)\right]\\
&-q^2(16K_{109}^r+8K_{115}^r)-\frac{M_M^4}{q^2}\left[8K_{113}^r+\frac{3}{2}n(n+1)L^2\right]\\
&+\pi_{16}L\left[\frac{M_M^4}{q^2}\left(\frac{13n^2}{8}+\frac{1}{2n^2}+\frac{43n}{24}-\frac{1}{2n}-\frac{1}{6}\right)+\frac{M_M^2}{6}n(n+1)\right]\\
&+\pi_{16}^2\left[\frac{M_M^4}{q^2}\left(-\frac{1}{8}n^2\pi^2-\frac{n\pi^2}{8}-\frac{17n^2}{64}+\frac{7}{8n^2}+\frac{5n}{192}-\frac{7}{8n}-\frac{7}{24}\right)\right.\\
&\left.+M_M^2n(n+1)\left(\frac{\pi^2}{36}+\frac{1}{72}\right)+\frac{n}{96}(n+1)q^2\right], \quad \text{(III.43)}
\end{aligned}$$

$$\begin{aligned}
\hat{\Pi}_{AA}^{(0)}(q^2) &= \left[-\frac{M_M^6}{q^2}\frac{n}{2}(n+1)+M_M^4(n-1)\left(\frac{1}{n^2}-\frac{1}{3}\right)\right]H^M(M_M^2,M_M^2,M_M^2,q^2)\\
&-\frac{3}{2}M_M^4n(n+1)H_{21}^M(M_M^2,M_M^2,M_M^2,q^2)+\frac{8M_M^4}{q^2}K_{113}^r\\
&+\pi_{16}\frac{M_M^4}{q^2}L\left(-\frac{n^2}{8}-\frac{1}{2n^2}-\frac{7n}{24}+\frac{1}{2n}+\frac{1}{6}\right)\\
&+\pi_{16}^2\frac{M_M^4}{q^2}\left(-\frac{15n^2}{64}-\frac{7}{8n^2}-\frac{101n}{192}+\frac{7}{8n}+\frac{7}{24}\right), \quad \text{(III.44)}
\end{aligned}$$

Pseudo − Real

$$\begin{aligned}
\hat{\Pi}_{AA}^{(1)}(q^2) &= \frac{n}{2}(n-1)\left[\frac{M_M^2}{q^2}H^F(M_M^2,M_M^2,M_M^2,q^2)-H_{21}^F(M_M^2,M_M^2,M_M^2,q^2)\right]\\
&-32M_M^2(K_{102}^r+2nK_{103}^r+K_{17}^r+2nK_{18}^r)-8q^2(2K_{109}^r+K_{115}^r)\\
&-\frac{8M_M^4}{q^2}K_{113}^r-\frac{M_M^4}{q^2}\frac{3n}{2}(n-1)L^2+\frac{M_M^2}{6}n(n-1)L^2-8M_M^2nLL_{10}^r\\
&+\pi_{16}\frac{LM_M^4}{q^2}\left(\frac{13n^2}{8}+\frac{1}{2n^2}-\frac{43n}{24}+\frac{1}{2n}-\frac{1}{6}\right)+\pi_{16}LM_M^2\left(\frac{n^2}{6}-\frac{n}{6}\right)\\
&+\pi_{16}^2\left[\frac{M_M^4}{q^2}\left(-\frac{1}{8}n^2\pi^2-\frac{17n^2}{64}+\frac{7}{8n^2}+\frac{n\pi^2}{8}-\frac{5n}{192}+\frac{7}{8n}-\frac{7}{24}\right)\right.\\
&\left.+M_M^2n(n-1)\left(\frac{\pi^2}{36}+\frac{1}{72}\right)+q^2\frac{n}{96}(n-1)\right], \quad \text{(III.45)}
\end{aligned}$$

$$\begin{aligned}\hat{\Pi}^{(0)}_{AA}(q^2) &= \left[-\frac{M_M^6}{q^2}\frac{n}{2}(n-1) - M_M^4(n+1)\left(\frac{1}{n^2}-\frac{1}{3}\right)\right] H^M(M_M^2, M_M^2, M_M^2, q^2) \\ &\quad -\frac{3}{2}M_M^4 n(n-1) H_{21}^M(M_M^2, M_M^2, M_M^2, q^2) + \frac{8M_M^4}{q^2}K_{113}^r \\ &\quad +\pi_{16}\frac{M_M^4}{q^2}L\left(-\frac{n^2}{8}-\frac{1}{2n^2}+\frac{7n}{24}-\frac{1}{2n}+\frac{1}{6}\right) \\ &\quad +\pi_{16}^2\frac{M_M^4}{q^2}\left(-\frac{15n^2}{64}-\frac{7}{8n^2}+\frac{101n}{192}-\frac{7}{8n}+\frac{7}{24}\right). \qquad \text{(III.46)}\end{aligned}$$

The axial two-point function is known in 3-flavour ChPT [23, 25]. We have checked that our result agrees with the one in [23] in the limit of equal masses.

III.3.4 The Scalar Two-Point Functions

The scalar two-point function is defined in (III.29), which contains the unbroken generator case ($T^a = Q^a$) and the singlet case ($a = 0$).

The Feynman diagrams for both cases are the same as those for the vector two-point function shown in Figure III.1 except that diagrams (2) and (5–7) are absent. Diagrams (1) and (3) are at NLO, and the diagrams (4) and (8–11) are at NNLO.

Q^a case

The scalar two-point functions are similar to the vector two-point functions, the LO results are zero for all the three cases since the vertex at LO is absent. We have rewritten again everything in terms of the physical mass and decay constant, M_M^2 and F_M. The results for the three cases are given below. The first line is the NLO contribution and the remainder is the NNLO contribution.

Complex

$$\begin{aligned}\Pi_{SS} &= B_0^2\left\{8H_2^r + 16L_8^r + \frac{1}{n}\left(n^2-4\right)\overline{B}(m^2,q^2)\right\} \\ &\quad +\frac{B_0^2}{F_M^2}\left\{q^2\left(8K_{113}^r + 32K_{47}^r\right) + M_M^2\left(192K_{25}^r + 64K_{26}^r n\right)\right. \\ &\quad\quad +M_M^2 L\left[\left(\frac{64}{n}-32n\right)L_8^r - 64L_7^r + \left(n^2-4\right)\frac{16}{n}L_5^r\right] \\ &\quad\quad \left.+\overline{B}(m^2,q^2)\left(n^2-4\right)\left[\frac{8q^2}{n}L_5^r + M_M^2\left(\frac{2}{n^2}L - 16L_4^r - \frac{32}{n}L_5^r - 32L_6^r + \frac{64}{n}L_8^r\right)\right]\right.\end{aligned}$$

$$+\overline{B}(m^2,q^2)^2\left(n^2-4\right)\left(\frac{q^2}{4}-\frac{2M_M^2}{n^2}\right)\Bigg\}, \tag{III.47}$$

Real

$$\begin{aligned}
\Pi_{SS} &= B_0^2\left\{8H_2^r+16L_8^r+\frac{1}{n}(n-1)(n+2)\,\overline{B}(m^2,q^2)\right\}\\
&+\frac{B_0^2}{F_M^2}\Bigg\{q^2\left(8K_{113}^r+32K_{47}^r\right)+M_M^2\left(192K_{25}^r+128nK_{26}^r\right)\\
&+M_M^2L\left[\left(\frac{32}{n}-32-32n\right)L_8^r-64L_7^r+(n-1)(n+2)\frac{16}{n}L_5^r\right]\\
&+\overline{B}(m^2,q^2)(n-1)(n+2)\left[\frac{8q^2}{n}L_5^r+M_M^2\left(\left(-\frac{1}{n}+\frac{1}{n^2}\right)L-32L_4^r\right.\right.\\
&\left.\left.-\frac{32}{n}L_5^r+64L_6^r+\frac{64}{n}L_8^r\right)\right]\\
&+\overline{B}(m^2,q^2)^2(n-1)(n+2)\left[\frac{q^2}{4}+M_M^2\left(\frac{1}{2n}-\frac{1}{n^2}\right)\right]\Bigg\},
\end{aligned} \tag{III.48}$$

Pseudo − Real

$$\begin{aligned}
\Pi_{SS} &= B_0^2\left\{8H_2^r+16L_8^r+\frac{1}{n}(n+1)(n-2)\,\overline{B}(m^2,q^2)\right\}\\
&+\frac{B_0^2}{F_M^2}\Bigg\{q^2\left(8K_{113}^r+32K_{47}^r\right)+M_M^2\left(192K_{25}^r+128nK_{26}^r\right)\\
&+M_M^2L\left[\left(\frac{32}{n}+32-32n\right)L_8^r-64L_7^r+(n+1)(n-2)\frac{16}{n}L_5^r\right]\\
&+\overline{B}(m^2,q^2)(n+1)(n-2)\left[\frac{8q^2}{n}L_5^r+M_M^2\left(\left(\frac{1}{n}+\frac{1}{n^2}\right)L-32L_4^r\right.\right.\\
&\left.\left.-\frac{32}{n}L_5^r+64L_6^r+\frac{64}{n}L_8^r\right)\right]\\
&+\overline{B}(m^2,q^2)^2(n+1)(n-2)\left[\frac{q^2}{4}+M_M^2\left(-\frac{1}{2n}-\frac{1}{n^2}\right)\right]\Bigg\}.
\end{aligned} \tag{III.49}$$

The definition of the one-loop function $\overline{B}(m^2,q^2)$ can be found in Appendix III.1.1.

Singlet case

We have also calculated the singlet case. This is the quark-antiquark combination that shows up in the mass term.

We write the expression up to NNLO as:

Complex

$$\begin{aligned}
\Pi^0_{SS} &= B_0^2\left\{8nH_2^r+32n^2L_6^r+16nL_8^r+2(n^2-1)\overline{B}(m^2,q^2)\right\}\\
&+\frac{B_0^2}{F_M^2}\left\{8q^2\left(nK_{113}^r+4nK_{47}^r+4n^2K_{48}^r\right)+192M_M^2\left(nK_{25}^r+n^2K_{26}^r+n^3K_{27}^r\right)\right.\\
&\quad+M_M^2L\left(n^2-1\right)\left(32nL_4^r+32L_5^r-64nL_6^r-64L_8^r\right)\\
&\quad+\overline{B}(m^2,q^2)\left(n^2-1\right)\left[16q^2\left(nL_4^r+L_5^r\right)\right.\\
&\qquad\left.\left.+M_M^2\left(\frac{4}{n}L+64\left(2L_8^r+2nL_6^r-L_5^r-nL_4^r\right)\right)\right]\right.\\
&\quad\left.+\overline{B}(m^2,q^2)^2\left(n^2-1\right)\left(nq^2-\frac{2M_M^2}{n}\right)\right\}, \qquad \text{(III.50)}
\end{aligned}$$

Real

$$\begin{aligned}
\Pi^0_{SS} &= B_0^2\left\{16nH_2^r+128n^2L_6^r+32nL_8^r+2(2n^2+n-1)\overline{B}(m^2,q^2)\right\}\\
&+\frac{B_0^2}{F_M^2}\left\{16q^2\left(nK_{113}^r+4nK_{47}^r+8n^2K_{48}^r\right)+384M_M^2\left(nK_{25}^r+2n^2K_{26}^r+4n^3K_{27}^r\right)\right.\\
&\quad+M_M^2L\left(2n^2+n-1\right)\left(64nL_4^r+32L_5^r-128nL_6^r-64L_8^r\right)\\
&\quad+\overline{B}(m^2,q^2)\left(2n^2+n-1\right)\left[16q^2\left(2nL_4^r+L_5^r\right)\right.\\
&\qquad\left.\left.+M_M^2\left(\left(-2+\frac{2}{n}\right)L+64(2L_8^r+4nL_6^r-L_5^r-2nL_4^r)\right)\right]\right.\\
&\quad\left.+\overline{B}(m^2,q^2)^2\left(2n^2+n-1\right)\left[nq^2+M_M^2\left(1-\frac{1}{n}\right)\right]\right\}, \qquad \text{(III.51)}
\end{aligned}$$

Pseudo − Real

$$\begin{aligned}
\Pi^0_{SS} &= B_0^2\left\{16nH_2^r+128n^2L_6^r+32nL_8^r+2(2n^2-n-1)\overline{B}(m^2,q^2)\right\}\\
&+\frac{B_0^2}{F_M^2}\left\{16q^2\left(nK_{113}^r+4nK_{47}^r+8n^2K_{48}^r\right)+384M_M^2\left(nK_{25}^r+2n^2K_{26}^r+4n^3K_{27}^r\right)\right.\\
&\quad\left.+M_M^2L\left(2n^2-n-1\right)\left(64nL_4^r+32L_5^r-128nL_6^r-64L_8^r\right)\right.
\end{aligned}$$

$$+\overline{B}(m^2,q^2)\left(2n^2-n-1\right)\left[16q^2\left(2nL_4^r+L_5^r\right)\right.$$
$$\left.+M_M^2\left(\left(2+\frac{2}{n}\right)L+64(2L_8^r+4nL_6^r-L_5^r-2nL_4^r)\right)\right]$$
$$+\overline{B}(m^2,q^2)^2\left(2n^2-n-1\right)\left[nq^2+M_M^2\left(-1-\frac{1}{n}\right)\right]\Bigg\}. \qquad \text{(III.52)}$$

We also written the result in term of physical M_M^2 and F_M. Notice that all loop diagrams are proportional to the number of Goldstone bosons in each case, i.e. n^2-1, $2n^2+n-1$, $2n^2-n-1$ for the complex, real and pseudo-real case respectively.

III.3.5 The Pseudo-Scalar Two-Point Functions

The pseudo-scalar two-point function is defined in (III.29). Just as in the case of the axial-vector two-point function there are one-particle-reducible diagrams. The diagrams are the same as those for the axial-vector two-point function with the axial-vector current replaced by a pseudo-scalar current. These are shown in Figure III.2 and III.3. There is also no vertex with two pseudo-scalar currents at LO so the equivalent of diagrams (1) and (7) in Figure III.2 and (13–15) in Figure III.3 vanish immediately. Just as in the scalar case, one should distinguish here between two cases: The adjoint case for the complex representation case which generalizes to the broken generators for the real and pseudo-real case, and the singlet operator with T^a in (III.28) the unit operator.

In Section III.3.3 we could simplify the final expressions very much by writing the final expression with the single pole at the meson mass in terms of the decay constant. The same happens here if we instead rewrite the result in terms of the meson pseudo-scalar decay constant G_M. So we first need to obtain that quantity to NNLO.

The meson pseudo-scalar decay constant G_M

The decay constant of the pseudoscalar density to the mesons, G_M is defined[4] similarly to F_M:

$$\langle 0|\bar{q}i\gamma_5 T^a q|\pi^b\rangle = \frac{1}{\sqrt{2}}\delta^{ab}G_M \qquad \text{(III.53)}$$

The calculation of G_M is very similar to F_M, the diagrams are exactly those shown in Figure 2 in [11] with one of the legs replaced by the pseudo-scalar

[4]The $\sqrt{2}$ is included in the definition to have the same normalization as [18].

current. There is here also a contribution from wave-function renormalization. In [11] we reported all the quantities M_M^2, F_M and $\langle\bar{q}q\rangle$ as an expansion in the bare or lowest order quantities F and $M^2 = 2B_0 m$. We therefore do the same here. We therefore use the quantity

$$L_0 = \frac{1}{16\pi^2}\log\frac{M^2}{F^2} \tag{III.54}$$

instead of L as in the other sections of this paper.

This quantity has been calculated to NLO in two-flavour ChPT in [18] and was called G_π there. We have checked that our NLO result agrees with theirs.

At leading order, all the three case have same expression:

$$G_M = G_0 = 2B_0 F\,. \tag{III.55}$$

We express the full results up to NNLO in terms of the LO meson mass M^2 and decay constant F as

$$G_M = 2B_0 F\left(1 + \frac{M^2}{F^2}\,a_G + \frac{M^4}{F^4}\,b_G\right) \tag{III.56}$$

At NLO and NNLO, the coefficients a_G and b_G are

Complex

$$\begin{aligned}
a_G &= \left(\frac{1}{n} - \frac{n}{2}\right)L_0 + 4(-nL_4^r - L_5^r + 4nL_6^r + 4L_8^r)\\
b_G &= -64(L_5^r + nL_4^r)(L_8^r + nL_6^r) + 24(L_5^r + nL_4^r)^2\\
&\quad -8n^2K_{22}^r + 48n^2K_{27}^r - 32K_{17}^r - 8K_{19}^r - 8K_{23}^r + 48K_{25}^r + 32K_{39}^r - 32nK_{18}^r\\
&\quad -8nK_{20}^r - 8nK_{21}^r + 48nK_{26}^r + 32nK_{40}^r\\
&\quad +L_0\Bigg[-(32 - 22n^2)\left(L_4^r + \frac{1}{n}L_5^r\right) + (4 - 8n^2)(L_1^r + 4L_6^r)\\
&\qquad + \left(\frac{80}{n} - 48n\right)L_8^r + \left(\frac{12}{n} - 10n\right)L_3^r - \left(8 + 2n^2\right)L_2^r + \left(\frac{12}{n} - 4n\right)L_0^r\Bigg]\\
&\quad +\pi_{16}\Bigg[(2 - n^2)\left(\frac{8}{n}L_8^r + 8L_6^r - \frac{4}{n}L_5^r - 4L_4^r - \frac{1}{n}L_3^r\right)\\
&\qquad + n^2L_2^r + 2L_1^r + 2\left(n - \frac{1}{n}\right)L_0^r\Bigg]\\
&\quad +\pi_{16}^2\left(\frac{113n^2}{256} - \frac{13}{24} + \frac{13}{8n^2}\right) - \pi_{16}L_0\left(\frac{55n^2}{96} - 1 + \frac{7}{2n^2}\right)\\
&\quad +L_0^2\left(\frac{3n^2}{16} - \frac{3}{2} + \frac{9}{2n^2}\right),
\end{aligned} \tag{III.57}$$

Real

$$
\begin{aligned}
a_G &= -\left(\frac{n}{2}+\frac{1}{2}-\frac{1}{2n}\right)L_0+(-8nL_4^r-4L_5^r+32nL_6^r+16L_8^r)\\
b_G &= -64(L_5^r+2nL_4^r)(L_8^r+2nL_6^r)+24(L_5^r+2nL_4^r)^2\\
&\quad -32K_{22}^r n^2+192K_{27}^r n^2-32K_{17}^r-8K_{19}^r-8K_{23}^r+48K_{25}^r+32K_{39}^r\\
&\quad -64K_{18}^r n-16K_{20}^r n-16K_{21}^r n+96K_{26}^r n+64K_{40}^r n\\
&\quad +L_0\Bigg[(-16+16n+22n^2)\left(2L_4^r+\frac{1}{n}L_5^r\right)+(4-8n-16n^2)L_1^r\\
&\qquad +16(1-3n-4n^2)L_6^r-\left(40-\frac{40}{n}+48n\right)L_8^r-\left(6-\frac{6}{n}+10n\right)L_3^r\\
&\qquad -\left(8+2n+4n^2\right)L_2^r-\left(6-\frac{6}{n}+4n\right)L_0^r\Bigg]\\
&\quad +\pi_{16}\Bigg[(1-n-n^2)\left(\frac{8}{n}L_8^r+16L_6^r-\frac{4}{n}L_5^r-8L_4^r-\frac{1}{n}L_3^r\right)\\
&\qquad +(n+2n^2)L_2^r+2L_1^r+\left(1-\frac{1}{n}+2n\right)L_0^r\Bigg]\\
&\quad +\pi_{16}^2\left(\frac{113n^2}{256}+\frac{443n}{768}-\frac{13}{96}-\frac{13}{32n}+\frac{13}{32n^2}\right)\\
&\quad -\pi_{16}L_0\left(\frac{55n^2}{96}+\frac{67n}{96}-\frac{3}{8}-\frac{5}{8n}+\frac{7}{8n^2}\right)\\
&\quad +L_0^2\left(\frac{3n^2}{16}+\frac{13n}{16}-\frac{1}{8}-\frac{3}{2n}+\frac{9}{8n^2}\right),
\end{aligned}
\tag{III.58}
$$

Pseudo − Real

$$
\begin{aligned}
a_G &= -L_0\left(\frac{n}{2}-\frac{1}{2}-\frac{1}{2n}\right)+(-8nL_4^r-4L_5^r+32nL_6^r+16L_8^r)\\
b_G &= -64(L_5^r+2nL_4^r)(L_8^r+2nL_6^r)+24(L_5^r+2nL_4^r)^2\\
&\quad -32K_{22}^r n^2+192K_{27}^r n^2-32K_{17}^r-8K_{19}^r-8K_{23}^r+48K_{25}^r\\
&\quad +32K_{39}^r-64K_{18}^r n-16K_{20}^r n-16K_{21}^r n+96K_{26}^r n+64K_{40}^r n\\
&\quad +L_0\Bigg[(-16-16n+22n^2)\left(2L_4^r+\frac{1}{n}L_5^r\right)+(4+8n-16n^2)L_1^r\\
&\qquad +16(1+3n-4n^2)L_6^r+\left(40+\frac{40}{n}-48n\right)L_8^r+\left(6+\frac{6}{n}-10n\right)L_3^r\\
&\qquad -\left(8-2n+4n^2\right)L_2^r+\left(6+\frac{6}{n}-4n\right)L_0^r\Bigg]
\end{aligned}
$$

$$
\begin{aligned}
&+\pi_{16}\left[(1+n-n^2)\left(\frac{8}{n}L_8^r+16L_6^r-\frac{4}{n}L_5^r-8L_4^r-\frac{1}{n}L_3^r\right)\right.\\
&\qquad\left.+(-n+2n^2)L_2^r+2L_1^r+\left(-1-\frac{1}{n}+2n\right)L_0^r\right]\\
&+\pi_{16}^2\left(\frac{113n^2}{256}-\frac{443n}{768}-\frac{13}{96}+\frac{13}{32n}+\frac{13}{32n^2}\right)\\
&-\pi_{16}L_0\left(\frac{55n^2}{96}-\frac{67n}{96}-\frac{3}{8}+\frac{5}{8n}+\frac{7}{8n^2}\right)\\
&+L_0^2\left(\frac{3n^2}{16}-\frac{13n}{16}-\frac{1}{8}+\frac{3}{2n}+\frac{9}{8n^2}\right). \qquad \text{(III.59)}
\end{aligned}
$$

X^a case

The pseudo-scale two point functions are similar to the axial-vector ones in the diagrams as described above. The LO result is the same for all the three cases:

$$\Pi_{PP}^a = -\frac{1}{2}\frac{G_0^2}{q^2-M^2}\,. \qquad \text{(III.60)}$$

The superscript "a" indicates the case with T^a in (III.28) an $SU(n)$ generator. For the real and pseudo-real case this is related by the conserved part of the symmetry group also to a number of diquark currents.

Subtracting the pole contribution in terms of the physical mass and decay constants, M_M^2, F_M and G_M, absorbs the major part of the higher order corrections. The final results are thus much simpler when written in this way. The remaining part at NLO is

$$\Pi_{PP}^a = B_0^2(8H_2^r-16L_8^r)\,. \qquad \text{(III.61)}$$

Thus we can define the full NNLO results as

$$\Pi_{PP}^a = -\frac{1}{2}\frac{G_M^2}{q^2-M_M^2}+B_0^2(8H_2^r-16L_8^r)+\frac{B_0^2}{F_M^2}\hat{\Pi}_{PP}^a\,, \qquad \text{(III.62)}$$

where the $\hat{\Pi}_{PP}$ is the remainder at NNLO. Its expression for the three different cases is:

Complex

$$
\begin{aligned}
\hat{\Pi}_{PP}^a \;=\;& -\frac{3}{2}n^2q^4H_{21}^M(M_M^2,M_M^2,M_M^2,q^2)\\
&+\left[\left(\frac{4}{3}-\frac{4}{n^2}\right)q^4-\frac{n^2}{2}M_M^2q^2\right]H^M(M_M^2,M_M^2,M_M^2,q^2)\\
&+8q^2K_{113}^r+64M_M^2(K_{17}^r+nK_{18}^r-K_{39}^r-nK_{40}^r)
\end{aligned}
$$

$$
\begin{aligned}
&+L^2M_M^2\left(-\frac{n^2}{2}-\frac{6}{n^2}+2\right)+LM_M^2\left(64L_6^r+32nL_8^r-\frac{64L_8^r}{n}\right)\\
&+\pi_{16}L\left[M_M^2\left(-\frac{8}{3}-\frac{n^2}{12}+\frac{8}{n^2}\right)+\left(\frac{2}{3}-\frac{n^2}{8}-\frac{2}{n^2}\right)q^2\right]\\
&+\pi_{16}^2\left[M_M^2\left(\frac{5}{3}-\frac{85n^2}{96}-\frac{5}{n^2}\right)+q^2\left(\frac{7}{6}-\frac{15n^2}{64}-\frac{7}{2n^2}\right)\right], \qquad \text{(III.63)}
\end{aligned}
$$

Real

$$
\begin{aligned}
\hat{\Pi}_{PP}^a \;=\;& -\frac{3}{2}q^4n(n+1)H_{21}^M(M_M^2,M_M^2,M_M^2,q^2)\\
&+\left[\left(-\frac{1}{n^2}-\frac{n}{3}+\frac{1}{n}+\frac{1}{3}\right)q^4-\frac{1}{2}M_M^2q^2n\,(n+1)\right]H^M(M_M^2,M_M^2,M_M^2,q^2)\\
&+8q^2K_{113}^r+64M_M^2(K_{17}^r+2nK_{18}^r-K_{39}^r-2nK_{40}^r)\\
&+M_M^2L^2\left(-\frac{n^2}{2}-\frac{3}{2n^2}-n+\frac{3}{2n}+\frac{1}{2}\right)+32M_M^2L\left(2L_6^r+L_8^rn-\frac{L_8^r}{n}+L_8^r\right)\\
&+\pi_{16}L\left[M_M^2\left(-\frac{n^2}{12}+\frac{2}{n^2}+\frac{7n}{12}-\frac{2}{n}-\frac{2}{3}\right)+q^2\left(-\frac{n^2}{8}-\frac{1}{2n^2}-\frac{7n}{24}+\frac{1}{2n}+\frac{1}{6}\right)\right]\\
&+\pi_{16}^2\left[M_M^2\left(-\frac{85n^2}{96}-\frac{5}{4n^2}-\frac{125n}{96}+\frac{5}{4n}+\frac{5}{12}\right)\right.\\
&\left.\quad+q^2\left(-\frac{15n^2}{64}-\frac{7}{8n^2}-\frac{101n}{192}+\frac{7}{8n}+\frac{7}{24}\right)\right], \qquad \text{(III.64)}
\end{aligned}
$$

Pseudo − Real

$$
\begin{aligned}
\hat{\Pi}_{PP}^a \;=\;& \frac{3}{2}q^4n(1-n)H_{21}^M(M_M^2,M_M^2,M_M^2,q^2)\\
&+\left[\left(-\frac{1}{n^2}+\frac{n}{3}-\frac{1}{n}+\frac{1}{3}\right)q^4+\frac{1}{2}M_M^2q^2n(1-n)\right]H^M(M_M^2,M_M^2,M_M^2,q^2)\\
&+8q^2K_{113}^r+64M_M^2(K_{17}^r+2nK_{18}^r-K_{39}^r-2nK_{40}^r)\\
&+M_M^2L^2\left(-\frac{n^2}{2}-\frac{3}{2n^2}+n-\frac{3}{2n}+\frac{1}{2}\right)+M_M^2L\left[64L_6^r+32\left(n-\frac{1}{n}-1\right)L_8^r\right]\\
&+\pi_{16}L\left[M_M^2\left(-\frac{n^2}{12}+\frac{2}{n^2}-\frac{7n}{12}+\frac{2}{n}-\frac{2}{3}\right)+q^2\left(-\frac{n^2}{8}-\frac{1}{2n^2}+\frac{7n}{24}-\frac{1}{2n}+\frac{1}{6}\right)\right]\\
&+\pi_{16}^2\left[M_M^2\left(-\frac{85n^2}{96}-\frac{5}{4n^2}+\frac{125n}{96}-\frac{5}{4n}+\frac{5}{12}\right)\right.\\
&\left.\quad+\left(-\frac{15n^2}{64}-\frac{7}{8n^2}+\frac{101n}{192}-\frac{7}{8n}+\frac{7}{24}\right)q^2\right]. \qquad \text{(III.65)}
\end{aligned}
$$

The loop integrals H^M and H_{21}^M are defined in Appendix III.1.2.

Singlet case

In the singlet case with $a = 0$, there is no contribution with poles. Only the one-particle-irreducible diagrams contribute. As a consequence, there is no order p^2 contribution and at order p^4 there is only a tree level contribution from the equivalent of diagram (3) in Figure III.2. At order p^6 or NNLO only the one-particle-irreducible diagrams contribute and since there is no order p^2 vertex with two pseudo-scalar currents only diagram (11–12) and (16) in Figure III.3 contribute.

Since there is no single pole contribution, there is also no need here to expand in the integrals around the meson mass. The integral H^F is defined in Appendix III.1.2.

The singlet pseudo-scalar two-point function we write as

$$\Pi^0_{PP} = B_0^2 \overline{\Pi}^0_{PP} + \frac{B_0^2}{F_M^2} \hat{\Pi}^0_{PP} \,. \tag{III.66}$$

The results for the three cases are

Complex :

$$\begin{aligned}
\overline{\Pi}^0_{PP} &= 8nH_2^r - 16nL_8^r - 32n^2L_7^r \,, \\
\hat{\Pi}^0_{PP} &= -\frac{2}{3n}\left(n^2-1\right)\left(n^2-4\right) H^F(M_M^2, M_M^2, M_M^2, q^2) \\
&\quad + q^2\left(8K_{113}^r n - 32K_{46}^r n^2\right) - 64M_M^2\left(K_{39}^r n + K_{40}^r n^2 + K_{41}^r n^2 + K_{42}^r n^3\right) \\
&\quad + L^2 M_M^2 \frac{1}{n}\left(n^2-1\right)\left(n^2-4\right) + 64LM_M^2(n^2-1)(nL_7^r + L_8^r) \\
&\quad + M_M^2 \pi_{16}^2 \frac{1}{n}\left(n^2-1\right)\left(n^2-4\right)\left(\frac{\pi^2}{6}+1\right) \,,
\end{aligned} \tag{III.67}$$

Real :

$$\begin{aligned}
\overline{\Pi}^0_{PP} &= 16nH_2^r - 128n^2L_7^r - 32nL_8^r \,, \\
\hat{\Pi}^0_{PP} &= -\frac{2}{3n}\left(2n^2+n-1\right)\left(n^2+n-2\right) H^F(M_M^2, M_M^2, M_M^2, q^2) \\
&\quad + q^2\left(16K_{113}^r n - 128K_{46}^r n^2\right) - 128M_M^2\left(nK_{39}^r + 2n^2K_{40}^r + 2n^2K_{41}^r + 4n^3K_{42}^r\right) \\
&\quad + L^2 M_M^2 \frac{1}{n}\left(2n^2+n-1\right)\left(n^2+n-2\right) + 64M_M^2 L(2n^2+n-1)(2nL_7^r + L_8^r) \\
&\quad + M_M^2 \pi_{16}^2 \frac{1}{n}\left(2n^2+n-1\right)\left(n^2+n-2\right)\left(\frac{\pi^2}{6}+1\right) \,,
\end{aligned} \tag{III.68}$$

Pseudo − Real :

$$\begin{aligned}
\overline{\Pi}^0_{PP} &= 16nH_2^r - 128n^2L_7^r - 32nL_8^r \,, \\
\hat{\Pi}^0_{PP} &= -\frac{2}{3n}\left(2n^2-n-1\right)\left(n^2-n-2\right) H^F(M_M^2, M_M^2, M_M^2, q^2)
\end{aligned}$$

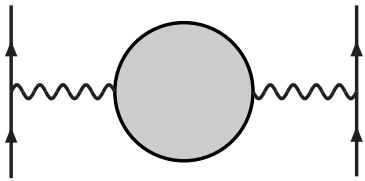

Figure III.4: The one-loop oblique correction to LEP process $e^+ + e^- \to q + \bar{q}$.

$$+q^2\left(16K^r_{113}n - 128K^r_{46}n^2\right) - 128M_M^2\left(nK^r_{39} + 2n^2K^r_{40} + 2n^2K^r_{41} + 4n^3K^r_{42}\right)$$
$$+L^2M_M^2\frac{1}{n}\left(2n^2-n-1\right)\left(n^2-n-2\right) + 64M_M^2L(2n^2-n-1)(2nL^r_7 + L^r_8)$$
$$+M_M^2\pi_{16}^2\frac{1}{n}\left(2n^2-n-1\right)\left(n^2-n-2\right)\left(\frac{\pi^2}{6}+1\right). \qquad \text{(III.69)}$$

Notice that just as for the scalar singlet two-point function, all loop contributions are proportional to the number of Goldstone bosons.

III.3.6 Large n

As one can see from all the explicit formulas, many of the expressions become equal for the different cases in the large n limit .

III.4 The Oblique Corrections and S-parameter

III

The physical process at the CERN LEP collider is $e^+ + e^- \to q + \bar{q}$. There are three types of one loop correction to this process: vacuum polarization corrections, vertex corrections, and box corrections. The vacuum polarization contribution is independent of the external fermions and it dominates the contributions from physics beyond SM. For the light fermions, the other two corrections are suppressed by factor of m_f^2/m_Z^2. That's why the vacuum polarization corrections are called "oblique corrections,", and the vertex and box corrections are called "nonoblique corrections."

The oblique polarization only affect the gauge bosons propagators and their mixing. The vacuum polarization amplitude can be defined as

$$g^{\mu\nu}\Pi_{XY} + (q^\mu q^\nu \text{ terms}) = i\int d^4x\, e^{iq\cdot x}\,\langle 0|T(J^\mu_X(x)J^\nu_Y(0))|0\rangle\,. \qquad \text{(III.70)}$$

The influence of new physics to the oblique corrections can be summarized to three parameters: S, T and U. One can find their definition in Ref. [15]. These parameters are chosen to be zero at a reference point in the SM. In the

past 20 years, they have been studied intensively in many models beyond the Standard Model physics.

For a beyond the Standard Model with strong dynamics at the TeV scale, there will in general be many resonances and other nonperturbative effects. At low momenta one can use the EFT as described above for these cases. In this paper, we will estimate the S parameter contribution from pseudo-Goldstone Boson sector within the EFT. The parameter T and U vanish because of the exact flavor symmetry, i.e. we work in the equal mass case.

The S parameter can be written as[5] [15]

$$S = -2\pi\left[\Pi'_{VV}(0) - \Pi'_{AA}(0)\right] = 2\pi\frac{d}{dq^2}\left(q^2\Pi^{(1)}_{VV} - q^2\Pi^{(1)}_{AA}\right)_{q^2=0}. \qquad \text{(III.71)}$$

$\Pi'_{VV}(0)$ and $\Pi'_{AA}(0)$ are the derivatives of the vector and axial-vector two-point functions at $q^2 = 0$. One should keep in mind that S is defined to be zero at a particular place in the standard model, as discussed at the end of section V in [15]. Our formulas are the equivalent of (5.12) in that reference.

The result can be written as

$$S = \overline{S} + \frac{\pi M_M^2}{F_M^2}\hat{S}, \qquad \text{(III.72)}$$

with

$$\begin{aligned}
&\textbf{Complex}: \\
\overline{S} &= -16\pi L^r_{10} - \frac{2n\pi}{3}(L+\pi_{16}), \\
\hat{S} &= 64\,(K^r_{102} - K^r_{81} + K^r_{17} + nK^r_{103} - nfK^r_{82} + nK^r_{18}) + \frac{n^2}{3}L^2 \\
&\quad +16n\,(L^r_9 + 2L^r_{10})\,L - \pi_{16}\frac{11n^2}{9}L + \pi^2_{16}n^2\left(\frac{85}{108} - \frac{5}{27}\tilde{\psi}\right) \qquad \text{(III.73)} \\
&\textbf{Real}: \\
\overline{S} &= -16\pi L^r_{10} - \frac{2(n+1)\pi}{3}(L+\pi_{16}), \\
\hat{S} &= 64\,(K^r_{102} - K^r_{81} + K^r_{17} + 2nK^r_{103} - 2nfK^r_{82} + 2nK^r_{18}) + \frac{n(n+1)}{3}L^2 \\
&\quad +16\,[(n+1)L^r_9 + (2n+1)L^r_{10}]\,L - \pi_{16}\frac{11n(n+1)}{9}L \\
&\quad +\pi^2_{16}n(n+1)\left(\frac{85}{108} - \frac{5}{27}\tilde{\psi}\right), \qquad \text{(III.74)} \\
&\textbf{Pseudo}-\textbf{real}: \\
\overline{S} &= -16\pi L^r_{10} - \frac{2(n-1)\pi}{3}(L+\pi_{16}),
\end{aligned}$$

[5] Our two point functions are normalized differently from those in [15].

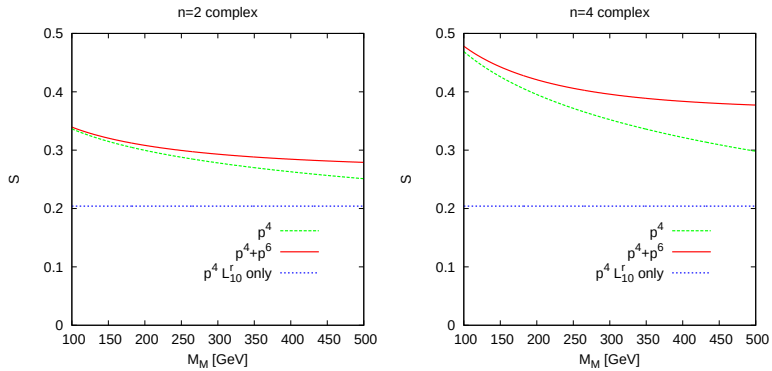

Figure III.5: The S-parameter for the values of L_9^r and L_{10}^r given in the text for the complex case. (a) $n = 2$ (b) $n = 4$.

$$\begin{aligned}\hat{S} &= 64\,(K_{102}^r - K_{81}^r + K_{17}^r + 2nK_{103}^r - 2nfK_{82}^r + 2nK_{18}^r) + \frac{n(n-1)}{3}L^2 \\ &\quad +16\,[(n-1)L_9^r + (2n-1)L_{10}^r]\,L - \pi_{16}\frac{11n(n-1)}{9}L \\ &\quad +\pi_{16}^2 n(n-1)\left(\frac{85}{108} - \frac{5}{27}\tilde{\psi}\right). \end{aligned} \tag{III.75}$$

The quantity $\tilde{\psi}$ is

$$\tilde{\psi} = 6\sqrt{3}\mathrm{Cl}_2\left(\frac{2\pi}{3}\right) = 7.0317217160684\,. \tag{III.76}$$

The real purpose of (III.73)-(III.75) is to be able to study the S-parameter in more general theories than just scaling up from QCD. However to provide some feeling about numerical results we choose parameters as if they are scaled up from QCD/ChPT. We change $F_\pi = 0.0922$ MeV to $F_M = 243$ GeV and the subtraction scale from 0.77 GeV to 2 TeV. We set the $K_i^r = 0$ and keep $L_9^r = 0.00593$ and $L_{10}^r = -0.00406$ at their values from ChPT [26, 27].

In Figures III.5, III.6 and III.7 we have shown the results for our three cases complex, real and pseudo-real for $n = 2$ and $n = 4$. Shown are the full p^4 and p^6 contributions as well as the p^4 part proportional to L_{10}^r only. The latter is what is the usual contribution to S corrected for the pieces that go into the reference point at p^4. We cannot do the same for the full result since that depends on how one treats the extra pseudo-Goldstone bosons that occur in the other models.

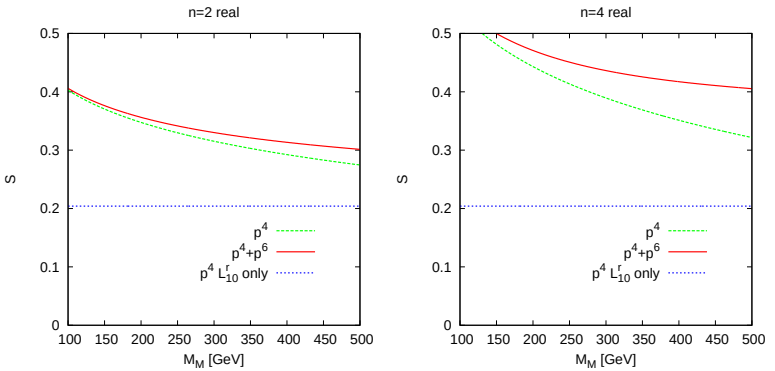

Figure III.6: The S-parameter for the values of L_9^r and L_{10}^r given in the text for the real case. (a) $n = 2$ (b) $n = 4$.

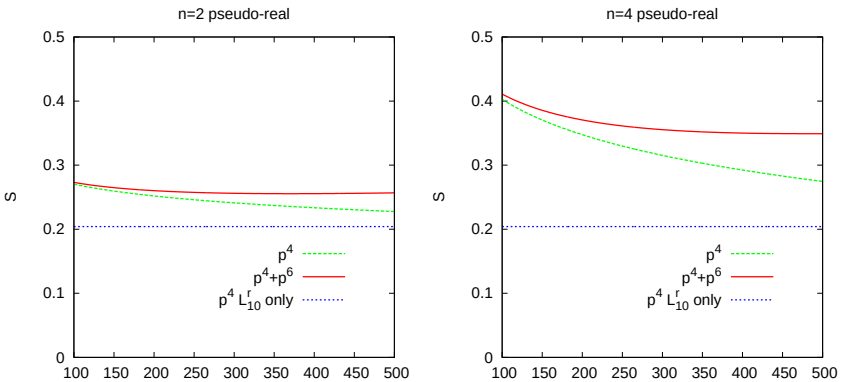

Figure III.7: The S-parameter for the values of L_9^r and L_{10}^r given in the text for the pseudo-real case. (a) $n = 2$ (b) $n = 4$.

III.5 Conclusion

In this paper, we have calculated the two-point correlation functions of vector, axial-vector, scalar and pseudo-scalar currents for QCD-like theories.

In the beginning of the paper, we gave a very brief overview of the QCD-like theories and their EFT treatment as developed earlier.

We then gave the analytic results of those two-point functions up to NNLO. The results are significantly shortened by using the physical meson mass M_M^2

and decay constants F_M and G_M when rewriting the pole contributions.

The main use of these formulas is expected to be in extrapolations to zero fermion mass of technicolour related lattice calculations. We have therefore also included precisely the combination needed for the S-parameter.

Acknowledgments

This work is supported in part by the European Community-Research Infrastructure Integrating Activity "Study of Strongly Interacting Matter" (HadronPhysics2, Grant Agreement n. 227431) and the Swedish Research Council grants 621-2008-4074 and 621-2010-3326. This work used FORM [28].

III.A Loop integrals

We use dimensional regularization and $\overline{MS}$ scheme to evaluate the loop integrals, $d = 4 - 2\epsilon$.

III.A.1 One-loop integrals

The loop integral with one propagator is

$$\begin{aligned} A(m^2) &= \frac{1}{i}\int \frac{d^dq}{(2\pi)^d}\frac{1}{q^2-m^2} \\ &= \frac{m^2}{16\pi^2}\left\{\lambda_0 - \ln(m^2) + \epsilon\left[\frac{C^2}{2}+\frac{1}{2}+\frac{\pi^2}{12}+\frac{1}{2}\ln^2(m^2) - C\ln(m^2)\right]\right\} \\ &\quad +\mathcal{O}(\epsilon^2)\,. \end{aligned} \tag{III.77}$$

Here

$$C = \ln(4\pi) + 1 - \gamma \qquad\qquad \lambda_0 = \frac{1}{\epsilon} + C$$

The extra $+1$ in C is the ChPT version of $\overline{MS}$.

The loop integrals with two propagators are

$$\begin{aligned} B(m_1^2,m_2^2,p^2) &= \frac{1}{i}\int \frac{d^dq}{(2\pi)^d}\frac{1}{(q^2-m_1^2)((q-p)^2-m_2^2)}\,, \\ B^\mu(m_1^2,m_2^2,p) &= \frac{1}{i}\int \frac{d^dq}{(2\pi)^d}\frac{q^\mu}{(q^2-m_1^2)((q-p)^2-m_2^2)} \\ &= p^\mu B_1(m_1^2,m_2^2,p^2)\,, \\ B^{\mu\nu}(m_1^2,m_2^2,p) &= \frac{1}{i}\int \frac{d^dq}{(2\pi)^d}\frac{q^\mu q^\nu}{(q^2-m_1^2)((q-p)^2-m_2^2)} \\ &= p^\mu p^\nu B_{21}(m_1^2,m_2^2,p^2) + g^{\mu\nu}B_{22}(m_1^2,m_2^2,p^2)\,. \end{aligned} \tag{III.78}$$

The two last integrals can be reduced to simpler integrals A and B via

$$\begin{aligned} B_1(m^2,m^2,p^2) &= \frac{1}{2}B(m_1^2,m_2^2,p^2)\,, \\ B_{22}(m^2,m^2,p^2) &= \frac{1}{2(d-1)}\left[A(m^2)+\left(2m^2-\frac{1}{2}p^2\right)B(m^2,m^2,p^2)\right], \\ B_{21}(m^2,m^2,p^2) &= \frac{1}{p^2}\left[A(m^2)+m^2B(m^2,m^2,p^2)-dB_{22}(m^2,m^2,p^2)\right] \end{aligned} \tag{III.79}$$

We quote here only the equal mass case results relevant for this paper. The explicit expression for B is

$$\begin{aligned} B(m^2,m^2,p^2) &= \frac{1}{16\pi^2}\lambda_0+\overline{B}(m^2,p^2)+\mathcal{O}(\epsilon)\,, \\ \overline{B}(m^2,p^2) &= \frac{1}{16\pi^2}\left(-1-m^2\log\frac{m^2}{\mu^2}\right)+\bar{J}(m_2,p^2)\,, \\ \bar{J}(m^2,p^2) &= -\frac{1}{16\pi^2}\int_0^1 dx\ln\left(\frac{m^2-x(1-x)p^2}{m^2}\right), \end{aligned} \tag{III.80}$$

The function $\bar{J}(m^2,p^2)$ is

$$\begin{aligned} \bar{J}(m^2,p^2) &= \begin{cases} 2+\sigma\ln\left(\frac{\sigma-1}{\sigma+1}\right), & p^2<0, \\ 2-2\sqrt{\frac{4}{x}-1}\cdot\operatorname{arccot}\left(\sqrt{\frac{4}{x}-1}\right), & 0\le p^2<4m^2, \\ 2+\sigma\ln\left(\frac{1-\sigma}{1+\sigma}\right)+i\pi\sigma, & p^2>4m^2, \end{cases} \\ &\sigma(x)=\sqrt{1-\frac{4}{x}}, \quad x=\frac{m^2}{p^2}\notin[0,4]. \end{aligned} \tag{III.81}$$

Taking derivatives w.r.t. p^2 at $p^2=0$ is most easily done in the form with the Feynman parameter integration explicit.

III.A.2 Sunset integrals

The sunset integrals are done with the methods of [23, 29]. They are defined as

$$\langle\langle X\rangle\rangle = \frac{1}{i^2}\int\frac{d^dq}{(2\pi)^d}\frac{d^dr}{(2\pi)^d}\frac{X}{\left(q^2-m_1^2\right)\left(r^2-m_2^2\right)\left[(q+r-p)^2-m_3^2\right]}\,, \tag{III.82}$$

The various sunset integrals with Lorenz indices are

$$\begin{aligned} H(m_1^2,m_2^2,m_3^2;p^2) &= \langle\langle 1\rangle\rangle\,, \\ H^\mu(m_1^2,m_2^2,m_3^2;p^2) &= \langle\langle q^\mu\rangle\rangle = p^\mu H_1(m_1^2,m_2^2,m_3^2;p^2)\,, \\ H^{\mu\nu}(m_1^2,m_2^2,m_3^2;p^2) &= \langle\langle q^\mu q^\nu\rangle\rangle \\ &= p^\mu p^\nu H_{21}(m_1^2,m_2^2,m_3^2;p^2)+g^{\mu\nu}H_{22}(m_1^2,m_2^2,m_3^2;p^2)\,. \end{aligned} \tag{III.83}$$

and

$$\begin{aligned}
\langle\langle r^\mu \rangle\rangle &= p^\mu H_1(m_2^2, m_1^2, m_3^2; p^2)\,, \\
\langle\langle r^\mu r^\nu \rangle\rangle &= p^\mu p^\nu H_{21}(m_2^2, m_1^2, m_3^2; p^2) + g^{\mu\nu} H_{22}(m_2^2, m_1^2, m_3^2; p^2)\,, \\
\langle\langle q^\mu r^\nu \rangle\rangle &= \langle\langle r^\mu q^\nu \rangle\rangle\,, \\
\langle\langle q^\mu r^\nu \rangle\rangle &= p^\mu p^\nu H_{23}(m_1^2, m_2^2, m_3^2; p^2) + g^{\mu\nu} H_{24}(m_1^2, m_2^2, m_3^2; p^2)\,, \qquad \text{(III.84)}
\end{aligned}$$

The function H is fully symmetric in m_1^2, m_2^2 and m_3^2, while H_1, H_{21} and H_{22} are symmetric under the interchange of m_2^2 and m_3^2. The relation between the above 3 functions

$$\begin{aligned}
p^2 H_{21}(m_1^2, m_2^2, m_3^2; p^2) + d H_{22}(m_1^2, m_2^2, m_3^2; p^2) = \\
m_1^2 H(m_1^2, m_2^2, m_3^2; p^2) + A(m_2^2) A(m_3^2)\,, \qquad \text{(III.85)}
\end{aligned}$$

allows to express H_{22} in terms of H_{21}.

Similar to the integral B and B_1, there is also a relation between H and H_1 which in the equal mass case becomes

$$H_1(m^2, m^2, m^2; p^2) = \frac{1}{3} H(m^2, m^2, m^2; p^2)\,. \qquad \text{(III.86)}$$

The other functions, H_{23} and H_{23}, can be written in term of H, H_1 and H_{21} by using relations derived from redefining the momenta and masses in its definition [23].

The full sunset integral expressions and the definition for finite part $H_i^F = \{H^F, H_1^F, H_{21}^F\}$ can be found in the appendix of [23]. In our case we take $m_1 = m_2 = m_3 = m$.

In order to eliminate the extra poles in the expressions, sometimes we need to expand the $H_i^F(m^2, m^2, m^2; q^2)$ around the pseudoscalar mass m^2, and we define

$$\begin{aligned}
H_i^M(m^2, m^2, m^2; q^2) &= \frac{1}{(q^2 - m^2)^2} \Big[H_i^F(m^2, m^2, m^2; q^2) - H_i^F(m^2, m^2, m^2; m^2) \\
&\quad - (q^2 - m^2) H_i^{F\prime}(m^2, m^2, m^2; m^2) \Big]\,, \qquad \text{(III.87)}
\end{aligned}$$

where

$$H_i^{F\prime}(m^2, m^2, m^2; m^2) = \left. \frac{\partial H_i^F(m^2, m^2, m^2; q^2)}{\partial q^2} \right|_{q^2 = m^2}\,. \qquad \text{(III.88)}$$

III References

[1] M. E. Peskin, "The Alignment Of The Vacuum In Theories Of Technicolor," *Nucl. Phys.* (1980) 197. pages

[2] J. Preskill, "Subgroup Alignment In Hypercolor Theories," *Nucl. Phys.* (1981) 21. pages

[3] S. Dimopoulos, "Technicolored Signatures," *Nucl. Phys.* (1980) 69. pages

[4] J. B. Kogut, M. A. Stephanov, D. Toublan, J. J. M. Verbaarschot and A. Zhitnitsky, "QCD-like theories at finite baryon density," *Nucl. Phys.* (2000) 477, arXiv:hep-ph/0001171. pages

[5] Y. I. Kogan, M. A. Shifman and M. I. Vysotsky, "Spontaneous Breaking Of Chiral Symmetry For Real Fermions And N=2 Susy Yang-Mills Theory," *Sov. J. Nucl. Phys.* **42** (1985) 318. pages

[6] H. Leutwyler and A. V. Smilga, "Spectrum of Dirac operator and role of winding number in QCD," *Phys. Rev. D* **46** (1992) 5607. pages

[7] A. V. Smilga and J. J. M. Verbaarschot, "Spectral Sum Rules And Finite Volume Partition Function In Gauge Theories With Real And Pseudoreal Fermions," *Phys. Rev. D* **51** (1995) 829, arXiv:hep-th/9404031. pages

[8] J. Gasser, H. Leutwyler, "Chiral Perturbation Theory: Expansions In The Mass Of The Strange Quark," *Nucl. Phys.* (1985) 465. pages

[9] J. Gasser and H. Leutwyler, "Light Quarks at Low Temperatures," *Phys. Lett.* (1987) 83. pages

[10] K. Splittorff, D. Toublan and J. J. M. Verbaarschot, "Diquark condensate in QCD with two colors at next-to-leading order," *Nucl. Phys.* (2002) 290, arXiv:hep-ph/0108040. pages

[11] J. Bijnens, J. Lu, "Technicolor and other QCD-like theories at next-to-next-to-leading order," *JHEP* **0911** (2009) 116, arXiv:0910.5424. pages

[12] J. Bijnens and J. Lu, "Meson-meson Scattering in QCD-like Theories," *JHEP* **1103** (2011) 028, arXiv:1102.0172. pages

[13] C. T. Hill, E. H. Simmons, "Strong dynamics and electroweak symmetry breaking," *Phys. Rep.* **381** (2003) 235–402, arXiv:hep-ph/0203079. pages

[14] F. Sannino, "Conformal Dynamics for TeV Physics and Cosmology," *Acta Phys. Polon.* (2009) 3533–3743, arXiv:0911.0931. pages

[15] M. E. Peskin, T. Takeuchi, "Estimation of oblique electroweak corrections," *Phys. Rev. D* **46** (1992) 381–409. pages

[16] G. Altarelli, R. Barbieri, "Vacuum polarization effects of new physics on electroweak processes," *Phys. Lett.* (1991) 161–167. pages

[17] S. Weinberg, "Phenomenological Lagrangians," *Physica A* **96** (1979) 327. pages

[18] J. Gasser, H. Leutwyler, "Chiral Perturbation Theory To One Loop," *Annals Phys.* **158** (1984) 142. pages

[19] S. R. Coleman, J. Wess and B. Zumino, "Structure of phenomenological Lagrangians. 1," *Phys. Rev.* **177** (1969) 2239. pages

[20] S. R. Coleman, J. Wess and B. Zumino, "Structure of phenomenological Lagrangians. 2," *Phys. Rev.* **177** (1969) 2247. pages

[21] J. Bijnens, G. Colangelo and G. Ecker, "The mesonic chiral Lagrangian of order p^6," *JHEP* **9902** (1999) 020, `arXiv:hep-ph/9902437`. pages

[22] J. Bijnens, G. Colangelo and G. Ecker, "Renormalization of chiral perturbation theory to order p^6," *Annals Phys.* **280** (2000) 100, `arXiv:hep-ph/9907333`. pages

[23] G. Amoros, J. Bijnens, P. Talavera, "Two point functions at two loops in three flavor chiral perturbation theory," *Nucl. Phys.* (2000) 319–363, `arXiv:hep-ph/9907264`. pages

[24] E. Golowich, J. Kambor, "Two loop analysis of vector current propagators in chiral perturbation theory," *Nucl. Phys.* (1995) 373–404, `arXiv:hep-ph/9501318`. pages

[25] E. Golowich and J. Kambor, "Two loop analysis of axial vector current propagators in chiral perturbation theory," *Phys. Rev. D* **58** (1998) 036004, `arXiv:hep-ph/9710214`. pages

[26] J. Bijnens and P. Talavera, "Pion and kaon electromagnetic form-factors," *JHEP* **0203** (2002) 046, `arXiv:hep-ph/0203049`. pages

[27] M. Gonzalez-Alonso, A. Pich, J. Prades, "Determination of the Chiral Couplings L(10) and C(87) from Semileptonic Tau Decays," *Phys. Rev. D* **78** (2008) 116012, `arXiv:0810.0760`. pages

[28] J. A. M. Vermaseren, "New features of FORM," `arXiv:math-ph/0010025`. pages

[29] J. Gasser, M. E. Sainio, "Two loop integrals in chiral perturbation theory," *Eur. Phys. J.* (1998) 297–306, `arXiv:hep-ph/9803251`. pages

IV

Constraining General Two Higgs Doublet Models by the Evolution of Yukawa Couplings

Johan Bijnens, Jie Lu and Johan Rathsman

Department of Astronomy and Theoretical Physics, Lund University,
Sölvegatan 14A, SE–223 62 Lund, Sweden
http://www.thep.lu.se/

LU TP 11-41
arXiv:1111.5760 [hep-ph]

We study how general two Higgs doublet models can be constrained by considering their properties under renormalization group evolution of the Yukawa couplings. We take into account both the appearance of a Landau pole as well as off-diagonal Yukawa couplings leading to flavour changing neutral currents in violation with experimental constraints at the electroweak scale. We find that the latter condition can be used to limit the amount of Z_2 symmetry breaking allowed in a given model.

IV.1 Introduction

The Standard Model (SM) has been compared to experiments with great success in the past decades and finding the Higgs boson is the only missing piece. However, there are still a few internal problems. The prime example is the so called hierarchy problem: why is the electroweak (EW) scale much smaller than the Plank scale? Thus, the SM cannot be seen as a fundamental theory of particle physics, but only as an effective description which will break down at higher energies, at least at the Planck scale where gravity becomes of the same magnitude as the gauge forces. The mission of the Large Hadron Collider at CERN is therefore not only to look for the SM Higgs boson but also for physics Beyond the Standard Model (BSM).

The general two Higgs Doublet Model (2HDM) was one of the earliest BSM models, proposed by T.D. Lee [1] already in 1973 as a model with spontaneous CP-violation. The 2HDM itself cannot give any solution to the problems of the SM, such as the hierarchy problem. On the contrary, it introduces more problems such as tree level flavour-changing-neutral-currents (FCNC) which are absent in the SM. However, a 2HDM is part of many other BSM models, especially supersymmetric ones, which require an even number of Higgs doublets. Therefore it is useful and interesting to study the 2HDM itself, since it can be thought of as an effective description of more general models at the TeV scale. One such example is the Minimal SuperSymmetric Model (MSSM) in the case of heavy superpartners such that the Higgs bosons only decays to SM particles.

The problem of tree level FCNC can be evaded by introducing an appropriate Z_2 symmetry that ensures that each fermion type only couples to one of the Higgs doublets, which is sufficient in order to avoid tree-level FCNC as shown by Glashow and Weinberg [2]. This is precisely what happens in the MSSM whose Higgs sector at tree-level is a so called type II 2HDM, meaning that one of the Higgs doublets couples only to down-type fermions and the other only to up-type ones. By enforcing a Z_2-symmetry one also ensures the absence of tree-level FCNC under renormalization group evolution of the model to other energy scales.

Recently another way of avoiding the tree-level FCNC, by having the Yukawa couplings to the two Higgs doublets proportional to each other, has been proposed [3]. This works fine at a given energy scale but if one evolves the model to another scale then the tree-level FCNC are reintroduced because the Yukawa couplings in this model do not respect any Z_2 symmetry as shown by Ferreira et al [4]. There has also been some discussion of the experimental constraints on this model under renormalization group evolution [5–7] and we will revisit these constraints more carefully below.

More generally, the FCNC at a given energy scale are avoided as long as

the Yukawa couplings are diagonal in the appropriate basis. The constraints on these more general models from low-energy flavour observables have also been studied [8], but not their properties under renormalization group evolution. Apart from these schemes, which are set up in order to avoid tree-level FCNC to a larger or lesser extent, one can also envision a top-down approach where one assumes a certain texture for the mass matrices and from this derives the Yukawa coupling matrices. In the present context the prime example is the Cheng-Sher ansatz [9] which gives a natural suppression of tree-level FCNC from the hierarchy of quark masses. Some generic properties of these models under renormalization group evolution have been studied [10] but not taking experimental constraints into account.

In this paper we will study the properties of all these types of models taking into account also experimental constraints on FCNC when evolving them according to the Renormalization Group Equations (RGE) for the Yukawa couplings. In this way we can see how stable the various assumptions are under RGE evolution, which in turn gives a measure of have plausible the assumptions are. A large sensitivity indicates that the assumptions behind the model are not stable meaning that they are either fine-tuned or incomplete such that there for example will be additional particles appearing when going to a higher energy. From this respect we will study both the appearance of a Landau pole as well as off-diagonal Yukawa couplings leading to FCNC at high energies, which are larger than what is experimentally allowed at the EW scale.

The layout of the paper is as follows. We first give a brief introduction to the general 2HDM in section IV.2 including the Yukawa sector with emphasis on the FCNC problem as well as some possible solutions and the RGEs for the Yukawa couplings. Section IV.3 gives the latest constraints on the non-diagonal Yukawa couplings from neutral meson mixing as well as the SM input values we use. Then in section IV.4 we present our numerical analysis of the running Yukawa couplings. We investigate the limits both from the absence of a Landau pole as well as from requiring the off-diagonal Yukawa couplings at higher energy scales to be in accordance with the experimental limits at the EW scale. Finally, in section IV.5 we present our conclusions.

IV.2 The general 2HDM

IV.2.1 The Scalar Sector

The two Higgs doublet model was introduced in [1] and for a more general overview of its properties and the constraints that can be put on it, we refer to the recent review [11]. Much of the phenomenology of the 2HDM is also closely related to the SM and MSSM for which we refer to the reviews by

Djouadi [12,13].

The most general renormalizable scalar potential with two Higgs doublets, Φ_1 and Φ_2, can be written as

$$\begin{aligned} V_\Phi &= m_{11}^2\Phi_1^\dagger\Phi_1 + m_{22}^2\Phi_2^\dagger\Phi_2 - (m_{12}^2\Phi_1^\dagger\Phi_2 + h.c) \\ &+\frac{1}{2}\lambda_1(\Phi_1\Phi_1)^2 + \frac{1}{2}\lambda_2(\Phi_2\Phi_2)^2 + \lambda_3(\Phi_1^\dagger\Phi_1)(\Phi_2^\dagger\Phi_2) + \lambda_4(\Phi_1^\dagger\Phi_2)(\Phi_2^\dagger\Phi_1) \\ &+\left\{\frac{1}{2}\lambda_5(\Phi_1^\dagger\Phi_2)^2 + \left[\lambda_6(\Phi_1^\dagger\Phi_1) + \lambda_7(\Phi_2^\dagger\Phi_2)\right](\Phi_1^\dagger\Phi_2) + h.c\right\}. \end{aligned} \tag{IV.1}$$

The coupling constants m_{11}^2, m_{22}^2 and $\lambda_{1,2,3,4}$ are real, while m_{12} and $\lambda_{5,6,7}$ can be complex if there are not any further restrictions. In the following we will however set them to be real such that there is no explicit CP-violation.

The vacuum expectation values (VEVs) of Φ_i are in general

$$\begin{aligned} \langle\Phi_1\rangle_0 &= \frac{1}{\sqrt{2}}e^{i\theta_1}\begin{pmatrix} 0 \\ v_1 \end{pmatrix}, \\ \langle\Phi_2\rangle_0 &= \frac{1}{\sqrt{2}}e^{i\theta_2}\begin{pmatrix} 0 \\ v_2 \end{pmatrix}, \end{aligned} \tag{IV.2}$$

and $\tan\beta$ is defined as the ratio of the v_i, $\tan\beta = v_2/v_1$.

The Higgs doublets can be rotated to a basis in which only one of the doublets has a vacuum expectation value using the angle β. This is called the Higgs basis and is related to the general basis as

$$\begin{aligned} H_1 &= \cos\beta\,\Phi_1 + \sin\beta\, e^{-i\theta}\Phi_2\,, \\ H_2 &= -\sin\beta\,\Phi_1 + \cos\beta\, e^{-i\theta}\Phi_2\,, \end{aligned} \tag{IV.3}$$

with $\theta = \theta_2 - \theta_1$. Hence the VEVs for the doublets in the Higgs basis, with $v^2 = v_1^2 + v_2^2$, are

$$\begin{aligned} \langle H_1\rangle_0 &= \frac{1}{\sqrt{2}}e^{i\theta_1}\begin{pmatrix} 0 \\ v \end{pmatrix}, \\ \langle H_2\rangle_0 &= \begin{pmatrix} 0 \\ 0 \end{pmatrix}. \end{aligned} \tag{IV.4}$$

We have defined both Φ_i to have weak hypercharge $+1$. Doublets with weak hypercharge -1 can be constructed out of the complex conjugate fields via

$$\widetilde{\Phi}_i = i\sigma_2\Phi_i^*\,. \tag{IV.5}$$

Φ_1 and Φ_2 consist of 8 real fields in total. Three of them correspond to the Goldstone bosons to be eaten by the weak gauge bosons $W^\pm$ and Z^0 upon

spontaneous breaking of the gauge group $SU(2)_L \times U(1)_Y$. One of the standard conventions to write the doublets without the Goldstone bosons is (setting for clarity $\theta_1 = 0$)

$$\begin{aligned} \Phi_1(x) &= \begin{pmatrix} -s_\beta H^+ \\ \frac{1}{\sqrt{2}}(c_\beta v - s_\alpha h + c_\alpha H - i s_\beta A) \end{pmatrix} \\ \Phi_2(x) &= \begin{pmatrix} c_\beta H^+ \\ \frac{1}{\sqrt{2}}(s_\beta v + c_\alpha h + s_\alpha H + i c_\beta A) \end{pmatrix} . \end{aligned} \tag{IV.6}$$

Here $H^\pm$ is the charged Higgs boson and the angle α ($s_\alpha = \sin\alpha, c_\alpha = \cos\alpha$) is introduced to diagonalize the CP eigenstates in the neutral sector, which can be divided into two CP even scalars: (H, h), and a CP odd pseudo-scalar: A.

IV.2.2 The Yukawa Sector

The weak eigenstates of the SM fermions (with massless neutrinos for simplicity) are denoted as

$$\begin{aligned} Q_L &= \begin{pmatrix} U_L \\ D_L \end{pmatrix} \qquad L_L = \begin{pmatrix} \nu_L \\ E_L \end{pmatrix} , \\ & U_R, \quad D_R, \quad E_R . \end{aligned} \tag{IV.7}$$

The most general Yukawa interaction can then be written as

$$\begin{aligned} -\mathcal{L}_Y &= \overline{Q}_L \widetilde{\Phi}_1 \eta_1^U U_R + \overline{Q}_L \Phi_1 \eta_1^D D_R + \overline{L}_L \Phi_1 \eta_1^L E_R \\ &\quad + \overline{Q}_L \widetilde{\Phi}_2 \eta_2^U U_R + \overline{Q}_L \Phi_2 \eta_2^D D_R + \overline{L}_L \Phi_2 \eta_2^L E_R + \text{h.c.} . \end{aligned} \tag{IV.8}$$

We leave the generation index implicit here, all entities are matrices or vectors in the three-dimensional generation space. The η_i^F are the 3×3 matrices of Yukawa couplings for $F = U, D, L$.

In order to show more explicitly the physical content in the Yukawa couplings, we rotate the Yukawa coupling matrices to the Higgs basis by inverting Eq. (IV.3) and inserting into Eq. (IV.8).

$$\begin{aligned} -\mathcal{L}_Y &= \overline{Q}_L \widetilde{H}_1 \kappa_0^U U_R + \overline{Q}_L H_1 \kappa_0^D D_R + \overline{L}_L H_1 \kappa_0^L E_R \\ &\quad + \overline{Q}_L \widetilde{H}_2 \rho_0^U U_R + \overline{Q}_L H_2 \rho_0^D D_R + \overline{L}_L H_2 \rho_0^L E_R + \text{h.c.} . \end{aligned} \tag{IV.9}$$

The relations between the two sets of Yukawa matrices are

$$\begin{aligned} \kappa_0^U &= \cos\beta\, \eta_1^U + \sin\beta (e^{-i\theta} \eta_2^U) , \\ \kappa_0^D &= \cos\beta\, \eta_1^D + \sin\beta (e^{+i\theta} \eta_2^D) , \\ \kappa_0^L &= \cos\beta\, \eta_1^L + \sin\beta (e^{+i\theta} \eta_2^L) ; \end{aligned} \tag{IV.10}$$

and

$$\begin{aligned}\rho_0^U &= -\sin\beta\,\eta_1^U + \cos\beta(e^{-i\theta}\eta_2^U)\,,\\ \rho_0^D &= -\sin\beta\,\eta_1^D + \cos\beta(e^{+i\theta}\eta_2^D)\,,\\ \rho_0^L &= -\sin\beta\,\eta_1^L + \cos\beta(e^{+i\theta}\eta_2^L)\,. \end{aligned} \tag{IV.11}$$

The couplings to H_1 produce the masses of the fermions. We can go over to the fermion mass basis by bi-diagonalizing the matrices κ^F with the unitary matrices V_L^F, V_R^F:

$$\kappa^F = V_L^F \kappa_0^F V_R^{F\dagger} = \frac{\sqrt{2}}{v}\mathcal{M}_{ii}^F \tag{IV.12}$$

$$\rho^F = V_L^F \rho_0^F V_R^{F\dagger} \tag{IV.13}$$

The κ^F are diagonal, real and positive and are fully determined from the fermion masses $\mathcal{M}_{ii}^F$ with $\mathcal{M}_{11}^U = m_u$ etc. ρ^F is still a general complex matrix whose non-diagonal matrix elements could cause tree level flavour-changing-neutral-currents. The reason is that we cannot in general diagonalize two different matrices simultaneously. The flavour changing charged currents are described by the matrix

$$V_{CKM} = V_L^U V_L^{D\dagger}\,. \tag{IV.14}$$

We now can derive the Yukawa interactions in the Higgs and fermion mass basis. Using the definitions of Eqs. (IV.3), (IV.6), and (IV.10-IV.13), the Yukawa interactions (IV.9) become (see e.g. [14])

$$\begin{aligned}-\mathcal{L}_Y &= \frac{1}{\sqrt{2}}\bar{D}\Big[\kappa^D s_{\beta-\alpha} + (\rho^D P_R + \rho^{D\dagger} P_L)c_{\beta-\alpha}\Big]Dh\\ &+\frac{1}{\sqrt{2}}\bar{D}\Big[\kappa^D c_{\beta-\alpha} - (\rho^D P_R + \rho^{D\dagger} P_L)s_{\beta-\alpha}\Big]DH + \frac{i}{\sqrt{2}}\bar{D}(\rho^D P_R - \rho^{D\dagger} P_L)DA\\ &+\frac{1}{\sqrt{2}}\bar{U}\Big[\kappa^U s_{\beta-\alpha} + (\rho^U P_R + \rho^{U\dagger} P_L)c_{\beta-\alpha}\Big]Uh\\ &+\frac{1}{\sqrt{2}}\bar{U}\Big[\kappa^U c_{\beta-\alpha} - (\rho^U P_R + \rho^{U\dagger} P_L)s_{\beta-\alpha}\Big]UH - \frac{i}{\sqrt{2}}\bar{U}(\rho^U P_R - \rho^{U\dagger} P_L)UA\\ &+\frac{1}{\sqrt{2}}\bar{L}\Big[\kappa^L s_{\beta-\alpha} + (\rho^L P_R + \rho^{L\dagger} P_L)c_{\beta-\alpha}\Big]Lh\\ &+\frac{1}{\sqrt{2}}\bar{L}\Big[\kappa^L c_{\beta-\alpha} - (\rho^L P_R + \rho^{L\dagger} P_L)s_{\beta-\alpha}\Big]LH + \frac{i}{\sqrt{2}}\bar{L}(\rho^L P_R - \rho^{L\dagger} P_L)LA\\ &+\Big[\bar{U}\left(V_{\rm CKM}\rho^D P_R - \rho^{U\dagger} V_{\rm CKM} P_L\right)DH^+ + \bar{\nu}\rho^L P_R L H^+ + \text{h.c.}\Big], \end{aligned} \tag{IV.15}$$

where $P_{R/L} = (1 \pm \gamma_5)/2$. One can clearly see, that if the Yukawa coupling matrices ρ^F are not diagonal, there are flavour-changing-neutral-currents (FCNC)

Type	U_R	D_R	L_R	ρ^U	ρ^D	ρ^L
I	$+$	$+$	$+$	$\kappa^U \cot\beta$	$\kappa^D \cot\beta$	$\kappa^L \cot\beta$
II	$+$	$-$	$-$	$\kappa^U \cot\beta$	$-\kappa^D \tan\beta$	$-\kappa^L \tan\beta$
III/Y	$+$	$-$	$+$	$\kappa^U \cot\beta$	$-\kappa^D \tan\beta$	$\kappa^L \cot\beta$
IV/X	$+$	$+$	$-$	$\kappa^U \cot\beta$	$\kappa^D \cot\beta$	$-\kappa^L \tan\beta$

Table IV.1: The different types of 2HDM with Z_2 symmetry. The nomenclature follows [8]. The Z_2 charges for Higgs doublets are odd or -1 for Φ_1 and even or $+1$ for Φ_2. The right-handed fermions have been given different Z_2 charges assignment as shown. The Yukawa matrices ρ^F are proportional to the κ^F and thus also diagonal with the relation shown in the last three columns.

at tree level, which are absent in the Standard Model and are severely constrained by experiments. Therefore, either these terms are completely forbidden by certain symmetries or mechanisms, or they are sufficiently small to avoid the current experimental bounds. An early discussion is the paper by Glashow and Weinberg [2].

There are different known solutions to the FCNC problem. In this paper we study three different cases:

- Z_2 **symmetry**

  If there is only one Higgs doublet coupling to each type of fermions, the situation becomes the same as in the standard model. The FCNC couplings vanish completely, known as naturally vanishing FCNC [2]. An elegant way to achieve this is to impose a Z_2 symmetry on the Lagrangian and set one of the Higgs doublets and some of the right handed fermions to be Z_2 odd. The different cases depending on which fermions couple to the same doublets are listed in Table IV.1. We also note that the Higgs sector of the MSSM is of type II at tree-level.

- **Yukawa Alignment**

  A more general way to diagonalize the Yukawa matrices simultaneously is the Yukawa Alignment model [3]. They proposed that the Yukawa coupling matrices η_1^F and η_2^F are proportional to each other. So the rotated Yukawa coupling matrices κ^F and ρ^F are also proportional to each other and can thus be diagonalized simultaneously. However, other than the models with Z_2 symmetry, this alignment may be spoiled at higher energy scales. Some of the non-diagonal couplings leading to FCNC may become sizable at higher scales. Studying limits on the proportionality constants from this source is one of the purposes of the present paper.

- **Cheng-Sher Ansatz**

  A third possibility is to keep the off-diagonal FCNC elements in the ρ^F

naturally small. The best known ansatz of this type was proposed by Cheng and Sher [9]

$$\rho^F_{ij} = \lambda^F_{ij}\frac{\sqrt{2m_i m_j}}{v}\,. \qquad \text{(IV.16)}$$

The m_i are the different fermion masses. Since the diagonal elements of the κ^F have a hierarchy in size corresponding to the fermion mass hierarchy it is natural to introduce this also for the ρ^F. The λ^F are expected to be of $\mathcal{O}(1)$ and should be small enough to suppress FCNC to the observed level. We discuss these limits below. One should be aware that there are different parameterizations of the Cheng-Sher ansatz, some papers do not have the factor of $\sqrt{2}$ in (IV.16), e.g. [15].

IV.2.3 RGE for Yukawa Couplings in 2HDM

The variation of couplings and masses with the subtraction scale μ is given by the renormalization group equations (RGE). The running of Yukawa couplings in the 2HDM can be found in many places, e.g. [4, 10, 11]. We have also rederived them using the methods of [10].

Using the notation $\mathcal{D} \equiv 16\pi^2 d/d(\ln\mu)$ the RGEs for the Yukawa couplings in the general basis are:

$$\begin{aligned}\mathcal{D}\eta^U_k &= -A_U\eta^U_k + \sum_{\ell=1}^{2}\mathrm{Tr}\left[N_c\left(\eta^U_k\eta^{U\dagger}_\ell + \eta^D_\ell\eta^{D\dagger}_k\right) + \eta^{L\dagger}_k\eta^L_\ell\right]\eta^U_\ell \\ &\quad + \frac{1}{2}\sum_{\ell=1}^{2}\left[\eta^U_\ell\eta^{U\dagger}_\ell + \eta^D_\ell\eta^{D\dagger}_\ell\right]\eta^U_k + \eta^U_k\sum_{\ell=1}^{2}\eta^{U\dagger}_\ell\eta^U_\ell - 2\sum_{\ell=1}^{2}\left[\eta^D_\ell\eta^{D\dagger}_k\eta^U_\ell\right],\end{aligned}$$

$$\begin{aligned}\mathcal{D}\eta^D_k &= -A_D\eta^D_k + \sum_{\ell=1}^{2}\mathrm{Tr}\left[N_c\left(\eta^D_k\eta^{D\dagger}_\ell + \eta^U_\ell\eta^{U\dagger}_k\right) + \eta^L_k\eta^{L\dagger}_\ell\right]\eta^D_\ell \\ &\quad + \frac{1}{2}\sum_{\ell=1}^{2}\left[\eta^U_\ell\eta^{U\dagger}_\ell + \eta^D_\ell\eta^{D\dagger}_\ell\right]\eta^D_k + \eta^D_k\sum_{\ell=1}^{2}\eta^{D\dagger}_\ell\eta^D_\ell - 2\sum_{\ell=1}^{2}\left[\eta^U_\ell\eta^{U\dagger}_k\eta^D_\ell\right],\end{aligned}$$

$$\begin{aligned}\mathcal{D}\eta^L_k &= -A_L\eta^L_k + \sum_{\ell=1}^{2}\mathrm{Tr}\left[N_c\left(\eta^{U\dagger}_k\eta^U_\ell + \eta^D_k\eta^{D\dagger}_\ell\right) + \eta^L_k\eta^{L\dagger}_\ell\right]\eta^L_\ell \\ &\quad + \sum_{\ell=1}^{2}\left[\frac{1}{2}\eta^L_\ell\eta^{L\dagger}_\ell\eta^L_k + \eta^L_k\eta^{L\dagger}_\ell\eta^L_\ell\right]. \qquad \text{(IV.17)}\end{aligned}$$

where A_F are given by the gauge couplings as follows

$$\begin{aligned} A_U &= 3\frac{(N_c^2-1)}{N_c}g_3^2 + \frac{9}{4}g_2^2 + \frac{17}{12}g_1^2\,, \\ A_D &= A_U - g_1^2\,, \\ A_L &= \frac{15}{4}g_1^2 + \frac{9}{4}g_2^2\,. \end{aligned} \tag{IV.18}$$

with $g_1 = e/\cos\theta_W$, $g_2 = e/\sin\theta_W$, and $g_3 = g_s$, $\sin\theta_W$ being the weak mixing angle. In turn the RGEs for the gauge couplings up to one loop level are

$$\begin{aligned} \mathcal{D}(g_1) &= \left(\frac{1}{3} + \frac{10}{9}n_q\right)g_1^3\,, \\ \mathcal{D}(g_2) &= -\left(7 - \frac{2}{3}n_q\right)g_2^3\,, \\ \mathcal{D}(g_3) &= -\frac{1}{3}\left(11N_c - 2n_q\right)g_3^3\,. \end{aligned} \tag{IV.19}$$

n_q is the number of active quarks above energy threshold. In this paper we will always use $n_q = 6$ since we start the evolution at m_Z.

Finally the RGEs for the fields and thus for the vacuum expectation values $e^{\theta_i}v_i$ are:

$$\begin{aligned} \mathcal{D}(e^{i\theta_k}v_k) &= -\sum_{\ell=1}^{2}\mathrm{Tr}\left[N_c\left(\eta_k^U\eta_\ell^{U\dagger} + \eta_\ell^D\eta_k^{D\dagger}\right) + \eta_\ell^L\eta_k^{L\dagger}\right]e^{i\theta_\ell}v_\ell \\ &\quad + \left(\frac{3}{4}g_1^2 + \frac{9}{4}g_2^2\right)e^{i\theta_k}v_k\,. \end{aligned} \tag{IV.20}$$

Note that the running of the Yukawa couplings as given in (IV.17) is independent of the couplings in the Higgs potential (IV.1). They only appear at the two-loop level.

Using the definitions (IV.3), (IV.10) and (IV.11), the RGEs can be rewritten in the Higgs basis. The vacuum expectation value v, the phase difference between the two vacuum expectation values θ and the angle β relating the general basis and the Higgs basis satisfy the following RGEs:

$$\mathcal{D}\left(v^2\right) = -2\mathrm{Tr}\left[N_c\left(\kappa_0^U\kappa_0^{U\dagger} + \kappa_0^D\kappa_0^{D\dagger}\right) + \kappa_0^L\kappa_0^{L\dagger}\right]v^2 + \left[\frac{3}{2}g_1^2 + \frac{9}{2}g_2^2\right]v^2\,,$$

$$\begin{aligned} \mathcal{D}(\tan\beta) &= -\frac{1}{2\cos^2\beta}\mathrm{Tr}\Bigg[N_c\left(\rho_0^U\kappa_0^{U\dagger} + \kappa_0^U\rho_0^{U\dagger} + \kappa_0^D\rho_0^{D\dagger} + \rho_0^D\kappa_0^{D\dagger}\right) \\ &\quad + \kappa_0^L\rho_0^{L\dagger} + \rho_0^L\kappa_0^{L\dagger}\Bigg]\,, \end{aligned}$$

$$\mathcal{D}(\theta) = \frac{1}{i\sin(2\beta)}\mathrm{Tr}\Big[N_c\left(\kappa_0^U\rho_0^{U\dagger}-\rho_0^U\kappa_0^{U\dagger}\right)-N_c\left(\kappa_0^D\rho_0^{D\dagger}-\rho_0^D\kappa_0^{D\dagger}\right) - \left(\kappa_0^L\rho_0^{L\dagger}-\rho_0^L\kappa_0^{L\dagger}\right)\Big]. \quad \text{(IV.21)}$$

Finally the Yukawa couplings in the Higgs basis, in other words the matrices κ_0^F and ρ_0^F satisfy:

$$\begin{aligned}\mathcal{D}\left(\kappa_0^U\right) = & -A_U\kappa_0^U+\mathrm{Tr}\left[N_c\left(\kappa_0^U\kappa_0^{U\dagger}+\kappa_0^D\kappa_0^{D\dagger}\right)+\kappa_0^{L\dagger}\kappa_0^L\right]\kappa_0^U \\ & -\frac{1}{2}\tan\beta\,\mathrm{Tr}\Big\{N_c\left(\kappa_0^U\rho_0^{U\dagger}-\rho_0^U\kappa_0^{U\dagger}\right)-N_c\left(\kappa_0^D\rho_0^{D\dagger}-\rho_0^D\kappa_0^{D\dagger}\right) \\ & -\left(\kappa_0^L\rho_0^{L\dagger}-\rho_0^L\kappa_0^{L\dagger}\right)\Big\}\kappa_0^U \\ & +\Big\{\frac{1}{2}\left[\rho_0^U\rho_0^{U\dagger}+\rho_0^D\rho_0^{D\dagger}+\kappa_0^U\kappa_0^{U\dagger}+\kappa_0^D\kappa_0^{D\dagger}\right]\kappa_0^U+\kappa_0^U\left[\rho_0^{U\dagger}\rho_0^U+\kappa_0^{U\dagger}\kappa_0^U\right] \\ & -2\rho_0^D\kappa_0^{D\dagger}\rho_0^U-2\kappa_0^D\kappa_0^{D\dagger}\kappa_0^U\Big\}, \end{aligned} \quad \text{(IV.22)}$$

$$\begin{aligned}\mathcal{D}\left(\kappa_0^D\right) = & -A_D\kappa_0^D+\mathrm{Tr}\left[N_c\left(\kappa_0^U\kappa_0^{U\dagger}+\kappa_0^D\kappa_0^{D\dagger}\right)+\kappa_0^L\kappa_0^{L\dagger}\right]\kappa_0^D \\ & +\frac{1}{2}\tan\beta\,\mathrm{Tr}\Big\{N_c\left(\kappa_0^U\rho_0^{U\dagger}-\rho_0^U\kappa_0^{U\dagger}\right)-N_c\left(\kappa_0^D\rho_0^{D\dagger}-\rho_0^D\kappa_0^{D\dagger}\right) \\ & -\left(\kappa_0^L\rho_0^{L\dagger}-\rho_0^L\kappa_0^{L\dagger}\right)\Big\}\kappa_0^D \\ & +\Big\{\frac{1}{2}\left[\rho_0^U\rho_0^{U\dagger}+\rho_0^D\rho_0^{D\dagger}+\kappa_0^U\kappa_0^{U\dagger}+\kappa_0^D\kappa_0^{D\dagger}\right]\kappa_0^D+\kappa_0^D\left[\rho_0^{D\dagger}\rho_0^D+\kappa_0^{D\dagger}\kappa_0^D\right] \\ & -2\rho_0^U\kappa_0^{U\dagger}\rho_0^D-2\kappa_0^U\kappa_0^{U\dagger}\kappa_0^D\Big\}, \end{aligned} \quad \text{(IV.23)}$$

$$\begin{aligned}\mathcal{D}\left(\kappa_0^L\right) = & -A_L\kappa_0^L+\mathrm{Tr}\Big\{N_c\left(\kappa_0^{U\dagger}\kappa_0^U+\kappa_0^D\kappa_0^{D\dagger}\right)+\kappa_0^{L\dagger}\kappa_0^L\Big\}\kappa_0^L \\ & +\frac{1}{2}\tan\beta\,\mathrm{Tr}\Big\{N_c\left(\kappa_0^U\rho_0^{U\dagger}-\rho_0^U\kappa_0^{U\dagger}\right)-N_c\left(\kappa_0^D\rho_0^{D\dagger}-\rho_0^D\kappa_0^{D\dagger}\right) \\ & -\left(\kappa_0^L\rho_0^{L\dagger}-\rho_0^L\kappa_0^{L\dagger}\right)\Big\}\kappa_0^L \end{aligned}$$

$$+\frac{1}{2}\left(\rho_0^L\rho_0^{L\dagger}+\kappa_0^L\kappa_0^{L\dagger}\right)\kappa_0^L+\kappa_0^L\left(\rho_0^{L\dagger}\rho_0^L+\kappa_0^{\dagger L}\kappa_0^L\right), \tag{IV.24}$$

$$\begin{aligned}\mathcal{D}(\rho_0^U) &= -A_U\rho_0^U+2\mathrm{Tr}\left[N_c\left(\rho_0^U\kappa_0^{U\dagger}+\kappa_0^D\rho_0^{D\dagger}\right)+\kappa_0^L\rho_0^{L\dagger}\right]\kappa_0^U\\ &+\mathrm{Tr}\left[N_c\left(\rho_0^U\rho_0^{U\dagger}+\rho_0^D\rho_0^{U\dagger}\right)+\rho_0^L\rho_0^{L\dagger}\right]\rho_0^U\\ &-\frac{1}{2}\cot\beta\,\mathrm{Tr}\Big\{N_c\left(\kappa_0^U\rho_0^{U\dagger}-\rho_0^U\kappa_0^{U\dagger}\right)-N_c\left(\kappa_0^D\rho_0^{D\dagger}-\rho_0^D\kappa_0^{D\dagger}\right)\\ &\quad-\left(\kappa_0^L\rho_0^{L\dagger}-\rho_0^L\kappa_0^{L\dagger}\right)\Big\}\rho_0^U\\ &+\Big\{\frac{1}{2}\left[\rho_0^U\rho_0^{U\dagger}+\rho_0^D\rho_0^{D\dagger}+\kappa_0^U\kappa_0^{U\dagger}+\kappa_0^D\kappa_0^{D\dagger}\right]\rho_0^U+\rho_0^U\left[\rho_0^{U\dagger}\rho_0^U+\kappa_0^{U\dagger}\kappa_0^U\right]\\ &\quad-2\rho_0^D\rho_0^{D\dagger}\rho_0^U-2\kappa_0^D\rho_0^{D\dagger}\kappa_0^U\Big\},\end{aligned} \tag{IV.25}$$

$$\begin{aligned}\mathcal{D}(\rho_0^D) &= -A_D\rho_0^D+2\mathrm{Tr}\left[N_c\left(\kappa_0^U\rho_0^{U\dagger}+\rho_0^D\kappa_0^{D\dagger}\right)+\rho_0^L\kappa_0^{L\dagger}\right]\kappa_0^D\\ &+\mathrm{Tr}\left[N_c\left(\rho_0^U\rho_0^{U\dagger}+\rho_0^D\rho_0^{D\dagger}+\rho_0^L\rho_0^{L\dagger}\right)\right]\rho_0^D\\ &+\frac{1}{2}\cot\beta\,\mathrm{Tr}\Big\{N_c\left(\kappa_0^U\rho_0^{U\dagger}-\rho_0^U\kappa_0^{U\dagger}\right)-N_c\left(\kappa_0^D\rho_0^{D\dagger}-\rho_0^D\kappa_0^{D\dagger}\right)\\ &\quad-\left(\kappa_0^L\rho_0^{L\dagger}-\rho_0^L\kappa_0^{L\dagger}\right)\Big\}\rho_0^D\\ &+\Big\{\frac{1}{2}\left[\rho_0^U\rho_0^{U\dagger}+\rho_0^D\rho_0^{D\dagger}+\kappa_0^U\kappa_0^{U\dagger}+\kappa_0^D\kappa_0^{D\dagger}\right]\rho_0^D+\rho_0^D\left[\rho_0^{D\dagger}\rho_0^D+\kappa_0^{D\dagger}\kappa_0^D\right]\\ &\quad-2\rho_0^U\rho_0^{U\dagger}\rho_0^D-2\kappa_0^U\rho_0^{U\dagger}\kappa_0^D\Big\},\end{aligned} \tag{IV.26}$$

$$\begin{aligned}\mathcal{D}\rho_0^L &= -A_L\rho_0^L+2\mathrm{Tr}\Big\{N_c\left(\kappa_0^U\rho_0^{U\dagger}+\rho_0^D\kappa_0^{D\dagger}\right)+\rho_0^L\kappa_0^{L\dagger}\Big\}\kappa_0^L\\ &+\mathrm{Tr}\Big\{N_c\left(\rho_0^U\rho_0^{U\dagger}+\rho_0^D\rho_0^{D\dagger}\right)+\rho_0^L\rho_0^{L\dagger}\Big\}\rho_0^L\\ &+\frac{1}{2}\cot\beta\,\mathrm{Tr}\Big\{N_c\left(\kappa_0^U\rho_0^{U\dagger}-\rho_0^U\kappa_0^{U\dagger}\right)-N_c\left(\kappa_0^D\rho_0^{D\dagger}-\rho_0^D\kappa_0^{D\dagger}\right)\\ &\quad-\left(\kappa_0^L\rho_0^{L\dagger}-\rho_0^L\kappa_0^{L\dagger}\right)\Big\}\rho_0^L\end{aligned}$$

$$+\frac{1}{2}\left(\rho_0^L\rho_0^{L\dagger}+\kappa_0^L\kappa_0^{L\dagger}\right)\rho_0^L+\rho_0^L\left(\rho_0^{L\dagger}\rho_0^L+\kappa_0^{\dagger L}\kappa_0^L\right). \tag{IV.27}$$

Before ending this section we note that the $\tan\beta$ dependent terms in the evolution equations for the Yukawa couplings disappear in the real case. In the CP-violating case ρ is no longer basis-independent and therefore there is a residual dependence on $\tan\beta$ in this case. For a thorough discussion of basis independent quantities in the CP-violating case we refer to [16].

IV.3 Constraints and SM input

IV.3.1 Low-energy constraints on λ_{ij}^F

In the recent review of 2HDM [11], the authors have given a comprehensive overview on the latest constraints on the λ_{ij}^F. The most stringent ones are in the quark sector, coming from the neutral meson mixing, and we will therefore limit ourselves to these constraints in the following.

The master formula for $F^0-\bar{F}^0$ mixing mediated by tree level Higgs scalars in the vacuum insertion approximation can be found in [17]:

$$\begin{aligned}\Delta M_F &= \frac{(\rho_{ij}^F)^2}{M_F}\left[S_F\left(\frac{c_{\beta-\alpha}^2}{m_h^2}+\frac{s_{\beta-\alpha}^2}{m_H^2}\right)+\frac{P_F}{m_A^2}\right] \\ S_F &= \frac{1}{6}B_F f_F^2 M_F^2\left[1+\frac{M_F^2}{(m_i+m_j)^2}\right] \\ P_F &= \frac{1}{6}B_F f_F^2 M_F^2\left[1+\frac{11M_F^2}{(m_i+m_j)^2}\right]\end{aligned} \tag{IV.28}$$

Here M_F and ΔM_F are the mass and mass difference of the neutral mesons respectively, and f_F is the corresponding pseudo-scalar decay constant. The parameter B_F is defined as the ratio of the actual matrix element compared to its value in the vacuum insertion approximation [17]. The numerical values of the parameters we use are listed in Table IV.2.

To calculate the limits on λ_{ij}^F, we require that the sum of the SM and 2HDM theoretical predictions for ΔM_F does not exceed the experimental value by more than 2 standard deviations:

$$\Delta M_F^{\mathrm{SM}}+\Delta M_F^{\mathrm{2HDM}}\leq\Delta M_F^{\mathrm{expt}}+2\sigma \tag{IV.29}$$

where $\sigma=\sqrt{\sigma_{\mathrm{expt}}^2+\sigma_{\mathrm{SM}}^2}$ is a combination of the experimental and theoretical uncertainties. For the $K^0-\bar{K}^0$ and $D^0-\bar{D}^0$ mixing, the non-perturbative interactions make the SM calculation very difficult. Here we therefore simply

Meson	M_F(GeV)	B_F	f_F (GeV)
$K^0\,(d\bar{s})$	0.4976 [18]	0.75 ± 0.026 [19]	0.1558 ± 0.0017 [19]
$D^0\,(\bar{u}c)$	1.8648 [18]	0.82 ± 0.01 [20]	0.165 [20]
$B_d^0\,(d\bar{b})$	5.2795 [18]	1.26 ± 0.11 [19]	0.1928 ± 0.0099 [19]
$B_s^0\,(s\bar{b})$	5.3663 [18]	1.33 ± 0.06 [19]	0.2388 ± 0.0095 [19]

Table IV.2: Parameters of the neutral mesons K^0, D^0,B_d^0 and B_s^0.

assume that the 2HDM contribution is not larger than the experimental value by more than 2 standard deviations. This corresponds to setting the SM contribution to zero in Eq. (IV.29) as was done in [15]. The experimental and SM values we thus use are listed below.

1. $K^0 - \bar{K}^0$:

$$\begin{aligned} \Delta M_{K^0}^{\text{expt}} &= (3.483 \pm 0.006) \times 10^{-15}\ \text{GeV} \quad [18] \\ \Delta M_{K^0}^{SM} &= 0 \end{aligned}$$

2. $D^0 - \bar{D}^0$

$$\begin{aligned} \Delta M_{D^0}^{expt} &= 1.57^{+0.39}_{-0.415} \times 10^{-14}\ \text{GeV} \quad [18] \\ \Delta M_{D^0}^{SM} &= 0 \end{aligned}$$

3. $B_d^0 - \bar{B}_d^0$

$$\begin{aligned} \Delta M_{B_d}^{expt} &= (3.344 \pm 0.0197 \pm 0.0197) \times 10^{-13}\ \text{GeV} \quad [18] \\ \Delta M_{B_d}^{SM} &= 3.653^{+0.48}_{-0.30} \times 10^{-13}\ \text{GeV} \quad [21] \end{aligned}$$

4. $B_s^0 - \bar{B}_s^0$

$$\begin{aligned} \Delta M_{B_s}^{expt} &= (116.668 \pm 0.270 \pm 0.171) \times 10^{-13}\ \text{GeV} \quad [22] \\ \Delta M_{B_s}^{SM} &= 110.6^{+17.1}_{-9.9} \times 10^{-13}\ \text{GeV} \quad [21] \end{aligned}$$

The 2HDM contribution is then calculated using Eq. (IV.28). We note that the quark masses appearing in Eq. (IV.28) are the low energy ones defined more or less at the scale of the respective meson masses. For internal consistency we use the following values from ref. [23] (in GeV):

$$\begin{aligned} m_u(2\,\text{GeV}) &= 2.2 \times 10^{-3}\,, \qquad m_c(m_c) = 1.25\,; \\ m_d(2\,\text{GeV}) &= 5.0 \times 10^{-3}\,, \qquad m_s(2\,\text{GeV}) = 0.095\,, \quad m_b(m_b) = 4.2\,. \end{aligned}$$

However, the impact of the actual quark masses used is very small since the masses appearing in $(\rho^F_{ij})^2$ and the dominant pseudo-scalar matrix element $M_F^2/(m_i+m_j)^2$ essentially cancel, and we get similar results using the masses defined at m_Z instead.

From Eq. (IV.28) we can see that the main uncertainty of this estimate is due to the unknown masses of the CP-even and CP-odd Higgs bosons. It is also clear that the contribution to the mixing from the CP-odd exchange is much larger due to the extra factor 11 in P_F for the dominant pseudo-scalar matrix element. We will consider three different representative cases. We also remind the reader that in some cases there is an extra factor of $\sqrt{2}$ in the definition of λ^F_{ij}. With all this in mind we get the following constraints on λ^F_{ij}:

- $m_h = m_H = m_A = 120$ GeV

$$\begin{aligned} \lambda_{uc} &\lesssim 0.13\,, \\ \lambda_{ds} &\lesssim 0.08, \quad \lambda_{db} \lesssim 0.03, \quad \lambda_{sb} \lesssim 0.05\,. \end{aligned}$$

- $m_h = m_H = m_A = 400$ GeV

$$\begin{aligned} \lambda_{uc} &\lesssim 0.44\,, \\ \lambda_{ds} &\lesssim 0.27\,, \quad \lambda_{db} \lesssim 0.12\,, \quad \lambda_{sb} \lesssim 0.18\,. \end{aligned}$$

- $m_h = m_H = 120$ GeV $m_A = 400$ GeV

$$\begin{aligned} \lambda_{uc} &\lesssim 0.30\,, \\ \lambda_{ds} &\lesssim 0.20\,, \quad \lambda_{db} \lesssim 0.08\,, \quad \lambda_{sb} \lesssim 0.12\,. \end{aligned}$$

The first and second cases are examples of typical low and intermediate masses for the Higgs bosons, whereas the last case illustrates that the main restriction comes from the exchange of the CP-odd Higgs. All in all we conclude from these different cases that a representative value for these constraints is given by $\lambda^F_{i\neq j} \lesssim 0.1$ and this is the generic value we will use when analyzing the effects of Z_2 breaking in the running of the Yukawa couplings in the next section.

IV.3.2 General input

For the RGE evolution towards high scales we need a set of input parameters at the low scale $\mu = m_Z = 91.186$ GeV. The experimental input we have are the masses and the measured parameters of the CKM-mixing matrix as well as the gauge couplings. We have neglected constraints coming from the neutrino sector. The quark and charged lepton masses at the scale m_Z we take from

Ref. [23], their values are (in GeV)

$$\begin{aligned} m_u &= 1.29 \times 10^{-3}\,, \quad m_c = 0.619\,, \quad m_t = 171.7\,; \\ m_d &= 2.93 \times 10^{-3}\,, \quad m_s = 0.055\,, \quad m_b = 2.89\,; \\ m_e &= 0.487 \times 10^{-3}\,, \quad m_\mu = 0.103\,, \quad m_\tau = 1.746\,. \end{aligned}$$

For the 3×3 CKM matrix we use the PDG [18] phase convention

$$V_{CKM} = \begin{pmatrix} c_{12}c_{13} & s_{12}c_{13} & s_{13}e^{-i\delta} \\ -s_{12}c_{23} - c_{12}s_{23}s_{13}e^{i\delta} & c_{12}c_{23} - s_{12}s_{23}s_{13}e^{i\delta} & s_{23}c_{13} \\ s_{12}s_{23} - c_{12}c_{23}s_{13}e^{i\delta} & -c_{12}s_{23} - s_{12}c_{23}s_{13}e^{i\delta} & c_{23}c_{13} \end{pmatrix}, \qquad \text{(IV.30)}$$

where $s_{ij} = \sin\theta_{ij}$ and $c_{ij} = \cos\theta_{ij}$. We will also use this convention for the phases at the high scale. The values for the angles and the phase follow from [18]

$$\begin{aligned} s_{21} &= \lambda\,, \quad s_{23} = A\lambda^2\,, \\ s_{13}e^{i\delta} &= \frac{A\lambda^3\,(\bar\rho + i\bar\eta)\,\sqrt{1 - A^2\lambda^4}}{\sqrt{1-\lambda^2}\,\left[1 - A^2\lambda^4\,(\bar\rho + i\bar\eta)\right]}\,. \end{aligned} \qquad \text{(IV.31)}$$

with

$$\lambda = 0.2253\,, \quad A = 0.808\,, \quad \bar\rho = 0.132\,, \quad \bar\eta = 0.341\,. \qquad \text{(IV.32)}$$

There is of course still a large freedom in how one chooses the remaining freedom at the weak scale m_Z. We chose to put the CKM-mixing always in the down quark sector and have thus at the EW scale

$$\begin{aligned} V_L^U &= V_R^U = I \\ V_L^D &= V_{CKM}^\dagger \qquad V_R^D = I \\ V_L^L &= V_R^L = I\,. \end{aligned}$$

The last two are a consequence of our neglecting neutrino masses and mixings. The Yukawa couplings at the EW scale are thus:

$$\begin{aligned} (\kappa_0^U)_{ij} &= \kappa_{ij}^U = \frac{\sqrt{2}m_i}{v}\,, & (\rho_0^U)_{ij} = \rho_{ij}^U & \qquad (i,j = u,c,t) \\ (\kappa_0^D)_{ij} &= V_{\rm CKM}\,\kappa_{ij}^D = V_{\rm CKM}\,\frac{\sqrt{2}m_i}{v}\,, & (\rho_0^D)_{ij} = V_{\rm CKM}\,\rho_{ij}^D & \qquad (i,j = d,s,b) \\ (\kappa_0^L)_{ij} &= \kappa_{ij}^L = \frac{\sqrt{2}m_i}{v}\,, & (\rho_0^L)_{ij} = \rho_{ij}^L & \qquad (i,j = e,\mu,\tau) \end{aligned}$$

At any energy higher than the EW scale, the Yukawa couplings κ_0 and ρ_0 in general become non-diagonal and complex. Thus they need to be transformed

to the mass eigenstates by the bi-diagonalization defined in Eq. (IV.13) in order to give κ and ρ. The latter can then be used together with the diagonal elements of the former to calculate $\lambda^F_{i\neq j}$. When performing the bi-diagonalization we always keep to the PDG conventions for how to write the CKM matrix.

For the electroweak VEV we use $v^2 = 1/(\sqrt{2}G_F)$ with $G_F = 1.16637 \cdot 10^{-5}$ GeV^{-2} from PDG [18] and for the phase difference between the two VEVs we start from $\theta = 0$ such that there is no spontaneous CP-violation. For the gauge couplings we use the PDG [18] values: $\alpha = 1/127.91$, $\alpha_s = 0.118$ and for the weak mixing angle we use the on-shell value $\sin^2\theta_W = 0.2233$.

IV.4 RGE analysis

We have implemented the RGE equations in the Higgs basis given above in three different computer codes. The matrix operations have been performed with either the C++ template library *Eigen* [24] or the *GNU Scientific Library (GSL)* [25] and the in total 114 ordinary differential equations are handled by the ODE-solver in GSL using the explicit Runge-Kutta-Fehlberg (4,5) method. The programs have been tested against each other and also by comparing with the results from [10].

In this section we will start by briefly exploring the behavior of Z_2-symmetric models and then study a number of Z_2-breaking models in more detail.

IV.4.1 Z_2-symmetric models

From table IV.1 and the definitions of κ^F and ρ^F, we get the diagonal elements of λ^F_{ii} in terms of $\tan\beta$ for the four different 2HDM types as shown in table IV.3. Since in this case the Yukawa couplings are given by $\tan\beta$ it is a real physical parameter. In addition the evolution of the Yukawa couplings will only depend on the initial value of $\tan\beta$.

Since the Z_2-symmetry is enforced the Yukawa couplings stay diagonal and the only thing that can happen during the evolution is that one or more of the Yukawas will blow up due to the presence of a Landau pole. This signals the breakdown of the perturbative description and calls for a new theory at the corresponding energy scale. The position of the Landau pole will depend on the initial value of $\tan\beta$ and which of the four types we are considering.

In Fig. IV.1 we show the position of the Landau pole as a function of the input $\tan\beta$. For the lower limits, the results are almost the same for all types, and the lines are more or less on top of each other. This is natural since in this regime the evolution is essentially driven by λ_{tt}, which is the same in all types. For the upper limits, on the other hand, there are some differences. First of all there is no upper limit on $\tan\beta$ in the type I model, which means there is no

Type	λ_{ii}^U	λ_{ii}^D	λ_{ii}^L
I	$1/\tan\beta$	$1/\tan\beta$	$1/\tan\beta$
II	$1/\tan\beta$	$-\tan\beta$	$-\tan\beta$
III/Y	$1/\tan\beta$	$-\tan\beta$	$1/\tan\beta$
IV/X	$1/\tan\beta$	$1/\tan\beta$	$-\tan\beta$

Table IV.3: The diagonal λ_{ii}^F in 2HDM models with Z_2 symmetry.

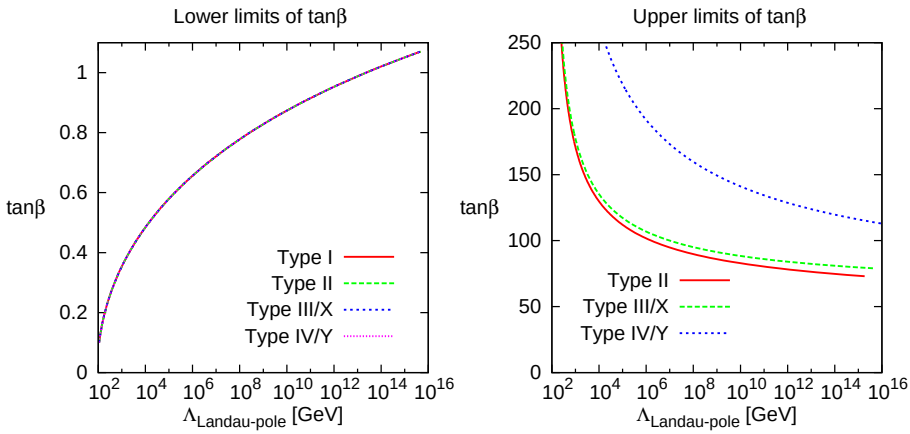

Figure IV.1: The starting value of $\tan\beta$ as a function of the position of the corresponding Landau pole ($\Lambda_{\text{Landau}-\text{pole}}$) in the different 2HDM types. There are lower limits on $\tan\beta$ for all four types (left), but only type II, type III/X and type IV/Y have an upper limit of $\tan\beta$ (right).

Landau pole below 10^{16} GeV if the input $\tan\beta > 1.1$. For the other types, the upper limits are shown in the right panel of Fig. IV.1. The differences can be understood from whether the evolution is driven by λ_{bb} (type III), $\lambda_{\tau\tau}$ (type IV) or both (type II).

IV

IV.4.2 Z_2-breaking models

Before starting to analyze the Z_2-breaking models we note that, as shown by [4], the Z_2-symmetry of the RGE's is still preserved if all the λ^F's for the different types are rescaled with a factor x for the $\cot\beta$ ones and $1/x$ for the $\tan\beta$ ones. In addition, when $\tan\beta$ is no longer related to the Yukawa couplings it does not have any physical meaning, since it only reflects the basis choice for the general 2HDM. In the following we will only be considering cases with ρ real at the starting scale. This means that the only source of CP-violation is from the CKM-matrix. Thus the CP-violating effects will be small and there-

fore the dependence on $\tan\beta$ very limited. We have verified this numerically for a number of cases and in the following we set $\tan\beta = 1$.

In this subsection, we will also explore the non-diagonal elements of FCNC Yukawa couplings. We know that in the Z_2 symmetric case, the tree level FCNC couplings will remain equal to zero (up to the numerical precision) up to arbitrarily high energy scales since they are protected by the symmetry. However once we break the Z_2 symmetry in some way, this protection is not effective anymore and the off-diagonal elements $\lambda^F_{i\neq j}$ may start to grow.

The actual values of the non-diagonal FCNC Yukawa couplings $\rho^F_{i\neq j}$ at different energy scales will depend on how much we break the Z_2 symmetry. We can thus use the size of the $\lambda^F_{i\neq j}$ as a measure of how severe different types of Z_2 symmetry breaking are. Of course we do not know how large the $\lambda^F_{i\neq j}$ can be at higher scales. Still it is reasonable to assume that the values should not be widely different from the ones at the EW scale. Thus we will use a generic value of $\lambda^F_{i\neq j} \leq 0.1$ as a limit on how much Z_2 symmetry breaking should be allowed and see at which energy scale this limit is reached.

The argument behind this is essentially that we can use the RGE evolution to analyze the stability of the assumptions underlying different 2HDMs under variations of the scale where the model is defined. A large sensitivity indicates that the assumptions behind the model are not stable meaning that they are either fine-tuned or incomplete such that there for example will be additional particles appearing when going to a higher energy. From this respect we will thus study both the appearance of a Landau pole as well as off-diagonal Yukawa couplings leading to FCNC larger than experimentally allowed at the EW scale. We also note that as will become clear below there is a small dependence on at which scale we apply the above argument. Requiring stability up to 10^3 GeV gives very similar constraints on the amount of Z_2-breaking that is allowed as when using 10^{15} GeV.

There are many possibilities to break the Z_2 symmetry and in the following we will consider three ways: aligned, diagonal and non-diagonal λ^F_{ij} as defined below. In most cases we will concentrate on the effects of breaking the symmetry starting from a type I or type II model. The reasons for this is on the one hand that these models are the most well studied cases in the literature and on the other hand that it is in the quark sector that we have the most stringent constraints on the FCNC Yukawa couplings. Thus the breaking of the Z_2 symmetry in the lepton sector will typically have small effects.

In order to be able to separate the effects of breaking the Z_2 symmetry in different ways we will limits ourselves to breaking the symmetry in one specific way at a time.

We start by noting that in the Z_2 symmetric models at least two of the λ^F are always equal whereas the third one is the same as the other two in type

I and the negative inverse of them in the other types. When going to the aligned models we will therefore keep two of the sectors in fulfillment with the Z_2-symmetry and only break the symmetry through the relation to the third sector. In other words either setting $\lambda^D_{ii} = \lambda^L_{ii}$, $\lambda^U_{ii} = \lambda^L_{ii}$, or $\lambda^U_{ii} = \lambda^D_{ii}$ and letting λ^F_{ii} of the third sector vary independently of the other two.

Another way of breaking the Z_2-symmetry is by keeping the λ^F_{ij} diagonal but letting the individual diagonal elements be non-equal as has been studied by Mahmoudi and Stål [8]. We will analyze the effects of this type of breaking in the up and down sectors separately again starting from the Z_2-symmetric cases with either $\lambda^D_{ii} = \lambda^L_{ii} = \lambda_{tt}$ or $\lambda^D_{ii} = \lambda^L_{ii} = -1/\lambda_{tt}$. In other words using the type I or II Z_2-symmetries as starting point.

The third way of breaking the Z_2-symmetry that we will consider is by setting the non-diagonal elements of λ^F_{ij} nonzero already at the starting scale. Again we will consider setting the up-sector and down-sector non-diagonal elements non-zero separately and apply the type I or type II symmetries for the diagonal elements.

Aligned models

We start by analyzing the three different versions of Aligned models with λ^U, λ^D, and λ^L pairwise equal. Based on the similarities with the Z_2-symmetric models we call them I/II, III, and IV respectively and their free parameters are as follows

- Aligned I/II: λ^U_{ii}, $\quad \lambda^D_{ii} = \lambda^L_{ii}$
- Aligned III: λ^D_{ii}, $\quad \lambda^U_{ii} = \lambda^L_{ii}$
- Aligned IV: λ^L_{ii}, $\quad \lambda^U_{ii} = \lambda^D_{ii}$

First we consider the effects of requiring that there is no Landau pole encountered when evolving to higher scales. We therefore plot in Fig. IV.2 the scale at which the Landau pole is reached as a function of the starting values for pairs of λ^U, λ^D, and λ^L. This means that for a given energy scale the points inside the corresponding contour is allowed by this requirement. As can be seen from the figure, the position of the Landau poles is very similar to the situation for the Z_2-symmetric cases and there is only a small correlation between the values of the aligned Yukawas where the Landau pole is reached.

Applying also the condition that the off-diagonal elements of should respect the limits given by the meson mixing constraints also at higher scales has a potentially large impact on the allowed regions. This is the case for the aligned models of type I/II and III, where λ^L is set equal to λ^D and λ^U respectively, as can be seen in Fig. IV.3. In fact, within the parameter region displayed in the figure (note the difference in scale compared to Fig. IV.2) there is no difference between the two cases and therefore we only show one of them. However, as may also have been expected, there are no additional

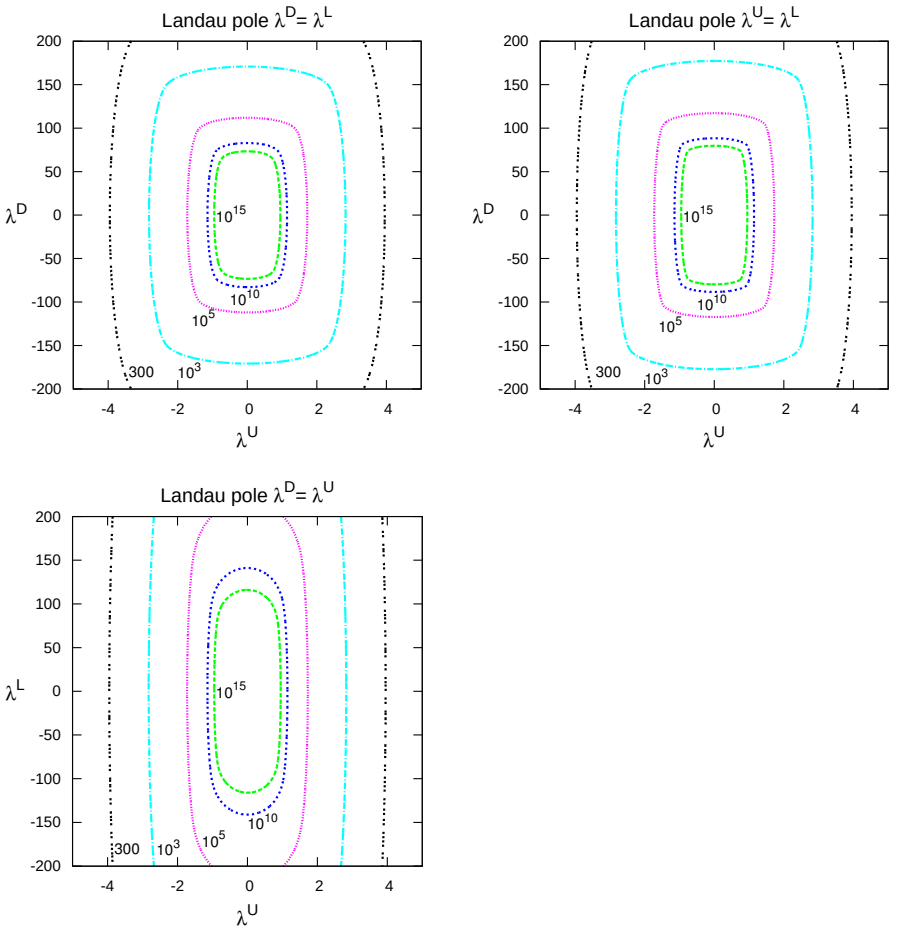

Figure IV.2: The energy scale at which the Landau pole is encountered as a function of pairwise combinations of the starting values for λ^U_{ii}, λ^D_{ii}, and λ^L_{ii} as indicated in the figure for the three different versions of aligned models explained in the text. The areas inside a given contour are allowed by the requirement of not having a Landau pole. The different contours are as follows starting from the center: 10^{15}, 10^{10}, 10^5, 10^3, and 300 GeV.

constraints in the case when λ^D and λ^U are set equal since the off-diagonal lepton Yukawas are always small as a consequence of the small lepton masses and the limited cross-talk between the quarks and leptons. In other words breaking the Z_2 symmetry between the quarks and leptons has no effect in this respect.

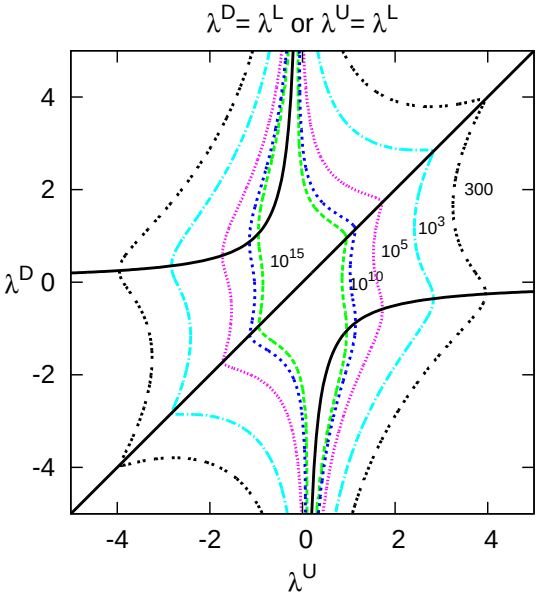

Figure IV.3: Same as Fig. IV.2 but also applying the constraints from the non-diagonal $\lambda^F_{i\neq j}$. The plot shows the results for $\lambda^L_{ii} = \lambda^D_{ii}$, but the same results are also obtained for $\lambda^L_{ii} = \lambda^U_{ii}$.

For reference we have also included lines corresponding to the Z_2 symmetric relations in Fig. IV.3. Along these lines it is the Landau pole that gives the limit but in the other regions the limit comes from the off-diagonal elements. We also note that the plot is symmetric under inversion through the origin $(x, y) \to (-x, -y)$, which follows since the evolution equations for ρ^F_0 are all even under $\rho^F_0 \to -\rho^F_0$ as long as the imaginary parts of κ^F_0 and ρ^F_0 are small.

It is also interesting to compare the results for non-equal λ^D and λ^U with the constraints on λ_{bb} and λ_{tt} obtained from $b \to s\gamma$ in [8]. Applying the conditions of stability when evolving to higher scales and that the non-diagonal Yukawas should stay small essentially removes the regions $|\lambda_{tt}| \gtrsim 1$ including the fine-tuned regions where λ_{bb} and λ_{tt} are both large ($\gtrsim 2$) and have the same sign.

As special cases we also show in Fig. IV.4 the results for $\lambda^U_{ii} = 0.02, 0.5$ and either $\lambda^D_{ii} = \lambda^L_{ii} = \xi\lambda^U_{ii}$ (type I) or $\lambda^D_{ii} = \lambda^L_{ii} = -\xi/\lambda^U_{ii}$ (type II). From these plots it is clear that for $\lambda^U_{ii} = 0.5$, the off-diagonal elements puts strong constraints on the Z_2-symmetry breaking parameter $\xi = \lambda^D_{ii}/\lambda^U_{ii}$ ($\xi = -\lambda^D_{ii}\lambda^U_{ii}$) with typical values being $\xi \lesssim 3 - 10\,(2 - 5)$ for type I (II). For $\lambda^U_{ii} = 0.02$ on the other hand the constraints are very mild in a type I set-up with $\xi \lesssim 100 - 1000$ al-

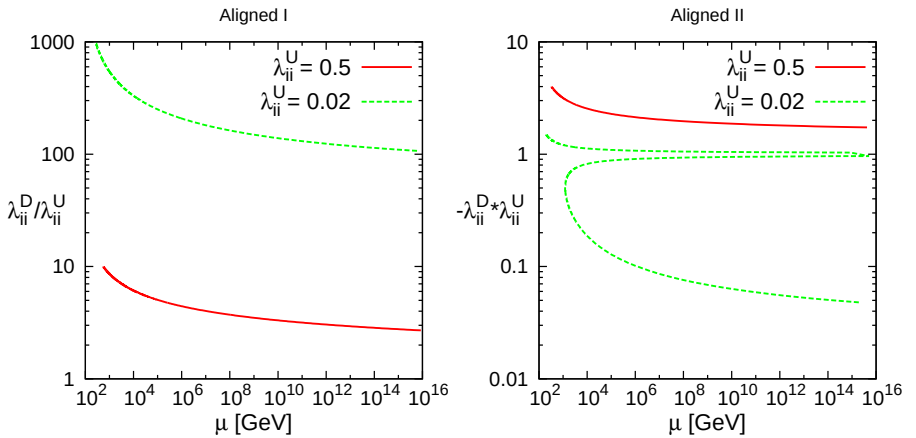

Figure IV.4: The constraints on the starting values of $\xi = \lambda^D_{ii}/\lambda^U_{ii}$ (left) and $\xi = -\lambda^D_{ii}\lambda^U_{ii}$ (right) as a function of the renormalization scale where the off-diagonal elements reaches 0.1 in the Aligned models of type I and type II respectively for the representative values $\lambda^U_{ii} = 0.02$ and 0.5.

lowed, whereas in a type II setup only ξ values very close to 1 or $\xi \lesssim 0.05 - 0.1$ are allowed. The two possibilities corresponds to two distinct regions in the $\lambda^D_{ii}, \lambda^U_{ii}$ plane. The first one where $\lambda^D_{ii} \approx -1/\lambda^U_{ii}$ and the second one where λ^D_{ii} is small ($\lesssim 2 - 5$). For comparison we recall that the Landau pole constrains $\lambda^D_{ii} \lesssim 70 - 200$ more or less irrespectively of λ^U_{ii}. So the constraints on ξ are more or less trivial in this case.

Diagonal models

Next we consider in more detail models with Z_2-breaking in either the up or the down sector. To make the discussion more clear we only consider models where λ_{tt} and λ_{bb} are related in a Z_2 symmetric way and since we have seen that the effects of the lepton sector is small we always set $\lambda^L_{ii} = \lambda_{bb}$. (If λ_{tt} and λ_{bb} are *not* related in a Z_2 symmetric way then we are more or less back in the aligned models since these two are the dominant Yukawas). In other words we only partially break the alignment.

Thus we start with considering Z_2-breaking in the up-sector with $\lambda^D = \lambda_{tt}$ (type I) or $\lambda^D = -1/\lambda_{tt}$ (type II). For simplicity we also set $\lambda_{uu} = \lambda_{cc}$.

First of all, as we show in Fig. IV.5, the Landau pole gives the restriction $\lambda_{cc} \lesssim 400 - 500$ both for type I and II, again more or less independently of the value of λ_{tt}. We also want to emphasize that even though it is not really discernable from the figure, there is also a lower limit on $\lambda_{tt} \gtrsim 0.01$ from the Landau pole for λ_{bb} for type II.

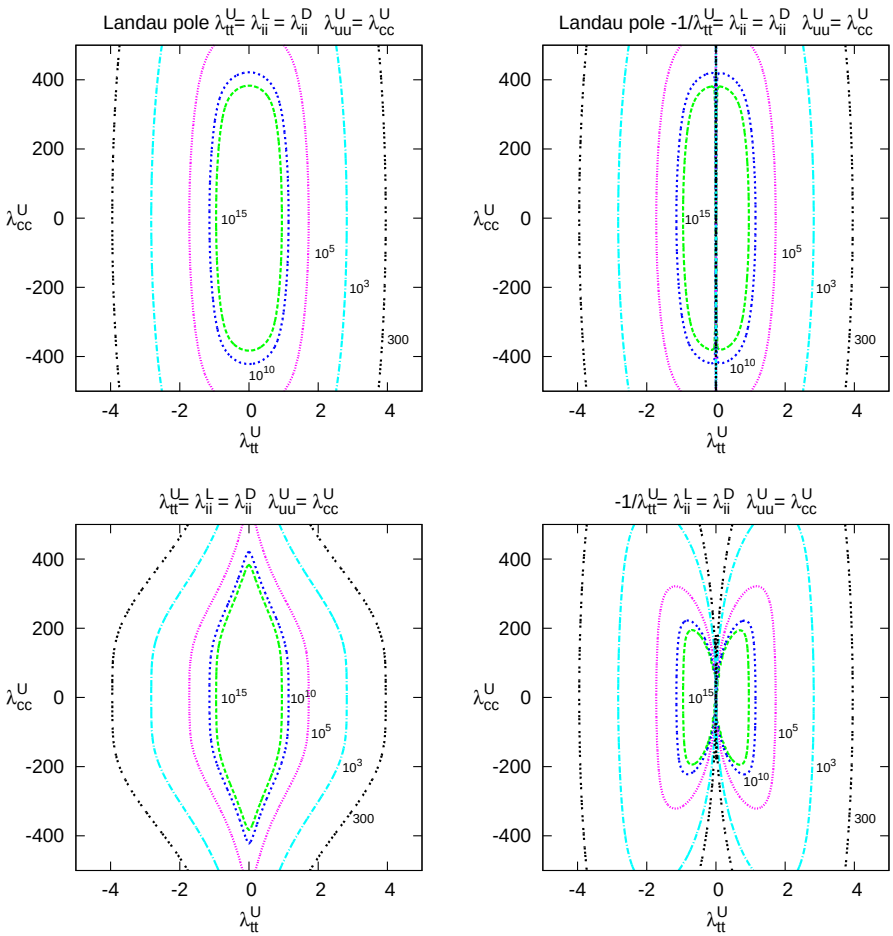

Figure IV.5: The energy scale where the Landau pole is reached (upper panels) together with the scale where one of the non-diagonal $\lambda^F_{i\neq j} = 0.1$ (lower panels) as a function of the input values λ_{cc} and λ_{tt}. In the left (right) panels $\lambda^D = \lambda^L = \lambda_{tt}(-1/\lambda_{tt})$.

IV

The figure also shows that the impact of constraining the off-diagonal elements to be less than 0.1 is limited for the type I set-up. In fact for $\lambda_{tt} = 0$ there is not additional constraint from the off-diagonal elements. In the type II set-up the constraints are more severe but even so quite mild.

To get a better picture of the range of the amount of Z_2-breaking allowed we also give in Fig. IV.6 the constraints on the ratio $\lambda_{cc}/\lambda_{tt}$ in type I and II set ups for our standard values $\lambda_{tt} = 0.02$ and 0.5. From the plots it is clear that this ratio can be as large as ~ 1000 without generating off-diagonal $\lambda^F \geq 0.1$ all

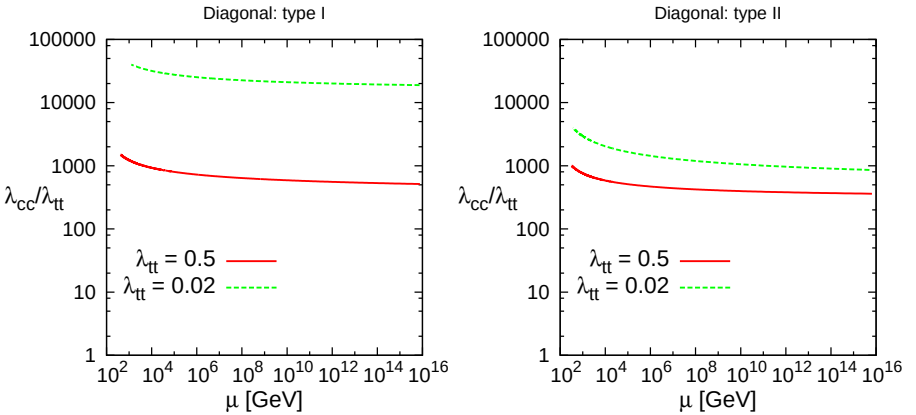

Figure IV.6: The constraints on the input values $\xi = \lambda_{cc}/\lambda_{tt}$ as a function of the renormalization scale where the off-diagonal elements reaches 0.1 in the diagonal models of type I (left) and type II (right) for the representative values $\lambda_{tt} = 0.02$ and 0.5.

the way up to the GUT scale.

Next we consider Z_2-breaking in the down-sector with $\lambda_{bb} = \lambda^U_{ii}$ (type I) or $\lambda_{bb} = -1/\lambda^U_{ii}$ (type II). Similarly to the up-sector we set $\lambda_{dd} = \lambda_{ss}$ for simplicity. Also in this case the constraints from the Landau pole are similar for the two set-ups with $\lambda_{ss} \lesssim 400 - 700$ in both cases with a small correlation with the value of λ^U_{ii} and λ_{bb} for a set up of type I and type II respectively as can be seen from Fig. IV.7 (upper panels). However, contrary to the up-sector the figure (lower panels) also shows that the effects from requiring the off-diagonal Yukawas to be small are quite severe. In the type II case one can even see a mild preference for solutions with $\lambda_{ss} \approx \lambda_{bb}$.

To get a more quantitative picture of the constraints we show in Fig. IV.8 the ratio $\xi = \lambda_{ss}/\lambda_{bb}$ for type I and type II using the values $\lambda^U_{ii} = 0.02$ and 0.5. In the type II set-up the constraints are especially restrictive with $\xi \lesssim 4 - 10$ for $\lambda^U_{ii} = 0.02$. In the type I set-up the constraints are less severe but even so stronger than the corresponding ones from the up-sector.

Non-diagonal models

Finally we consider the case of breaking the Z_2-symmetry from having non-zero non-diagonal elements in the up- or down sectors. As starting point we again use the Z_2 symmetric models of type I or II for the diagonal elements and then set either $\lambda^U_{i\neq j} = 0.1$ or $\lambda^D_{i\neq j} = 0.1$ at the EW scale in order to break the Z_2 symmetry.

Quite unexpectedly the additional constraints from requiring the off-

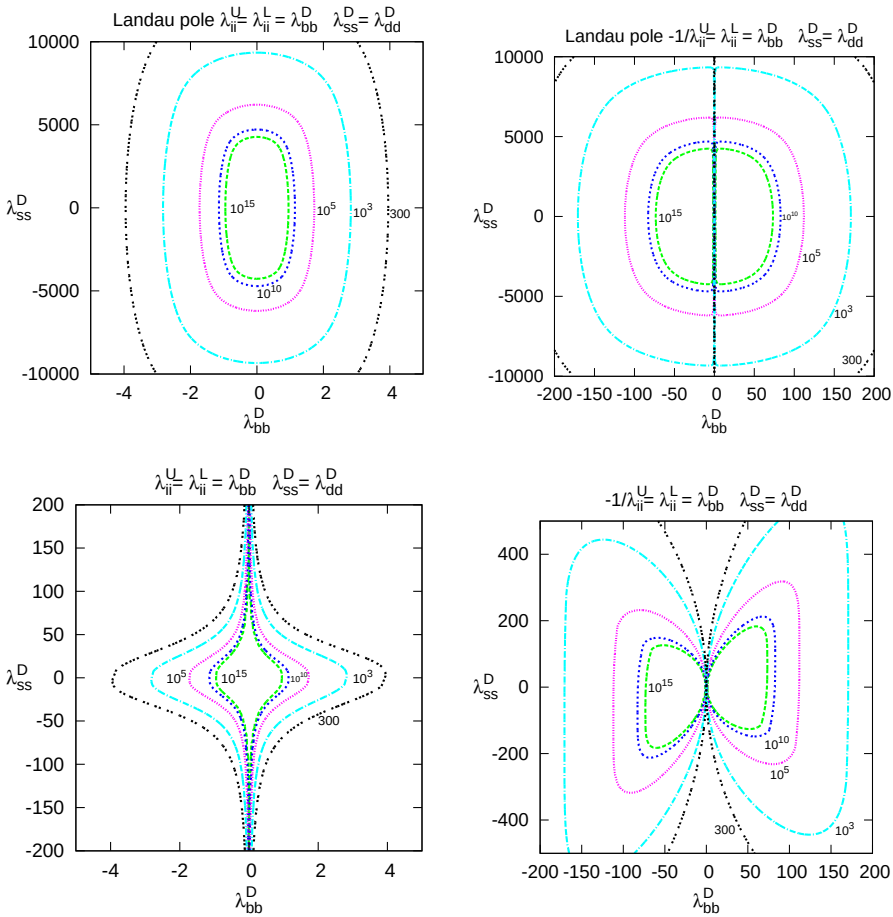

Figure IV.7: The energy scale where the Landau pole is reached (upper panels) together with the scale where one of the non-diagonal $\lambda^F_{i\neq j} = 0.1$ (lower panels) as a function of λ_{ss} and λ_{bb}. In the left (right) panels $\lambda^U = \lambda_{bb}(-1/\lambda_{bb})$ and in all cases $\lambda^L = \lambda_{bb}$.

IV

diagonal elements to stay small are limited. The corresponding plots for the case of only considering the Landau pole are essentially straight vertical lines. Thus we do not show the effects of applying the two constraints separately. In fact it is only in case II with $\lambda^D_{ii} = \lambda^L_{ii} = -1/\lambda^U_{ii}$ and $\lambda^U_{i\neq j} = 0.1$ that the requirement of having $\lambda^U_{i\neq j}(\mu) \leq 0.1$ gives any discernable effect and then only for small $\lambda^U_{ii} \lesssim 0.2$. On the other hand, in this case the constraints are very strong as also illustrated in Fig. IV.10. It is interesting to note that it is actually the off-diagonal elements in the down-sector that become large whereas the ones

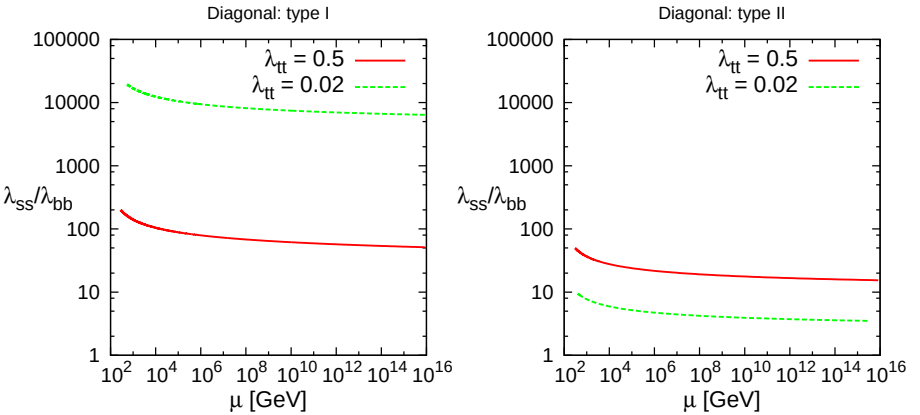

Figure IV.8: The constraints on the input values $\xi = \lambda_{ss}/\lambda_{bb}$ as a function of the renormalization scale where the off-diagonal elements reaches 0.1 in the diagonal models of type I (left) and type II (right) for the representative values $\lambda_{tt} = 0.02$ and 0.5.

in the up-sector remain in accord with the limit $\lambda^U_{i\neq j}(\mu) \leq 0.1$. This means that even though there are presently no direct experimental constraints on λ_{ct} and λ_{ut} they are in this case highly constrained from the link to the down-sector through the RGE evolution. This is then the case in the MSSM, the prime example of a type II 2HDM, for large $\tan\beta$. To see more clearly what happens we show also in Fig. IV.10 the RGE evolution of the relevant off-diagonal elements for the input values $\lambda^U_{ii} = 0.02$ and $\lambda^U_{i\neq j} = 0.001$, $\lambda^D_{i\neq j} = 0$.

IV.5 Conclusion

We have seen that the RGE evolution is a useful tool to analyze the stability of the assumptions underlying different versions of the 2HDM under variations of the scale where the model is defined. A large sensitivity indicates that the assumptions behind the model are not stable meaning that they are either fine-tuned or incomplete such that there for example will be additional particles appearing when going to a higher energy. From this respect we have studied both the appearance of a Landau pole as well as off-diagonal Yukawa couplings leading to FCNC larger than experimentally allowed at the EW scale.

Based on our studies we have seen that the constraints from avoiding a Landau-pole are in general the same irrespective of the Z_2-symmetry. They appear as soon as the magnitude of one of the Yukawa couplings becomes of order 1.

The constraints from the off-diagonal elements on the other hand depend

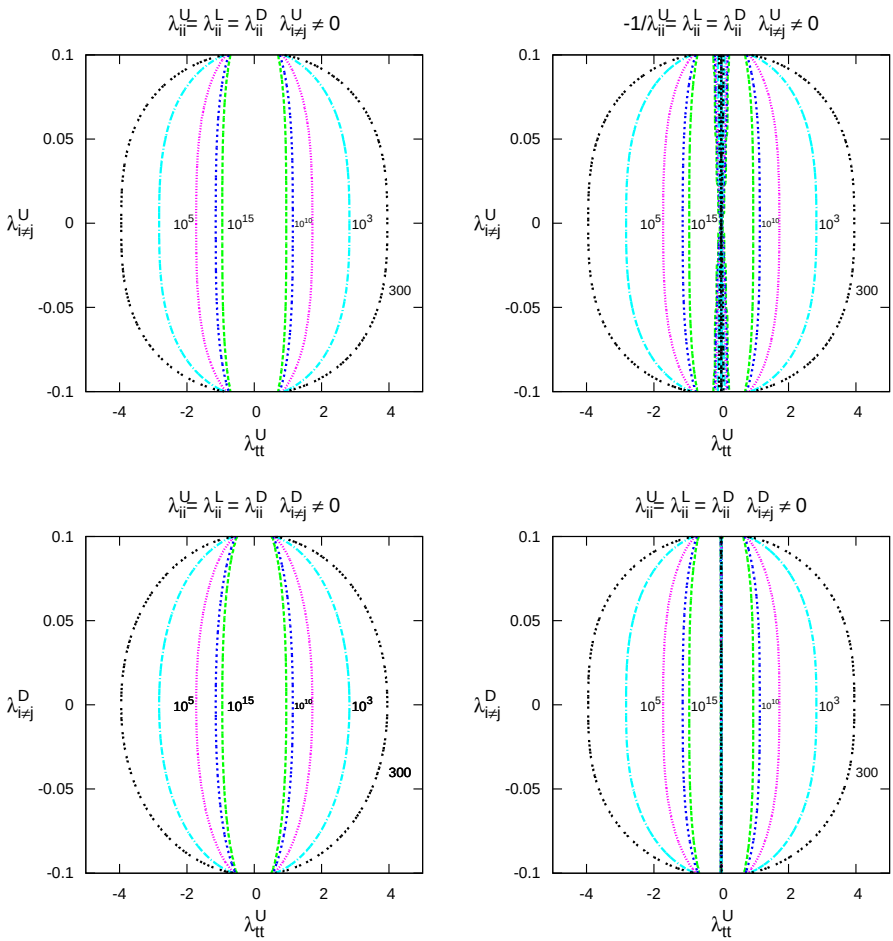

Figure IV.9: The constraints from the Landau pole and the off-diagonal elements as a function of λ^U_{ii} and the off-diagonal elements $\lambda^U_{i\neq j}$ (up) or $\lambda^D_{i\neq j}$ (down) at the input scale for the type I (left) and type II (right) relations for the diagonal elements.

on the details of how the Z_2-symmetry is broken:

- breaking the Z_2 relation between λ^D and λ^U as in the Aligned models is highly constrained with $\lambda^D/\lambda^U \lesssim 10$ or $-\lambda^D\lambda^U \lesssim 10$ unless λ^D and λ^U are both $\lesssim 2$,
- breaking it instead in the up-sector by having λ_{cc} and λ_{tt} non-equal gives a small difference compared to the constraints coming from the Landau pole with ratios $\lambda_{cc}/\lambda_{tt} > 1000$ allowed,

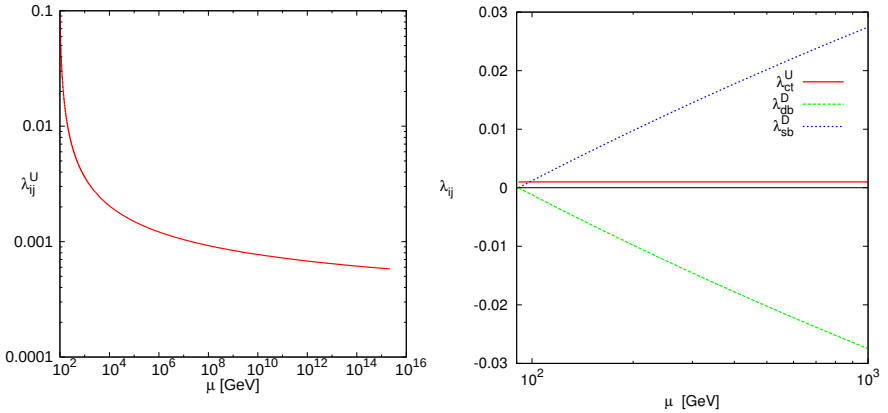

Figure IV.10: Left: The starting value $\lambda^U_{i\neq j}$ as a function of the energy scale μ where one of the non-diagonal elements of $\lambda^{U,D}_{i\neq j}$ becomes larger than 0.1 for $\lambda^U_{ii} = 0.02$ and a type II relation between the diagonal elements, $\lambda^D_{ii} = \lambda^L_{ii} = -1/\lambda^U_{ii}$. Right: The RGE-evolution of the non-diagonal elements $\lambda_{ct}(\mu)$, $\lambda_{sb}(\mu)$, and $\lambda_{db}(\mu)$ in the same case for $\lambda^U_{i\neq j} = 0.001$.

- in the down sector the constraints can be much stronger, but also more dependent on the relation between λ_{bb} and λ_{tt}, ranging from $\lambda_{ss}/\lambda_{bb} \lesssim 10$ for $\lambda_{bb} = 50$ and $\lambda_{tt} = -0.02$ to $\lambda_{ss}/\lambda_{bb} \lesssim 10000$ for $\lambda_{bb} = \lambda_{tt} = 0.02$,
- in the non-diagonal case the constraints are weak when starting from $\lambda^{D,U}_{i\neq j} = 0.1$ except in the case $\lambda_{bb} = -50$ and $\lambda_{tt} = 0.02$ where we find $\lambda^U_{i\neq j} \lesssim 0.001$. In all cases it is the $\lambda^D_{i\neq j}$

From this we can conclude that starting from a type I Z_2 symmetry there is quite a lot of room for breaking the symmetry as long as one does not encounter a Landau pole except that $\lambda^D/\lambda^U \lesssim 10$ has to be respected. In the type II case however, the room for breaking the symmetry is much smaller for large λ_{bb}. This is natural since in the latter case κ_{tt} and ρ_{bb} are both large. It is also interesting to note that this corresponds to the situation in the MSSM with large $\tan\beta$. Finally we conclude that there is little hope to see effects of non-diagonal Yukawa couplings in the top system in a type II model such as MSSM if $\tan\beta$ is large.

Acknowledgements

This work is supported in part by the European Community-Research Infrastructure Integrating Activity "Study of Strongly Interacting Matter" (Hadron-

Physics2, Grant Agreement n. 227431) and the Swedish Research Council grants 621-2008-4074, 621-2008-4219 and 621-2010-3326.

IV References

[1] T. D. Lee, "A Theory of Spontaneous T Violation," *Phys. Rev. D* **8** (1973) 1226. pages

[2] S. L. Glashow and S. Weinberg, "Natural Conservation Laws for Neutral Currents," *Phys. Rev. D* **15** (1977) 1958. pages

[3] A. Pich and P. Tuzon, "Yukawa Alignment in the Two-Higgs-Doublet Model," *Phys. Rev. D* **80** (2009) 091702, arXiv:0908.1554. pages

[4] P. M. Ferreira, L. Lavoura and J. P. Silva, "Renormalization-group constraints on Yukawa alignment in multi-Higgs-doublet models," *Phys. Lett.* (2010) 341, arXiv:1001.2561. pages

[5] A. J. Buras, M. V. Carlucci, S. Gori, and G. Isidori, "Higgs-mediated FCNCs: Natural Flavour Conservation vs. Minimal Flavour Violation," *JHEP* **1010** (2010) 009, arXiv:1005.5310 [hep-ph]. pages

[6] C. B. Braeuninger, A. Ibarra, and C. Simonetto, "Radiatively induced flavour violation in the general two-Higgs doublet model with Yukawa alignment," *Phys.Lett.* **B692** (2010) 189–195, arXiv:1005.5706 [hep-ph]. pages

[7] M. Jung, A. Pich, and P. Tuzon, "Charged-Higgs phenomenology in the Aligned two-Higgs-doublet model," *JHEP* **1011** (2010) 003, arXiv:1006.0470 [hep-ph]. pages

[8] F. Mahmoudi, O. Stal, "Flavor constraints on the two-Higgs-doublet model with general Yukawa couplings," *Phys. Rev. D* **81** (2010) 035016, arXiv:0907.1791. pages

[9] T. P. Cheng and M. Sher, "Mass Matrix Ansatz and Flavor Nonconservation in Models with Multiple Higgs," *Phys. Rev. D* **35** (1987) 3484. pages

[10] G. Cvetic, S. S. Hwang and C. S. Kim, "One loop renormalization group equations of the general framework with two Higgs doublets," *Int. J. Mod. Phys. A* **14** (1999) 769, arXiv:hep-ph/9706323. pages

[11] G. C. Branco, P. M. Ferreira, L. Lavoura, M. N. Rebelo, M. Sher and J. P. Silva, "Theory and phenomenology of two-Higgs-doublet models," arXiv:1106.0034. pages

[12] A. Djouadi, "The Anatomy of electro-weak symmetry breaking. I: The Higgs boson in the standard model," *Phys.Rept.* **457** (2008) 1–216, arXiv:hep-ph/0503172 [hep-ph]. pages

[13] A. Djouadi, "The Anatomy of electro-weak symmetry breaking. II. The Higgs bosons in the minimal supersymmetric model," *Phys.Rept.* **459** (2008) 1–241, arXiv:hep-ph/0503173 [hep-ph]. pages

[14] S. Davidson and H. E. Haber, "Basis-independent methods for the two-Higgs-doublet model," *Phys.Rev.* **D72** (2005) 035004, arXiv:hep-ph/0504050 [hep-ph]. pages

[15] R. S. Gupta, J. D. Wells, "Next Generation Higgs Bosons: Theory, Constraints and Discovery Prospects at the Large Hadron Collider," *Phys. Rev. D* **81** (2010) 055012, arXiv:0912.0267. pages

[16] H. E. Haber and D. O'Neil, "Basis-independent methods for the two-Higgs-doublet model. II. The Significance of tan beta," *Phys.Rev.* **D74** (2006) 015018, arXiv:hep-ph/0602242 [hep-ph]. pages

[17] D. Atwood, L. Reina, A. Soni, "Phenomenology of two Higgs doublet models with flavor changing neutral currents," *Phys. Rev. D* **55** (1997) 3156–3176, arXiv:hep-ph/9609279. pages

[18] K. Nakamura *et al.* [Particle Data Group Collaboration], "Review of particle physics," *J. Phys. G* **37** (2010) 075021. pages

[19] J. Laiho, E. Lunghi, R. S. Van de Water, "Next Generation Higgs Bosons: Theory, Constraints and Discovery Prospects at the Large Hadron Collider," *Phys. Rev. D* **81** (2010) 034503, arXiv:0910.2928. pages

[20] E. Lunghi, A. Soni, "Footprints of the Beyond in flavor physics: Possible role of the Top Two Higgs Doublet Model," *JHEP* **0709** (2007) 053, arXiv:0707.0212. pages

[21] A. Lenz, U. Nierste, J. Charles, S. Descotes-Genon, A. Jantsch, C. Kaufhold, H. Lacker, S. Monteil *et al.*, "Anatomy of New Physics in $B - \bar{B}$ mixing," *Phys. Rev. D* **83** (2011) 036004, arXiv:1008.1593. pages

[22] LHCb collaboration, "Measurement of Δm_s in the decay $B_s^0 \to D_s^-(K^+K^-\pi^-)\pi^+$ using opposite-side and same-side flavour tagging algorithms,". LHCb-CONF-2011-050. pages

[23] Z. z. Xing, H. Zhang and S. Zhou, "Updated Values of Running Quark and Lepton Masses," *Phys. Rev. D* **77** (2008) 113016, arXiv:0712.1419. pages

[24] G. Guennebaud, B. Jacob, *et al.*, "Eigen v3." http://eigen.tuxfamily.org/, 2010. pages

[25] M. Galassi, J. Davies, J. Theiler, B. Gough, G. Jungman, P. Alken, M. Booth, F. Rossi, *GNU Scientific Library Reference Manual - Third Edition (v1.12)*. pages